01 Jan 1970

Effects of cold work in cold-formed steel structural members

S. J. Britvec

Alexander Chajes

K. W. Warren

Jairo Uribe

et. al. For a complete list of authors, see https://scholarsmine.mst.edu/ccfss-library/170

CORNELL ENGINEERING
RESEARCH BULLETIN □ 70-1

Effects of cold work in cold-formed steel structural members

By S. J. Britvec, A. Chajes,
K. W. Karren, J. Uribe, and
G. Winter

DEPARTMENT OF STRUCTURAL
ENGINEERING ☐ SCHOOL OF
CIVIL ENGINEERING ☐
CORNELL UNIVERSITY
ITHACA, NEW YORK

Effects of cold work in cold-formed steel structural members

By S. J. Britvec, A. Chajes,
K. W. Karren, J. Uribe, and
G. Winter

ACKNOWLEDGEMENTS

When this investigation was in progress, the various co-authors were, respectively:

S. J. Britvec, assistant professor,
A. Chajes, K.W. Karren, and Jairo Uribe, research assistants and research associates,
George Winter, Professor of Engineering (Class of 1912 Chair) and chairman

all in the Department of Structural Engineering, Cornell University.

Drs. Chajes and Karren, at this time, are associate professors at the University of Massachusetts and Brigham Young University, respectively. Dr. Uribe is now Professor of Civil Engineering at the Universidad de los Andes in Bogota, Colombia.

CONTENTS

PREFACE

The mechanical properties of steel in cold-formed structural members differ from those of the flat material from which they are formed by cold-rolling or in press-brakes. This is so because the forming process subjects the material to strain-hardening; this increases the yield strength and, in most cases also the ultimate strength, at the expense of some reduction in ductility.

Structural economy can be improved if the design of such members is based on the as-formed properties, rather than on the properties of the flat sheet, strip, or plate before forming. This can be done only, however, if the strength properties of the material in the formed shape can be reliably ascertained, by calculation, test, or a combination of the two. Realizing this potential gain in economy, the American Iron and Steel Institute sponsored a research investigation at Cornell University for the purpose of identifying the effects of cold-forming on the mechanical properties of the as-formed steel, as well as on structural behavior of members so formed.

The four papers in this bulletin present a condensed account of this investigation. The first three have been previously published in the Journal of the Structural Division, Proc., Am. Soc. Civ. Eng. and, together with their published discussions, are reprinted herein. The fourth and last paper is published here for the first time. Together they constitute the basis for new provisions in the 1968 edition of the Specification for the Design of Cold-Formed Steel Structural Members, A.I.S.I.; these provide the methods for utilizing in design the improved strength properties obtained in the process of cold-forming.

George Winter
Professor of Engineering
(Class of 1912 Chair)

Journal of the
STRUCTURAL DIVISION
Proceedings of the American Society of Civil Engineers

EFFECTS OF COLD-STRAINING ON STRUCTURAL SHEET STEELS

By Alexander Chajes,[1] M. ASCE, S. J. Britvec,[2] A.M. ASCE, and George Winter,[3] F. ASCE

SYNOPSIS

The cold working to which sheet steels are subjected when being cold-formed into structural shapes for light-gage steel construction affects their mechanical properties. In order to study the basic features of this process, the effects of various amounts of simple, uniform cold stretching on the stress-strain characteristics of various mild carbon structural sheet steels have been investigated. The results of tension and compression tests of cold stretched material, both in the direction of prior stretching and transverse to it, are presented. The effects of such cold work are found to be strongly directional, and are different for various types of structural carbon sheet steels. A general discussion of strain hardening, the Bauschinger effect, and strain aging is presented, based on current concepts of the crystalline nature of the material and of dislocation theory, and the experimental results are interpreted in terms of these concepts.

Note.–Discussion open until September 1, 1963. To extend the closing date one month, a written request must be filed with the Executive Secretary, ASCE. This paper is part of the copyrighted Journal of the Structural Division, Proceedings of the American Society of Civil Engineers, Vol. 89, No. ST2, April, 1963.

[1] Research Asst., Dept of Structural Engrg., Cornell Univ., Ithaca, N. Y.
[2] Asst. Prof., Dept. of Structural Engrg., Cornell Univ., Ithaca, N. Y.
[3] Prof. and Head, Dept. of Structural Engrg., Cornell Univ., Ithaca, N. Y.

INTRODUCTION

The structural members that are used in light-gage steel construction[4] are produced by various cold-forming processes, such as cold-rolling or brake-forming. It is well known that cold working by stretching, bending, and so forth, affects the mechanical properties of mild structural steels and other ductile metals. Generally, such operations produce an increase in the yield point and ultimate strength and a decrease in ductility. Cold working of one type or another occurs in the forming of all cold formed light gage steel structural shapes. As a result, the mechanical properties of the steel in the member, as formed, are, to various degrees, different from those of the sheet prior to forming.

The cold-forming operations produce plastic deformations in the direction transverse to the axis of the member as well as parallel to it. Tests that were performed on coupons cut from various places along the cross section of a formed member indicate that the increase in yield strength is much higher at the corners than along the flat parts.[5] This observation leads to the assumption that plastic deformation transverse to the direction of subsequent loading, such as that which results from the bending of corners, is a major factor in the increase of strength observed in cold-formed structural members. In order to derive all possible advantage from this phenomenon, a deeper understanding of the effects of cold work on the properties of light gage steel sheet is essential.

The cold work that is exerted on sheet steels during the forming processes is of a complex nature and is not yet well undertstood. Therefore, in order to gain a fundamental understanding of the effects of such forming, it appeared necessary as a first step, to investigate the consequences of the simplest type of cold work, that is, of uniform cold-stretching. To this end, flat sheets of five different types of mild carbon structural steel were given known amounts of plastic deformation by simple uniform stretching. Next, the effect of this prior cold stretching on the stress strain diagram, in tension and in compression, both in the direction parallel to that of cold stretching and perpendicular to it, was determined. The particular steels investigated were chosen because they are representative of materials actually being used in cold-formed structural members.

---

[4] "Cold-Formed, Light-Gage Steel Construction," by George Winter, Journal of the Structural Division, ASCE, Vol. 86, No. ST9, Proc. Paper 2270, November, 1959.

[5] "Applications of Cold-Formed Sections," by R. M. Kenedi and W. S. Smith, Journal of the West of Scotland Iron and Steel Institute, Vol. 66, 1958–1959.

The cold work performed during the actual cold-forming of structural steel shapes consists of a complex combination of cold bending and other deformations. For this reason, the results of simple uni-axial cold stretching, obtained in the present investigation, cannot be applied directly to the cold-forming process. These results merely lay the groundwork of understanding for later investigations of the specific effects of cold-forming.

MATERIALS

The five carbon steels used in this investigation are described in Table 1, which includes the main mechanical properties, and the chemical composition for each steel. These compositions are the average values from analyses for the entire width of the sheet. In each case the virgin material consisted of coupons cut from a straightened sheet coil. Four of the steels used were 16 gage and one was 10 gage material. The four 16-gage steels consisted of two cold reduced and two hot rolled steels. One of the cold reduced steels was killed and the other rimmed, while one of the hot rolled steels was semi-killed and the other rimmed. The 10-gage steel was hot rolled and semi-killed. The two cold reduced coils were manufactured by hot rolling to a thickness of 0.109 in., and by further cold reduction, annealing, and temper rolling they were reduced to a final thickness of 0.062 in.

As carbon is removed from pig iron during the steel refining operation, the quantity of oxygen in the molten steel increases. Carbon steels are classified as rimmed or killed steels according to the method of elimination or reduction of this oxygen. In rimmed steels, the oxygen combines with carbon during solidification, and the resultant carbon monoxide gas rises through the liquid steel. The resultant ingot has a "rimmed zone" that occupies 25% to 40% of its cross section. The rimmed zone is relatively purer than the center of the ingot that freezes last. Killed steels are deoxidized by the addition of silicon or aluminum. Since no gas is evolved, they lie quietly in the mold during solidification. Killed steels normally possess less chemical segregation than rimmed steels.

Aluminum was used as a deoxidizing agent for the killed and semi-killed steels that were produced for this investigation. Deoxidation was performed in the mold rather than in the ladle because of the relatively small quantity of steel required. This practice sometimes results in a slightly less homogeneous material.

The deoxidizing process may have the effect of producing a non-aging steel. This is, however, not necessarily true in every case. In this investigation, the term "killed" or "semi-killed" refers only to the deoxidation practice used in the production of the steel and it does not imply a non-aging steel.

Table 1. Material Properties

Material	Gage	Chemical Composition by Random Check Analysis				Tensile Properties		
		C	Mn	S	P	Yield Strength, in psi	Ultimate Strength, in psi	% Elong. 2 inch gage length
1. Cold Reduced Annealed, Temper-Rolled Killed, Sheet Coil	16	0.15	0.40	0.024	0.008	38,300	51,100	40
2. Cold Reduced Annealed, Temper-Rolled Rimmed, Sheet Coil	16	0.09	0.39	0.028	0.008	36,400	50,700	35
3. Hot Rolled Semi-Killed Sheet Coil	16	0.04	0.32	0.025	0.008	37,500	49,000	37
4. Hot Rolled Rimmed Sheet Coil	16	0.08	0.32	0.045	0.008	40,500	50,700	35
5. Hot Rolled Semi-Killed Sheet Coil	10	0.18	0.50	0.029	0.008	37,000	57,500	36

TESTING

Tests Performed.—Tensile and compressive tests were made on flat specimens in the virgin state and with four degrees of uniform cold-stretching for each of the five different types of steel investigated. The four degrees of plastic deformation were: 0.010 inches per inch (10 mils), 0.025 inches per inch (25 mils), 0.050 inches per inch (50 mils), and 0.100 inches per inch (100 mils). The lowest of these, as a rule, is still on the yield plateau of steels that display a sharp yielding stress-strain curve Strains of 25 mils and 50 mils are usually in the strain hardening range of the material and a strain of 100 mils is located in the region in which the stress-strain curve begins to level out.

In order to determine the effects of aging after plastic deformation, one artificially aged companion specimen (held at 100°C for 30 min) was tested for every non-aged specimen. In addition, several tests were performed at various time intervals subsequent to the cold stretching operation so that the progress of aging at room temperature with elapsed time could be observed.

Compression and tension tests were made for transverse as well as longitudinal specimens. The term "longitudinal," as used in this investigation refers to specimens of which the axis of loading during testing coincided with the direction of prior uniform cold stretching and "transverse" refers to specimens loaded in a direction normal to that of cold stretching.

In each case, except for the aged specimens, duplicate tests were made.

Preparation of Specimens.—Flat coupons of over-all size, 49 in. by 14 in. (Fig. 1), cut from straightened sheets of each of the five steels were given four degrees of uniform cold stretching in the direction of rolling. By means of seven high strength bolts, the coupon was inserted at each end into specially fabricated, practically rigid tension jaws. A 20 in. gage length was laid off, on which extensions were determined by means of a steel scale graduated to 0.01 in. Each plate was pulled to the desired permanent strain in a 400,000 lb universal testing machine.

Compressive and tensile specimens were then cut from the plate longitudinally and transversely, as indicated in Fig. 1.

Except for the test series that was conducted specifically in order to investigate the effects of aging, all tests were performed an average of five days after the cold stretching operation. Therefore, even the so-called non-aged specimens had been exposed to a certain amount of natural aging, and the term aged, as applied to specimens hereafter, means artificially aged at 100°C for 30 min and has a relative, rather than absolute connotation.

Testing Apparatus.—Tensile specimens of standard ASTM shape (over-all 9 in. by 0.687 in.) were tested in self-alining grips, and strains on a 2 in. gage length were measured by means of an autographic microformer gage.

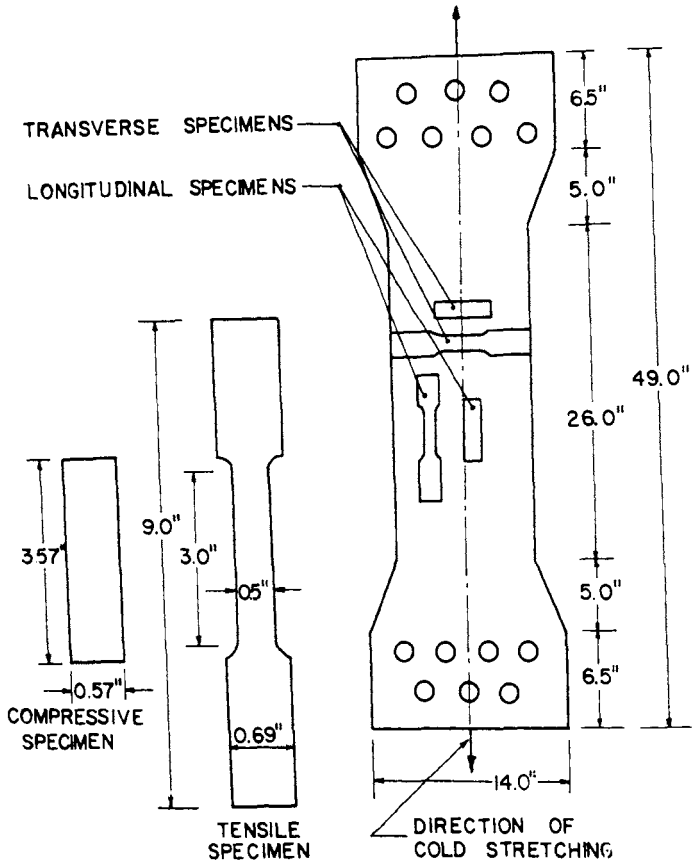

Fig. 1. Plate used in cold stretching operation and typical tensile and comprehensive specimens.

Tests of compressive specimens were performed by means of a device that was designed to prevent buckling of the compressive flat specimens. This device consists of two rigid longitudinally serrated flat I-shaped counterparts, connected by means of screws between which the compression specimen is held. The jig is of the type produced by Tinius Olsen Testing Machine Company except that its length was increased so that a 2 in. autographic microformer gage could be accommodated. The assembly, which consisted of the specimen, jig, and microformer gage, was placed in a sub-press in order to assure a high degree of axiality of loading. Compressive specimens were approximately 3.570 in. by 0.570 in.

TEST RESULTS

Notation.–The properties described herein, except for the proportional limit, are defined in the conventional manner. The 0.2% offset yield strength is used when referring to gradually yielding steels and the lower yield point for sharply yielding steels.

Because structural strength, in particular buckling strength, strongly depends on the tangent modulus, it was thought necessary to define a quantity that characterizes the stress at which deviation from linearity of the stress-strain diagram becomes pronounced. Because the proportional limit, as ordinarily understood, depends on sensitivity of instrumentation and personal judgment, it was decided to define proportional limit, for purposes herein, as that stress at which the permanent strain is 0.02%, that is, one-tenth of that of the conventional definition of yield strength. For sharp yielding steels, the lower yield point is taken for the proportional limit.

Proportional limit, yield strength, and ultimate strength are each defined as a specific load divided by the cross-sectional area of the specimen at the beginning of the test during which this property is determined. For virgin specimens, this definition simply states that engineering stress-strain characteristics are considered. This is, however, not the case for specimens cut from prestretched material. For these specimens, the cross-sectional area is measured after the prestretching operation and therefore includes the reduction in area resulting from the preceding plastic deformation.

Because of this manner of computing strength, any difference between one of the aforementioned properties in the prestretched specimen and the same property in the virgin material will consist of two parts. One is a change in strength per unit mass of material because of cold stretching, which is of primary interest in this investigation, whereas the other is a change in strength resulting from a decrease in cross-sectional area occurring during prestretching.

Table 2 gives reductions in area for all degrees of cold stretching used in the investigation. It also lists factors by which any of the strength properties

Table 2[a]

Amount of Cold Stretching, in mils	% Reduction in Cross Sectional Area	Stress Correction Factor
10	1	0.99
25	2	0.98
50	5	0.95
100	9	0.91

[a] Factors by which Proportional Limit, Yield Strength, and Ultimate Strength must be multiplied to give stress based on cross sectional area existing prior to cold stretching.

of a given specimen can be multiplied in order to give the same property based on the cross-sectional area existing prior to cold stretching. The difference between this new or corrected strength and the corresponding property in the virgin material would then be the change in strength per unit mass of material because of cold stretching.

Since a cold-formed member is aged by the time it becomes part of an actual structure, the properties of the material in the aged condition are of primary interest. For this reason, the stress-strain characteristics recorded in Figs. 2 through 5 and Figs. 8 through 10, which are presented subsequently, are for the aged condition.

Virgin Stress-Strain Curves.—Fig. 2 shows three virgin stress-strain curves which are representative of the types of steel investigated. The hot rolled steels are seen to display the sharp yielding stress-strain relationship usually associated with mild steel. The stress-strain curve of the cold reduced steel, however, is of the gradually yielding type. Evidently the lack of a yield plateau in the case of cold reduced steel is the result of the plastic deformation during the cold rolling operation.

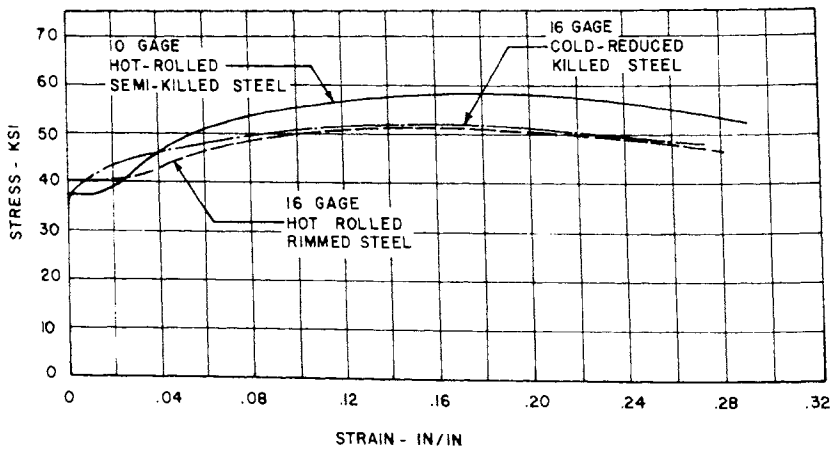

Fig. 2. Typical virgin stress-strain curves.

Yield Strength and Proportional Limit.—A summary of the data obtained from the various tests is shown in Tables 3 and 4. The yield strength and the proportional limit in compression and tension, transversely and longitudinally, were observed to increase with increasing amounts of cold-stretching. This was true for every steel except for the cold reduced killed steel. In the latter, for increasing amounts of cold-stretching, the yield strength in longitudinal

Table 3. Summary of Tension Test Results

		Proportional Limit, in kips per square inch		Yield Strength, in kips per square inch		Tensile Strength, in kips per square inch	% Elong.
		Non Aged	Aged	Non Aged	Aged	Aged	Aged
Cold Reduced	Virgin-L	31.0		38.3		51.1	40
Killed	10Mil-L	30.0	32.0	37.5	37.5	47.0	41
16 Gage	25Mil-L	39.0	38.0	44.7	44.6	50.8	37
	50Mil-L	40.0	38.0	45.0	45.5	53.5	39
	100Mil-L	38.0	37.0	52.5	52.5	55.7	31
	Virgin-T	31.0		38.3		51.1	40
	10Mil-T	20.5	24.0	39.5	35.8	45.9	40
	25Mil-T	25.5	23.0	38.7	38.0	50.0	37
	50Mil-T	21.0	22.0	38.5	38.5	49.7	27
	100Mil-T	24.0	23.0	43.5	43.5	55.0	30
Cold Reduced	Virgin-L	34.0		36.4		50.7	35
Rimmed	10Mil-L	44.0	44.0	45.0	45.3	51.5	31
16 Gage	25Mil-L	48.0	49.0	48.4	49.2	52.2	29
	50Mil-L	49.0	56.5	51.5	56.5	57.4	22
	100Mil-L	54.0	59.0	57.5	59.0	59.0	9
	Virgin-T	34.0		36.4		50.7	35
	10Mil-T	32.0	39.0	40.0	42.0	52.4	16
	25Mil-T	36.5	42.0	44.5	45.0	53.2	18
	50Mil-T	40.0	46.0	50.5	51.0	57.8	12
	100Mil-T	44.5	46.0	56.0	57.0	63.0	9
Hot Rolled	Virgin-L	40.7		37.5		49.0	37
Semi-Killed	10Mil-L	40.5	40.5	40.5	40.5	49.7	25
16 Gage	25Mil-L	45.5	49.0	45.5	49.0	54.5	20
	50Mil-L	53.0	54.7	53.0	54.7	58.0	20
	100Mil-L	60.3	60.5	60.3	61.0	61.5	12
	Virgin-T	40.7		40.7		50.3	30
	10Mil-T	41.3	42.7	41.3	42.7	49.6	35
	25Mil-T	40.0	47.5	42.0	47.5	54.2	21
	50Mil-T	43.5	50.0	46.0	50.0	57.5	15
	100Mil-T	51.5	55.7	56.1	58.0	64.6	10
Hot Rolled	Virgin-L	40.5		40.5		50.7	35
Rimmed	10Mil-L	39.5	39.6	39.5	39.6	49.5	30
16 Gage	25Mil-L	41.5	41.6	41.6	41.6	53.0	15
	50Mil-L	51.8	54.3	51.8	54.3	58.3	18
	100Mil-L	59.5	59.7	59.5	59.7	61.0	11
	Virgin-T	39.8		39.8		49.0	34
	10Mil-T	43.0	41.1	43.0	41.1	50.2	22
	25Mil-T	42.6	46.2	42.6	46.2	55.0	21
	50Mil-T	47.6	51.4	47.6	51.4	57.4	14
	100Mil-T	53.5	56.0	56.0	56.0	61.0	10
Hot Rolled	Virgin-L	37	37	37	37	57.5	36
Semi-Killed	10Mil-L	39	39	39	39	60	35
10 Gage	25Mil-L	49.5	49.5	49.5	49.5	59.5	27
	50Mil-L	57	57	57	57	63.0	21
	100Mil-L	70	70	70	70	70.0	15
	Virgin-T	39	39	39	39	58	35
	10Mil-T	38	41	38	41	59	31
	25Mil-T	37.5	42	40.5	42	59.5	38
	50Mil-T	44	44	46.5	46.5	61.0	20
	100Mil-T	50	50	57	57	68.0	14

L: Longitudinal T: Transverse

Table 4. Summary of Compression Test Results

		Proportional Limit, in kips per square inch		Yield Strength, in kips per square inch	
		Non Aged	Aged	Non Aged	Aged
Cold Reduced	Virgin-L	25.0		34.6	
Killed	10Mil-L	20.0	20.0	33.0	32.5
16 Gage	25Mil-L	19.0	16.5	33.0	33.0
	50Mil-L	19.0	17.5	34.0	34.0
	100Mil-L	15.5	17.0	35.0	35.5
	Virgin-T	33.0		40.3	
	10Mil-T	31.0	32.0	39.0	39.0
	25Mil-T	39.0	37.0	47.7	47.7
	50Mil-T	35.5	37.0	51.5	52.5
	100Mil-T	42.0	43.0	56.5	56.5
Cold Reduced	Virgin-L	27.5		33.0	
Rimmed	10Mil-L	27.0	38.5	36.0	38.5
16 Gage	25Mil-L	33.0	37.0	40.5	41.0
	50Mil-L	37.0	42.0	44.0	46.5
	100Mil-L	38.0	44.0	47.0	51.0
	Virgin-T	33.0		35.7	
	10Mil-T	38.5	42.0	44.0	44.7
	25Mil-T	41.0	45.0	50.0	50.0
	50Mil-T	44.5	45.0	53.0	53.0
	100Mil-T	52.0	54.0	63.5	64.0
Hot Rolled	Virgin-L	40.5		40.5	
Semi Killed	10Mil-L	39.5	43.6	40.2	43.6
16 Gage	25Mil-L	42.0	45.0	42.0	46.0
	50Mil-L	42.5	48.0	45.0	48.0
	100Mil-L	48.0	51.5	53.2	54.0
	Virgin-T	40.5		42.3	
	10Mil-T	44.0	43.0	44.0	43.0
	25Mil-T	43.5	46.5	43.5	46.5
	50Mil-T	49.5	54.5	51.0	54.5
	100Mil-T	58.0	61.0	62.0	62.0
Hot Rolled	Virgin-L	40.3		40.3	
Rimmed	10Mil-L	40.0	40.7	40.5	40.7
16 Gage	25Mil-L	36.0	41.0	41.0	41.0
	50Mil-L	43.0	47.0	46.5	47.0
	100Mil-L	46.5	48.0	52.6	50.0
	Virgin-T	43.0		43.0	
	10Mil-T	45.5	49.4	46.5	49.4
	25Mil-T	45.0	48.5	46.6	48.5
	50Mil-T	49.0	54.6	52.3	54.6
	100Mil-T	53.0	58.0	60.0	60.0
Hot Rolled	Virgin-L	38.5	38.5	38.5	38.5
Semi Killed	10Mil-L	36	42	38.5	42
16 Gage	25Mil-L	36.5	46	39.5	46
	50Mil-L	40	50	42.5	50
	100Mil-L	40	48.5	47.5	50
	Virgin-T	42.5	42.5	42.5	42.5
	10Mil-T	44	50.5	44	50.5
	25Mil-T	46.5	52	48	52
	50Mil-T	51.5	59	57	59
	100Mil-T	58	58	68	68

L: Longitudinal T: Transverse

compression remained constant and the proportional limit decreased for longitudinal compression and transverse tension. The rates of increase of the aforementioned properties for the remaining four steels differed considerably, depending on the properties of the material and the direction of loading.

The directionality of the effects of cold work is shown in Fig. 3. Fig. 3(a) describes the variation of the yield strength with cold stretching for 10-gage hot rolled semi-killed steel. This material had a tension yield strength of 37,000 psi before cold stretching [indicated on Fig. 3(b) as virgin longitudinal tension]. It is seen that increasing amounts of cold stretching raise the tension yield strength in the longitudinal direction by increasing amounts to 70,000 psi for 10% of cold stretching. At the same time, the tension yield strength in the transverse direction is increased to a considerably smaller degree, approximately half of that in the longitudinal direction for this particular steel. In regard to compression properties it is seen that the gain in yield strength in the longitudinal direction is on the whole considerably smaller than in tension. In contrast, the compression yield strength in the transverse direction is considerably larger than that in the longitudinal direction. Fig. 3(b) depicts the directional effect of cold stretching on the proportional limit of the foregoing steel, whereas Figs. 3(c) and 3(d) give similar descriptions for two other steels.

These results illustrate two facts: (1) The magnitude of the effects of cold work depends largely, though in varying degrees, on the extent of cold work that has been done; and (2) the effects of cold work are strongly directional, being different in tension than in compression and varying from the longitudinal to the transverse direction.

Another important feature is that the magnitude of the effects of cold work also vary strongly with the type of mild steel, that is, with the chemical composition and method of manufacture of the steel. This is illustrated by the test results plotted in Fig. 4. Fig. 4(a) compares the main longitudinal properties of two cold reduced 16-gage steels, one rimmed and the other killed. Both steels had roughly the same mechanical properties when in the virgin condition. It is evident that any given degree of cold stretching had a much larger effect on the yield strength of the rimmed steel than on that of the killed steel. Generally, the effect of cold work is to raise the tensile yield strength of the rimmed steel more than that of the killed steel and to raise the compression yield strength of the rimmed steel while having little or no effect on that of the killed steel.

A comparison of the transverse properties for the same two steels [Fig. 4(b)] indicates similar effects. The properties of the rimmed steel are again affected to a greater degree, by the same amount of cold stretching, than those of the killed steel.

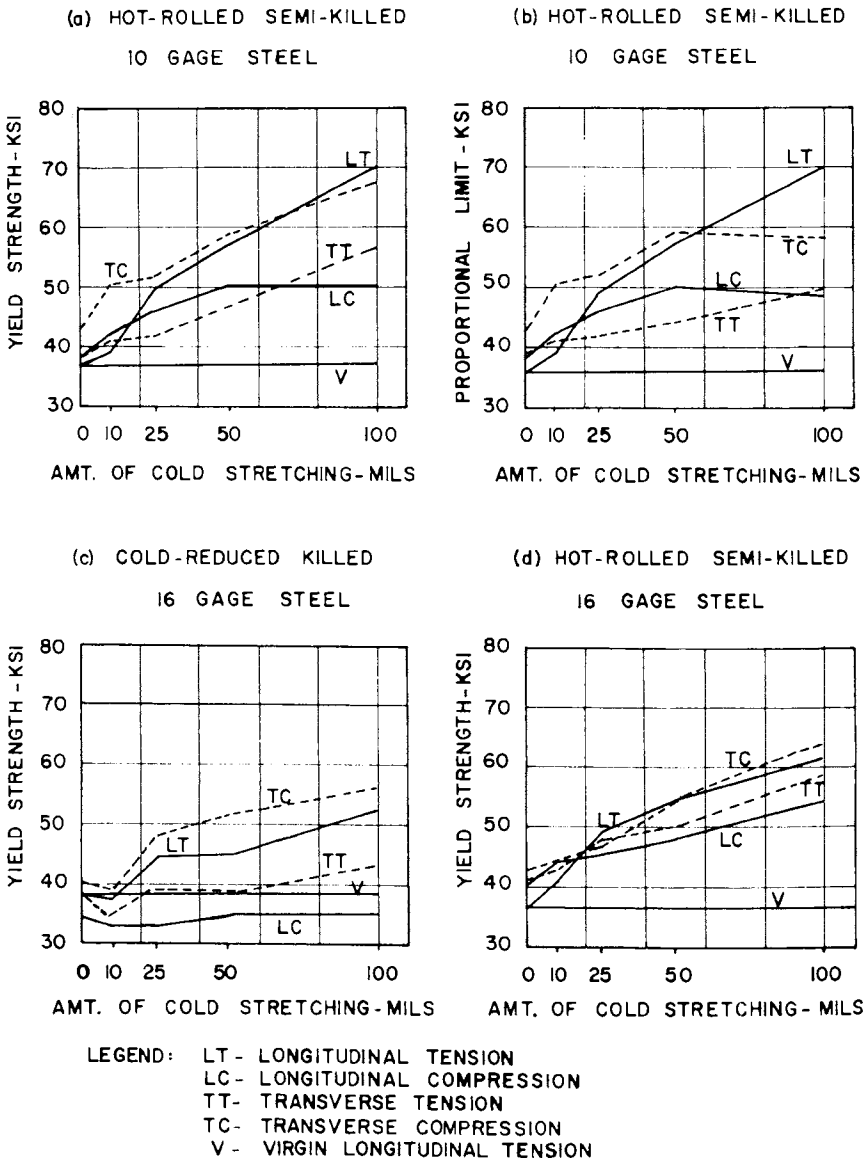

Fig. 3. Directional effect of cold stretching on yield strength and proportional limit.

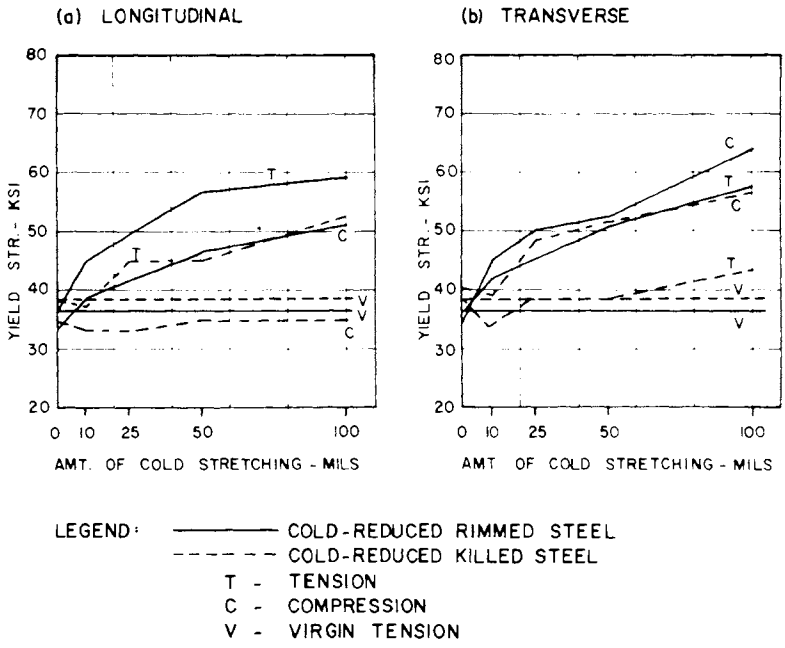

Fig. 4. Effect of cold stretching on yield strength of two different 16-gage steels: cold reduced killed steel and cold reduced rimmed steel.

It follows that if the same cold forming operation is performed on two steels of the same thickness and virgin strength but of different metallurgical characteristics, the effective structural properties of the shaped members are apt to be different. In order to make economical use of the increases in strength resulting from cold forming, it seems therefore essential to maintain a constant steel quality.

Bauschinger Effect.—A comparison of the results for longitudinal specimens in Fig. 3(a) shows that the increase in yield strength caused by cold stretching is considerably greater in tension than in compression. Fig. 3(a) also indicates that the opposite is true for transverse specimens; that is, the increase in yield strength is larger in compression than in tension. The same observation can be made for each of the steels tested, regardless of whether they were hot rolled or cold reduced, rimmed or killed, as it is evident from Figs. 3 and 4.

These results appear to indicate that the well known Bauschinger effect has an appreciable influence on the mechanical properties in the transverse as well as in the longitudinal direction, but in different ways. In the longitudinal direction, the observations agree with the Bauschinger effect, and as a result,

the yield strength in tension is higher than that in compression following cold stretching. However, in the transverse direction, a reversed Bauschinger effect is observed to exist. That is, the compressive yield strength is greater than the tensile yield strength for the same cold stretched material. Both of these effects are examined in detail subsequently under the subheading "Bauschinger Effect."

Ratio of Ultimate Strength to Yield Strength.—Fig. 5 compares the effect of cold stretching on the longitudinal tensile yield strength of two hot rolled semi-killed steels. Aside from a difference in gages, the only variation in properties in these two materials is a different ratio of ultimate strength to

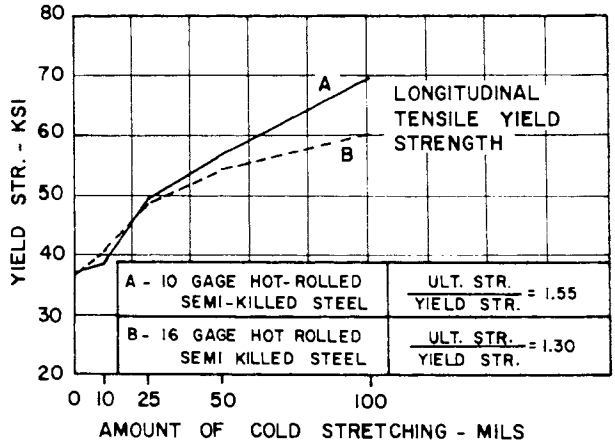

Fig. 5. Effect of ratio of ultimate strength to yield strength on strain hardening.

yield strength. This ratio, in the virgin steel, was 1.55 for the 10-gage material and 1.30 for the 16-gage material. A comparison of the test results for any degree of cold stretching shows that the yield strength increase in longitudinal tension is higher for the 10-gage steel than for the 16-gage material. Thus, the larger the ratio of tensile strength to yield strength in the virgin material, the larger is the amount of strain hardening subsequent to cold stretching.

Aging.—Increases in the yield strength and proportional limit as a result of aging, that is, with passage of time after cold stretching, were observed in all steels tested (see Tables 3 and 4) except for the cold reduced killed steel. The latter steel exhibited no increase in either of these properties as a result of aging.

Fig. 6(a) shows the results of a special test series which indicates the effect of aging subsequent to 50 mils cold stretching, on the longitudinal proportional limit of cold reduced rimmed 16-gage steel. The solid lines indicate the

variation of the proportional limit with time, subsequent to prestretching, whereas the dashed lines give the proportional limit after holding the specimen at 100°C for 30 min. In both tension and compression, the proportional limit is seen to increase quite rapidly during the first week and then much more slowly during the remaining interval. The data plotted in Fig. 6(a) also indicate that the strength obtained as a result of artificial aging is a reasonable approximation of the maximum strength caused by natural aging.

As far as the 0.2% offset yield strength is concerned, Fig. 6(b) indicates that the effect of aging on this property is similar to that on the proportional limit. The only difference appears to be that the proportional limit increases more than the yield strength for any given period of aging.

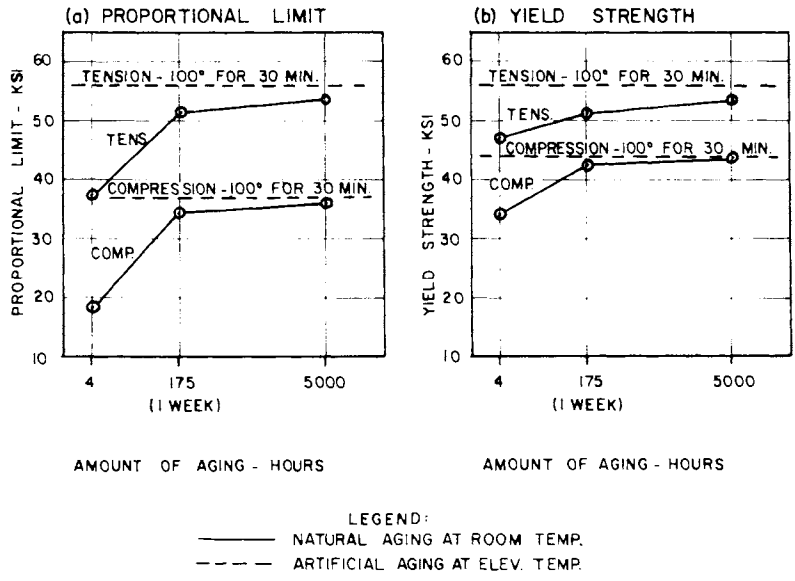

Fig. 6. Effect of aging on yield strength and proportional limit of 16-gage cold reduced rimmed steel after 50 mils of cold stretching.

Fig. 7 depicts the stress-strain relationship to a strain of 0.008 inches per inch for various cold stretched specimens. In each instance, the solid line represents the unaged specimen and the dashed line represents the aged specimen. The term "aged" refers to specimens held at 100°C for 30 min. In those instances where the curve of the aged specimen did not differ materially from that of the unaged one, a single solid curve is used to represent both.

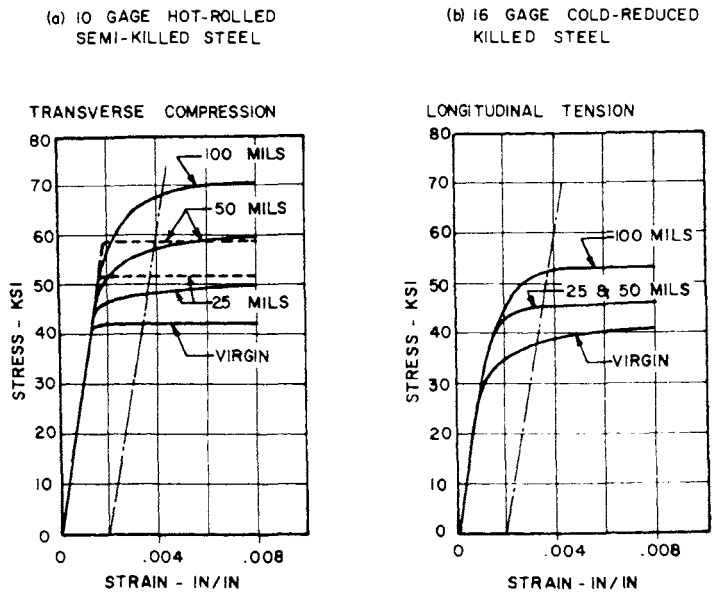

Fig. 7. Effect of aging on shape of stress-strain curve of cold stretching specimens.

In addition to showing the increases in the yield strength and proportional limit, these curves also display the tendency of aging to recover the well defined yield point of mild steel. The curves for 50 mils of prestretching in Fig. 7(a) offer a good comparison between the gradual type of yielding curve obtained shortly after cold stretching and the sharp yielding curve resulting after aging.

The curve for 100 mils in Fig. 7(a) and the curves in Fig. 7(b) demonstrate that not all specimens displayed a recovery of the well defined yield point subsequent to artificial aging. Fig. 7(b) refers to cold reduced killed steel, a material that apparently was not susceptible to aging. There occurred neither an increase in the yield strength or proportional limit, nor a recovery of the well defined yield point for any specimen of this steel.

The other illustration of a failure to recover the yield plateau as a result of aging [Fig. 7(a)] was typical of all hot rolled specimens. For this type of steel, absence of the sharp yielding stress-strain curve subsequent to cold working was limited almost exclusively to transverse specimens with 100 mils of cold stretching. Almost all longitudinal specimens and the transverse specimens with less than 100 mils of cold stretching gave evidence of a return of the yield plateau as a result of aging.

Ultimate Strength.—Fig. 8 indicates the increase in the ultimate strength caused by prior cold stretching. The increase varies directly with the amount of cold stretching and is present in all steels investigated.

As explained previously, the difference between the ultimate strength of the virgin specimen and that of the cold stretched material consists of two parts: The increase in strength per unit mass as a result of cold stretching and the increase in strength because of the decrease in area during prestretching. Of these, only the increase in strength per unit mass should be considered when comparing the ultimate strength of the prestretched specimen with that of the virgin specimen. Table 2 gives reduction factors by which the tabulated values of ultimate strength must be multiplied in order to remove the effect of the reduction in area during cold stretching. For 100 mils, the factor is 0.91.

From the curves in Fig. 8, the increase in the ultimate strength, as a result of 100 mils cold stretching, is seen to be approximately 10% for the cold reduced killed material and approximately 20% for each of the other steels. Applying the correction factor for 100 mils results in reducing the ultimate strength by 9% in each case. If the resulting value of the ultimate strength is now compared with the same property in the virgin material, it is evident that an increase in ultimate strength because of cold stretching exists for all steels except the cold reduced killed steel.

The instantaneous effect of cold work known as strain hardening results in an increase of the yield strength but does not have any effect on the ultimate strength. If an increase in ultimate strength occurs subsequent to cold working, it must be attributed entirely to strain aging (Fig. 13 in the next section of the paper is a pictorial presentation of these concepts). The importance of this distinction lies in the fact that not all steels are susceptible to strain aging, and as a result, cold work does not always result in an increase of ultimate strength.

For the cold reduced killed material, the observation of no increase in ultimate strength as a result of cold stretching agrees with the earlier results pertaining to this steel, namely, that aging did not appear to have any effect on the yield strength, or proportional limit of the material either.

Percentage Elongation.—According to Fig. 9, a marked decrease in the percentage elongation, with increasing amounts of prior cold stretching, was observed in all specimens except killed cold reduced steel. For the latter, a reduction was present, but to a much lesser degree. With this exception, cold stretching to a permanent elongation of 10% (100 mils) was sufficient to lower the percentage elongation from 35% to approximately 12%. These values appear to indicate that strain hardening is not the only factor responsible for the decrease of ductility resulting from cold work. If the percentage elongation were decreased solely as a result of strain hardening, a

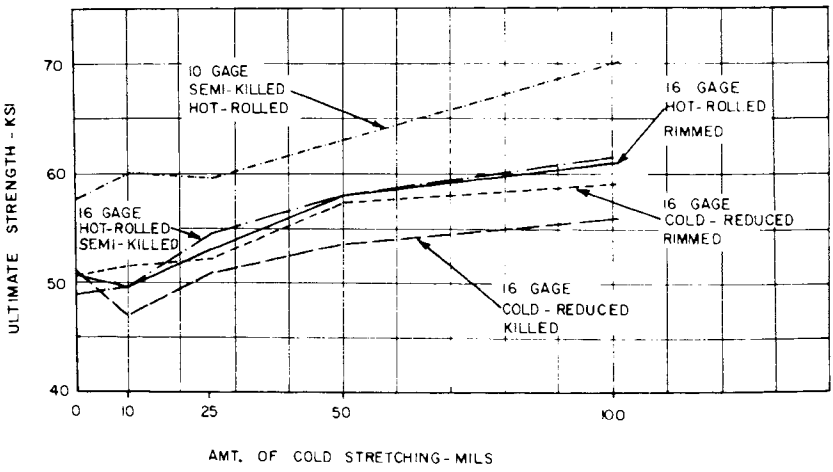

Fig. 8. Effect of cold stretching on ultimate strength.

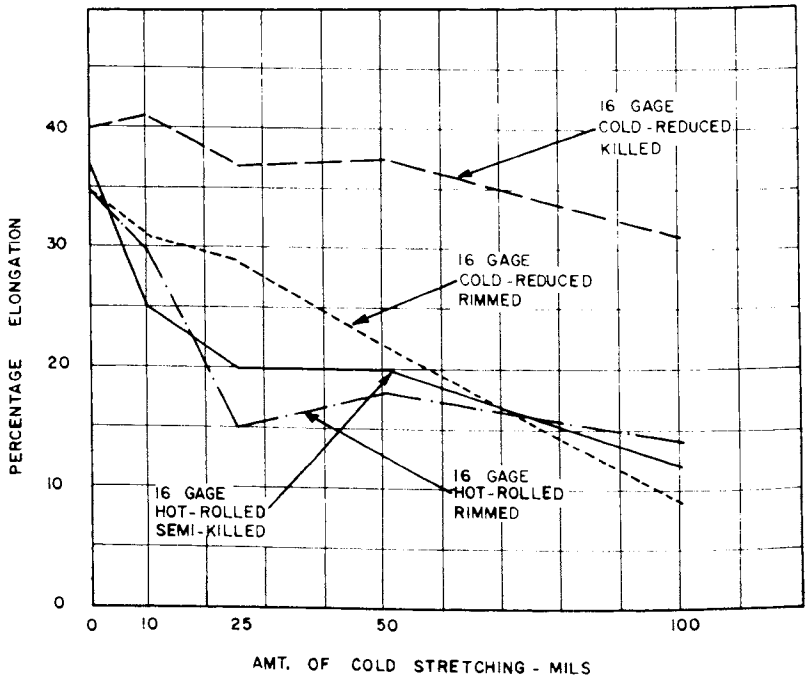

Fig. 9. Effect of cold stretching on percentage elongation

10% plastic elongation would be expected to reduce the over-all elongation by approximately the same 10% instead of the 23% noted previously.

The reduction in percentage elongation, beyond the increment that can be attributed to strain hardening, is believed to be caused by aging. In other words, it is felt that the ductility of a cold stretched specimen is reduced first because of strain hardening, and then an additional amount because of aging. This is illustrated by the behavior of the cold reduced, killed, non-aging steel. For this steel, the observed 9% decrease in elongation after 100 mils of cold stretching (Fig. 9) is near the 10% reduction that can be attributed to strain hardening alone. Because the non-aging characteristic of this material has already been repeatedly demonstrated, it is consistent that the increment of the reduction in ductility caused by aging is absent in this case. In all other cases of aging steel, the total decrease in elongation was significantly larger than the quantity attributable to strain aging. (The reductions in ductility as a result of strain hardening and strain aging are shown subsequently, in Fig. 13.)

Stress-Strain Curves.—Fig. 10 gives tension and compression stress-strain curves for several cases. Only that part of the curve below 0.008 inches per inch strain is given. Each of the curves pertains to a specimen that has been cold stretched and aged artificially at 100°C for 30 min. The gradual yielding curves in Figs. 10(a) and 10(b) are for cold reduced killed steel, a material on which aging had no effect. By comparison, the sharp yielding curves in Figs. 10(c) and 10(d) are for hot rolled rimmed steel and hot rolled semi-killed steel, both of which were susceptible to the aging. Figs. 10(a), 10(c), and 10(d) are for longitudinal specimens. In each case, a comparison of the tensile and compressive curve gives evidence of the presence of the Bauschinger effect. The inverse Bauschinger effect in the transverse direction is illustrated in Fig. 10(b), which compares two transverse specimens.

These curves offer a good example of the radical effect that a change in the steel or direction of the applied stress can have on the shape and position of the stress-strain curve.

DISCUSSION OF THEORETICAL BACKGROUND AND EXPERIMENTAL RESULTS

Plastic Deformation.—Yielding in crystalline materials is the result of slip in which two adjacent planes of atoms slide with respect to one another causing a permanent displacement of one section of the crystal relative to the other (Fig. 11). Considering the type of movement involved, it is evident that shearing stress causes slip. Because of the presence of imperfections in the crystal lattice, known as dislocations, the stress required to initiate yielding is

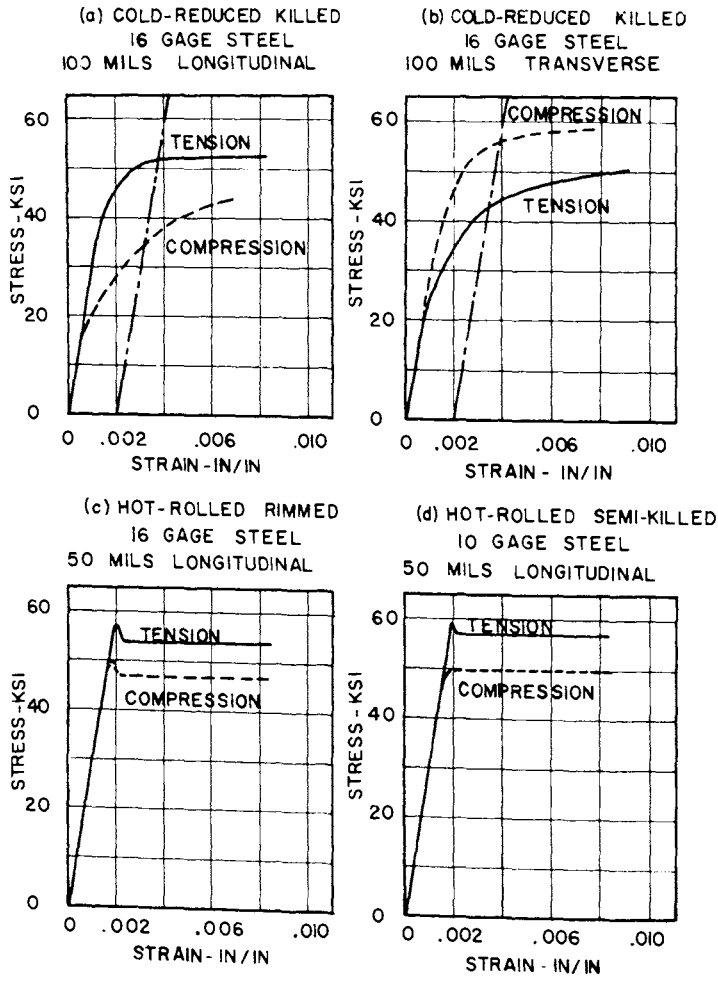

Fig. 10. Typical stress-strain curves of cold stretched specimens.

smaller by several orders of magnitude than that which would be necessary in order to overcome the interatomic bonds in a perfect crystal.

At a dislocation several atoms are pushed out of their ordinary lattice position by an extra plane of atoms in one section of the crystal (Fig. 12). The travel of such a dislocation through the crystal, as a result of an applied shear stress, causes a slip of one atomic distance. Instead of having to overcome every bond along an entire slip plane, simultaneously, which would be necessary to cause slip in a perfect crystal, dislocations make it possible to overcome these bonds successively, one at a time. Furthermore, the strained

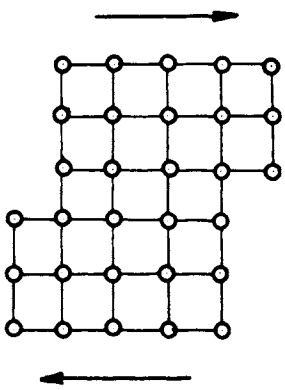

Fig. 11. Slip.

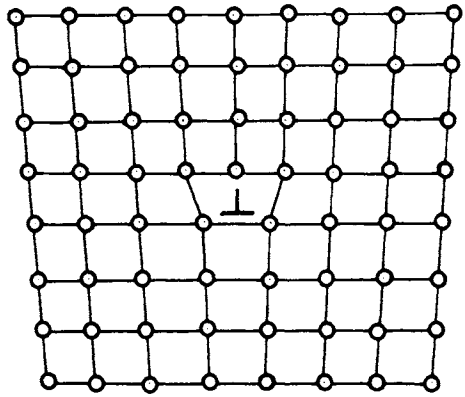

Fig. 12. Line dislocation.

lattice in the vicinity of the dislocation results in a bond that is less stable and therefore easier to break than the ordinary interatomic bond. The actual yielding process is the result of the motion of thousands of dislocations similar to the one described previously.

A specific shear stress is required to move dislocations in a given direction on any specific plane in a crystal. Most metals have certain crystallographic planes along which a minimum stress is required to initiate motion. These planes of easy slip are usually the ones along which the atoms are most closely spaced. Their exact location, for any particular material, depends on the lattice structure of the crystal.

This rather simple process of yielding, as a result of slip, becomes complex in a polycrystalline material consisting of numerous small crystals oriented at random. The direction of easiest slip will be different for every crystal as a result of the random manner in which the crystals are oriented. On application of an external load, the direction of maximum shear stress in the specimen will coincide with the preferred slip planes in some crystals but not in others, resulting in so-called weakly and strongly oriented crystals. Yielding will then begin, at a relatively low stress, in a few weakly oriented crystals and gradually spread to the more favorably oriented ones as the stress increases. This results in a gradual yielding process, an example of which is the deformation of aluminum.

Certain metals, of which mild steel is the most important, do not yield in this gradual manner. Instead, there is apparently no yielding to a relatively high stress, after which yielding commences rather abruptly. A simple explanation of discontinuous yielding in mild steel, based on the presence of

foreign atoms (such as nitrogen, oxygen, or carbon) has been offered by A. H. Cottrell.[6] Even at ordinary room temperatures, the atoms of a solid crystalline structure have sufficient thermal energy to allow them to move about in the lattice. This atomic motion in a solid is called diffusion. There is usually a tendency for things to move from an unstable state of high energy to a more stable condition, represented by less excess energy. In a lattice, any imperfection such as a vacant space, a dislocation, or a foreign atom occupying an interstitial position between several other atoms, constitutes a state of excess energy. In an attempt to bring about a more stable configuration, interstitial foreign atoms migrate to vacant spaces at dislocations. These foreign atoms surround the dislocation and form an "atmosphere" which restricts the mobility of the dislocation. If most of the dislocations in a material are thus anchored by "atmospheres," no yielding can occur until the applied stress is high enough to tear the dislocations away from their atmospheres. Because a dislocation without an atmosphere is at a higher energy level than one with an atmosphere, less strain energy need be added to produce motion of the free dislocation than the one surrounded by an atmosphere. The stress required in order to move a dislocation once it has been freed from its atmosphere is therefore less than that required to set it free. This gives rise to the well-known phenomenon of the upper and lower yield point, and to the discontinuous shape of the stress-strain curve in mild steel.

Another factor that influences the character of slip in a polycrystalline material is the presence of grain boundaries. Because of the difference in orientation of adjacent crystals, boundaries are regions of atomic disorder. The distortion of the lattice in this area gives rise to an excess quantity of strain energy, as a result of which impurity atoms congregate. These foreign atoms, as well as the distorted structure, form a barrier against the movement of the dislocations across crystal boundaries. The stress sufficient to move dislocations along a slip plane in the undistorted crystal lattice is not large enough to push them past the obstacles presented by the grain boundary, with the result that the dislocations pile up in this area.

Strain Hardening.—As a mild steel specimen is strained beyond the yield plateau, an increasing stress is required to produce further deformation. The region of the stress-strain curve representative of this type of yielding, that is, increasing stress with increasing plastic deformation, lies between the yield plateau and the ultimate strength and is known as the strain hardening range. Curve C in Fig. 13 represents the stress-strain curve of a specimen previously

6 "Dislocation Theory of Yielding and Strain Aging of Iron," by A. H. Cottrell and B. A. Bilby, Proceedings of the Physical Society, Vol. 64, 1951.

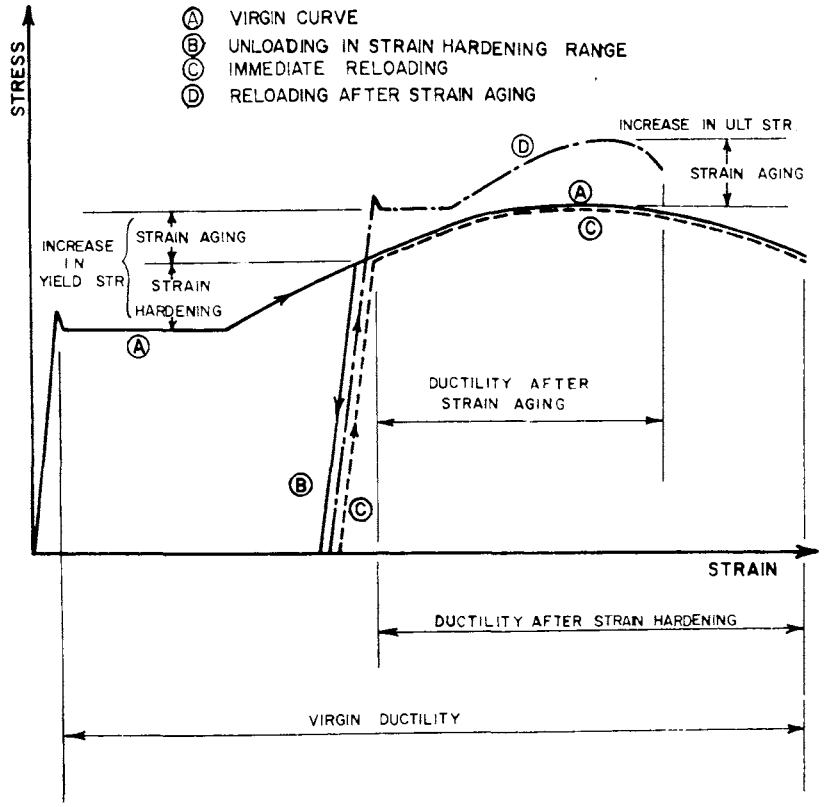

Fig. 13. Effects of strain hardening and strain aging on stress-strain characteristics of structural steel.

loaded into the strain hardening range and unloaded along curve B. If this curve, typical of a strain hardened specimen, is compared with curve A for the virgin material, it is evident that strain hardening increases the proportional limit and decreases the ductility of the material.

In the section on plastic deformation, it was indicated that slip will be restrained whenever the mobility of dislocations is impeded by obstacles such as grain boundaries. The latter produce a pile-up of dislocations which in turn puts additional restraints on the yielding process. Fig. 12 shows that the spacing between atoms is less than normal on one side of the dislocation and greater on the other. This results in the existence of compressive and tensile

stresses, above and below a dislocation. As dislocations pile up at crystal boundaries or other obstacles, the stress pattern that surrounds each dislocation gives rise to an interaction between adjacent dislocations. Opposite dislocations attract each other, combine, and cancel one another, whereas similar dislocations repel each other. Both of these processes cause strain hardening, one by removing two dislocations, and the other by creating resistence to motion.

Strain hardening can also be the result of multiple slip in a cubic lattice structure.[7] In this case, dislocations originating on intersecting planes interact with one another at the intersection producing a combined immobilized dislocation.

Strain Aging.—If a mild steel specimen is plastically stretched and a period of time is allowed to elapse before reloading, a further increase in the tensile yield strength occurs, beyond that which results from strain hardening. This is known as strain aging. Another aspect of strain aging in mild steel is the recovery of a well defined yield plateau. As indicated by curve C in Fig. 13, a specimen that is reloaded immediately after having been cold stretched begins to strain harden as soon as the proportional limit is exceeded. There is no yielding at constant stress in this case. The aged specimen, represented by curve D, exhibits both the previously mentioned increase in the yield strength as well as the sharp yielding type of stress-strain curve typical of virgin mild steel.

A comparison of curve D for the aged specimen with curve A for the virgin material and with curve C representing strain hardening alone illustrates two more effects of strain aging, namely, an increase in the ultimate strength and a further reduction in ductility beyond that already present in the strain hardening specimen.

As was indicated previously, yielding in mild steel occurs subsequent to the dislocations having been freed from their "atmospheres." If enough time is allowed to lapse following this disengagement, the foreign atoms will again diffuse to the vicinity of the dislocations, with the accompanying return of a sharp yield point. Although this theory appears to give a satisfactory explanation of the recovery of a yield plateau and the ensuing increase in the yield strength, it does not explain the significant increase in the ultimate strength and the decrease in ductility, beyond that resulting from strain hardening, that were observed in this investigation.

---

[7] "Modern Concepts of Flow and Fracture," by E. R. Parker, Transactions, ASM, Vol. 50, 1958.

Both of these effects could be attributed to the presence of a precipitate. The latter need not necessarily be similar to that produced during precipitation hardening in nonferrous metals such as aluminum. In fact, G. V. Smith[8] noted several characteristics of precipitation hardening that are definitely absent in strain aging.

Since the addition of thermal energy increases the diffusion rate of foreign atoms, it is evident that the aging process can be expedited by an increase in temperature. Aging at elevated temperatures is known as artificial aging, in contrast to natural aging at room temperature. As the temperature is increased, a point (about 250°C) is reached beyond which, instead of continually increasing, the yield strength begins to decrease. This decrease is caused by the relaxation of the initially distorted lattice resulting from increased atomic mobility at elevated temperatures.

The time that must lapse after cold working in order to attain the maximum yield strength depends on the temperature at which the material is being aged and on the specific steel under consideration. In general, however, the greatest part of the increase in strength appears to occur in the first two weeks at room temperature or in 30 min at 100°C [Fig. 6(b)]. Klöppel,[9] in a similar series of tests, indicates 10 to 15 days at room temperature as being sufficient to attain the maximum strength.

Both Smith[8] and Klöppel[9] give indication of a decrease in the yield strength and tensile strength with further lapse of time beyond the attainment of the maximum strength. Klöppel noted drops in yield strength after 500 hr at room temperature of as much as 25% of the prior gain due to strain aging, whereas Smith records similar decreases ranging from 30% to 60% after aging for 10^4 hr at 75°F. The results obtained in the present investigation were all similar to that shown in Fig. 14, that is, no decrease in the yield strength was noted after aging for 5,000 hr at room temperature. It is apparent from the foregoing that the exact aging characteristics depend on the specific type of steel used.

One of the observations made during the investigation [Fig. 7(a)] is the absence of the yield point recovery in some of the transverse specimens. Several other investigators[8,10] have indicated similar results. Smith,[8] having

---

8 "The Effect of Time and Temperature on Various Mechanical Properties during Strain Aging of Normalized Low Carbon Steels," by F. Garofalo and G. V. Smith, Transactions, ASM, Vol. 47, 1955.

9 "Versuche mit Kaltgereckten Stählen," by K. Klöppel and R. Schardt, Der Stahlbau, Vol. 30, No. 7, July, 1961.

10 "Effect of Direction of Rolling, Direction of Straining, and Aging on the Mechanical Properties of a Mild Steel Plate," by C. F. Tipper, Journal of the Iron and Steel Institute, October, 1952.

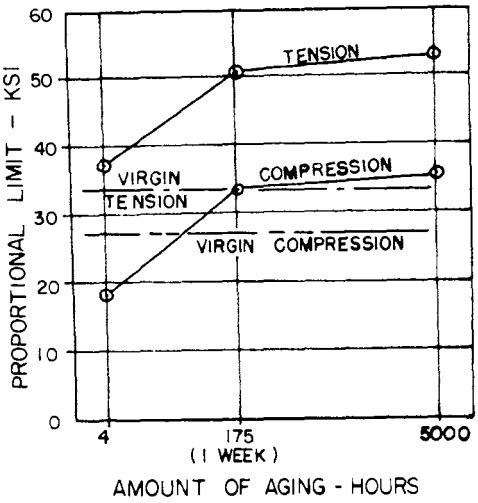

Fig. 14. Effect of aging on longitudinal proportional limit of 16-gage cold reduced rimmed steel after 50 mils of cold stretching.

gone somewhat deeper into the matter, was able to show that steels with no recovery of sharp yielding after 9,000 hr at room temperature did exhibit such a recovery after being aged for an additional 100 hr at 230°C. According to the results observed in the present investigation, it always appeared to be the transverse specimens with the maximum amount of prior cold stretching that did not recover the well defined yield point.

The Bauschinger Effect.—The phenomenon that results in an increase in the proportional limit and yield strength by reloading a plastically deformed specimen in the same direction, (tension after prestretching), or in a decrease by reloading it in the opposite direction (compression after prestretching), is known as the Bauschinger effect. The same principle applies regardless of whether the initial deformation is extension, compression, or twisting.

Because aging causes an increase in the compressive as well as tensile yield strength, the full Bauschinger effect, as described, can only be observed immediately after prestraining or in non-aging steels. The majority of tests of this investigation, having been performed several days after prestretching, include the effects of at least some natural aging. As a result, the Bauschinger effect manifested itself merely as a difference between the increase of the tensile and compressive yield strength instead of the familiar drop of one and increase of the other. The superposition of aging on the Bauschinger effect is

clearly evident in the curves of Fig. 14, which describe the variation of the proportional limit of a specimen cold stretched to 50 mils with increasing time subsequent to cold working. After 4 hr at room temperature, the proportional limit in compression is well below the value for the virgin material. With passing time, this property is seen to increase until after a week, it exceeds its virgin value. The proportional limit in tension also increases because of aging and, as expected, is always more than its virgin value and more than the proportional limit in compression. These curves appear to substantiate the concept that aging transforms the Bauschinger effect from the absolute concept described in textbooks, which includes weakening as well as strengthening, to a relative effect where both properties increase, but by different amounts.

Specimens tested in a direction transverse to that of prior cold stretching display an increase in the compressive yield strength that is greater than the corresponding increase in the transverse tensile yield strength. In other words, there exists an "Inverse Bauschinger Effect" in the transverse direction. Actually, a specimen stretched inelastically in one direction, if free to deform laterally, will receive a permanent transverse compressive strain simultaneously with the longitudinal plastic extension. Viewed in this manner, a transverse specimen from a cold stretched plate behaves similarly to a longitudinal cold compressed specimen and shows the appropriate ordinary Bauschinger effect. Similar results have been obtained by several other authors.[10,11]

Hoff and Fisher,[11] in a rather extensive investigation including precompressed as well as prestretched specimens, obtained the same results regarding the inversion of the Bauschinger effect at 90° from the direction of prestraining as were obtained in the present investigation. Furthermore, by letting the axis of testing assume various orientations between the longitudinal and transverse direction, they were able to show that no Bauschinger effect exists for the direction along which the plastic prestrain was zero. These results appear to substantiate the supposition that the Bauschinger effect depends on the type of deformation in the direction of subsequent loading to which the specimen has been subjected.

The Bauschinger effect in a polycrystalline material is a complex phenomenon not fully understood. Based on present knowledge, it can be examined in two stages—the action of a single crystal and the interaction of several crystals in a polycrystalline specimen. The behavior of a single crystal is illustrated in Fig. 15, which depicts a crystal of which the only active slip planes lie at 45° to the axis of prestretching. During prestretching, the shear stress along these

11 "Beobachtungen über den Bauschinger–Effekt an weichen und mittelharten Stählen," by von H. Hoff and G. Fischer, Stahl und Eisen, Vol. 78, No. 19, September 18, 1958.

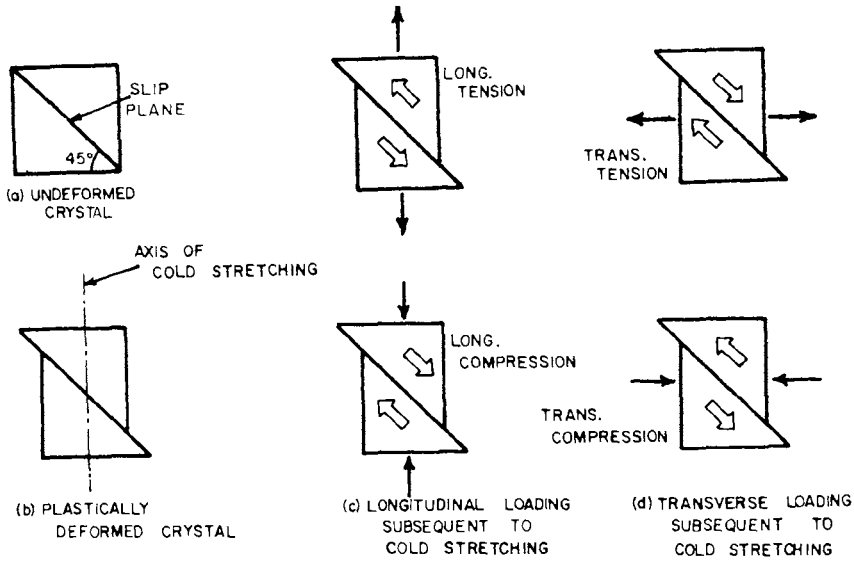

Fig. 15. Bauschinger effect in single crystals.

planes causes dislocations to move and eventually pile up in the vicinity of barriers. Opposite dislocations cancel one another when brought into close proximity, leaving only those of the same sign which repel each other. These dislocations, which are being prevented by the barrier and their mutual repulsion from moving in the direction of preceding slip, are free to move in the opposite direction should the applied stress be reversed. Because of the repulsive interaction, a smaller stress will be required to move the dislocations in the reversed direction than the stress originally necessary to initiate motion. This means that the proportional limit and the yield strength have been lowered. This is the Bauschinger effect in the longitudinal direction. Experimental evidence of the presence of the Bauschinger effect in single crystals has been gathered by several investigators.[7,12]

If a load is applied to the same plastically deformed crystal, but in a direction transverse to that of prior cold stretching, slip will occur on substantially the same 45° planes on which slip had occurred and dislocations had been piled up during the prior cold stretching. If the transverse load is compressive, it tends to promote further slip in the direction of the prior slip

12 "Versuche an Messing Einkristallen," by von G. Sachs and H. Shoji, Zeitschrift fur Physik, Vol. 45, 1927.

during cold stretching. It is for this direction that the described dislocation effects have produced strain hardening. Consequently, while in the longitudinal direction, a "softening" was produced for subsequent compression stresses, in the transverse direction, strain hardening was produced for subsequent compression stresses. Conversely, for transverse tension stresses that tend to reverse the direction of slip from what it had been during cold stretching, "strain softening" is being produced, whereas for longitudinal tension stresses that produced slip in the same direction as that which had occurred during cold stretching, strain hardening had been produced. This is the reverse Bauschinger effect.

Superimposed on this single crystal effect is the interaction of adjacent grains in a polycrystalline aggregate. The residual stresses developed as a result of the interaction of strongly and weakly oriented crystals in a polycrystalline specimen are believed to be at least partly responsible for the Bauschinger effect in bulk material. Weakly oriented crystals will tend to yield at a stress well below the yield strength of the entire specimen. They are prevented from deforming freely, however, by the more strongly oriented crystals that surround them. A simplified model of a crystal assembly illustrating this principle is presented in Appendix I. The model gives a semi-qualitative picture of the Bauschinger effect in the transverse as well as in the longitudinal direction.

SUMMARY AND CONCLUSIONS

The stress-strain characteristics of five types of structural mild carbon sheet steel have been investigated for four degrees of uniform cold stretching. These characteristics were observed in the longitudinal and the transverse direction for tension and compression. The results are recorded in Tables 3 and 4 and reviewed in the section entitled "Test Results."

The changes in the mechanical properties, brought about by cold work are considered as being caused mainly by three phenomena: Strain hardening, the Bauschinger effect, and strain aging.

The following are the specific conclusions that can be drawn from this investigation.

1. Uniform cold stretching in one direction has a pronounced effect on the mechanical properties of the material, not only in the direction of stretching but also in the direction normal to it.
2. Regardless of the direction of testing, increases in the yield strength and ultimate strength as well as decreases in ductility were always found to be approximately proportional to the amount of prior cold stretching.

3. A comparison of the yield strength in tension with that in compression indicates the presence of the familiar Bauschinger effect in the longitudinal direction and the existence of a less familiar inverse Bauschinger effect in the transverse direction. The fact that uniform plastic stretching in one direction causes inelastic compressive strains in the direction normal to that of stretching affords a qualitative explanation of the inverse Bauschinger effect.
4. A comparison of two steels with different ratios of ultimate strength to yield strength indicates that the larger this ratio the larger is the effect of strain hardening. As a result, two steels with the same yield strength but different ultimate strength, will react in a different manner to the same amount of cold work.
5. Aging at room temperature for one to two weeks, or at 100°C for a much shorter period of time, subsequent to cold stretching, results in marked increases in the proportional limit, the yield strength, and the ultimate strength. These increases occur in tension as well as compression in both the longitudinal and the transverse direction. They were observed to occur in every steel tested, except for the cold reduced killed steel.
6. Two other effects of aging on the mechanical properties of mild steel, subsequent to cold stretching, are a reduction in ductility and a conversion of the stress-strain curve from gradual to sharp yielding. Both of these effects were observed in every steel tested except for the cold reduced killed steel. Several transverse specimens with 100 mils of cold stretching coming from the four steels that gave all other indications of being susceptible to aging did not indicate a recovery of the well defined yield point.
7. Whereas the increase in the yield strength and the recovery of a well defined yield plateau due to aging can be satisfactorily explained by Cotrell's theory of "atmospheres," the increase in ultimate strength and the decrease in ductility that were also observed to be a consequence of aging give rise to the belief that some type of precipitate may form during aging.
8. A comparison of the results for the different types of steel investigated indicates that the increase in yield strength and ultimate strength due to cold working is much greater for the hot rolled steels and the cold reduced rimmed material than for the cold reduced killed steel. This is mainly attributed to the non-aging characteristic of the killed steel. The absence of aging in the cold reduced killed steel is also responsible for a much smaller loss of ductility as a result of cold stretching.

As a general conclusion, it is evident that various types of mild structural carbon sheet steels (approximately the same yield strength, ultimate strength, and ductility, but of different processes of manufacture) react in markedly

different ways to the same amount of cold work. Likewise, a given amount of cold work may have markedly different effects on the properties in tension as compared to those in compression and on those in the longitudinal as compared to the transverse direction. Finally, of two steels with the same yield strength but different tensile strengths, the one with the higher tensile strength will undergo more strain hardening because of cold work. This leads to the conclusion that in order to utilize the increased strength of cold formed light gage structural shapes the type, grade, and quality of the steel and the amount and kind of cold work performed should be closely controlled.

APPENDIX I.—BAUSCHINGER EFFECT MODEL

In a crystalline material, such as any ductile metal, there are two phases to the Bauschinger effect. One of them, the Bauschinger effect in the individual, constituent crystals, has already been described herein. The other occurs as a result of the interaction of differently oriented, neighboring crystals in the bulk material, particularly if the individual crystal shows preferred planes of slip. This second phase will be illustrated by the behavior of a model.

Let blocks A, B, and A [Fig. 16(a)] represent three adjacent crystals, located in a prismatical bar, as shown in Fig. 16(b). Subject to the tension forces, P, the bar undergoes a uniform unit elongation, ϵ in the z direction, and uniform unit contraction, $\mu\epsilon$ in the x and y directions. That is, the axial force P results in a stress σ_z acting on the face a-b-f-e whereas σ_y and σ_x on the faces b-c-g-f and a-d-b-c are zero.

A single crystal begins to yield when the component of the applied shear stress in a certain direction along one of the planes of slip reaches a critical value. It is assumed in the model that the orientation of the preferred slip planes is different in crystal B from those in crystals A, as shown in Fig. 16(c). If a tension stress σ_z is applied to each of the crystals A and B, the maximum shear stress occurs at 45° to the z direction. Thus, the shear stress along the plane of easiest slip will be larger for crystal B than for crystal A. Crystal B will therefore yield under the application of a smaller tension stress σ_z and will be referred to as an unfavorably oriented crystal when compared to A. It is evident that crystals that are unfavorably oriented for resisting slip resulting from stress applied in the z direction are likewise unfavorably oriented for resisting slip caused by a stress in the y direction.

The model, therefore, consists of an unfavorably oriented crystal, B, between two favorably oriented crystals, A. It is assumed that as a result of mutual restraint, the two crystals A will not be able to deform independently

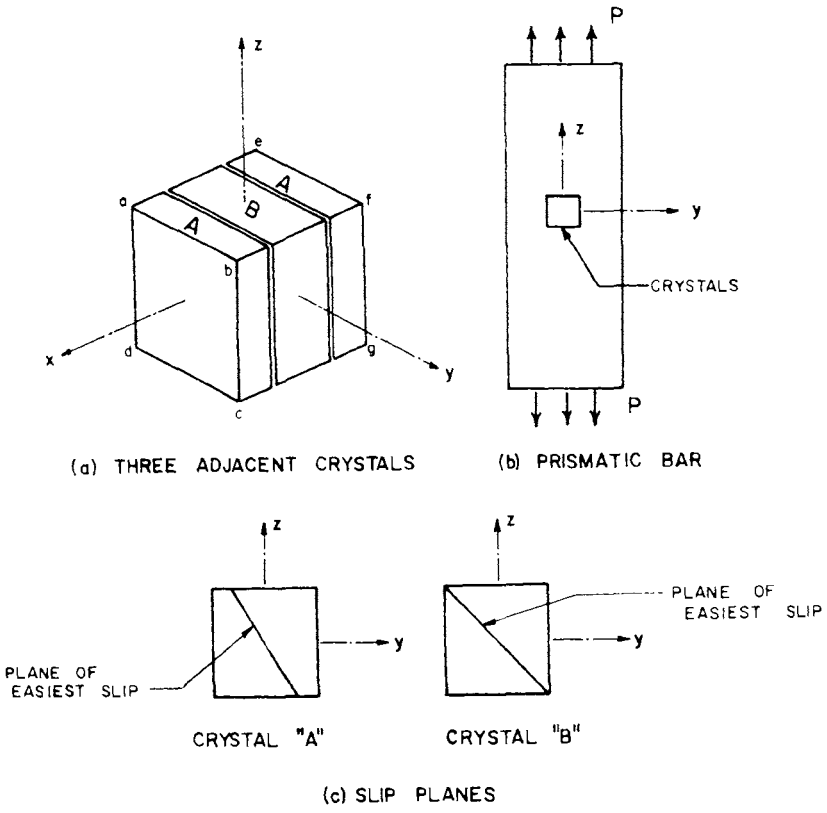

Fig. 16. Bauschinger effect model.

of crystal B. This means that in the bulk material, the planes d-c-g-h, a-b-f-e, b-c-g-f, and a-d-h-e remain plane during deformation. As long as all crystals are stressed in the elastic range, plane sections remain plane as a direct consequence of the state of homogeneous deformation assumed earlier. It is only after the yield strength has been exceeded that the mutual restraining action of crystals A and B is responsible for keeping the sections plane during deformation. The physical and geometrical properties listed in Table 5 are assumed for the three crystals.

The stresses and strains created in the individual crystals by the load P are tabulated in Table 6 for several load increments.

All crystals behave elastically to P = 120 kips. At P = 120 kips, crystal B has reached its yield point, whereas crystal A has not. As the load is increased to more than 120 kips, crystal A continues to deform elastically with increasing stress. Crystal B, however, is in the plastic range and deforms without an

Table 5.

	Crystal A Favorably oriented	Crystal B Unfavorably oriented
Area^{a}_{z}	1 sq in.	2 sq in.
Area^{a}_{y}	1 sq in.	2 sq in.
$(\text{Yield Str.})^{a}_{z}$	70 Ksi	30 Ksi
$(\text{Yield Str.})^{a}_{y}$	70 Ksi	30 Ksi

[a] The subscript always refers to the normal of the plane in question.
In addition to the above, both crystals have the following properties: $E = 30 \times 10^6$ psi, $\mu = 0.3$ in the elastic range, and $\mu = 0.5$ in the inelastic range.

Table 6. Stresses and Strains In Individual Crystals

	σ_z, in kips per square inch	ϵ_z, in inches per inch	$\sigma^{1\,a}_{y}$	ϵ_y
1) P = 120 Kips				
A	+ 30	+ 0.001	0	- 0.0003
B	+ 30	+ 0.001	0	- 0.0003
2) P = 180 Kips				
A	+ 60	+ 0.002	- 3	- 0.0007
B	+ 30	+ 0.002	+ 3	- 0.0007
3) P = 60 Kips				
A	+ 30	+ 0.001	- 3	- 0.0004
B	0	+ 0.001	+ 3	- 0.0004
4) P = 0				
A	+ 15	+ 0.0005	- 3	- 0.00025
B	- 15	+ 0.0005	+ 3	- 0.00025

[a] σ^{1}_{y} is the internal stress that exists only as a result of the interaction among the three crystals. There is, of course, no external stress in the y-direction.

increase in stress. When P = 180 kips, the following situation exists. The 60-kips increase beyond 120 kips has all been absorbed by the A crystals, and because they are still elastic, their stress σ_z and strain ϵ_z are easily determined. The stress σ_z, for crystal B has remained constant at the yield stress, and the requirement that sections d-c-g-h and a-b-f-e remain plane results in crystal B having the same ϵ_z as crystal A. Turning now to the y direction, it is evident that $\mu = 0.3$ for the elastic crystal A while the plastic crystal B has $\mu = 0.5$. If, as the load is increased from 120 kips to 180 kips, crystals A and B were free to contract independently of each other, crystal B would contract more than crystal A. Continuity in the bulk material requires, however, that sections a-d-h-e and b-c-g-f remain plane, so that the A crystals prevent the B crystals

from contracting more than the A crystals. As a result, crystal B is put into transverse tension and crystals A into transverse compression. The stresses and strains in the y direction are determined from the deformation compatibility requirement and from the assumption that no net external stress σ_y acts on the free body determined by the three crystals; they are entered in Table 6.

As load is removed, all crystals unload elastically. Because crystals A and B are beginning with different longitudinal stresses and because external equilibrium must prevail at P = 0, crystal A has a residual tension ($+ \sigma_z$) equal to the residual compression ($- \sigma_z$) in crystal B when the entire load has been removed. During the unloading process $\mu = 0.3$ for all crystals, and as a result, there is no tendency of one to deform relative to the other in the y direction. The transverse stresses (σ_y) that were present at P = 180 kips are therefore still acting when P = 0.

The load deformation curve for the three crystals acting as a unit is shown in Fig. 17. Point 1 indicates the load at which crystal B becomes inelastic and is the proportional limit of the entire assembly. Unloading begins at point 2 and continues elastically to point 3 representing zero applied load. At this point, permanent deformations exist as well as residual stresses in both the longitudinal and transverse directions of the model, caused by the cold stretching of the bar.

The effect of the residual stresses in the z direction (tension in crystal A and compression in crystal B) on the level of the longitudinal proportional limit of the model during subsequent loading will now be considered. Reloading in tension in the z direction occurs along the dashed line 3–2. For this direction, the residual compression stress in the unfavorably oriented crystal B causes this crystal to yield, that is, the proportional limit to occur, at point 2. In other words, yielding now begins at a load P which is higher than that during the initial loading. Conversely, if longitudinal compression is applied after cold stretching, the residual compression stresses cause crystal B to yield, that is, the proportional limit to occur at point 4, a load numerically smaller than that corresponding to the virgin proportional limit. (The virgin stress-strain curve in compression, 5–6–7 in Fig. 17, is assumed to be identical with that in tension.) This illustrates the contribution of the intercrystalline residual stresses to bhe Bauschinger effect in the longitudinal direction.

The values in Table 6 indicate that residual stresses also exist in the y direction. These are opposite in sign and smaller in magnitude than those in the x direction. If the bar is loaded in the y direction after having been cold stretched in the z direction, the proportional limit during this second loading will again be affected by a set of residual stresses resulting from the prior plastic deformation. Because the sign of the residual stresses in the y direction

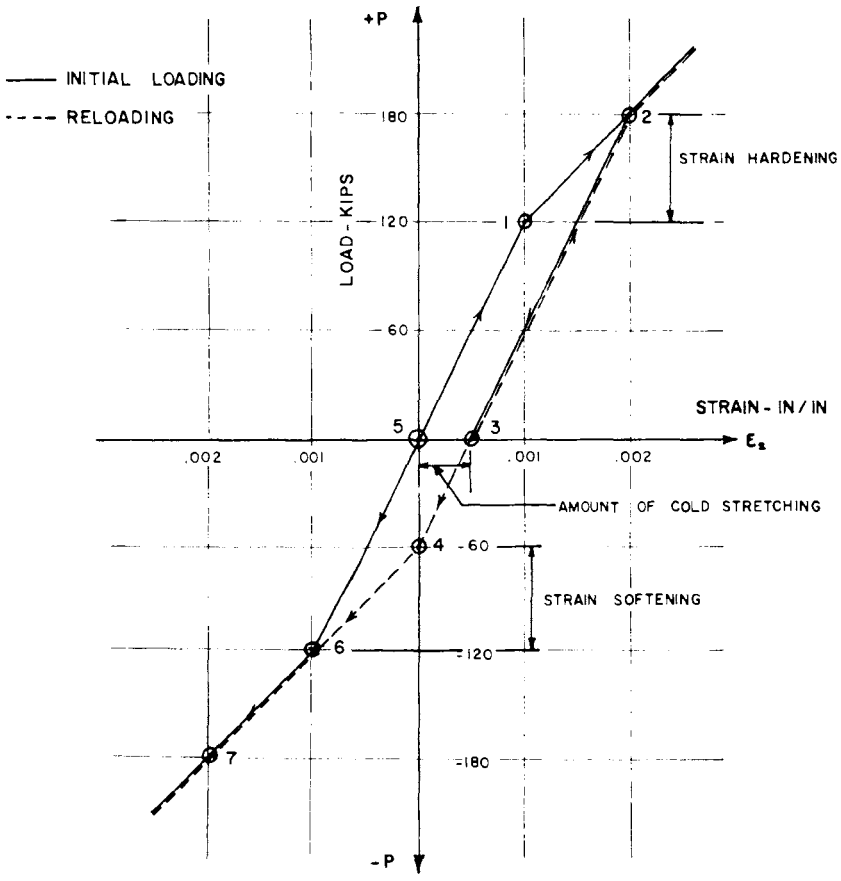

Fig. 17. Load deformation curve for Bauschinger effect model.

is opposite that in the z direction, reloading transverse to the direction of prior stretching will now cause an increase in the elastic range for compression and a decrease in the elastic range for tension. This is the inverse Bauschinger effect in the transverse direction. If the two effects, longitudinal and transverse, are regarded as being related to the previous inelastic deformation in the respective directions, the same Bauschinger effect, though different in intensity, is found to be present in both directions. This is so because a bar plastically stretched in the z direction has in effect been plastically compressed in the y direction, although to a lesser degree.

The foregoing is only a model, which depicts certain experimentally observed phenomena on the basis of interaction between favorably and unfavorably oriented crystals. It is not a complete portrayal of the actual

complex intercrystalline behavior found in bulk materials. Also, it is probable that the behavior described by this model is more pronounced in metals of which the single crystals exhibit stronger directionality in strength properties than steel.

The actual Bauschinger effect is a superposition of the effect occurring in single crystals and described in the body of the paper, and of the crystal interaction of which the foregoing model gives a simplified presentation.

ACKNOWLEDGMENTS

This investigation is part of a continuing research undertaking concerning light gage, cold-formed steel structures, sponsored at Cornell University by the American Iron and Steel Institute. The sponsorship is within the province of the Committee on Building Research and Technology, AISI.; of its Light Gage Steel Subcommittee, Tappan Collins, Chairman; and of W. G. Kirkland, Chief of Engineering Division and Assistant Vice-President, AISI. The unfailing cooperation on the part of the sponsoring organization is gratefully acknowledged.

The advice and comments of George V. Smith and Malcolm S. Burton, Professors of Metallurgical Engineering at Cornell University, Ithaca, N. Y., have been most helpful and are sincerely appreciated. The writers wish to express their appreciation to Imre A. Kovach, mechanician, for his valuable contributions to the experimental work.

EFFECTS OF COLD-STRAINING ON STRUCTURAL SHEET STEELS[a]

Discussion by S. T. Rolfe

S.T. ROLFE,[13] A. M. ASCE.—Some interesting observations concerning the effects of cold-straining on the mechanical properties of mild steel have been presented. Differences that can exist in the mechanical properties of materials before and after fabrication may be significant and the designer should be aware of such changes.

According to the authors, an "inverse Bauschinger effect" existed for specimens oriented transverse to the direction of cold stretching. That is, a permanent compressive strain existed in the transverse direction because of the particular specimen geometry and, as noted in Fig. 3, caused an increase in the transverse compressive yield strengths (TC) above those of the transverse tensile yield strengths (TT). The rise in all properties above the original undeformed values was explained by strain aging. Nevertheless, a significant difference in compressive and tensile properties existed and was referred to as the "inverse Bauschinger effect" by the authors.

Preliminary results of an investigation at United States Steel Corporation's Applied Research Laboratory offer further information on the effect of state-of-stress during cold deformation on the Bauschinger effect and other changes in mechanical properties of cold-deformed material.

Three HY-80 (United States Navy Specification for all 80,000 psi minimum yield strength quenched and tempered alloy steel) steel plates, 2-1/2 in. thick, 36 in. wide, and 60 in. long, were cold-formed to different radii to obtain material cold-deformed to large values of surface strain. Duplicate 0.252-in. diameter tensile and 0.40-in. diameter compressive specimens (longitudinal and transverse to the direction of cold deformation) were machined from material near the surfaces of the three formed plates to obtain specimens having different amounts of cold deformation in bending. Thus, these specimens had a strain gradient across the test section. In additon, material from an undeformed part of the plates was axially deformed various amounts in tension or compression to obtain material for specimens (longitudinal only) having a uniform cold deformation (no strain gradient across

[a] April 1963, by Alexander Chajes, S. J. Britvec, and George Winter (Proc. Paper 3477).

[13] Applied Research Lab., United States Steel Corporation, Monroeville, Pennsylvania.

the test section). Results of tests on the above-mentioned specimens were compared with values from test specimens machined from an undeformed part of the plates.

Results of tests on specimens oriented transverse to the direction of cold deformation showed that regardless of the direction of cold deformation (tension of compression) both the tensile and compressive yield strengths were increased. Because of the plane strain condition that existed during bending of the wide plates, the transverse strain was zero. Therefore, no Bauschinger effect was observed in either transverse tensile or compressive tests. However, the cold deformation perpendicular to the transverse specimens strain-hardened the material so that increased yield strengths (tensile and compressive) were observed for both tensile and compressive longitudinal cold deformation. For material cold-deformed in simple tension and free to contract laterally (thus, subjected to permanent transverse compressive strains), the "inverse Bauschinger effect" should exist because of the particular state-of-stress, as observed by the authors.

For specimens oriented in the same direction (longitudinal) as the cold deformation, a larger Bauschinger effect existed for axially deformed material than for material cold-deformed by bending, even though the magnitudes of the cold deformation were similar. This behavior was attributed to the micro-residual stress distribution resulting from the difference in the state-of-stress during cold deformation by axial or bending loads. The axially deformed specimens were machined from 1/2 in. by 1-in. bars that were not restrained laterally during cold deformation whereas the specimens from the material deformed by bending were machined from material at the top surface of wide plates which was restrained laterally during cold deformation. Thus, the axially deformed specimens were cold-deformed under uniaxial stress conditions whereas the specimens from the material deformed by bending were cold-deformed under conditions of plane strain.

The Bauschinger effect is attributed to the residual compressive stress existing in individual grains after tensile yielding (or vice versa), i.e., micro-residual stresses. This residual compressive stress leads to a premature yielding when the material is tested in compression (for material originally yielded in tension). Thus, if a condition of biaxial stress existed (as would be the case in highly restrained material such as 2-1/2-in.-thick by 36-in.-wide plates), the component of residual compressive stress (in the testing direction) within the individual grains of the bent plates would be less than in grains of uniaxially strained material. Therefore, it would be expected that the maximum Bauschinger effect should occur under conditions of uniaxial stress (axial deformation) and a lower Bauschinger effect occur under conditions of biaxial stress (cold deformation in bending of wide plates).

The significance of these results is that the apparent loss in yield strength in actual structural members because of the Bauschinger effect should not be as great as would be expected based on tests of uniaxially prestrained material. Furthermore, since actual structures generally are not composed of simple unrestrained elements but rather of large restrained members (which deform under conditions approaching plane strain), a "plane strain tension test" (rather than standard 0.252-diameter tension tests) might be more representative of the actual strain distribution during deformation of structures. Thus, the apparent loss in yield strength because of the Bauschinger effect would probably be even less in "plane strain tension tests."

The statement was made by the authors that "The phenomenon that results in an increase in the proportional limit and yield strength by reloading a plastically deformed specimen in the same direction, (tension after prestretching), or in a decrease by reloading it in the opposite direction (compression after prestretching), is known as the Bauschinger effect."

The generally accepted concept of the Bauschinger effect is a lowering in yield strength caused by yielding in the opposite direction of testing whereas strain hardening is generally believed to be responsible for an increase in yield strength following yielding in the same direction. However, the Bauschinger effect is defined in the ASM Metals Handbook as follows: "Bauschinger effect. Usually refers to the phenomenon by which plastic deformation of a polycrystalline metal, caused by stress applied in one direction, reduces the yield strength where the stress is applied in the opposite direction. Sometimes used in a broad sense to include all changes in the stress-strain characteristics of both single and polycrystalline metals that may be ascribed to changes in the microscopic stress distribution within the metals, as distinguished from those caused by strain hardening."

It would be helpful if the authors could expand on this definition as related to their test results, especially because there appears to be some question as to whether strain hardening or the Bauschinger effect is responsible for increasing the yield strength of material previously cold-deformed in the same direction as tested.

EFFECTS OF COLD-STRAINING ON STRUCTURAL SHEET STEELS[a]

Discussion by W. Carl Anderson

W. CARL ANDERSON,[14] M. ASCE.—As properly noted, the investigation by the authors is confined to cold tension, stretched material of 16 gage and 10 gage of killed, semikilled, and rimmed steel. Experience and observations of thousands of tests lead the writer to remark that there are variances within the classes and gages described that may be greater than those differences between the classes, as observed by a few random tests. The variations, all of which are manifested by the final metallurgy of the steel, would be caused by the following:

1. Variances in chemistry of the steel. These would depend on carbon, manganese, sulphur, phosphorous, silicon, and the traces of nickel, chromium, etc., introduced by either the raw materials or the scrap.
2. Freezing rates and size of ingots in the molds.
3. Rolling temperatures, speed of rolling, and amount of reduction at the various stands, including the amount of water at the various stands.
4. Specific handling of the sheets after rolling, and size of coil, rate of cooling in coil, or if cooled in cut sheets, etc.
5. Cold treatment in mill, such as roller levelling, stretcher handling, temper pass on cold rolled anneal, etc.
6. The gage of the material, as already noted.

Undoubtedly, there are other variables, and the writer does not wish to pose as an expert in the field of steel production. There are many experts in this field, in general agreement about cause and effect, but they are concerned mainly with the problem of producing the steel at an ever increased demand on economy, quality, and quick delivery to the customer in time to meet the customer's increasing demands for prompt delivery. In general, the steel metallurgists are not structural engineers and have not looked for specific effects noted by the authors. Thus, it is the writer's opinion that a broad statistical approach must be made before any general statements can be legitimate. This does not detract from the value of the work of the authors on certain specific samples.

[a] April 1963, by Alexander Chajes, S. J. Britvec, and George Winter (Proc. Paper 3477).

[14] Chf. Research and Development Engr., The Union Metal Mfg. Co., Canton, Ohio.

Cold straining need not result from stretching (as performed by the authors) or bending, as mentioned previously. Cold straining can also be accomplished by peening, local rolling, and other methods, some of which may alter greatly the physical (or, more properly termed, mechanical) properties of the steel. In at least one case, the steel may have its yield strength increased by over 60% and, at the same time, have its bonding properties unharmed or even improved, as shown in Figs. 18 and 19. In the process being examined, the steel is cold-formed to a cylindrical shape, seam welded, and then cold-rolled longitudinally by simultaneous gang rolls fitting the contour of the cylinder, over a hard mandrel that fits the inside of the cylinder. The cylinder may have various degrees of taper. Wall thicknesses may vary from 12 gage to 5/16 in.; lengths may extend to 40 ft, and O.D.'s to 24 in.

With destructive tests, it is impossible to observe the same square inch of steel before and after this process; however, with a large number of observations, adequate statistical conclusions can be made. The following shows typical values and statistics of certain steels of different gages and general class of steel production.

The photo-micrographs (Figs. 20 through 27) demonstrate the lack of any great disturbance in the grain structure of the steel. The electron photo-micrographs (Figs. 28 and 29) show radial disturbance caused by this cold work. The statistical curve in Fig. 30 is for 7 gage SAE 1015 hot-rolled, semikilled steel, after processing. The samples with photo-micrographs are of 11 gage and 5/16 in. of the above SAE 1015 steel. Details of the illustrations are shown in Table 7.

The photo-micrographs are at 100 diameters and the electron photo-micrographs are at 65,000 decimeters.

The photomicrographs of the cold bend are of the following chemistry and physical characteristics after processing. Bend test specimen had been tensile tested prior to bending (see Table 8).

Fig. 30 shows 131 samples plotted in steps of 1,000 psi and shows the statistical values of cold working process. Details are not given, although this steel, prior to working, had a yield strength of 34,000 psi to 39,000 psi. Average thickness reduction was approximately 1%.

Fig. 18. Sample No. 539.

Fig. 19. Sample No. 558.

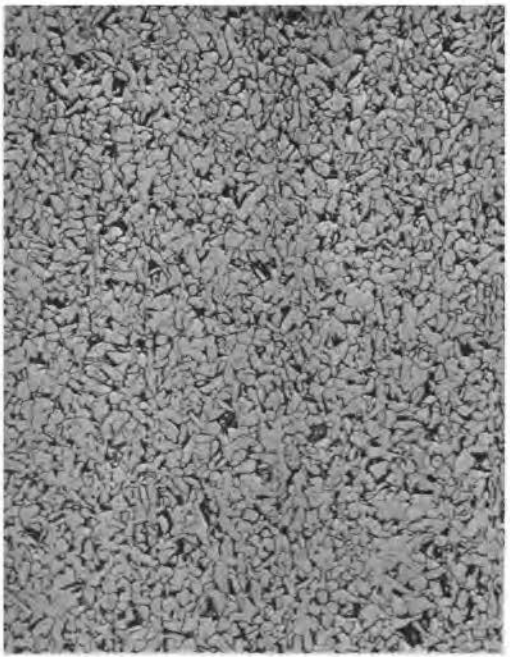

Fig. 20. Sample No. 676b (transverse): before process.

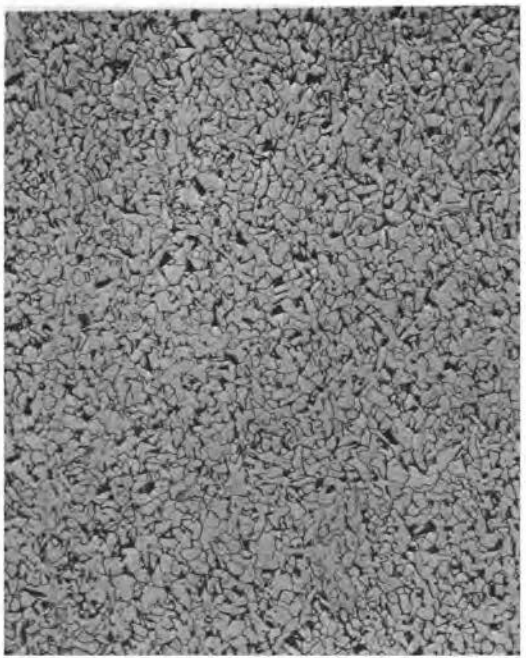

Fig. 21. Sample No. 677b (transverse): after process.

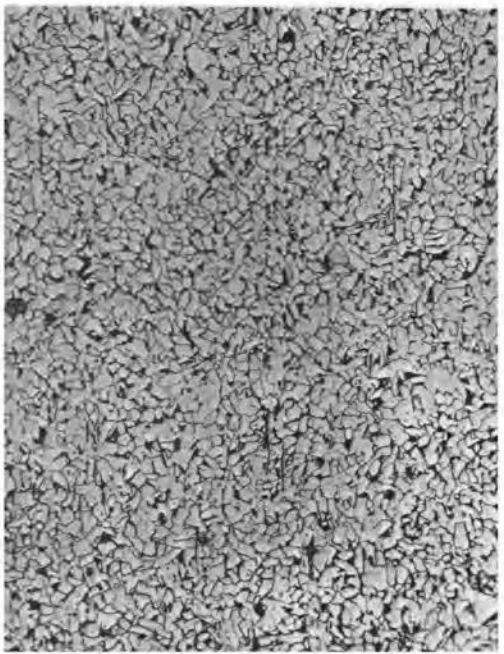

Fig. 22. Sample No. 676b (longitudinal): before process.

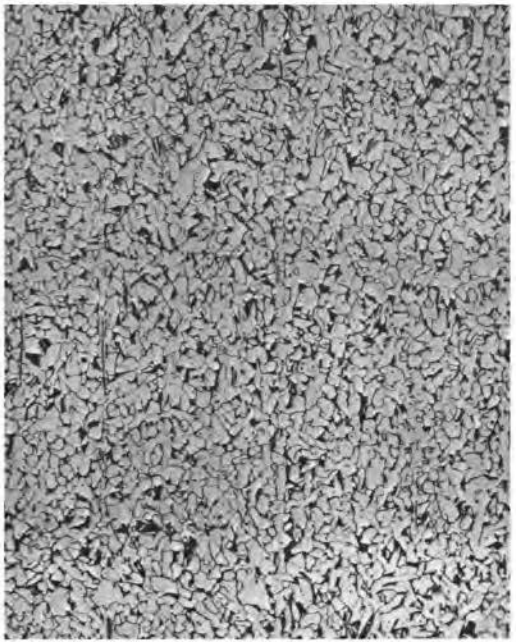

Fig. 23. Sample No. 677b (longitudinal): after process.

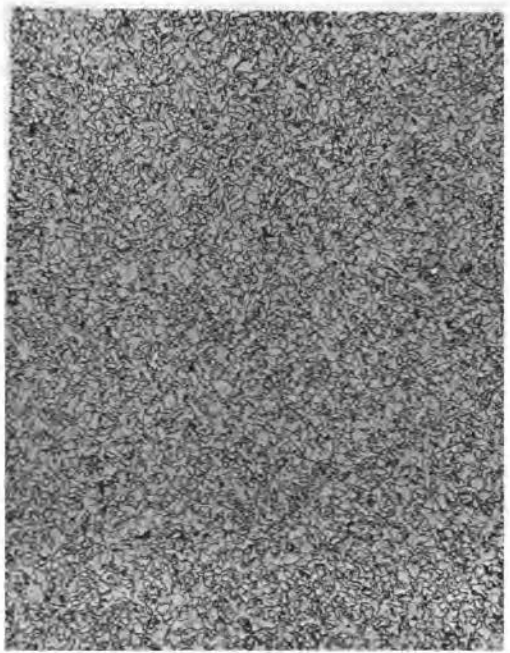

Fig. 24. Sample No. 680b (transverse): before process.

Fig. 25. Sample No. 681b (transverse): after process.

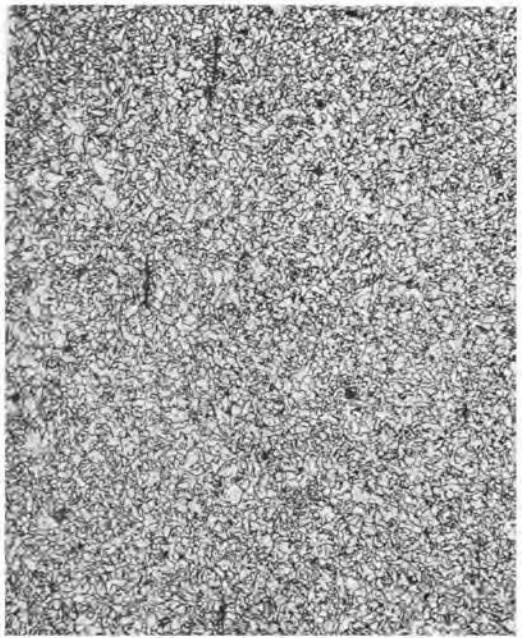

Fig. 26. Sample No. 680b (longitudinal): before process.

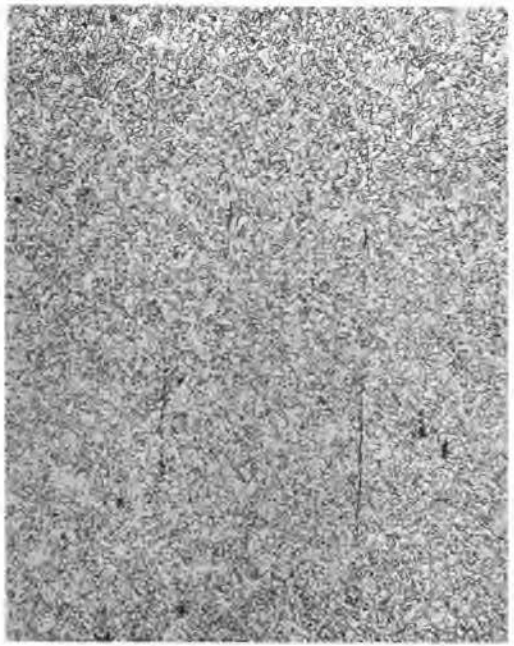

Fig. 27. Sample No. 681b (longitudinal): after process.

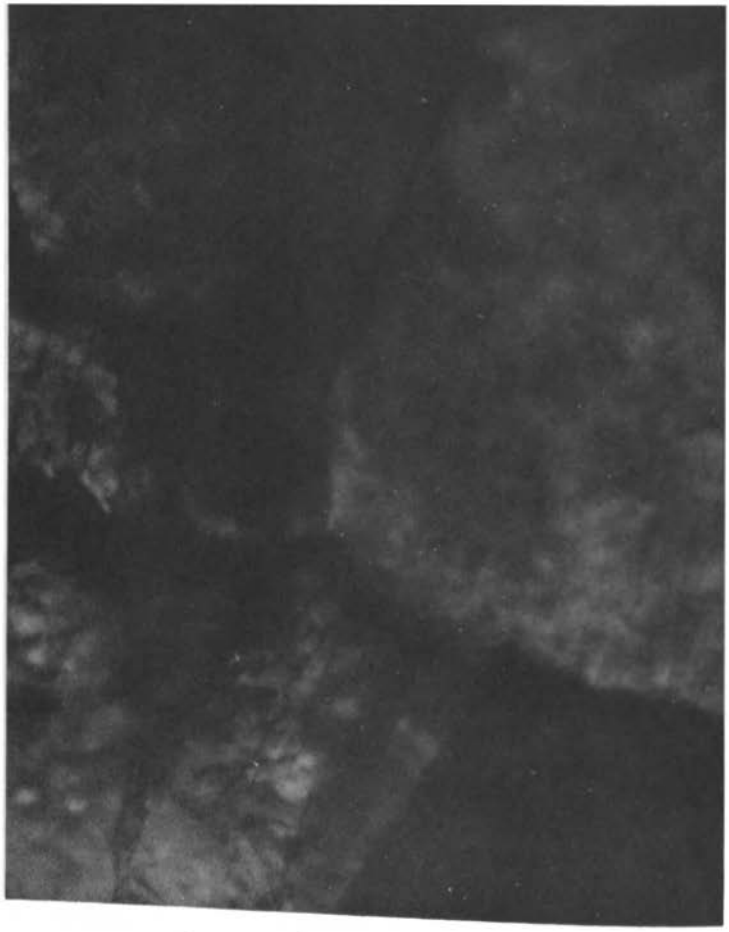

Fig. 28. Sample No. 1690b: before process (65,000 electron micrograph).

Fig. 29. Sample No. 1693e: after process.

Table 7. Details Of Illustrations

Sample Number	676B	677B	680B	681B	1690B	1693B
Heat Number	4210423	4210423	4210615	4210615	420018	420018
Chemistry, ladle or check	Ladle	Ladle	Ladle	Ladle	Check	Check
Carbon	0.18	0.18	0.16	0.16	0.146	0.146
Manganese	0.52	0.52	0.43	0.43	0.53	0.53
Silicon	0.03	0.03	0.03	0.03	0.07	0.07
Sulphur	0.033	0.033	0.029	0.029	0.028	0.028
Phosphorus	0.012	0.012	0.012	0.012	0.012	0.012
Aluminum	0.02	0.02			0.008	0.008
Physicals: before or after spec. cold work	Before	After	Before	After	Before	After
Gage or thickness	5/16 in.	5/16 in.	11 Ga.	11 Ga.	7 Ga.	7 Ga.
Number cold cylindrical passes	--	27	--	11	--	11
Yield 0.005 in. per in.	43,400	56,200	38,650	60,400	52,000	67,900
Magnifications	100X	100X	100X	100X	65,000X	65,000X

Table 8

Band Test Number	539	558
Thickness, in inches	5/16	5/16
Type Steel	Semi-killed	Semi-killed
(a) Ladle Analysis		
C	0.16	0.13
Mn	0.42	0.40
Si	0.04	0.02
Ph	0.010	0.013
Sul	0.029	0.30
(b) Properties from Mill Report		
Yield, in psi	38,100	36,300
Tensile, in psi	60,300	59,000
Elongation	28%	29%
(c) Properties after Cold Work		
Yield, in psi	64,000	59,700
Tensile,[a] in psi	70,700	68,550
Elongation[a]	16.5%	20.7%
Bend flat test	OK	OK

[a] Specimens are rough surfaced and do not show elongation and tensile as high as warranted with smoother specimens.

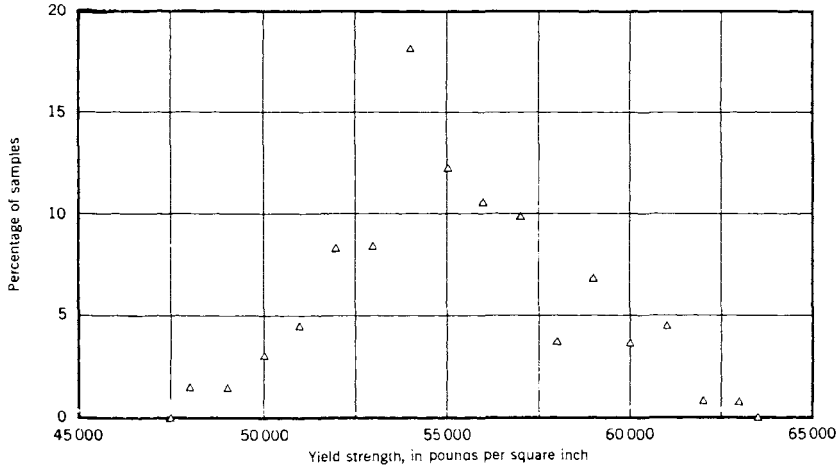

Fig. 30. Yield strength versus frequency.

EFFECTS OF COLD-STRAINING ON STRUCTURAL SHEET STEELS[a]

Closure by Alexander Chajes, S. J. Britvec, and George Winter

ALEXANDER CHAJES,[15] M. ASCE, S. J. BRITVEC,[16] A. M. ASCE, AND GEORGE WINTER,[17] F. ASCE.—The contribution by S. T. Rolfe is appreciated as providing valuable complementary evidence concerning the effects of cold-straining on mechanical properties of steel.

Rolfe's experimental observations demonstrate the point made by the writers at the end of the Introduction; namely, that results obtained for simple uniaxial stress cannot be applied directly to the more complex stress conditions existing in most actual cold-formed members. An investigation of the complex effects of realistic cold forming operations is in fact being conducted at Cornell University at present. It was felt, however, that such a study should be preceded by an investigation of the basic mechanisms of strain hardening, strain aging, and related phenomena since in the end they are responsible for the effects of cold work, regardless of how simple or complex it may be.

The fact that Rolfe's work refers to a heat treated high strength alloy steel, in contrast to the writers' mild carbon steels, makes the two investigations not directly comparable, but rather emphasizes the complementary character of Rolfe's contribution. Its value would have been considerably enhanced if quantitative data, rather than qualitative descriptions, had been furnished.

Rolfe reported on the effects of cold work produced in the process of bending flat plates to different radii, in contrast to the writers' tests which were concerned with uniform cold stretching. Rolfe noted that the difference between these two types of cold work consists mainly in the fact that in his tests a plane strain situation was obtained which caused zero strains but definite stresses in the direction transverse to that of cold-forming, whereas the writers' uniaxial tests resulted in zero transverse stress, but in definite transverse strain. Rolfe's observation that under such plane strain conditions no Bauschinger effect results in the transverse direction, whereas it does occur in the longitudinal direction, is of considerable general and practical interest.

---

[a] April 1963, by Alexander Chajes, S. J. Britvec, and George Winter (Proc. Paper 3477).

[15] Asst. Prof., Dept. of Civ. Engrg., Univ. of Massachusetts, Amherst, Mass.; formerly, Cornell Univ., Ithaca, N. Y.

[16] Asst. Prof., Dept. of Structural Engrg., Cornell Univ., Ithaca, N. Y.

[17] Prof. and Head, Dept. of Structural Engrg., Cornell Univ., Ithaca, N. Y.

Rolfe's observations are in qualitative agreement with a large body of test evidence obtained at Cornell University since the publication of the paper. This concerns mechanical properties of corners shaped to various radius to thickness ratios from the same five sheet steels described in the paper. It was found that the flexural cold work produced in shaping the corners increased the yield strength in the direction of the corners both in tension and in compression, somewhat more so in the latter than the former. The effect was smallest in the cold reduced killed steel, a fact which again emphasizes the contribution of strain aging to this complex phenomenon.

Rolfe seems to attribute the entire phenomenon of strain hardening and Bauschinger effect to intergranular residual stresses. As was noted and documented in the paper, strain hardening and Bauschinger effect both have been observed and measured in single crystals. In this case intergranular stresses evidently do not exist, and the entire phenomenon is interpreted in terms of dislocation theory. The phenomena observed in polycrystalline material such as steel, as was also noted and documented, appear to be a complex interaction of the effects of dislocation behavior, of intergranular residual stresses as illustrated in Appendix I, and of strain aging.

Rolfe questioned the writers' definition of the Bauschinger effect. Different definitions can be found in different authoritative texts. The reason for these differences is that terms such as strain hardening, Bauschinger effect, and strain aging are broad and general. Instead of referring to specific well defined phenomena, they describe a large number of not too well understood changes in crystalline structure and the effects which these changes have on the mechanical properties of the material. If the word "or" were replaced by "but," the statement would more clearly represent the writers' intention, to wit: "The phenomenon that results in an increase in the proportional limit and yield strength by reloading plastically deformed specimens in the same direction, but in a decrease by reloading it in the opposite direction is known as Bauschinger effect."

Anderson's enumeration of all the variables that occur in steel making, and the few results he presented from a different and somewhat incompletely described process of cold-working do not seem to add significantly to the topic of the paper. It was the aim of this investigation to deal specifically with sheet steels representative of those used for cold-formed structural members, and results seem to show that this has been achieved. The effects of cold work are of considerable interest to industry in a variety of practical situations, and extensive experimental work appears to be underway in industry laboratories. For understandable reasons such investigations are seldom published in full; yet partial and incomplete results rarely contribute to the advancement of general understanding.

CORNER PROPERTIES OF COLD-FORMED STEEL SHAPES[a]

By Kenneth W. Karren,[1] M. ASCE

INTRODUCTION

The various methods of cold-forming, such as roll forming, brake forming, and deep drawing, bring about changes in the mechanical properties of steel sheets and plates. Cold working generally increases yield and ultimate strengths and decreases ductility. The nature of these changes depends on the chemical composition of the steel, its prior metallurgical history, its prior history of cold work, and the type and magnitude of plastic strains caused by the cold work. In a prior phase[2] of this continuing investigation, specimens subjected to a simple type of cold work were tested to provide an understanding of the fundamental effects of cold-straining before attempting to investigate the more complex types of cold work caused by the cold-forming of members. These specimens, subjected to unidirectional permanent tensile prestrains of 10, 25, 50, and 100 mils, were tested in tension and in compression both in and transverse to the direction of prestrain. It was concluded that the changes brought about in the mechanical properties of sheet steels can be attributed to three phenomena: strain hardening, strain aging, and the Bauschinger Effect.

Included herein are the results of the phase of the investigation dealing with cold-formed corners. Empirical plastic stress-strain relationships are established for virgin tensile specimens of nine sheet steels. The plastic strains occurring in cold-formed corners are measured by a photogrid technique and are approximated by somewhat simplified models of plastically deformed corners. These results are used to develop an equation for predicting the yield strength of corners. The resulting analytical corner-yield strength values are found to compare well with test values. The experimental ultimate strength and ductility of corners are also determined for all nine sheet steels used in the investigation.

Note.–Discussion open until July 1, 1967. To extend the closing date one month, a written request must be filed with the Executive Secretary, ASCE. This paper is part of the copyrighted Journal of the Structural Division, Proceedings of the American Society of Civil Engineers, Vol. 93, No. ST1, February, 1967. Manuscript was submitted for review for possible publication on March 8, 1966.

[a] Presented at the January 31–February 4, 1966 ASCE Structural Engrg. Conf., held at Miami Beach, Fla., where it was available as Preprint 301.

[1] Assoc. Prof., Dept. of Civ. Engrg., Brigham Young Univ., Provo, Utah; formerly, Research Asst., Cornell Univ., Ithaca, N.Y.

[2] Chajes, Alexander, Britvec, S. J., and Winter, George, "Effect of Cold-Straining on Structural Steels," Journal of the Structural Division, ASCE, Vol. 89, No. ST2, Proc. Paper 3477, April, 1963, pp. 1–32.

COLD-FORMING METHODS

Light-gage structural members are cold-formed by a variety of methods falling into two main categories: (1) roll-forming and (2) brake forming. Roll-forming is a mass-production process requiring rolling machines with a series of two or more roll stands. As the section passes successive stations in the rolling machine, it is changed by small stages from a flat sheet into the final desired shape. Roll design and the number of roll passes required depend on several factors including the complexity of the shape. Roll design has not been completely reduced to a science, depending considerably on the skill and judgment of the designer. Therefore, it is assumed that the type, amount, and locations of cold work resulting from roll-forming will depend, at least within certain limits, on roll design and on roll wear. However, forming by press brake is a straight bending, semi-manually operated process of more limited production capacity, requiring only a standard set of punches, dies, and tools for most shapes which can be braked. A corner may be either "air" or "coin" press braked, the terms "air" and "coin" being descriptive of what actually happens in the forming process. In coin press braking, both the punch and the die match the final shape desired in the corner, the die having been cut to the same angle as is subtended by the flats of the final formed corner. The piece to be formed is "coined" or bottomed in the die to eliminate springback. For "air" press braking there are a variety of shapes which may be used for the dies. The corner is bent sharper than the desired final angle to allow for springback. Air press braking is illustrated in Fig. 1. Bending progresses from the centerline outward in this type of forming. The curvature is not constant in the final corner, being larger for its middle portion[3] (Fig. 1). At the point where bending is occurring, there is considerable pressure on the inside surface. However, this radial pressure is probably not as large as that which may occur in either the roll-forming or coin press braking operations. The three forming methods used in this investigation were (1) roll-forming, (2) air press braking, and (3) coin press braking.

MATERIALS

The nine carbon steels used in this investigation are listed in Table 1. (The first five of these materials were used in the work of the prior phase on simple unidirectional prestrain.[2]) The table contains the main properties of the virgin materials in their as-rolled state prior to further cold working. Chemical

[3] Sangdahl, G. S., Aul, E. L., and Sachs, G., "An Investigation of the Stress and Strain States Occurring in Rectangular Bars," Proceedings, Soc. for Experimental Stress Analysis, Cambridge, Mass., Vol. 6, No. I.1, 1948.

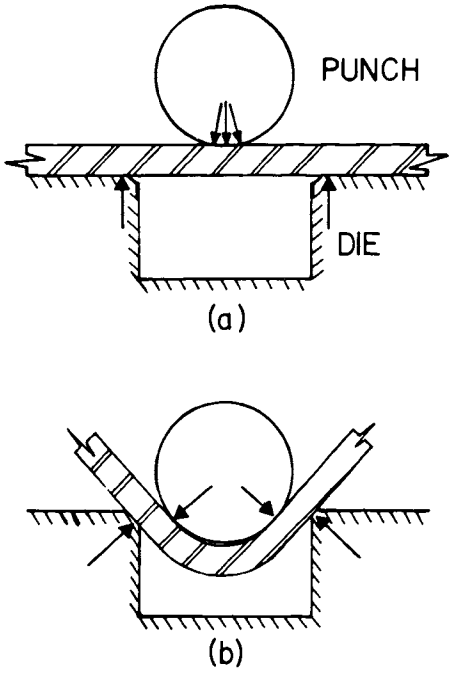

Fig. 1. Air-press braking.

compositions are shown for each steel. Because it was cold-reduced and semikilled, the first virgin material of Table 1 was gradual yielding. The other eight materials were orginally sharp yielding.

The following abbreviations are used herein: CRK–Cold reduced killed, CRR–Cold reduced rimmed, HRSK–Hot rolled semikilled, and HRR–Hot rolled rimmed sheet steel. The abbreviation HRSK10-37.0 is typical of the abbreviations used for the nine sheet steels of this investigation. The 10 indicates that the material is of 10-gage thickness and the 37.0 is the virgin tensile yield strength of the sheet, in kips per square inch, taken in the direction in which the sheet was rolled. The virgin yield strength is defined as that of the material prior to the cold-forming operation. For example, the first eight materials were received in the form of flat sheets. The last material (HRSK9-30.7) was received in a curved condition as it was cut directly from the coil. This was done because it was roll-formed into a joist chord directly from the coil without stretcher-straightening. The procedures used in testing these virgin materials are described below in the section entitled "Tests." Tensile and compressive corner yield strengths were determined experimentally for all nine materials.

Table 1. Material Properties of Test Specimens

Material	Gage	Chemical Composition by Random Check Analysis				Compressive yield strength, in kips per square inch	Tensile Properties			
		C	Mn	S	P		Yield strength, in kips per square inch	Ultimate strength, in kips per square inch	Percentage elongation in 2-inch gage length	$\frac{\sigma_u}{\sigma_y}$
1. Cold Reduced Annealed, Temper-Rolled Killed, Sheet Coil	16	0.15	0.40	0.024	0.008	34.6	38.3	51.1	40	1.34
2. Cold Reduced Annealed, Temper-Rolled Rimmed, Sheet Coil	16	0.09	0.39	0.028	0.008	33.0	36.4	50.7	35	1.39
3. Hot Rolled Semi-Killed Sheet Coil	16	0.04	0.32	0.025	0.008	40.5	37.5	49.0	37	1.31
4. Hot Rolled Rimmed Sheet Coil	16	0.08	0.32	0.045	0.008	40.3	40.5	50.7	35	1.25
5. Hot Rolled Semi-Killed Sheet Coil	10	0.18	0.50	0.029	0.008	38.5	37.0	57.5	36	1.55
6. Hot Rolled Semi-Killed Sheet Coil	16	0.16	0.46	0.024	0.009	37.6	39.7	55.9	35	1.41
7. Hot Rolled Semi-Killed Sheet Coil	10	0.22	0.43	0.024	0.008	43.2	42.8	66.6	31	1.55
8. Hot Rolled Semi-Killed Sheet Coil	16	0.23	0.45	0.025	0.012	39.1	40.7	61.4	31	1.51
9. Hot Rolled Semi-Killed Sheet Coil	9	0.09	0.52	0.033	0.010	32.0	30.7	52.9	35	1.72

ANALYTICAL DETERMINATION OF CORNER YIELD STRENGTH

A method for calculating the tensile yield strength of cold-formed corners is outlined as follows: (1) An empirical function relating uniaxial stress to strain in the plastic range is established from the stress-strain curves of several tensile specimens from each of nine sheet steel materials. (2) It is assumed that such an empirical function is also applicable to certain states of strain other than simple tension. (3) A corner model is assumed to be produced by a simplified system of forces, e.g., by pure flexure only. (4) An equation is established for the circumferential strain at an arbitrary point in a corner in terms of the radius to the point and of the ratio of the inside radius to the

thickness of the corner. The situation in cold-formed corners being that of plane strain, the longitudinal strain component is zero. From the constant volume concept of plasticity it is determined that the third component, the radial strain, is equal and opposite to the circumferential strain when strains are expressed as natural strains. (5) Using the parallel concepts of effective stress and effective strain, the function relating stress to strain (Step 1) is integrated over the full area of the corner to obtain the average yield strength of the corner after cold working.

GENERAL STRAIN HARDENING THEORY

One theory of strain hardening[4,5] may be expressed in the form

$$\bar{\sigma} = F(\bar{\epsilon}) \tag{1}$$

in which $\bar{\sigma}$ = a quantity known variously as the generalized stress, equivalent stress, or effective stress, and which may be determined from the Huber-Mises-Hencky distortion energy yield condition as

$$\bar{\sigma} = \frac{1}{\sqrt{2}} \sqrt{(\sigma_1 - \sigma_2)^2 + (\sigma_2 - \sigma_3)^2 + (\sigma_3 - \sigma_1)^2} \tag{2}$$

in which σ_1, σ_2, and σ_3, are the principal stresses. (For large plastic strains, such as will be considered herein, these principal stresses must be expressed in terms of true stress. True stress is defined as load divided by instantaneous area. However, it is customary and convenient to omit reference to true stresses when dealing with three-dimensional plasticity problems.) Note that for the condition of uniaxial tension, $\bar{\sigma}$ is equal to σ_1', where the prime indicates that the stress is in terms of true stress. The symbol $\bar{\epsilon}$ is a somewhat analogous quantity variously called the generalized strain, equivalent total strain, or effective strain,

$$\bar{\epsilon} = \frac{\sqrt{2}}{3} \sqrt{(\epsilon_1' - \epsilon_2')^2 + (\epsilon_2' - \epsilon_3')^2 + (\epsilon_3' - \epsilon_1')^2} \tag{3}$$

in which ϵ_1', ϵ_2', and ϵ_3' are the natural principal strains. Natural or logarithmic strain, ϵ', is related to engineering strain, ϵ, by

$$\epsilon' = \ln(1 + \epsilon) \tag{4}$$

For the case of uniaxial stress in the plastic range, $\epsilon_2' = \epsilon_3' = -1/2\ \epsilon_1'$. The constant in Eq. 3 is chosen such that substitution of these values of principal

---

[4] Hill, R., The Mathematical Theory of Plasticity, Oxford University Press, London, England, 1950.

[5] Nadai, A., Theory of Flow and Fracture of Solids, Vol. 1, McGraw-Hill Book Co., Inc., New York, N. Y., 1950.

strains gives an effective strain equal to ϵ_1'. In Eq. 1, F is a function depending on the characteristics of the metal involved; and F may be found, for example, from the stress-strain curve of a simple tensile specimen, and is assumed to be valid for other states of stress, subject to some limitations which are enumerated below.

Eq. 1 is subject to the following assumptions: (1) The material is isotropic under plastic conditions; (2) Elastic strains are negligible in comparison with plastic strains; (3) Shearing stresses are responsible for plastic deformations, but normal stresses are not; (4) The ratios of the principal strains remain constant throughout the straining which takes place, i.e., ϵ_2/ϵ_1 and ϵ_3/ϵ_1 remain constant; (5) The principal axes of successive strain increments do not rotate with respect to the element. (6) The tensile and compressive stress-strain curves coincide when expressed in terms of true stress and true strain; (7) No Bauschinger Effect is present in the direction normal to the direction of cold work; and (8) There is no change in volume as a result of plastic deformation. Assumption 8 has been verified to be accurate by a number of investigators. For the large plastic strains occurring in cold-formed corners the elastic strains, Assumption 2, are indeed negligible. Assumptions 4 and 5 are shown below to be true for a somewhat idealized model of a cold-formed corner. Assumption 7 is found below to be reasonable from a theoretical standpoint. Experimental evidence from this investigation and that of S.T. Rolfe[6] also appears to justify the use of this assumption. From results obtained in this investigation it will be shown that the cumulative error caused by these and the remaining assumptions (Nos. 1, 3, and 6) is reasonably small.

REPRESENTATION OF STRAIN HARDENING FUNCTION BY POWER EQUATION

For some metals the strain hardening function, F, of Eq. 1 may be represented in the plastic part of the stress-strain curve by a power function:[5,7,8]

$$\bar{\sigma} = k\,(\bar{\epsilon})^n \tag{5}$$

in which k = the strength coefficient, and n - the strain-hardening exponent. Eq. 5 is possible when a plot of the logarithm of $\bar{\epsilon}$ versus the logarithm of $\bar{\sigma}$ in the plastic domain appears as a straight line, which is the case for many steels

---

[6] Rolfe, S. T., discussion of "Effect of Cold-Straining on Structural Sheet Steels," by Alexander Chajes, S. J. Britvec, and George Winter, Journal of the Structural Division, ASCE, Vol. 89, No. ST5, Proc. Paper 3688, October, 1963.

and some other metals.[7,8] For uniaxial tension, Eq. 5 reduces to $\sigma' = k(\epsilon')^n$ by use of Eqs. 2 and 3. To use this equation, it is first necessary to investigate k and n experimentally.

Tensile Test Procedure.—For determination of plastic stress-strain characteristics, three 15-in.-long tensile specimens were prepared for each of the nine materials of Table 1. These specimens were standard ASTM tensile specimens except that the narrow (1/2-in.-wide) middle part was 9 in. long rather than the standard 3 in. Marks 8 in. apart were accurately punched on the specimens. Dividers were preset to appropriate lengths. When the specimen had elongated such that the distance between punch marks matched the present dividers, the load was read and recorded. The data was converted to true stress and true strain and plotted on log-log paper.

Analysis of Results.—Typical true stress-strain curves are shown in Fig. 2 for the first three materials. Values of k and n obtained from similar true stress-strain curves for each of the nine materials are given in Table 2. Values of k vary from 70 ksi to 114 ksi, and values of n vary from 0.13 to 0.28.

From the nondimensional plot of k/σ_y versus σ_u/σ_y of Fig. 3 it can be seen that the empirical formula

$$k = 2.80\,\sigma_u - 1.55\,\sigma_y \tag{6}$$

gives a good approximation for k, in which, σ_u = the virgin ultimate strength, in kips per square inch, and σ_y = the virgin tensile yield strength, in kips per square inch. From the plot of Fig. 4 where values of n are plotted versus σ_u/σ_y, it can be seen that values of n tend to increase in a general way with increase in the σ_u/σ_y, ratio. These experimental values of n may be approximated by

$$n = 0.225\,\frac{\sigma_u}{\sigma_y} - 0.120 \tag{7}$$

Eqs. 5, 6, and 7 are useful below in deriving equations for predicting the tensile yield strength of cold-formed corners.

PLASTIC STRAINS IN COLD-FORMED CORNERS

Circumferential strains at any point in a cold-formed corner are established for a simplified theoretical model of a corner. The results are compared to experimental evidence obtained by using a photogrid method.

---

[7] Holloman, J. H. "Tensile Deformation," Transactions, AIME, Vol. 162, 1945, pp. 268–290.

[8] Lowe, J., and Garafalo, F., "Precision Determination of Stress-Strain Curves in the Plastic Range," Proceedings, Soc. for Experimental Stress Analysis, Cambridge, Mass., Vol. 4, No. 2, pp. 16–25.

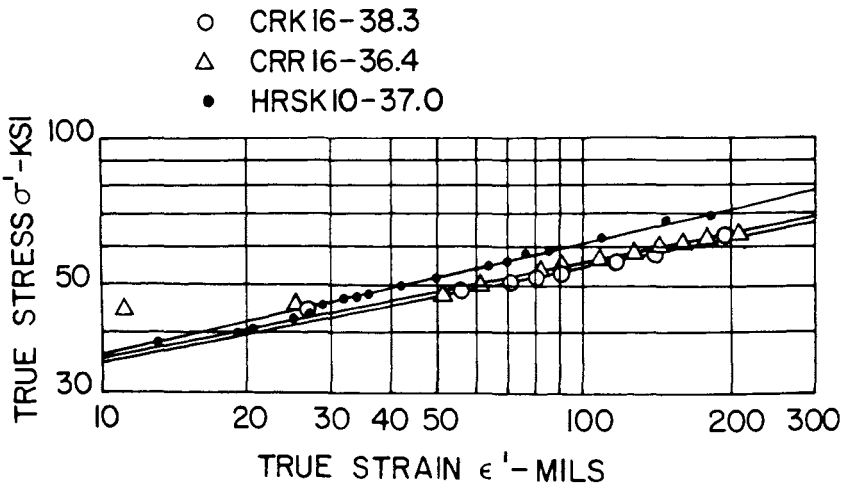

Fig. 2. Tensile stress-strain curves of virgin materials in terms of true stress and true strain.

Theoretical Model.—To attempt an analysis of strains in a corner caused by cold work it is helpful to choose a model[4,9] with a somewhat simpler force system acting on it than actually exists in any of the common methods of cold-forming. Such a model, in which application of a pure bending moment to a wide flat sheet produces a uniform curvature and uniform tangential strain, is shown in Fig. 5. A certain amount of radial pressure is present in die bending in addition to bending moment. In coin press braking and in roll-forming, the metal in the corner is even more highly compressed in the radial direction. Despite these complexities, however, it proves instructive and worthwhile to begin by investigating the simplified model.

It is assumed that sections in the radial direction which are plane before plastic bending remain plane after bending. From symmetry it can be seen that the principal directions for stress and strain will be the radial or r, the tangential or θ, and the longitudinal, or z-directions. The Levy-Mises theory of plastic flow,[4,5,9] in which it is assumed that elastic strains are negligible in comparison to plastic strains, relates the deviator stress tensor to the strain-increment tensor by

$$S' \, d\lambda = dE, \tag{8}$$

in which S' = deviator stress tensor, dE = strain increment tensor, and $d\lambda$ = a scalar factor of proportionality. The first equation contained in this matrix equation may be written as

$$\frac{d\lambda}{3} \, (2\,\sigma_z - \sigma_r - \sigma_\theta) = d\epsilon_z \tag{9}$$

[9] Hoffman, O. and Sachs, G., Plasticity, McGraw-Hill Book Co., Inc., New York, N.Y., 1953.

Table 2. Values For k and n From Virgin Tensile Specimens

Material	Tensile Properties, in kips per square inch		σ_u/σ_y	n	k, in kips per square inch
	Yield strength, σ_y	Ultimate strength, σ_u			
1. CRK16-38.3	40.1	50.7	1.27	0.149	77.7
	40.7	51.0	1.25	0.143	77.2
	40.2	50.8	1.27	0.155	78.8
	37.0	45.7	1.24	0.149	69.6[a]
2. CRR16-36.4	38.2	49.8	1.30	0.149	76.3
	38.9	50.3	1.29	0.155	78.8
	38.6	50.3	1.30	0.143	76.2
	37.8	51.4	1.36	0.137	76.5[a]
3. HRSK16-37.5	40.3	49.8	1.23	0.161	77.4
	40.5	49.3	1.22	0.161	76.8
	40.5	49.3	1.22	0.158	76.8
	41.0	50.8	1.24	0.198	85.2[a]
4. HRR16-40.5	34.7	45.5	1.31	0.195	75.2
	33.7	45.3	1.34	0.203	76.1
	38.7	46.8	1.21	0.152	71.7
	41.5	51.5	1.24	0.198	87.0[a]
5. HRSK10-37.0	39.1	58.1	1.49	0.208	99.2
	42.5	60.5	1.42	0.197	101.5
	42.7	60.2	1.41	0.236	109.0
	37.5	58.0	1.55	0.228	101.7[a]
6. HRSK16-39.7	35.8	52.3	1.46	0.210	90.1
	35.8	52.0	1.45	0.212	90.4
	36.0	51.3	1.43	0.201	86.7
7. HRSK10-42.8	41.4	65.0	1.57	0.215	114.0
	40.8	64.0	1.57	0.212	111.0
	45.2	66.1	1.46	0.208	114.0
8. HRSK16-40.7	44.8	64.8	1.45	0.208	111.2
	45.3	65.5	1.45	0.204	112.8
	45.7	66.0	1.45	0.199	110.9
9. HRSK9-30.7	30.9	52.0	1.68	0.262	99.2
	29.5	52.2	1.77	0.276	99.6
	31.1	50.6	1.63	0.281	103.7

[a]Computed from data from tests conducted more than 2 yr prior to those for other data shown.

in which σ_z, σ_r, and σ_θ are the principal stresses and ϵ_z = the strain in the longitudinal direction. However, because $\epsilon_z = 0$ and $d\epsilon_z = 0$, this becomes

$$\sigma_z = \frac{\sigma_r + \sigma_\theta}{2} \tag{10}$$

Substituting this in the Huber-Mises-Hencky distortion-energy yield condition

$$(\sigma_z - \sigma_r)^2 + (\sigma_r - \sigma_\theta)^2 + (\sigma_\theta - \sigma_z)^2 = 2\,\sigma_y^2 \tag{11}$$

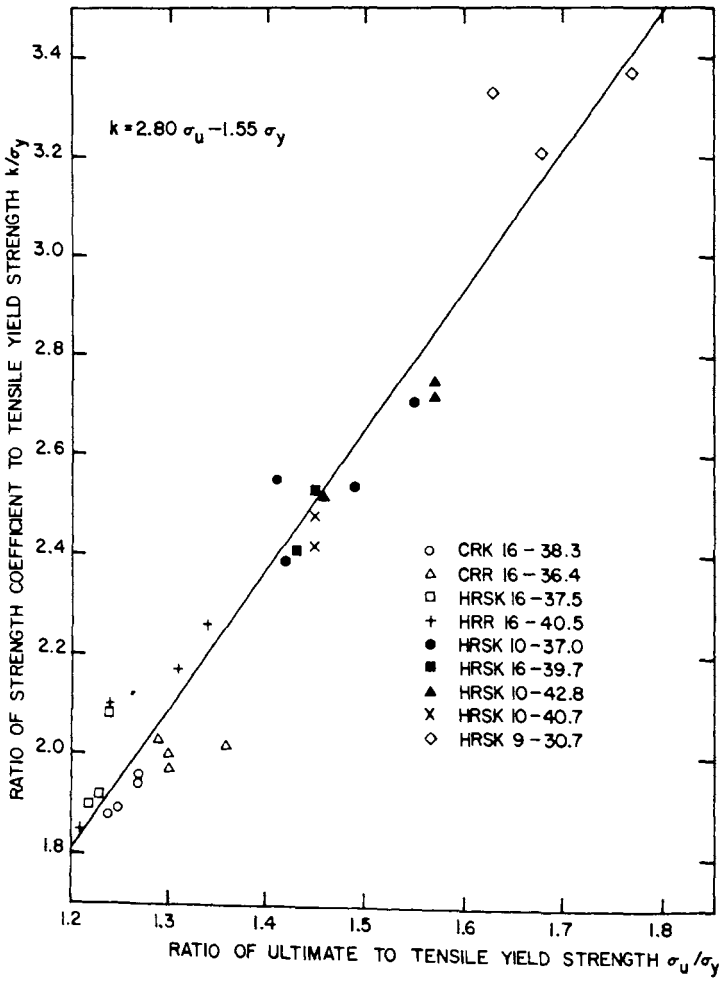

Fig. 3. Strength coefficient, k, as function of tensile yield and ultimate strengths.

gives $\sigma_r - \sigma_\theta = \pm 2K$ (12)

in which $K = \dfrac{\sigma_y}{\sqrt{3}}$ (13)

Note that the use of the Huber-Mises-Hencky yield criterion tacitly assumes isotropy and the absence of the Bauschinger Effect.

The equilibrium equation of the element of volume of Fig. 5 is

$$\frac{d\sigma_r}{dr} = \frac{\sigma_\theta - \sigma_r}{r} = \pm \frac{2K}{r} \tag{14}$$

Separation of variables and integration using the boundary condition $\sigma_r = 0$ at $r = b$ the outside radius, yields

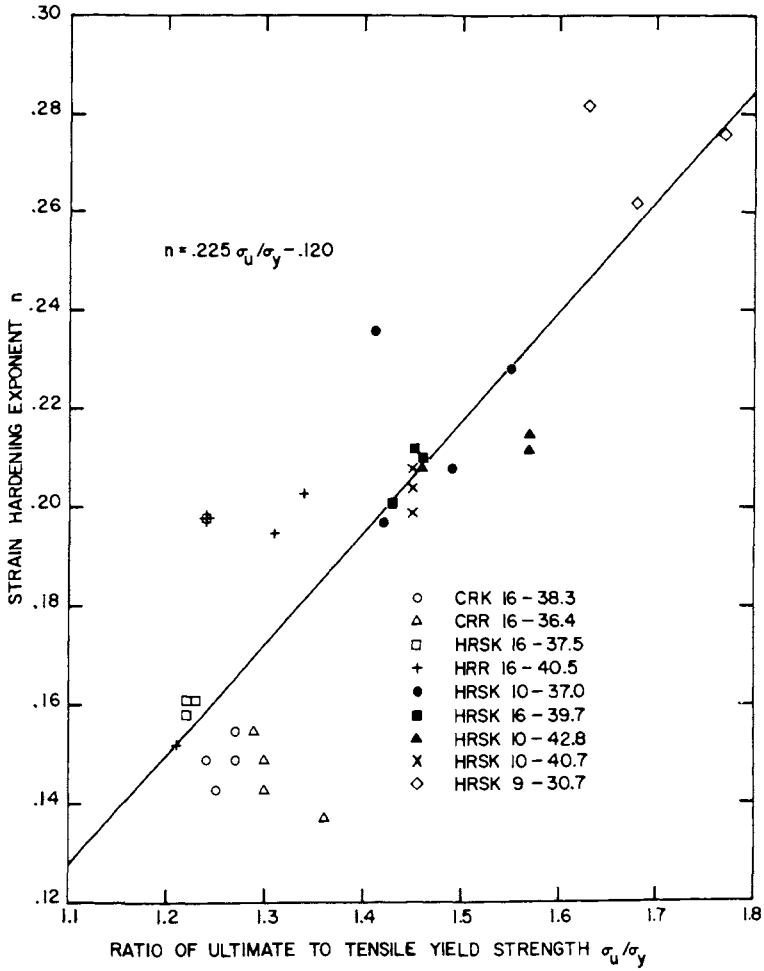

Fig. 4. Strain hardening exponent, n, as function of tensile yield and ultimate strengths.

$$\frac{\sigma_r}{2K} = \ln \frac{r}{b} \quad \text{for } r_n \leqslant r \leqslant b \tag{15}$$

and using the boundary condition $\sigma_r = 0$ at $r = a$, the inside radius, gives

$$\frac{\sigma_r}{2K} = \ln \frac{a}{r} \quad \text{for } a \leqslant r \leqslant r_n \tag{16}$$

Eqs. 15 and 16 for radial stress must be equal at the neutral surface. Equating them gives the radius to the neutral surface,[4,10] or

$$r_n = \sqrt{a\,b} \tag{17}$$

[10] Lubahn, J.D., and Sachs, G., "Bending of an Ideal Plastic Metal," Transactions, ASME, Vol. 72, 1950, pp. 201 and 208.

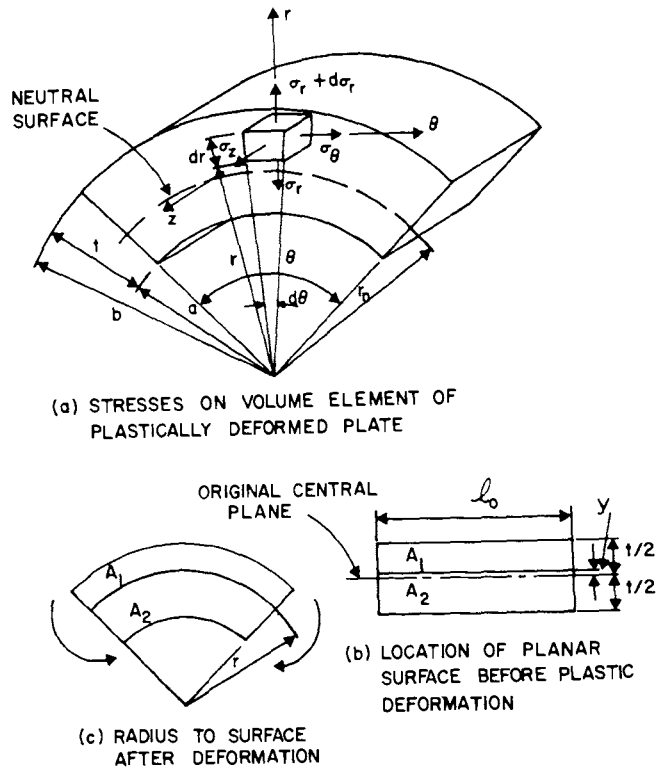

Fig. 5. Wide plate plastically deformed by pure flexural loading.

The tangential stress, σ_θ, is compressive on the inside and tensile on the outside of the neutral surface. The radial stress, σ_r, is maximum at the neutral surface.[4]

It may also be shown that the thickness of the model does not change during the plastic deformation.[4,9] This does not mean that the thickness of the volume element of Fig. 5 does not change. It simply means that the overall thickness $t = b - a$ remains constant. Hill showed that the neutral surface (i.e., the surface where the sign of σ_θ reverses) and the fiber of zero strain are not the same.[4] The neutral surface is initially at the midplane of the sheet. As bending progresses, all fibers on the inside of the neutral surface are compressed and those on the outside stretched. Then, as bending progresses still further and the neutral surface moves toward the inside radius, an area that was under compression is now stretched.

The relationship between the original fiber length, l_o, and the inside and outside radii may be expressed by equating initial and final corner areas and simplifying to obtain

$$l_o = (a + b)\frac{\theta}{2} \tag{18}$$

The radius to the fiber of zero strain is then given by

$$r_o = \frac{l_o}{\theta} = \frac{a+b}{2} \tag{19}$$

The engineering strain in the tangential direction is linear with r, i.e.,

$$\epsilon_\theta = \frac{l - l_o}{l_o} = \frac{r - r_o}{r_o} = \frac{r}{r_o} - 1 \tag{20}$$

in which $r = l/\theta$. At the inner ($r = a$) and outer ($r = b = a + t$) surfaces the tangential strain may be found from[9]

$$\epsilon_a = -\epsilon_b = -\frac{1}{2\,a/t + 1} \tag{21}$$

The volume strain, Δ, is given by

$$\Delta = (1 + \epsilon_1)(1 + \epsilon_2)(1 + \epsilon_3) - 1 \tag{22}$$

and the logarithmic volume strain, Δ', is given by

$$\Delta' = \ln(1 + \Delta) = \epsilon_1' + \epsilon_2' + \epsilon_3' \tag{23}$$

Because $\Delta = 0$ for constant volume,

$$\Delta' = \epsilon_1' + \epsilon_2' + \epsilon_3' = 0 \tag{24}$$

In the case of the purely flexural model which is in a condition of plane strain, $\epsilon_z = 0$ and, consequently,

$$\epsilon_r' = -\epsilon_\theta' \tag{25}$$

Using this in Eq. 3 results in $\bar{\epsilon} = 2/\sqrt{3}\ (\epsilon_\theta')$, from which

$$\bar{\epsilon} = \frac{2}{\sqrt{3}} \ln(1 + \epsilon_\theta) = \frac{2}{\sqrt{3}} \ln \frac{r}{r_o} \tag{26}$$

Eq. 26 will be used below in deriving equations for predicting the tensile yield strength of cold-formed corners.

Plastic Strains by the Photogrid Method.—A photographic emulsion was applied to the surfaces of the sheets. They were then exposed to an accurately gridded contact negative with divisions of 200 lines per inch, developed, and the grid image dyed black.

Sixteen-gage cold reduced rimmed sheets with both surfaces photogridded were air and coin press braked into corners of various radii. Measurement of the maximum plastic strains on the inside and outside surfaces was accomplished by means of a vernier microscope. Thickness to inside radius ratios were obtained by cutting thin sections from the photogridded corners and examining them on a 32-power comparator. Concentric circles were

compared with the corner image until the circle which best matched the central part of the inside radius was found. A slight reduction in thickness was observed in most of these corner images. The reduction varied from 0% for the largest to 3% for the smallest a/t ratios.

The plastic strains, measured in the tangential direction on the inside and outside corner surfaces, are shown in Fig. 6. The theoretical strains given by Eq. 21 for the purely flexural model are shown by the dashed lines. The experimental strains are somewhat larger on the tensile surface and slightly smaller on the compressive surface than the theoretical strains. The differences between the experimental and the theoretical values are largest for low values of the a/t ratio (i.e., high values of the t/a ratio). Quite similar results were obtained by J. D. Lubahn and G. Sachs[10] for plastic bending of an aluminum alloy. The theoretical strains shown by the solid lines will be examined below in connection with a second model which includes, in addition to bending, the effect of radial pressure during the forming of the corner. Note that the correlation of experimental points is better for the second model than for the first. Strains measured in the longitudinal direction of these specimens were negligible. Consequently, a plane strain condition may be considered to exist during and after the plastic condition of cold-forming.

Grids were also applied to the edges of 10-gage sheet so that the distribution of plastic strains over cross sections could be studied in addition to those on the inside and outside surfaces of sheets bent into corners. When a wide flat plate or sheet is bent by applying equal bending moments to two opposite edges, distortions occur at the two edges where no moment is applied. Thus, the application of photogrids to the unrestrained edges of such sheets or plates will not give precise values of the plastic strains that have occurred in the locations in which restraint is present. Despite such edge distortions, however, the photogridded specimen of Fig. 7 appears roughly to justify the assumption that plane sections before plastic bending remain plane after bending.

THEORETICAL TENSILE YIELD STRENGTH OF CORNERS

In this section an equation is established to relate the corner yield strength, σ_{yc}, directly to the fundamental material properties, k and n. This is done for (1) a corner model with purely flexural loads, and (2) a corner model with flexural plus radial pressure loads.

First Corner Model.—Because of the condition of plane strain it is logical to assume that the Bauschinger Effect is not present (in the z-direction) in the plastically formed corner model of Fig. 5(a). Indeed, a typical volume element located outside the surface of zero strain will have a tensile natural plastic strain in the tangential direction and a compressive natural plastic strain of equal magnitude in the radial direction (as was shown by Eq. 25).

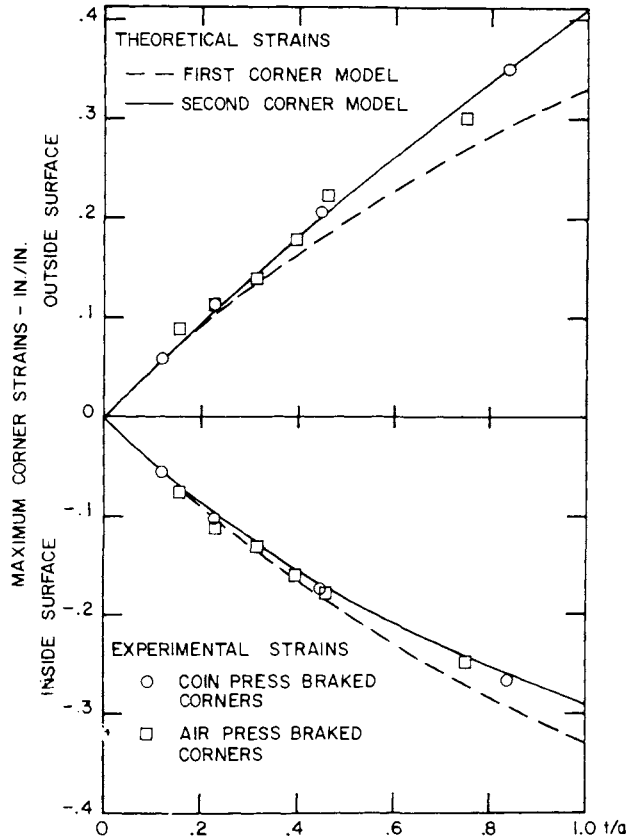

Fig. 6. Maximum corner strains by photogrid method.

Similarly, a volume element located inside the surface of zero strain will have a compressive natural plastic strain in the tangential direction and a tensile natural plastic strain of equal magnitude in the radial direction. In each of these two typical elements, the plastic strains ϵ'_θ and ϵ'_r of equal size and opposite sign are oriented at right angles to the final direction of testing or loading, the longitudinal z-direction. Thus, considering one strain component at a time and superimposing the two effects, there is no net effect on the yield strength in the longitudinal direction from the "inverse Bauschinger Effect". ("The phenomenon that results in an increase in the proportional limit and yield strength by reloading a plastically deformed specimen in the same direction, but in a decrease by reloading it in the opposite direction is known as the Bauschinger effect."[2] However, when testing is at right angles to prior cold-straining, a prior tensile strain produces a larger increase in the compressive than in the tensile yield strength. This is called the "Inverse Bauschinger Effect" by Chajes, Britvec, and Winter in a thorough treatment of the Bauschinger Effect.[2])

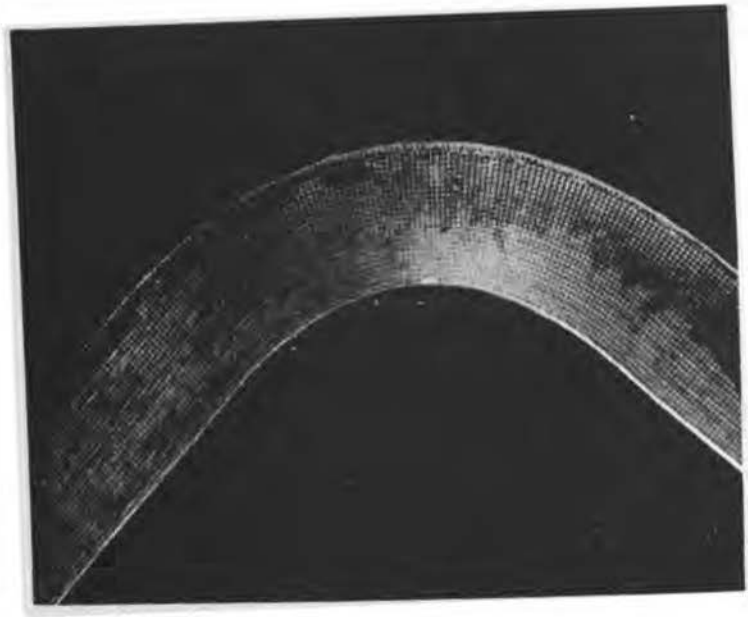

Fig. 7. Photogrid on edge of 10–gage air press braked corner.

For example, the increase in tensile yield strength in the longitudinal direction from a compressive plastic strain in the tangential direction is offset by the reduction from the equal tensile plastic strain in the radial direction. S. T. Rolfe[6] reported that specimens taken from locations of high plastic deformation in 2-1/2-in.-thick HY-80 steel plates cold-formed to different radii exhibited no Bauschinger Effect when tested in the longitudinal z-direction. There is, however, an increase in both tensile and compressive yield strength as a result of strain hardening.

It is desired to find the stress at which a corner will yield when tested in uniaxial tension. A corner may be considered to be composed of a series of elements each of which has its own stress-strain curve. Suppose a composite stress-strain curve for the corner were calculated from those of the individual elements. (A technique for constructing composite stress-strain curves is as follows: (1) Divide the cross section to be investigated into several subareas, each of which has its own characteristic stress-strain curve. (2) Find the stress of each subarea corresponding to a given value of strain. (3) Multiply the stress from each subarea by the ratio of the subarea to the total cross-sectional area. (4) The sum of these products for all of the subareas is the mean stress for the total area.) Then the corner yield strength could be determined from this composite curve. However, in the case at hand this is neither practical nor necessary. As an alternative, the yield stress may be approximated by taking the weighted average of the yield strengths of the

various elements of the corner.[11] Suppose that the material has been cold worked to a certain "effective stress" and then unloaded. Next, suppose that the material is reloaded by a different system of forces. It should now yield when the "effective stress" of the second loading equals that of the first. For uniaxial tension, the effective stress is equal to the applied tensile stress. Because the Bauschinger Effect is assumed to be absent, it follows that the average corner yield strength is given by the average effective stress attained in the prior cold-forming.[12]

No correction from true stress to engineering stress is required. If a specimen is loaded plastically and unloaded, its area may or may not be reduced, depending on the system of forces causing the plastic deformation. A reduction in area would occur in a specimen loaded plastically in uniaxial tension. However, if elastic strains are neglected as being small compared to plastic strains, the new area becomes the initial area for any subsequent loading. Therefore, it is concluded that the true stress of any prior plastic loading is the engineering yield stress for a subsequent loading.

Although no tests were made on unidirectionally precompressed sheets, it is assumed that Eq. 5 for the plastic tensile strain of a material is also valid for plastic compressive strains in the same material using the values of k and n determined from tensile tests. On this basis, the average corner yield strength, σ_{yc}, is obtained by integrating the effective stress from Eq. 5 over the full area of a corner, or

$$l_o\, t\, \sigma_{yc} = k \int_A |\bar{\epsilon}|^n\, dA = k \int_{-t/2}^{t/2} |\bar{\epsilon}|^n\, l_o\, dy \tag{27}$$

$$\text{or} \quad \sigma_{yc} = \frac{k}{t} \int_{-t/2}^{t/2} |\bar{\epsilon}|^n\, dy \tag{28}$$

From the volume constancy relationship, it may be assumed that an area after deformation is equal to the same area before deformation. Thus, $dA = l_o\, dy = \theta\, r_o\, dy = \theta\, r\, dr$ from which the relationship

$$dy = \frac{r}{r_o}\, dr \tag{29}$$

is obtained. Substituting the expressions for dy and ϵ from Eqs. 29 and 26 in Eq. 28, gives

$$\frac{\sigma_{yc}}{k} = \frac{1}{t} \int_a^b \left| \frac{2}{\sqrt{3}} \ln \frac{r}{r_o} \right|^n \frac{r}{r_o}\, dr \tag{30}$$

---

11 Karren, K. W., "Effects of Cold-Forming on Light-Gage Steel Members," thesis presented to Cornell University, at Ithaca, N. Y., in 1965, in partial fulfilment of the requirements for the degree of Doctor of Philosophy.

12 "Sixth Progress Report of Effects of Cold-Forming on Light-Gage Steel Members," Report No. 318, by the Dept. of Civ. Engrg., Cornell Univ., Ithaca, N. Y., for Amer. Iron and Steel Inst., New York, N. Y., June, 1965.

Separating this integral into two parts (corresponding to the inside and outside of the surface of zero strain) and using the change of variable $x = r/r_o$ yields

$$\frac{\sigma_{yc}}{k} = \frac{r_o}{t}\left[\int_1^{b/r_o}\left(\frac{2}{\sqrt{3}}\ln x\right)^n x\,dx + \int_{a/r_o}^{1}\left|\frac{2}{\sqrt{3}}\ln x\right|^n x\,dx\right] \quad (31)$$

Using the Eq. 19 expression for r_o, the integrals in Eq. 31 were evaluated numerically by means of Simpson's Rule for values of n held constant. Values of the integrals are plotted in Fig. 8(*a*). The final result is that σ_{yc} is a product of the strength coefficient, k, and a value determined from Fig. 8(*a*) as a function of the a/t ratio and the strain hardening exponent, n.

It is found that for values of a/t less than 10, Eq. 31 may be closely approximated by

$$\sigma_{yc} = \frac{k\,b}{\left(\frac{a}{t}\right)^m} \quad (32)$$

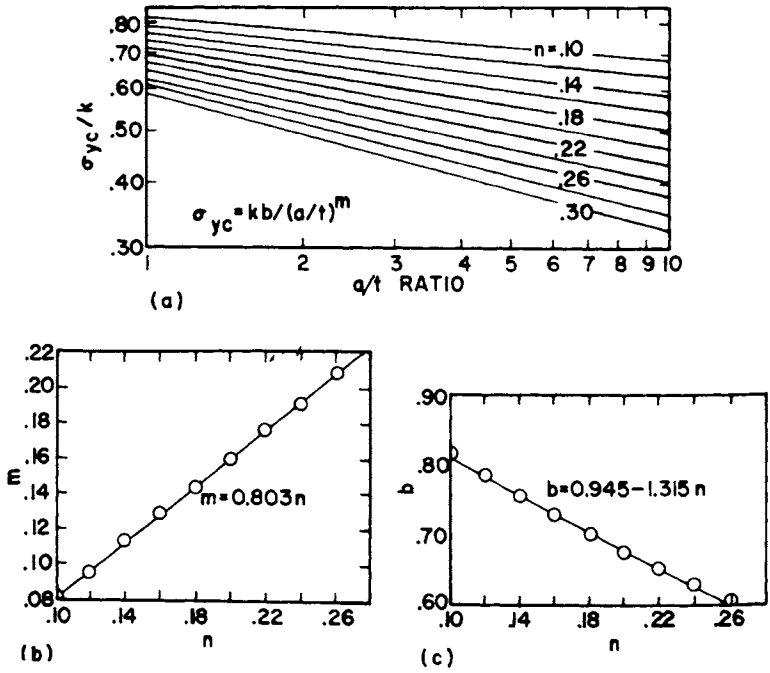

Fig. 8. Yield strength for first corner model subjected to pure flexural loads: (*a*) corner yield strength as function of b, k, m, and a/t; (*b*) constant m as function of strain hardening exponent n; (*c*) constant b as function of strain hardening exponent, n.

This is true because the plot [Fig. 8(*a*)] of Eq. 31 on log-log paper, holding n constant, closely approximates a straight line. Furthermore, using Eq. 32, it was found that the relationships between the constants b and n and between m and n are linear, as shown in Figs. 8(*b*) and 8(*c*). The empirical equations for b and m are

$$b = 0.945 - 1.315\,n \tag{33}$$

and $$m = 0.803\,n \tag{34}$$

With values of k and n available for sheet materials, Eqs. 32, 33, and 34 may be used to establish σ_{yc} values. This will be detailed further after a description of the second corner model.

Second Corner Model.–Radial pressures of unknown magnitudes are present during the plastic bending of corners by air and coin press braking or by roll-forming. The effect of an inside radial pressure during the plastic bending is explored analytically; this is done by means of a second corner model with a uniformly distributed outward radial pressure, p, on the inside surface of the corner. The uniform radial pressure is equilibrated by circumferential tensile forces equal to p times a per unit length of the corner. Cylindrical surfaces will remain cylindrical, but R. Hill has shown that these conditions cause the neutral surface to displace inward and the thickness of the sheet to decrease.[4] (Note that the maximum decrease in thickness measured for the press braked photogridded corners was 3%.) Integrating Eq. 14, using the corresponding boundary conditions $\sigma_r = -p$ at $r = a$, and $\sigma_r = 0$ at $r = b$, the radial stresses are

$$\sigma_r = -2K \ln \frac{b}{r}, \text{ for } r_n \leqslant r \leqslant b \tag{35}$$

and $$\sigma_r = -p - 2K \ln \frac{r}{a}, \text{ for } a \leqslant r \leqslant r_n \tag{36}$$

Equating the expressions for σ_r at the neutral surface, the radius to the neutral surface is

$$r_n = \sqrt{a\,b\,e^{-p/2K}} \tag{37}$$

Comparison with Eq. 17 shows that the neutral surface is closer to the inside surface for the second than for the first model (subjected to pure flexure only). If the neutral surface is displaced inward, so will be the fiber of zero strain. Larger strains will be expected on the outside fiber and smaller strains on the inside fiber.

The exact amount of radial pressure produced by any of the three forming methods is not known. However, the location of the axis of zero strain may be adjusted by trial until better agreement is obtained between the experimental and theoretical strains of Fig. 6. In so doing, it is assumed that the

slight thinning effect can be ignored and that the strain distribution remains linear. If it is thus assumed that the axis of zero strain is located at

$$r_o = \sqrt{a\,b} \tag{38}$$

the resulting theoretical strains are $ea = \sqrt{b/a} - 1$ and $eb = \sqrt{a/b} - 1$ and are shown by the solid lines on Fig. 6. Comparison of Eqs. 38 and 19 shows that the axis of zero strain is closer to the inside surface for the second than for the first corner model. It appears that this assumption tends to give closer agreement between theoretical and experimental strains than the assumption of pure flexural bending.

Eq. 31 was again evaluated numerically, using the Eq. 38 expression for r_o. The results show that Eq. 31 can also be closely approximated by Eq. 32 for the second corner model, provided that the relationships between b, m, and n are now given by

$$b = 1.0 - 1.3\,n \tag{39}$$

and $$m = 0.855\,n + 0.035 \tag{40}$$

Eq. 32 may be written in nondimensional form as

$$\frac{\sigma_{yc}}{\sigma_y} = \frac{(k\,b/\sigma_y)}{(a/t)^m} \tag{41}$$

By inspection of Eqs. 6, 7, 39, and 40, it may be seen that the right side of this form of Eq. 32 is a function of only two parameters: the ratios σ_u/σ_y and a/t. This fact made possible the preparation of Fig. 9 for practical use. It gives the corner yield strength, σ_{yc}, directly as a function of the virgin yield strength, σ_y, the materials parameter, σ_u/σ_y and the geometrical parameter, a/t. The σ_u/σ_y ratio is a measure of the strain hardenability of the virgin material. A material which has a large σ_u/σ_y ratio is capable of relatively large amounts of strain hardening. However, a material with a low σ_u/σ_y ratio (e.g., 1.1) will strain harden little before fracturing. Consequently, it may be seen in Fig. 9 that as the σ_u/σ_y ratio increases, the ratio of the corner to the virgin yield strength increases markedly. The a/t ratio to which a corner is bent determines the amount of plastic cold-straining which occurs; i.e. the smaller the a/t ratio, the larger is the degree of cold working. Correspondingly, it is seen in Fig. 9 that the ratio of corner yield strength to virgin yield strength is largest for the smallest a/t ratios.

Analytical curves of σ_{yc} versus the a/t ratio are plotted in Figs. 12 to 15 for four of the nine materials tested. Values for these curves were calculated by means of Eq. 31. Values of b and m were evaluated by means of Eqs. 33

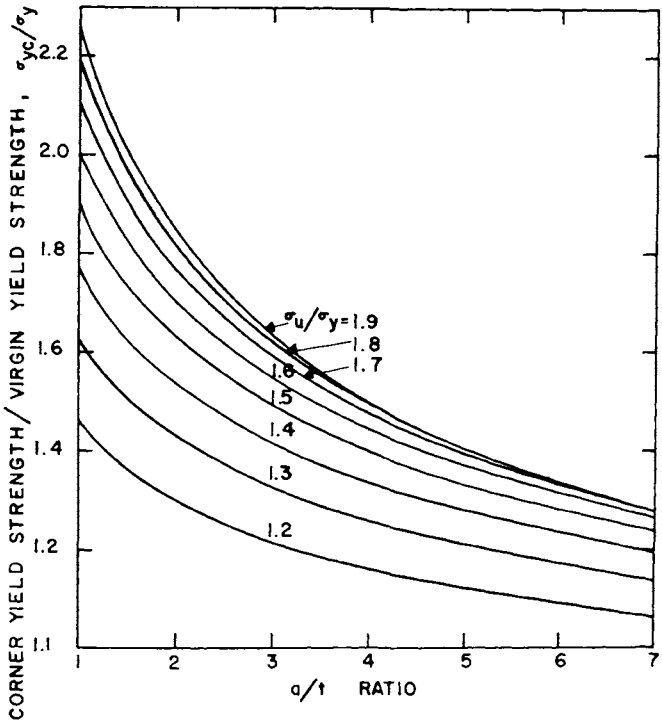

Fig. 9 Corner yield strength design chart (based on second corner model).

and 34 (first corner model) and Eqs. 39 and 40 (second corner model) in obtaining values for the dashed and solid curves, respectively. Corner yield strength values obtained experimentally are also shown in these figures.

Values for the materials constants k and n were established for use with Eq. 31 by means of empirical Eqs. 6 and 7 which require that representative values of σ_u and σ_y be available from standard tensile tests. The σ_{yc} versus a/t curves obtained using Eq. 32 will be examined further in the next section where corner test results are treated in detail.

TESTS

Tensile and compressive test specimens for corners, as well as flat specimens, are shown in Fig. 10. Special methods for cutting and testing corner specimens were devised.

Virgin Tensile Test Procedure.–The tensile properties of the virgin materials were established by using standard 9-in. coupons, as shown in Fig. 10(*c*). Tensile coupons for the ninth material, HRSK9-30.7, were cut directly from a length of unstraightened sheet coil 4-5/8-in. wide. The material had a

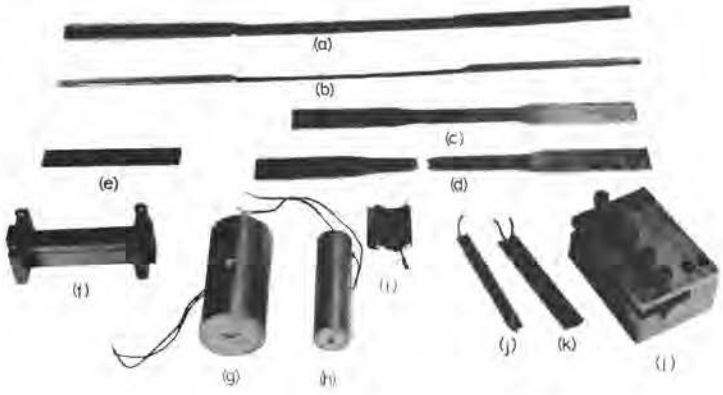

Fig. 10. Test specimens: (*a*) tensile specimen inside radius of 1/4 in., (*b*) tensile specimen radius 1/8 in., (*c*) standard flat tensile specimen, (*d*) flat tensile specimen after testing, (*e*) flat compression specimen, (*f*) jig for compression specimen, (*g*) and (*h*) compression corner specimen cast in hydrostone, (*i*), (*j*), and (*k*) compression specimen (corners) of 7/16 in., 1/8 in., and 1/4 in., respectively, with foil type electric SR4 strain gages, (*l*) steel jig for compression corner specimen.

radius of curvature of approximately 18.2 in. These tensile coupons were standard except for the longitudinal curvature. Two SR-4 strain-gages were mounted on opposite sides of each of these three specimens and were connected to eliminate bending strains from the strain readings. The specimens were tested in the curved condition, the force of the testing maching gradually straightening them as testing progressed. The resulting stress-strain curves are somewhat gradual yielding as a result of the bending stresses caused by the curvature. The stress-strain curves show a definite flattening out at the yield plateau so that the yield point is not difficult to determine.

Virgin Compressive Test Procedures.–Flat rectangular specimens, Fig. 10(*e*), (either 0.57-in.-by-3.57-in. or 0.50-in.-by-3.00-in.) were taken to determine the compressive properties of the virgin materials. These flat specimens were tested in a greased jig [Fig. 10(*f*)] to keep them from buckling in the weak direction. Strains were obtained by means of a microformer gage mounted on the protruding edges of the specimens.

Tensile Corner Test Procedure.–Tension tests on corner specimens were also conducted using self-alining grips and a microformer strain gage. The specimens were made extra long: 16-in. and 18 in., rather than the standard 9 in. ordinarily used for flat sheet specimens, as shown in Figs. 10(*a*) and (*b*). This extra length was considered necessary to minimize bending and flattening of the corner in the center of the specimen during testing.

Table 3. Material Properties of Corner Specimens

Material and forming method	Compression Tests				Tension Tests					Percentage elongation in 2 inches
	a/t	σ_p, in kips per square inch	σ_y, in kips per square inch	$\frac{\sigma_p}{\sigma_y}$	a/t	σ_p, in kips per square inch	σ_y, in kips per square inch	σ_u, in kips per square inch	$\frac{\sigma_p}{\sigma_y}$	
CRK16-38.3	1.59	44.0	60.0	0.73	1.59	49.3	61.1	65.3	0.80	8
Roll	1.59	36.0	54.5	0.66	1.59	45.7	57.5	57.5	0.79	
Formed	1.59	37.0	54.5	0.67	1.59	43.0	57.7	59.0	0.74	8
	1.59	46.0	59.0	0.77	3.02	32.2	49.2	52.0	0.65	31
	3.02	51.0	58.5	0.87						
	3.02	43.0	53.0	0.81						
	3.03	38.0	51.5	0.73						
	3.03	37.0	51.5	0.71						
	3.03	36.0	50.0	0.72						
CRK16-38.3	1.00	41.5	62.5	0.66	1.06	44.8	64.7	67.0	0.69	5
Coin	1.62	43.0	63.0	0.68	1.05	42.0	58.0	62.0	0.72	6
Press	2.29	30.0	53.0	0.56	1.06	51.7	65.6	66.2	0.78	9
Braked	2.16	39.0	51.0	0.76	2.43	42.0	58.6	60.0	0.71	7
	4.32	36.0	48.5	0.74	4.58	40.3	48.2	50.3	0.83	26
	4.50	39.0	53.0	0.73						
CRK16-38.3	1.62	44.6	61.5	0.72	1.61	38.3	57.5	57.5	0.66	5
Air	2.04	44.0	55.0	0.80	2.12	41.7	57.5	58.2	0.72	8
Press	2.38	39.0	57.6	0.67	4.23	36.9	50.3	52.3	0.73	32
Braked	3.98	36.0	46.5	0.77						
	4.32	33.0	52.0	0.63						
CRR16-36.4	1.54	50.0	63.0	0.79	1.54	52.8	61.0	71.0	0.86	
Roll	1.54	44.0	59.0	0.74	1.54	50.0	61.7	64.8	0.81	10
Formed	1.54	46.0	61.5	0.74	3.23	44.0	52.0	58.7	0.84	
	3.23	50.0	59.0	0.84	3.23	45.7	53.7	60.4	0.85	14
	3.23	38.0	53.0	0.71						
	3.23	49.0	56.0	0.87						
	3.23	46.5	55.5	0.83						
	3.23	44.0	54.0	0.81						
CRR16-36.4	1.02	54.0	68.2	0.79	1.06	49.0	67.6	67.6	0.72	
Coin	1.54	54.0	65.8	0.82	1.06	41.3	62.3	70.0	0.66	5
Press	2.18	42.0	60.5	0.69	1.30	49.6	64.1	68.1	0.77	10
Braked	4.10	39.5	54.0	0.73	2.34	46.3	60.8	65.2	0.76	8
	4.56	41.0	52.0	0.78	4.62	34.2	48.8	55.2	0.70	18
CRR16-36.4	1.89	50.0	63.8	0.78	1.89	42.3	58.7	61.7	0.72	4
Air	2.05	44.0	64.0	0.68	2.08	43.8	59.1	62.8	0.74	7
Press	4.10	41.5	53.0	0.78	4.36	33.7	47.5	54.5	0.70	24
Braked	4.36	42.5	53.0	0.80						
HRSK16-37.5	1.49	56.0	62.5	0.89	1.42	53.0	60.0	67.0	0.88	
Roll	1.49	58.5	62.5	0.93	1.49	54.3	58.7	65.0	0.92	10
Formed	3.02	54.5	54.5	1.00	3.02		53.3	57.0		
	3.03	52.8	54.1	0.97	3.02	50.0	52.7	59.0	0.94	18
	3.03	54.5	56.0	0.97						
	3.03	53.0	55.0	0.96						
HRSK16-37.5	1.05	67.5	69.0	0.97	1.00	67.0	67.0	69.0	1.00	
Coin	1.51	54.1	63.8	0.84	1.00	55.3	64.5	70.0	0.85	6
Press	2.11	53.5	56.5	0.94	1.76	55.2	61.9	67.0	0.89	6
Braked	2.14	47.5	56.0	0.84	1.24	48.2	56.9	61.3	0.84	7
	3.72	51.0	53.0	0.96	2.23	49.8	54.2	58.3	0.91	10
	4.03	48.0	54.5	0.88	2.24	51.0	59.0	64.3	0.86	8
					4.22	47.1	47.4	55.2	0.99	16
HRSK16-37.5	1.76	56.7	62.2	0.91	1.49	54.8	61.5	67.4	0.89	8
Air	2.02	46.0	58.0	0.79	1.98	52.8	57.3	63.8	0.92	10
Press	3.97	47.5	49.0	0.96	3.78	47.6	49.8	57.3	0.95	20
Braked	3.72	50.0	53.5	0.93						
HRR16-40.5	1.75	54.0	64.0	0.84	1.75	58.0	64.5	70.5	0.89	
Roll	1.75	46.5	66.0	0.70	1.75	55.7	62.0	68.0	0.89	9
Formed	1.75	58.0	65.7	0.88	3.02		54.0	62.5		
	1.75	58.0	67.0	0.86	3.02	53.2	56.0	64.0	0.95	19
	3.02	55.0	59.0	0.93						

Table 3. *(Continued)*

Material and forming method	Compression Tests				Tension Tests					Percentage elongation in 2 inches
	a/t	σ_p, in kips per square inch	σ_y, in kips per square inch	$\frac{\sigma_p}{\sigma_y}$	a/t	σ_p, in kips per square inch	σ_y, in kips per square inch	σ_u, in kips per square inch	$\frac{\sigma_p}{\sigma_y}$	
	3.03	54.5	55.5	0.98						
	3.03	43.0	56.5	0.76						
HRR16-40.5	1.06	68.3	72.6	0.94	1.02	59.7	71.2	76.6	0.83	10
Coin	2.02	53.0	61.0	0.86	1.02	60.7	69.0	74.8	0.87	7
Press	2.02	49.0	55.0	0.89	1.24	51.0	60.0	67.0	0.85	10
Braked	3.97	45.0	55.0	0.81	1.24	64.5	66.4	69.6	0.97	11
	3.97	45.0	50.0	0.90	2.27	47.0	56.0	63.0	0.83	9
					4.22	48.0	50.0	57.0	0.96	17
HRR16-40.5	1.74	53.5	64.0	0.83	1.74	48.0	56.0	61.0	0.85	10
Air	1.98	57.0	62.0	0.91	1.74	47.6	59.0	64.5	0.80	6
Press	1.88	53.0	59.0	0.89	1.98	50.0	56.0	62.0	0.89	9
Braked	3.72	52.0	53.0	0.98	3.72	48.0	51.0	58.0	0.94	19
HRSK16-39.7	0.96	55.0	69.0	0.80	0.97	52.0	65.5	70.5	0.79	6
Air	0.96	52.6	70.0	0.75	0.96	50.6	64.7	69.5	0.78	5
Press	0.96	52.0	68.0	0.76	0.96	54.5	66.4	70.3	0.82	6
Braked	1.97	44.0	64.2	0.69	1.74	43.3	59.8	68.8	0.72	7
	1.97	51.2	65.2	0.79	1.75	46.8	59.7	68.0	0.78	8
	1.97	42.3	62.4	0.68	1.73	47.2	59.6	68.4	0.79	8
	4.97	39.3	53.6	0.73	4.52	39.9	48.3	60.1	0.82	25
	4.97	43.3	53.0	0.82	4.53	39.5	47.9	59.1	0.82	24
	4.47	40.3	53.5	0.76	4.51	42.7	49.4	60.7	0.86	22
	5.83	45.2	47.2	0.96	5.93	40.4	47.2	59.0	0.86	30
	5.83	43.2	47.3	0.91	5.94	41.1	48.7	61.1	0.85	29
	6.32	37.9	46.4	0.82	5.92	41.4	47.7	59.2	0.87	33
HRSK10-42.8	0.71	66.5	87.0	0.76	0.96	67.3	79.7	88.2	0.85	10
Air	0.71	64.5	82.0	0.79	0.96	58.2	76.3	87.0	0.76	11
Press	0.71	62.8	81.0	0.78	0.96	58.2	75.0	86.3	0.78	10
Braked	1.78	57.5	75.4	0.76	1.92	49.1	69.0	80.2	0.71	17
	1.78	55.7	75.5	0.76	1.92	51.3	69.3	80.8	0.74	15
	1.78	57.0	74.6	0.76	1.92	50.8	69.2	80.1	0.74	14
	2.85	53.7	64.2	0.84	2.99	45.8	57.0	71.5	0.80	26
	2.85	51.2	57.8	0.89	2.99	46.7	57.9	72.4	0.81	25
	2.85	57.7	65.6	0.88	2.99	46.7	58.0	72.0	0.80	25
	5.71	48.2	56.9	0.85	5.73	39.1	53.3	70.0	0.73	32
	5.71	48.4	54.8	0.88	5.73	42.2	53.7	69.5	0.67	32
	5.71	51.1	57.3	0.89	5.73	44.8	54.7	70.5	0.82	32
HRSK16-40.7	1.03	68.3	77.9	0.88	1.06		67.2	75.3		8
Air	1.03	52.9	68.8	0.73	1.06	50.5	66.3	73.5	0.76	8
Press	1.03	58.8	72.7	0.81	1.04	45.1	65.7	74.0	0.69	8
Braked	2.10	53.5	67.5	0.79	1.83	48.8	61.3	68.6	0.80	14
	2.10	47.5	67.5	0.70	1.83	52.6	62.3	69.2	0.84	14
	2.10	45.5	66.2	0.69	1.84	44.7	61.8	69.8	0.72	12
	4.21	40.5	60.1	0.67	4.18	38.2	53.9	65.3	0.71	28
	4.21	46.0	62.3	0.74	4.18	38.5	54.5	65.6	0.70	27
	4.21	40.7	58.0	0.70	4.21	39.7	55.2	65.7	0.72	32
	6.30	30.5	48.3	0.63	6.33	39.3	50.4	63.7	0.78	30
	6.30	37.2	45.4	0.82	6.33	38.3	49.3	62.8	0.78	30
	6.30	37.7	47.7	0.79	6.32	37.9	49.7	63.7	0.76	31
HRSK9-30.7	1.34	61.5	68.8	1.12	1.45	50.6	59.6	69.3	0.83	12
Roll-formed	1.55	60.2	67.4	1.12	1.45	50.0	65.5	73.5	0.76	10
	1.55	55.0	66.1	1.20	1.55	52.0	62.9	71.8	0.82	13
	1.45	54.0	67.7	1.25	1.45	52.7	65.4	74.0	0.80	11
HRSK10-37.0	0.89	66.0	74.0	0.89	0.89	59.0	66.4	72.9	0.88	9
Roll Formed	0.89	65.0	74.0	0.87	0.89	62.0	68.8	76.0	0.90	10
HRSK10-37.0	0.78	64.0	75.0	0.85	0.78	47.8	71.0	79.2	0.67	9
Coin	0.78	43.5	73.0	0.59	1.90	57.3	63.2	73.2	0.90	14
Press	1.90	54.0	63.5	0.85	3.10	42.0	55.0	68.2	0.76	22
Braked	1.90	50.5	63.0	0.80						

Table 3. *(Continued)*

Material and forming method	Compression Tests				Tension Tests					Percentage elongation in 2 inches
	a/t	σ_p, in kips per square inch	σ_y, in kips per square inch	$\frac{\sigma_p}{\sigma_y}$	a/t	σ_p, in kips per square inch	σ_y, in kips per square inch	σ_u, in kips per square inch	$\frac{\sigma_p}{\sigma_y}$	
	3.10	46.0	56.0	0.82						
	3.10	41.0	55.0	0.74						
HRSK10-37.0	1.00	52.0	72.0	0.72	0.78	57.0	70.3	80.0	0.81	9
Air	0.78	71.0	86.5	0.82	1.89	52.2	61.5	72.1	0.84	14
Press	1.90	50.5	63.0	0.80	1.90	54.3	60.7	70.8	0.89	14
Braked	1.90	48.0	62.0	0.77	3.12	46.5	54.6	68.7	0.85	26
	3.10	43.0	57.0	0.75	3.12	49.7	58.3	70.0	0.85	15
	3.10	43.0	55.0	0.78	3.10	52.0	58.4	68.7	0.89	22

Compressive Corner Test Procedure.–Compression tests were more difficult than tension tests because of the necessity of measuring strains while preventing buckling in the specimen. Compressive tests such as shown in Figs. 10(*g*) through (*k*) were accomplished by two main methods. In the first, the specimen was greased, wrapped in aluminum foil, and enclosed in hydrostone in a pipe, as in Figs. 10(*g*) and (*h*). (Hydrostone is a proprietary material of white color containing gypsum which hydrates and hardens much more rapidly than Portland Cement and has ultimate compressive strengths on the order of 9,000 psi.) In the second method, the specimen was greased and inserted into a special metal jig for corners [Fig. 10(*l*)]. For the 10-gage specimen shown in Fig. 10(*i*), which had an inside radius of 7/16-in., no jig or hydrostone was necessary as the specimen had an L/r ratio of less than 15 so that buckling was not a problem.

SR-4 foil-type strain gages were mounted on one side of each specimen. One test was conducted with strain gages on both sides of the corner specimen. The results from the two gages were so close that it was considered unnecessary to mount two gages on each specimen.

Measurement of the inside radii of the corners was accomplished with radius gages.

Corner and flat specimens for the first five materials listed in Table 1 were taken from structural shapes made by three forming methods: air press braking, coin press braking, and roll-forming. Corners from the sixth, seventh, and eighth materials of Table 1 were taken from air press braked angles. Corners from the ninth material were roll-formed.

Corner Test Results.–The appropriate as-formed material properties, such as proportional limit, σ_p, yield strength, σ_y, tensile ultimate strength, σ_u, and percentage elongation in 2 in., of each tensile and compressive corner specimen tested are given in Table 3. Yield strength is defined as the stress at which the permanent strain is 0.2% for gradually yielding steels or the level of the yield plateau for sharp yielding steels. Proportional limit is taken as the stress at which the permanent strain is 0.02%.

The compressive experimental corner yield strengths are approximately equal to the tensile experimental corner yield strengths in the nonaging

CRK16-38.3 material. This tends to check the assumption that the Bauschinger Effect is not present in cold-formed corners. However, for all of the aging materials, the compressive corner specimens give from 5% to 15% larger increases in yield strength than tensile specimens. It was found that the method of forming makes little difference in the yield strength of corners, although it does have an important influence on the properties of flats.

Typical stress-strain curves for corners are given in Figs. 11(*b*) and (*c*). It is seen that the curves are highest for corners with the smallest a/t ratios, corresponding to the highest amounts of cold work. It is also apparent that as the a/t ratio decreases, the σ_p/σ_y ratio decreases. Low values of the σ_p/σ_y ratio indicate gradual yielding stress-strain curves; whereas high values correspond to sharp yielding stress-strain curves. Aging also affects the σ_p/σ_y ratio to a certain extent, the ratio being larger for aging than for nonaging materials. For example, corners formed from the nonaging CRK16-38.3 steel

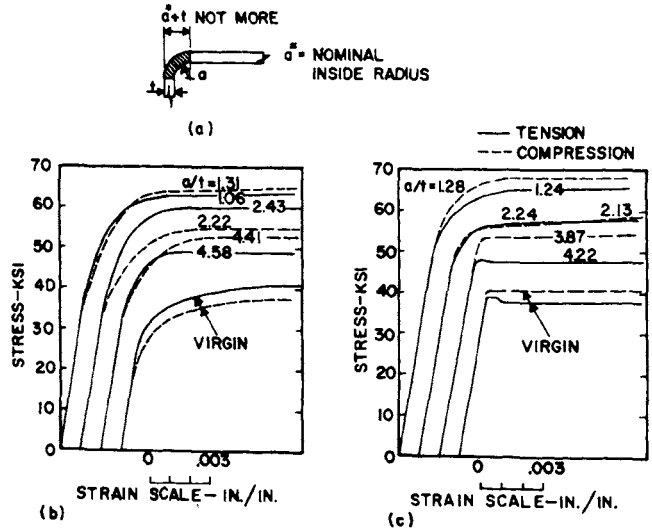

Fig. 11. (*a*) Cross-sectional dimensions of corner specimens: Typical stress-strain curves for (*b*) CRK16-38.3 and (*c*) HRSK16-37.5 corners.

have the lowest σ_p/σ_y ratios (Table 3), with values varying from 0.65 to 0.87. Corners formed from the aging HRSK16-37.5 steel have the highest σ_p/σ_y ratios, varying from 0.79 to 0.97. However, with increasing amounts of cold work, even the curves for originally sharp yielding materials become more rounded at the knees or more gradual yielding and do not seem to completely regain a plateau with aging as many simply prestrained flat specimens do;[2] this is true of both tensile and compressive corner specimens. Possible explanations for this phenomenon follow. The various fibers in a cold-formed corner do not have the same yield strength, having been subjected to varying

amounts of cold work. Consequently, as a corner is tested, various elemental parts of it yield at different stresses, resulting in a gradual yielding stress-strain curve. The tendency may be explained further by the fact that the amounts of plastic strain in the corners are considerably larger than in the simply prestrained flats of the first phase of the investigation.[2] (In the first phase it was found that the flat specimens for longitudinal compression and transverse tension and compression for the three aging materials which had been subjected to 100 mils of prestretch remained of the gradual yielding type after aging. The rest of the specimens for the three aging materials regained sharp yielding characteristics after aging.)

Typical experimental results of tensile and compressive corner tests are given in Figs. 12 to 15. The dashed and solid curves in these figures represent the theoretical tensile yield strength based on the first and second corner models. Note that the compressive experimental points are also plotted for comparative purposes with curves established for the tensile, σ_{yc}, from Eq.32. (It is difficult to obtain accurate experimental stress-strain curves in the plastic region for compressive sheet metal specimens. For the purposes of the theoretical analysis for σ_{yc} presented above, it was necessary to assume that the plastic material constants k and n are the same in compression as in tension. Therefore, no theoretical evaluation for compressive corner yield strength was attempted.) Several conclusions may be drawn from these and similar curves not reproduced: (1) For a/t ratios greater than about 5, there is little difference between the solid curves and the dashed curves, the latter being based on the purely flexural model. For smaller a/t ratios, however, the yield strengths predicted for the second model are up to 9% larger than for the purely flexural model. (2) The theoretical σ_{yc} versus a/t curves of the second model correlate better than those of the first for most of the nine materials tested; i.e., for all but the sixth, seventh and eighth materials. The correlation between the theoretical curves and experimental values is good, the curves giving for most of the nine materials conservative, yet reasonable values of σ_{yc}. (3) The calculated curves for σ_{yc} are, in general, more conservative when compared to experimental compressive corner yield strengths than to tensile yield strengths. (4) The variations between experimental values in a given sheet material cold-formed into corners by coining, by air press braking, or by roll-forming are not significant. (5) Variations between curves of corner yield strength for different materials are sufficiently large to be of significance.

The majority of experimental points lie above the theoretical (solid) curves, however. How much of this is caused by aging, by a different strain distribution than that assumed, or by a combination of causes, is uncertain. Other possible sources of difference between the theoretical curves and the experimentally obtained points are:

1. Variation in virgin properties of individual specimens;

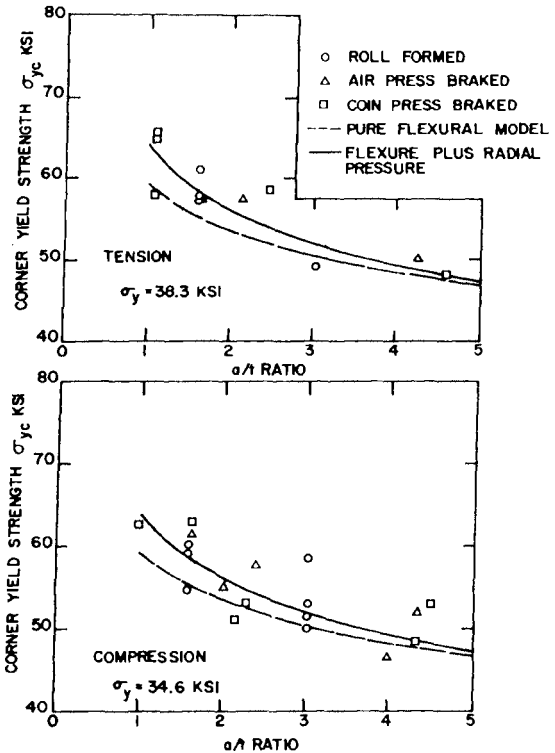

Fig. 12. Yield strength of corners versus a/t ratio for CRK16-38.3 steel.

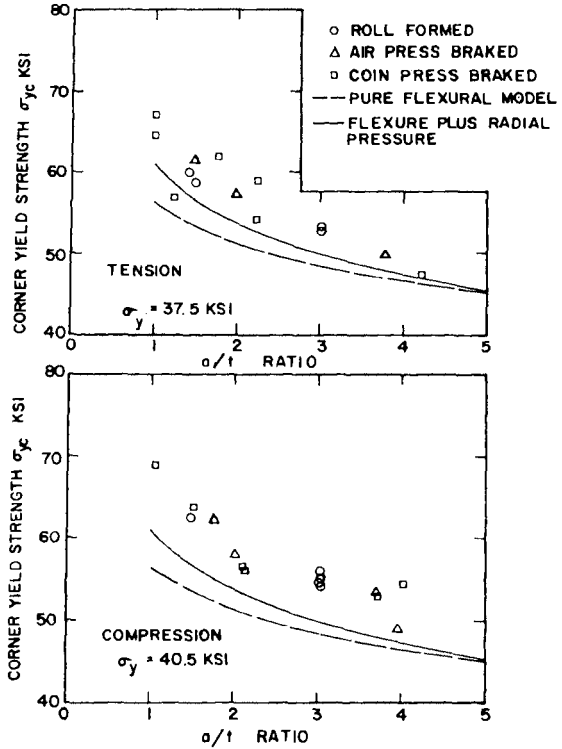

Fig. 13. Yield strength of corners versus a/t ratio for HRSK16-37.5 steel.

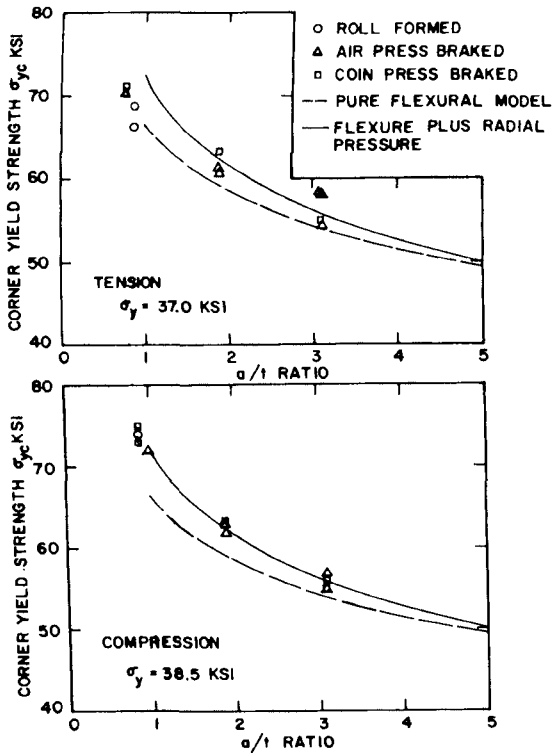

Fig. 14. Yield strength of corners versus a/t ratio for HRSK10-37.0 steel.

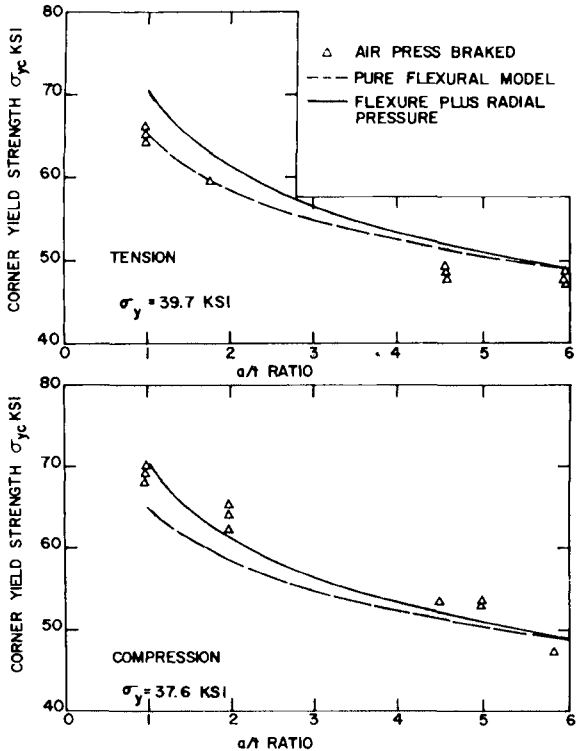

Fig. 15. Yield strength of corners versus a/t ratio for HRSK16-39.7 steel.

2. lack of uniform curvature and possible deviation from the assumption that plane surfaces remain plane;
3. anisotropy, which is present in virgin sheet steel and is also caused by the cold-forming operations themselves, and which tends to render the "effective strain" concept somewhat inaccurate;
4. the fact that no experimental stress-strain curves are available from which compressive values of the constants k and n can be determined.
5. ignoring the effects of residual stresses; and
6. the fact that plastic straining in the corners was at right angles to the grain, whereas k and n values were established for specimens tested in the direction of the grain.

However, comparison of tests and analysis indicates that the total influence of these factors is relatively small. Thus, the tensile corner yield strength, σ_{yc}, has been successfully related to the a/t ratio and to the fundamental material properties k and n. It should be noted that Eq. 32 should not be used for a/t ratios in excess of about 7.0 without further verification, because no corner specimens were tested beyond that range. With b and m calculated for Eqs. 39 and 40, and k and n from Eqs. 6 and 7, Eq. 32 should be useful in predicting the effects of cold work on the yield strength of corners within reasonable limits.

In regard to ultimate strength, inspection of Table 3 shows that the percentage increase in corners is considerably less than the increase in yield strength. Consequently, there is a marked reduction in the spread between yield and ultimate strength in corners. For example, for two coin press braked HRR16-40.5 corners with a/t equal to 1.02, the yield and ultimate strengths averaged 70.1 ksi and 75.7 ksi, respectively. This gives a ratio of ultimate to yield strength of 1.08 for the corners, compared to 1.25 for the virgin material. In these two specimens the corner yield strength was 69% above the virgin yield strength, and the corner ultimate strength was 45% above the virgin ultimate strength. This was the maximum percentage increase in ultimate strength observed in the corner tests. Also, Table 3 and Fig. 16 show that the percentage elongation drops rapidly with increasing amounts of cold work in the corner, indicating a loss of ductility with increasing strength. The reduction in percentage elongation as compared to that of the virgin material varies from 20% to as much as 90% in CRK16-38.3 corners. However, even for the sharpest corners tested, the elongation was between 5% and 10%, indicating sufficient remaining ductility for structural use.

SUMMARY AND CONCLUSIONS

1. The cold work of forming causes large changes in the mechanical properties of the corners of cold-formed structural shapes. In fact, the yield strength after cold working may be considerably higher than the original

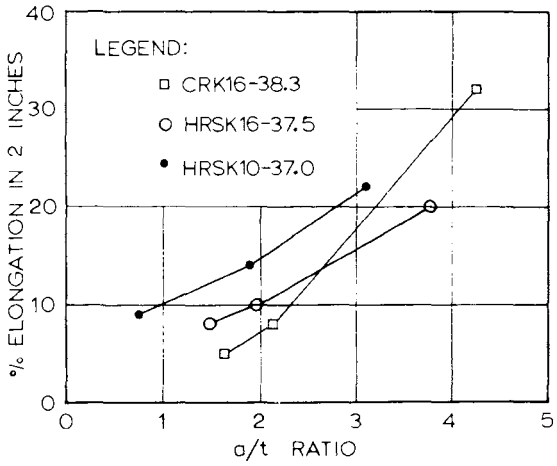

Fig. 16. Percentage elongation for corners.

ultimate strength of the material. The percentage increase in ultimate strength in the corners is considerably smaller than the increase in yield strength, with a consequent marked reduction in the spread between yield and ultimate strength. Also, the percentage alongation drops rapidly with increasing amounts of cold work in the corner, indicating a loss of ductility with increasing strength. The reduction in percentage elongation as compared to that of the virgin material varies from 20% to as much as 90%, but permanent elongation even for the sharpest corners tested was in the range of 5% to 10%, indicating considerable remaining ductility.

2. Three methods of cold-forming were used in this investigation: air press braking, coin press braking, and cold roll-forming. Nine different sheet steel materials of varying gages, chemical compositions, and metallurgical history were used (see Table 1). Only one of these, the cold-reduced killed material, was a gradual yielding, nonaging material. The rest were sharp yielding, aging materials. It was found that the forming method used had little influence on the properties of cold-formed corners. However, differences in the mechanical properties of the virgin materials had a significant influence on corner properties.
3. By plotting the logarithm of the true yield strength versus the logarithm of true plastic strain, it was found that a straight line could be fitted to the stress-strain data, establishing the power relationship of plastic strain to stress of Eq. 5 for each of the nine materials used in the investigation. (This relationship was observed to be valid in tensile specimens for plastic strains from approximately 15 to 200×10^{-3} in. per in., and is presumably valid until fracture of the material occurs.) Values of k, the strength coefficient, and n the strain hardening exponent, were established from

virgin tensile specimens tested in the plastic range. Values of n varied from 0.13 to 0.28 and values of k varied from 70 ksi to 114 ksi. Empirical equations (Eqs. 6 and 7) were established which enable k and n to be computed directly from the yield strength, σ_y, and the ultimate strength, σ_u, of virgin tensile specimens, rather than from log-log plots of true stress and true strain.

4. Two analytical corner models were used in analyzing the changes which cold-forming causes in corners. The first consisted of a wide flat sheet subjected to pure flexure, as shown in Fig. 5. The second included the effect of radial pressure during plastic forming. Consideration of the mechanics of the cold-forming operations used in the investigation indicates that there are radial pressures present in all of the three methods of cold-forming studied.
5. To study the plastic distortions occurring during the various kinds of cold-forming operations, photogrids of 200 lines per inch were applied to the surfaces of sheets before cold-forming them into corners. It was found that circumferential plastic strains on the outside of a corner are somewhat larger than predicted by the first corner model (see Fig. 6). The second corner model was so chosen that better agreement with photogrid strains was obtained.
6. Equations for theoretical tensile yield strengths were derived for both analytical corner models. For this purpose: (*a*) It was assumed that a condition of plane strain exists; i.e., that the strain in the longitudinal direction is negligible because of the restraint imposed on the corner by the adjacent undeformed flats. (*b*) It was further assumed, using the plain strain condition and the volume constancy concept for large plastic deformations, that the natural strain in the circumferential direction is equal in magnitude and opposite in sign to the natural strain in the radial direction. (*c*) From Assumption *b*, it was concluded that there will be no Bauschinger Effect in volume elements taken from such a corner and tested in the longitudinal direction. This conclusion is verified by test results. (*d*) Using the concepts of "effective strain" given by Eqs. 2 and 3, the power function, Eq. 5, was applied to a volume element and integrated over the area of a corner to obtain the yield strength of corners, Eq. 31. Eq. 32 is a simple, but accurate approximation of Eq. 31.
7. Both the experimentally observed strains and the experimentally obtained corner yield strengths agree better with the second model than with the first.
8. The tensile strength can, therefore, be adequately predicted from Eqs. 32, 39, and 40. The virgin material constants k and n which are used in these equations may be obtained most readily by means of Eqs. 6 and 7.
9. Virgin materials having large values of the σ_u/σ_y ratio have more ability to strain harden than those with small ratios. Consequently, as the σ_u/σ_y

ratio increases, the ratio of the corner yield strength, σ_{yc}, to the virgin yield strength, σ_y, increases (see Fig. 9).

10. Small inside radius to thickness (a/t) ratios correspond to a large degree of cold work in a corner. Therefore, for a given material, values of the corner yield strength are largest for the smallest a/t ratio (see Figs. 12 to 15).

ACKNOWLEDGMENTS

This investigation is part of a continuing research program relating to light-gage cold-formed steel construction, sponsored at Cornell University by the American Iron and Steel Institute. Appreciation is expressed for the capable guidance of George Winter, Head, Department of Structural Engineering, Cornell University, who served as the Project Director. S.J. Britvec served as Assistant Project Director during a part of this investigation. One of his contributions was the suggestion to use a photogrid technique for the measurement of plastic strains. The unfailing cooperation of W.G. Kirkland, Vice-President, AISI; Tappan Collins, former Chairman of the Light-Gage Steel Subcommittee; D.S. Wolford, Chairman, Light-Gage Steel Research Subcommittee; and C.R. Clauer, Chairman of the Task Group on the Effects of Cold Work, is gratefully acknowledged.

Materials used in this investigation were furnished by Stran Steel Corporation, U.S. Steel Corporation, and Armco Steel Corporation.

APPENDIX.–NOTATION

The following symbols are used in this paper:

A = instantaneous cross-sectional area;
A_o = original area;
a = inside corner radius;
b = outside corner radius and empirical constant;
dE = strain increment tensor;
$d\lambda$ = a scalar factor of proportionality;
K = constant = $\sigma_y/\sqrt{3}$;
k = strain-hardening coefficient having same units as stress;
l = instantaneous length of a fiber;
l_o = original length;
m = empirical constant;
n = strain hardening exponent (nondimensional);
r = radius to a point in a cold-formed corner;
r_n = radius to neutral surface (surface of zero circumferential stress);

r_o = radius to surface of zero strain;
S' = deviator stress tensor;
t = thickness of sheet, element, or corner;
w = width of a plate element;
x = a variable of integration or a distance;
y = vertical distance of a point from midsurface of undeformed sheet (except where defined otherwise);
Δ = volume strain = $\epsilon_1 + \epsilon_2 + \epsilon_3$;
Δ' = logarithmic volume strain = $\epsilon'_1 + \epsilon'_2 + \epsilon'_3$;
ϵ = engineering strain = $(l - l_o)/l_o$;
ϵ' = natural or logarithmic strain = $\ln (1 + \epsilon)$;
$\epsilon_1, \epsilon_2, \epsilon_3,$
$\epsilon_\theta, \epsilon_r, \epsilon_z$ = principal strains;
σ_o = load/A_o, engineering stress;
σ' = load/A, true stress;
$\sigma_1, \sigma_2, \sigma_\theta,$
$\sigma_\theta, \sigma_r, \sigma_z$ = principal stresses;
σ_p = proportional limit determined by 0.02% offset method;
σ_u = ultimate strength;
σ_y = yield strength determined by 0.2% offset method;
σ_{yc} = yield strength of corner;
σ_{yf} = yield strength of flats of cold-formed member; and
σ_{ys} = yield strength of full section.

CORNER PROPERTIES OF COLD-FORMED STEEL SHAPES[a]

Discussion by John N. Macadam

JOHN N. MACADAM,[13] M. ASCE.—Karren's theory for predicting cold-formed corner yield strengths is reasonably substantiated by tests on corner specimens with a/t ratios less than 7 and supposedly 90° included angles. It is noted in the paper that the theory (Eq. 32) should not be used for a/t ratios larger than 7 without further experimental verification. However, the possibility of using this theory for predicting yield strengths of cold-formed electric welded structural and mechanical tubing is of interest. Cold forming of common sizes of round tubing with D/t ratios to approximately 60 (a/t = 29) is known to increase the yield strength over the virgin flat strip properties.

In applying Karren's theory to common sizes of round tubing, it is first necessary to check the linear extension of Eq. 31 on log-log paper for $a/t >$ 10. Computer calculated values were obtained up to a/t = 30 and remained linear on the log-log plot. Thus, the curves shown in Fig. 9 were justifiably extended by use of Eqs. 5, 6, 39, 40, and 41. Although it might appear in Fig. 9 that the family of curves becomes asymptotic to the σ_{yc}/σ_y = 1.0 axis, these curves in fact intersect the axis at a/t ratios ranging from 10.2 to 18.6. This leads to the illogical prediction that no increase and even a decrease in yield strength from cold forming will occur at $a/t > 10.2$ to 18.6 for steels with σ_u/σ_y = 1.2 to 1.9.

The writer has recently investigated the mechanical properties of medium carbon semikilled tubing. Sixteen-gage continuously galvanized material was used to produce 1-1/8-in., 1.9-in., and 3-in. diam tubing. Tensile properties of the three sizes are given in Table 4.

Using Karren's theory for the second corner model and a tensile-to-yield ratio of 1.45, an as-formed-to-virgin yield strength curve can be drawn similar to Fig. 9 of the paper. The round tubing data is compared to this curve in Fig. 17. The tubing exhibited considerably higher yield strengths than predicated by the extension of Karren's theory.

Also shown in Fig. 17 are theoretical values computed directly from Eq. 31 using the actual n and k values determined from tensile tests on the virgin material (Table 4). Considerably better agreement with the test data was found in this case. Hence, it appears that using Karren's empirical Eqs. 6 and 7 relating k and particularly n to the virgin tensile properties can result in conservative errors. The scatter of n value data in Fig. 4 is quite large, and n

---

[a] February, 1967, by Kenneth W. Karren (Proc. Paper 5112).
[13] Research Engr., Armco Steel Corp., Middletown, Ohio.

values of the tubing material deviate significantly from the assumed relationship when plotted on Fig. 4. There are evidently other factors, as yet unexplained, that prohibit application of Karren's theory to cold-formed tubing of larger a/t ratios.

Table 4. Material Properties Of Round Tubing[a]

Round Tubing Dimensions, 16 gage	a/t	0.2% Yield Strength, in pounds per square inch	Flat Strip Yield Strength, in pounds per square inch	Flat Strip Tensile Strength, in pounds per square inch	Ratio $\frac{\sigma_u}{\sigma_y}$	Flat strip n	Flat Strip k, in pounds per square inch
1-1/8-in. diameter	8.24	66,500	48,000	69,700	1.45	0.16	113,000
1.9-in. diameter	14.65	63,500	48,200	70,200	1.45	0.15	108,400
3-in. diameter	23.79	57,500	47,600	69,200	1.45	0.16	111,500

[a] Average of replicated tests.

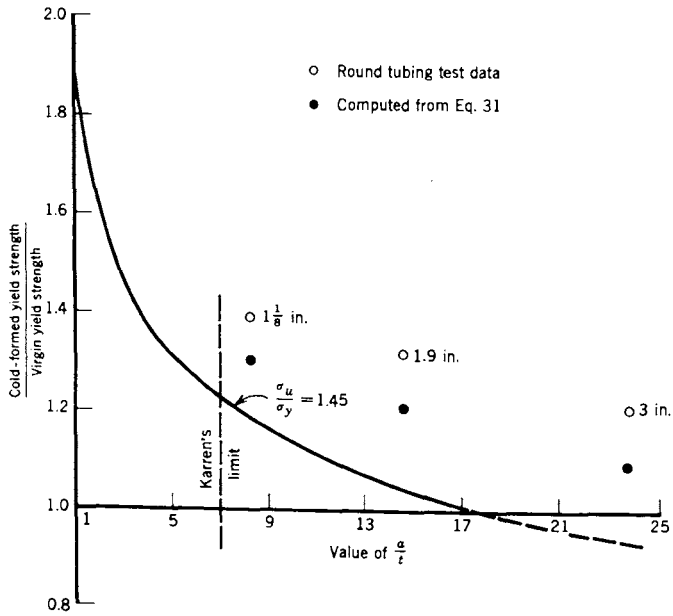

Fig. 17. Tubing data compared to Karren's theory (second corner model).

CORNER PROPERTIES OF COLD-FORMED STEEL SHAPES[a]

Closure

KENNETH W. KARREN,[14] M. ASCE.—The writer expresses his thanks to J. N. Macadam and the Armco Steel Corporation for their interest in the paper. It is gratifying that additional practical application has been found for this development. The scope of the original research was limited to sharply curved corners with inside radius to thickness ratios (a/t) of not more than 7. Macadam's interest in extending the development to larger a/t ratios is logical not only for the application to cold-formed electric welded tubing, but also as a check on the validity of the original work.

Whether or not Eq. 32 can be used to predict the yield strength of cold-formed round tubing depends (among other things) on whether a log log plot of Eq. 31 remains linear for large a/t ratios. Macadam verified this for a/t ratios up to 30. Subsequently, this has also been verified by the writer for a/t ratios up to 100. However, in doing so it was discovered that Eqs. 39 and 40 could be improved somewhat to read $b = 0.94 \cdot n$ and $m = n$.

These revisions make little difference in the curves of Fig. 9. The resulting values of σ_{yc}/σ_y in these curves are a maximum of 2% larger than those based on Eqs. 39 and 40. Even with this change, the curves of Fig. 9 still have the deficiency noted by Macadam; i.e., when they are extended for values of a/t larger than 10 to 20, the curves predict zero or negative increases in yield strength.

It should be noted that this limitation to a/t ratios smaller than about 7 to 10 applies only to the simple approximations given in Eqs. 6, 7, 32, 39, and 40 which were developed for routine design use when dealing with sharp corners. This limitation does not apply to the fundamental approach used to derive Eq. 31.

As was pointed out in the paper, differences between theoretical and experimental corner yield strength values can likely be attributed either to strain aging or to the existence of a different plastic strain distribution than was assumed by the writer for the second corner model. Chajes, Britvec, and Winter[2] found that the phenomenon of strain aging is more significant for small plastic strains than for large ones. In fact, the influence of strain aging is negligible for plastic strains in excess of 100 mils. Therefore, it is quite likely that strain aging is of much more significance in the case of small plastic strains associated with large a/t ratios than it is in the case of large plastic strains associated with small a/t ratios. Preliminary indications are that the

---

[a] February, 1967, by Kenneth W. Karren (Proc. Paper 5112).

[14] Assoc. Prof., Dept. of Civ. Engrg., Brigham Young Univ., Provo, Utah; formerly, Research Asst., Cornell Univ., Ithaca, N. Y.

influence of strain aging can be included in a reduced value of the strain hardening exponent and a slightly modified value of the strength coefficient k for corners with a/t ratios significantly larger than 10. The assumption that strains in the longitudinal direction are zero may not be valid for cold-formed round tubing.

Macadam mentions that the scatter in Fig. 4 is quite large. It is certainly true that the scatter of Fig. 4 is larger than that of Fig. 3. However, it should also be pointed out that the ordinates of these two graphs do not begin at zero. Because of the scale of the graphs, the scatter appears to be worse than it really is. Nevertheless, it has been noted that strain aging resulting from small plastic strains can have a significant influence on the value of n. The previous history of cold work such as coiling and stretcher-straightening of sheet stock may also have significance in this scatter.

EFFECTS OF COLD-FORMING ON LIGHT-GAGE STEEL MEMBERS

By Kenneth W. Karren,[1] M. ASCE, and George Winter,[2] F. ASCE

INTRODUCTION

This is the third in a series of papers concerning the effects of the cold work of forming on the mechanical properties of light-gage steel members. The first[3] dealt entirely with one type of cold work, i.e., simple undirectional tensile straining of flat sheets. The goal of this first phase of the investigation was to lay a foundation of understanding of the basic phenomena of cold working in preparation for later phases. The second paper[4] dealt specifically with the more complex type of cold straining which occurs in the forming of corners. This type of cold straining occurs in nearly all cold-formed light-gage structural members whose cross sections generally consist of flat elements and of corners.

The interrelated topics included in this paper are (1) the mechanical properties of flats, i.e., the flat elements of sections, (2) the mechanical properties of full sections, and (3) the inelastic buckling strength of cold-formed axially loaded pin-ended columns. Only open sections cold-formed from flat or coiled sheet steel were considered in this investigation. Consequently, the results may not be applicable to closed shapes such as square and rectangular tubes cold-formed from round pipe.

The yield strength of corners was found to be to 100% above that of the virgin material.[4] (Virgin material refers to the condition, i.e., coiled or straight, of the material prior to the cold-forming operation.) The increase in ultimate strength of corners is considerably less than the increase in yield strength, the maximum value found experimentally being 47% above the virgin value. Flats have smaller increases in strength than corners. The

Note.–Discussion open until July 1, 1967. To extend the closing date one month, a written request must be filed with the Executive Secretary, ASCE. This paper is part of the copyrighted Journal of the Structural Division, Proceedings of the American Society of Civil Engineers, Vol. 93, No. ST1, February, 1967. Manuscript was submitted for review for possible publication on March 7, 1966.

[1] Assoc. Prof., Dept. of Civ. Engrg., Brigham Young Univ., Provo, Utah; formerly Research Asst., Cornell Univ., Ithaca, N. Y.

[2] Prof., and Head, Dept. of Structural Engrg., Cornell Univ., Ithaca, N. Y.

[3] Chajes, A., Britvec, S. J., and Winter, G., "Effect of Cold-Straining on Structural Sheet Steels," Journal of the Structural Division, ASCE, Vol. 89, No. ST2, Proc. Paper 3477, April, 1963, pp. 1–32.

[4] Karren, K. W., "Corner Properties of Cold-Formed Steel Shapes," Journal of the Structural Division, ASCE, Vol. 93, No. ST1, Proc. Paper 5112, February, 1967, pp. 401–432.

maximum increase in yield strength found in the flats of a roll-formed section was 52% and is generally much smaller. Cold-forming decreases the ductility (as measured by percentage elongation in 2 in.) of both corners and flats. The stress-strain curves of corner specimens are always gradual yielding, whereas those of flats may be sharp or gradual yielding, depending on the type of material used and on the method used to form the member.

In general, stability of thin-walled compression members depends on an interaction between local and general buckling. As the L/r ratio is decreased, the general buckling stress of a column increases to meet the maximum stress which plate elements are capable of sustaining. Tests were conducted on compact column shapes fabricated by connecting two roll-formed channels back to back and by connecting two roll-formed joist chord sections together. The tangent modulus equation for inelastic column buckling is applicable in modified form despite (1) the nonuniform distribution of the yield strength and (2) the gradual yielding nature of stress-strain curves of the flat and corner elements in cold-formed sections. The tensile and compressive properties of flat and corner elements of sections are used to obtain analytical column curves that are compared with column test values. On the basis of these comparisons, procedures are proposed for the design of cold-formed columns.

COLD-FORMING METHODS

The methods used for cold-forming of light-gage structural members may be divided into two main categories—roll-forming and brake-forming. Brake-forming may be accomplished by bend braking, by "air" press praking, or by "coin" press braking. The forming methods covered in this investigation are (1) roll-forming, (2) air-press braking, and (3) coin-press braking. These three methods are described in some detail elsewhere.[4] It was found that the method of forming used makes little difference in the yield strength of corners, but does have an important effect on the properties of flats. Because of the pressure of the rolls, roll-formed members may have significant strength increases in the flats. Ordinarily, either bend or press braking has no effect on flats. One exception to this occurs in sections such as deep channels. To brake-form such sections, it may be necessary to temporarily put a reverse bend in the web. When the corners have all been formed, the reverse bend is flattened out. This will, of course, increase the yield strength of the cold-worked part of the web.

MATERIALS

The four carbon steels used in this investigation are listed in Table 1. These sheet steel materials are four of the nine used in the investigation of the

effects of cold work on cold-formed corners.[4] Table 1 contains the main properties of the virgin materials in their as-rolled state prior to further cold working. Chemical compositions are shown for each steel. The following abbreviations are used herein: CRK—cold-reduced killed sheet steel, and HRSK—hot-rolled semikilled sheet steel. In the designation CRK16-38.3, the number 16 indicates the gage of the material and 38.3 indicates the virgin tensile yield strength of the sheet taken in the direction of rolling.

Table 1. Material Properties

Material	Gage	Chemical Composition By Random Check Analysis				Compressive yield strength, in kips per square inch	Tensile Properties		
		C	M_n	S	P		Yield strength, in kips per square inch	Ultimate strength, in kips per square inch	Percentage elongation in 2-in. gage length
(1)	(2)	(3)	(4)	(5)	(6)	(7)	(8)	(9)	(10)
Cold-reduced annealed, temper-rolled killed, sheet coil	16	0.15	0.40	0.024	0.008	34.6	38.3	51.1	40
Hot-rolled semikilled sheet coil	16	0.04	0.32	0.025	0.008	40.5	37.5	49.0	37
Hot-rolled semikilled sheet coil	10	0.18	0.50	0.029	0.008	38.5	37.0	57.5	36
Hot-rolled semikilled sheet coil	9	0.09	0.52	0.033	0.010	32.0	30.7	52.9	35

TEST METHODS

Tests of Virgin Materials and Corners.—The specimens and test procedures used to determine the mechanical properties of the virgin materials and of corners are described in detail in Reference 4.

Tests of Specimens from the Flats of Cold-Formed Sections.—Tests were conducted to determine how cold-forming changes the tensile and compressive mechanical properties of the flats of members made from all four of the test steels. These specimens were taken from locations distributed throughout the flat portions of the cross sections.

Tensile flat specimens were 1/4-in. wide by 10-in. long strip specimens cut from the cross sections of the cold-formed shapes indicated in Figs. 1(*a*), 3(*a*), 4(*a*), and 5(*a*). These specimens were made narrow and without shoulders to obtain the desired test information reasonably close to the corners and to get more points in the flats between the corners than would have been possible

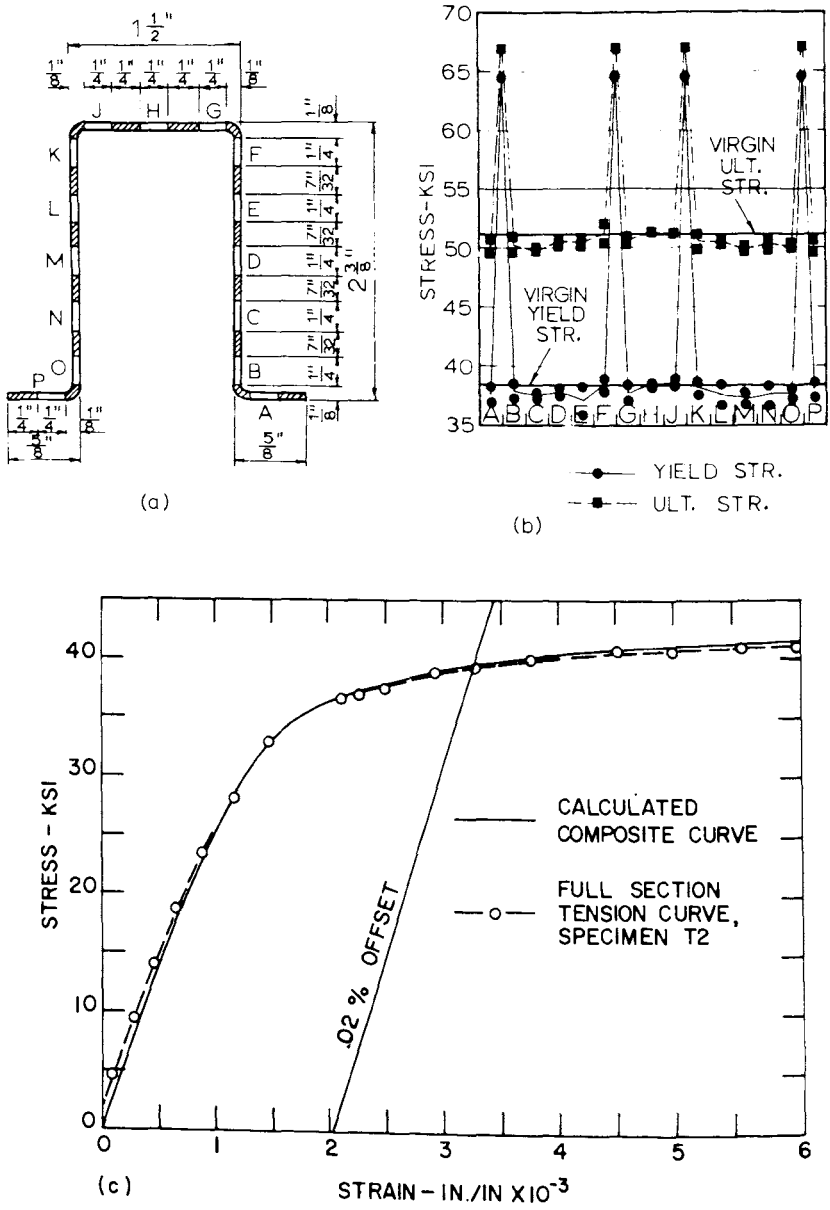

Fig. 1. Tensile stress-strain characteristics of a press-braked CRK16-38.3 hat.

SEE FIG. 1 FOR SECTION DIMENSIONS AND SPECIMEN LOCATIONS.

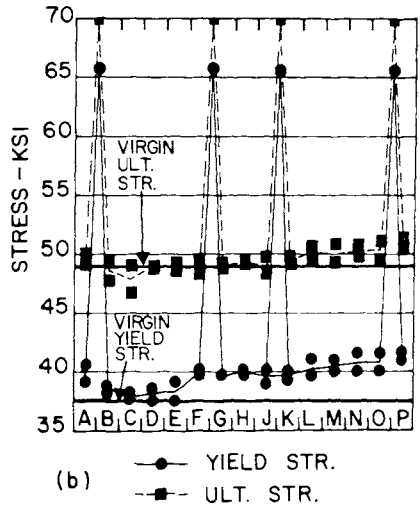

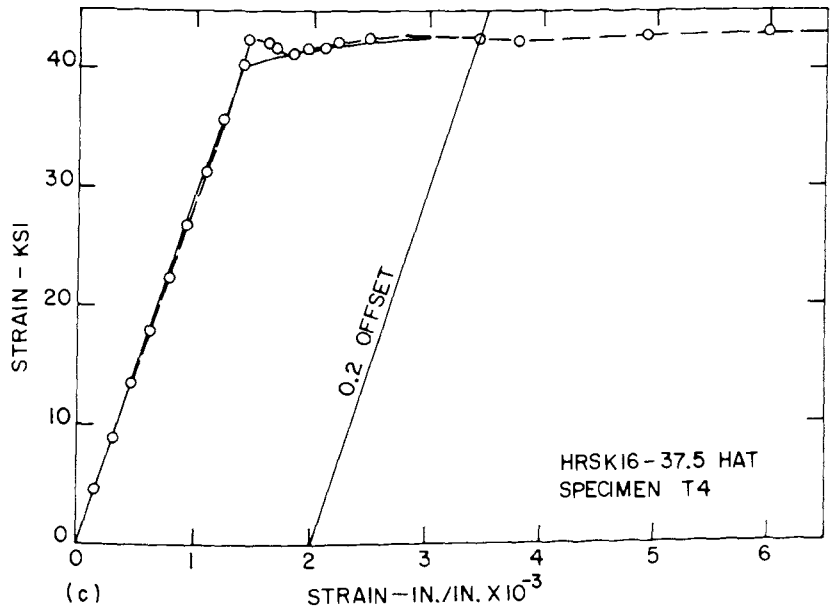

Fig. 2. Tensile stress-strain characteristics of a press-braked HRSK16-37.5 hat.

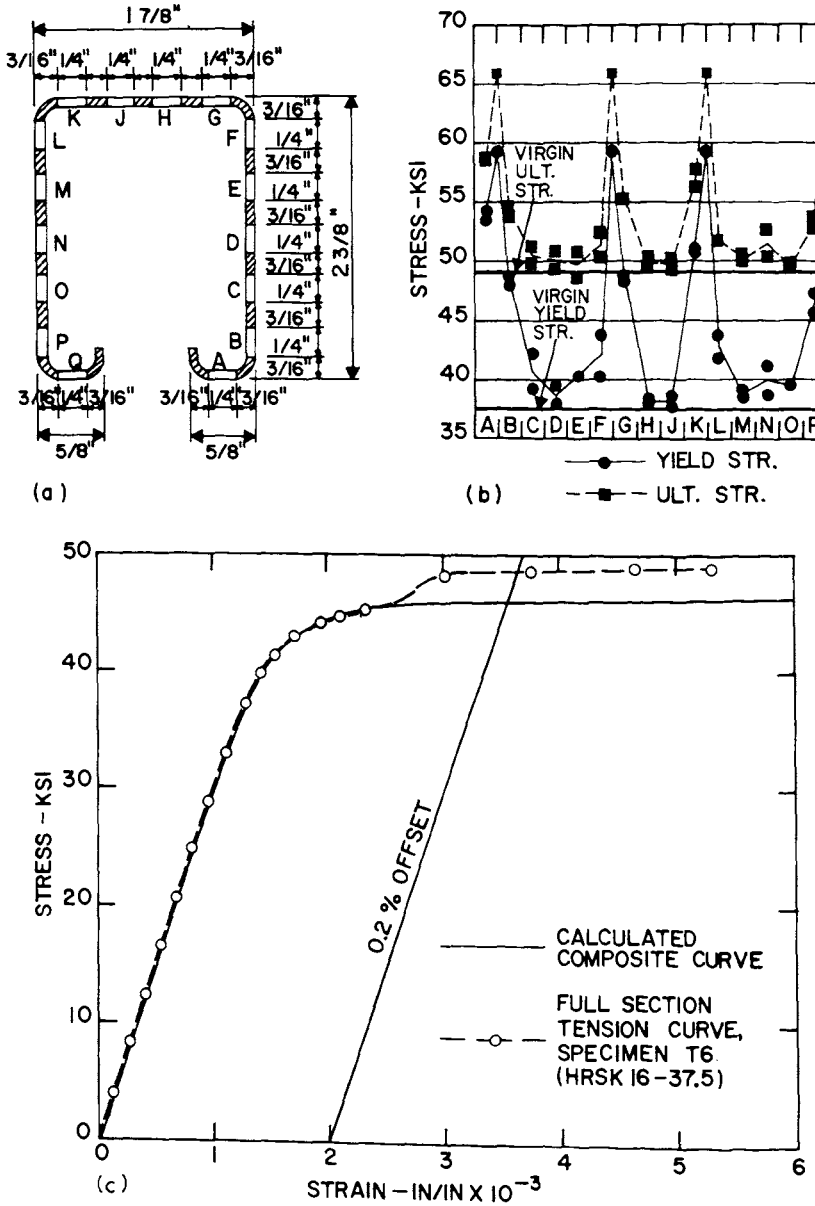

Fig. 3. Tensile stress-strain charactistics of a roll-formed HRSK16-37.5 track.

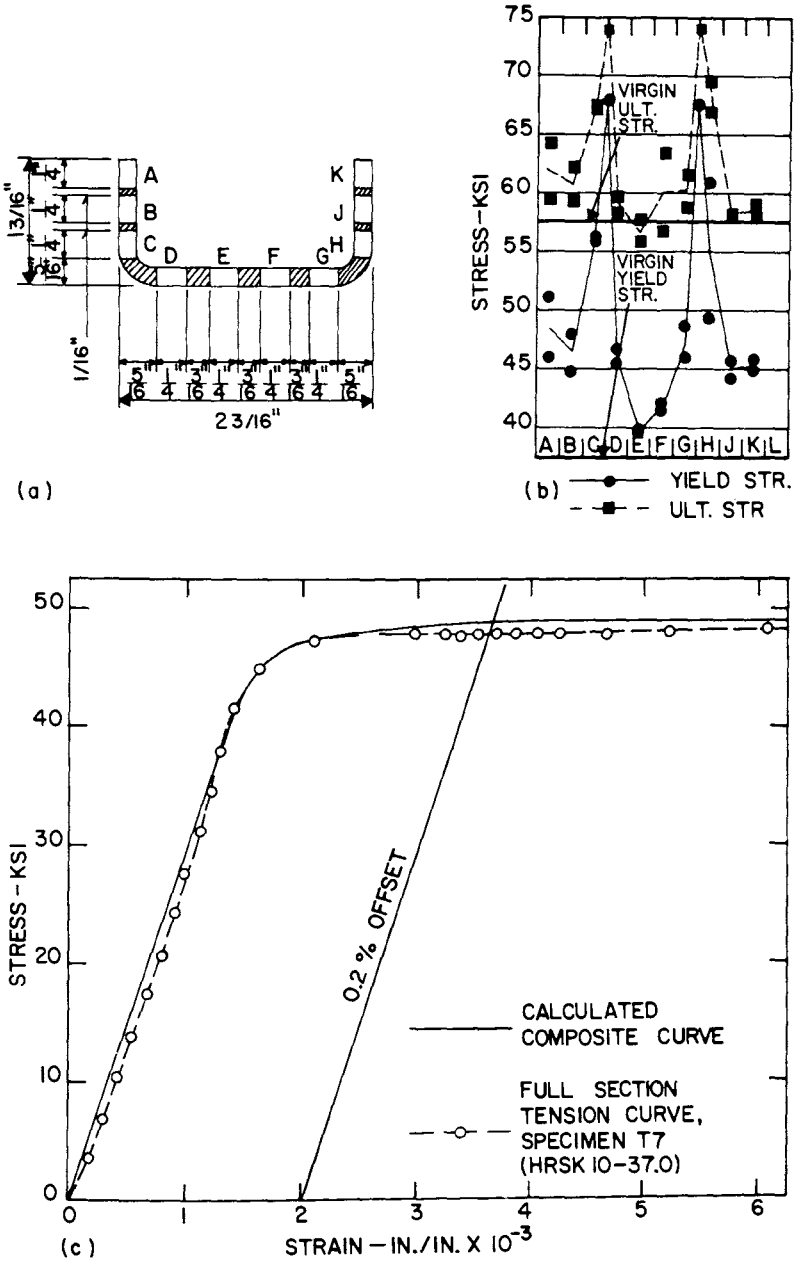

Fig. 4. Tensile stress-strain characteristics of a roll-formed HRSK10-37.0 channel.

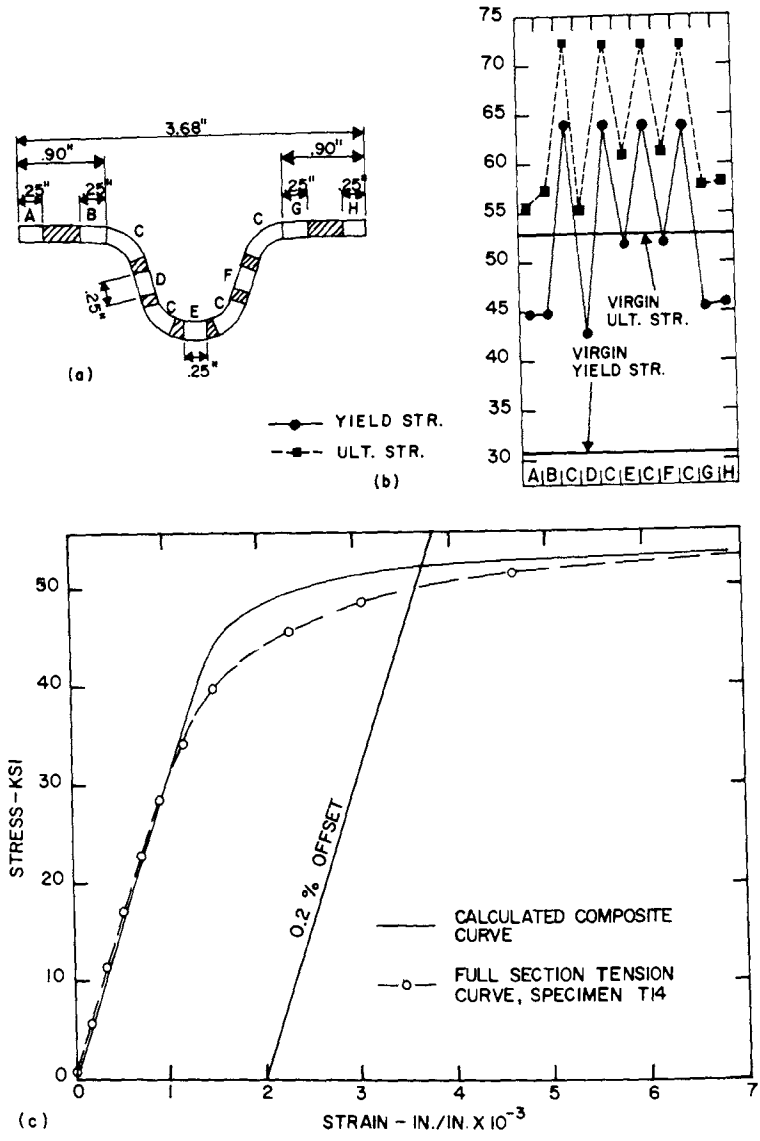

Fig. 5. Tensile stress-strain characteristics of a roll-formed HRSK9-30.7 joist chord.

with standard-width tensile coupons. The specimens were tested with the middle 3 in. of length exposed between the grips. Most of these nonstandard tensile specimens failed in the middle of the specimen away from the jaws of the self-alining tension grips. Strains were measured with an autographic microformer gage. Final elongation in 2 in. was taken.

The compressive properties of the flats from cold-formed members were determined by the same method as for the virgin materials described above.

Full-Section Tension Test Procedure.—Full-Section tension tests were performed by welding pull plates to the sections in the neutral plane of the member [Fig. 6(*a*)]. The end plates were slotted rather than the specimens.

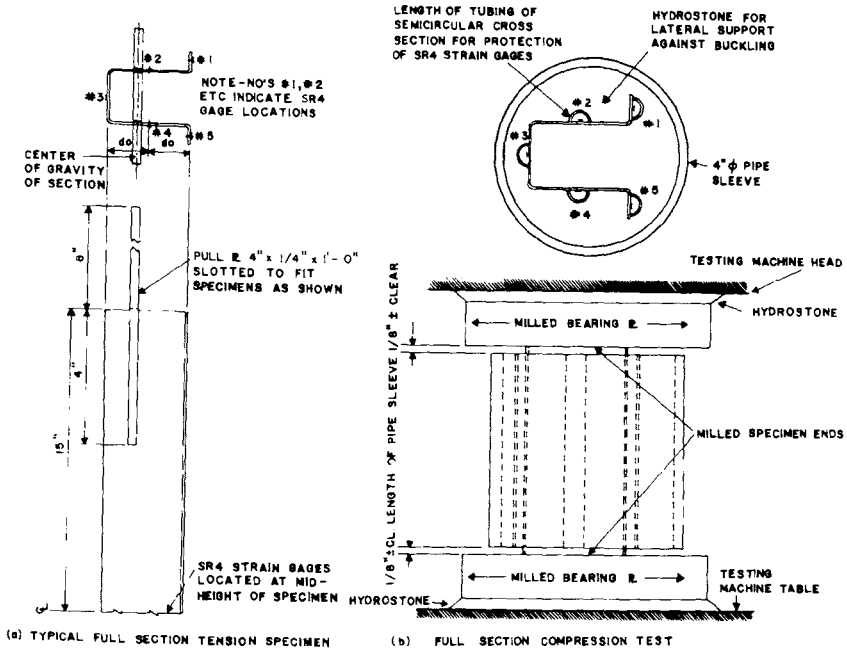

Fig. 6. Full-section test specimens.

This made welding easier and more reliable because the tendency to burn through a thin sheet is reduced when welding in an uncut location rather than along a cut edge. Full-section tension tests were made on all of the sections shown in Fig. 7.

SR-4 strain gages were mounted on each of these full section tensile specimens. Strains were recorded as long as they could be read. Thereafter, strains were taken visually by means of a scale reading to the nearest 0.01 in. in a 6-in. gage length.

Laterally-Supported Full-Section Compression Test Procedure.—Full-section compression specimens were prepared by casting short lengths of the sections in hydrostone within slightly shorter lengths of 4-in.-diam pipes [Fig. 6(*b*)]. The purpose of the hydrostone was to limit local bending of flat portions of the section and to prevent local buckling. SR-4 strain gages were mounted on each specimen. All of the sections shown in Fig. 7 were tested as full-section compression specimens with hydrostone lateral support.

The gages were waterproofed, and the specimens were greased, wrapped in aluminum foil, and cast in hydrostone. The protruding ends were milled to a plane surface after the hydrostone had hardened. The milled ends were placed against thick bearing plates which were, in turn, seated against the head and table of the testing machine with hydrostone [Fig. 6(*b*)]. The hydrostone was allowed to harden for approximately 1 hr before each test. Testing was done with the spherical-seated compression head fixed. The object of this procedure was to apply uniform compressive strains to all parts of the cross section.

Stub Column Test Procedure.—Two full-section compression tests without lateral support were performed for each of the sections shown in Figs. 7(*c*),

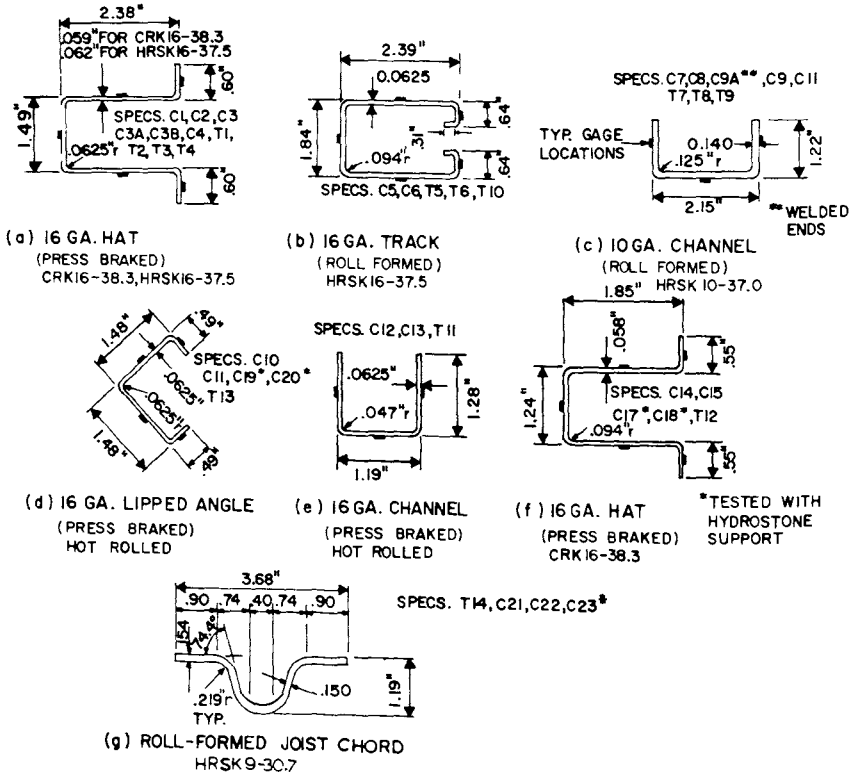

Fig. 7. Full-section specimens and average dimensions.

7(*d*), 7(*e*), 7(*f*), and 7(*g*). These tests were conducted in the same manner as shown in Fig. 6(*b*), except that the hydrostone surrounding the specimen and the 4-in.-diam tubes were omitted.

PROPERTIES OF CORNERS AND FLATS

The yield strength of cold-formed corners[4] is considerably larger than that of the virgin material from which they are formed, by as much as 102% larger in this investigation. The percentage increase in tensile ultimate strength is not as large as for yield strength, the maximum value found being 47% above the virgin ultimate strength. Stress-strain curves for corners are rounded at the knee and do not seem to regain the sharp yielding characteristic that simply prestrained flat specimens do. This is true of both tensile and compressive corner specimens. This is so because the various fibers in a cold-formed corner are plastically strained by widely different amounts. Consequently, as a corner is tested, the different fibers yield at different stresses, resulting in a gradual yielding composite stress-strain curve. However, the ratio of the proportional limit, σ_p, to the yield strength, σ_y, is larger for aging materials than for nonaging materials.[4] The ductility of corners may be reduced considerably. The reduction in percentage elongation as compared to that of the virgin material varied from 20% to as much as 90%.

The tensile yield strength of corners, σ_{yc}, may be calculated from[4]

$$\sigma_{yc} = \frac{k\,b}{\left(\frac{a}{t}\right)^m} \tag{1}$$

in which $b = 1.0 - 1.3\,n$ (2)

$$m = 0.855\,n + 0.035, \tag{3}$$

the strength coefficient, $k = 2.80\,\sigma_u - 1.55\,\sigma_y$ (4)

$$\text{the strain hardening exponent, } n = \frac{0.225\,\sigma_u}{\sigma_y - 0.120} \tag{5}$$

and a/t = the ratio of the inside corner radius to the thickness of the material. Herein, σ_y and σ_u are the tensile yield and ultimate strengths of the virgin material.

Figs. 1(*b*) through 5(*b*) show the variation of tensile yield and ultimate strengths in the corners and in the flat portions of the cross sections. The yield and ultimate strengths are plotted as ordinates, and the locations of the elemental strip specimens are shown on the abscissa. The virgin tensile yield and ultimate strengths of the material are indicated as solid horizontal lines.

The values for corner strengths are plotted as equal for all of the corners shown for each particular type of member. In each case, the values of yield and ultimate strength of the corners can easily be identified because they are much higher than the values for the flat material. In fact, the yield-strength values for the cold-worked corners are significantly above the virgin ultimate strength of the material in all cases.

From the average tensile values for flats shown in Table 2, the following observations may be made: (1) changes in the yield and ultimate strengths of the flats of the CRK16-38.3 press braked sections, Fig. 1(*b*), are negligible; (2) the increase in yield strength of the HRSK16-37.5 press braked hat flats, Fig. 2(*b*), is small, being on the order of 6%; (3) roll-forming as conducted on the three HRSK sections of Figs. 3(*a*), 4(*a*), and 5(*a*) increases the yield strength in the flats by the most significant amounts, i.e., averaging 17%, 29%, and 50%, respectively; (4) roll-forming seems to raise the average ultimate strength of the flats by a more significant amount than does press braking.

The general appearance of compressive yield-strength distributions (omitted here for brevity) is quite similar to that of their respective tensile counterparts. As is seen from Table 2, in the CRK16-38.3 hat section, the average value of the compressive yield strength of flats was somewhat lower than the average tensile yield strength whereas, in all other sections tested, the reverse was true.

Table 2. Average Test Results in Flat Portions of Sections

Section				0.2% Offset Yield Strength						Tensile Strength		
				Compressive			Tensile					
Gage	Material	Forming method	Shape	Virgin, in kips per square inch	Average flats, in kips per square inch	Percentage increase	Virgin, in kips per square inch	Average flats, in kips per square inch	Percentage increase	Virgin, in kips per square inch	Average flats, in kips per square inch	Percentage increase
(1)	(2)	(3)	(4)	(5)	(6)	(7)	(8)	(9)	(10)	(11)	(12)	(13)
16	CRK	Press Braked	Hat	34.6	36.0	4	38.3	37.9	- 1	51.1	50.5	- 1
16	HRSK	Press Braked	Hat	40.5	42.2	4	37.5	39.7	6	49.0	49.5	1
16	HRSK	Roll Formed	Track	40.5	47.3	17	37.5	43.8	17	49.0	52.7	6
10	HRSK	Roll Formed	Channel	38.5	49.8	29	37.0	45.6	23	57.5	60.1	5
9	HRSK	Roll Formed	Joist Chord	32.0	48.1	50	30.7	46.8	52	52.9	58.0	10

The change in ductility of cold-formed flats is generally quite small. The largest reduction in percentage elongation as compared to that of the virgin material was 26% in the flats of the HRSK9-30.7 roll-formed joist chord.

The increases in yield strength of flats appear to be attributable to strain hardening and aging caused by two main factors: (1) The aging which occurs after stretcher-straightening (i.e., flattening of the sheet from the coils in which it is stored); and (2) the normal pressure of the rolls in roll-forming on the flat portions of the sections being formed.

That the former may increase the yield strength seems to be substantiated by the fact that no increases occurred in the flats of the nonaging CRK16-38.3 press-braked hat, Fig. 1(*b*), whereas increases occurred in the flats of all of the materials which exhibit the property of aging.

The pressure of the rolls increased the average yield strength of the flats of all three roll-formed sections (Figs. 3, 4, and 5) considerably. The small shearing strains which occur in the flats of members as they pass from station to station in a rolling mill do not appear to cause significant changes in yield strength. For example, in the roll-formed track section of Fig. 3(*a*), the two webs were probably subjected to shearing strains, and the 1.84-in. flange probably was not, because of symmetry. The yield strength values of specimens C, D, E, M, N, and O tend to indicate that these shearing strains do not contribute significant increases in yield strength, because these values are about the same as those for the flats of the press-braked hat section of Fig. 2(*b*).

The large plastic deformations which occur in corners do not extend far into the adjacent flats.[5,6] For example, in coin press braked channels, the influence of corner plastic strains extended less than one sheet thickness from the corner. The flat tensile specimens taken without a scarf directly adjacent to the corners of the press-braked hat sections of Figs. 1(*b*) and 2(*b*) were evidently not affected by any such extension of plastic strains. Conversely, comparing the yield-strength values of the flat specimens from locations next to the corners for the roll-formed track section of Fig. 3(*b*) and for the roll-formed channel of Fig. 4(*b*), it is seen that increases in yield strength in these specimens are significantly above those of specimens located further from the corners. Because there is no reason to believe that corner plastic strains should extend into roll-formed flats any further than into press-braked flats, it is concluded that these increases in yield strength are caused by the pressure of the rolls.

Two factors have been suggested above, as being of significance in strain hardening and aging of the flats of cold-formed members. The increase in yield strength caused by the first factor, strain aging subsequent to stretcher-straightening of stored materials, is assumed to be fairly uniform throughout the flats, both for roll-formed and for press-braked members. To determine the magnitude of such increases is a simple matter requiring only a few representative standard tensile coupons from the central regions of the flats of cold-formed members. The second factor, normal pressure on the flats produced by roll-forming, may cause increases in yield strength at locations remote from corners. These increases are evidently dependent on roll design, adjustments made by the rolling mill operator, wear on the rolls, etc. Predictions of such increases prior to the rolling of a particular member would be

---

5 Karren, K. W., "Effects of Cold-Forming on Light-Gage Steel Members," thesis presented to Cornell University, at Ithaca, N. Y., in 1965, in partial fulfilment of the requirements for the degree of Doctor of Philosophy.

6 Karren, K. W., and Winter, George, "Sixth Progress Report on Effects of Cold-Forming on Light-Gage Steel Members," Report No. 318, the Amer. Iron and Steel Inst., New York, N. Y. by the Dept. of Civ. Engrg., Cornell Univ., Ithaca, N. Y. June, 1965.

necessarily uncertain even if based on a certain amount of experience and judgment.

PROPERTIES OF FULL SECTIONS

Full-Section Tension Test Results.—Typical full-section tensile stress-strain curves for five cold-formed shapes are shown in Figs. 1(*c*) through 5(*c*). With the arrangement of Fig. 6(*a*), it was possible to carry tension tests of all of the full-section tensile specimens to stresses beyond the yield point; in fact, nearly all specimens were taken to their ultimate load with necking down and fracture occurring near midlength of the specimen. However, in the track specimens, it proved impossible to reach the potential ultimate load because of difficulties encountered in welding. Failure did not occur in the central portions of any of these track specimens. The discontinuity which occurs between strains of 2 and 3 mils in specimen T6, Fig. 3(*c*), was caused by a distortion of the section which occurred shortly after yielding commenced. However, the full-section curve follows closely the calculated composite curve (see below) up to a strain of 2.5 mils, indicating that the composite curve is a valid representation of the properties of the section.

Composite stress-strain curves were obtained analytically from the stress-strain curves of all the component corner and flat test coupons taken from a particular shape. Composite curves may be constructed as follows: (1) The cross section to be investigated is divided into several subareas, each having reasonably uniform stress-strain characteristics: (2) average stress-strain curves are established for each region of the cross section from corner and flat coupons; (3) the stress for each subarea corresponding to a given value of strain is multiplied by the ratio of the subarea to the total cross-sectional area; (4) the sum of these products for all of the subareas is the mean stress for the total area for the given value of strain; (5) the process is repeated for a number of different values of strain and the composite stress-strain curve is plotted. This is a tedious procedure and would not be practical for routine use, but it did serve to give an excellent check on full-section test values. Such composite stress-strain curves compared to full-section tension test curves are also shown in Figs. 1(*c*) through 5(*c*).

The experimental stress-strain curves from the full-section tests as compared to the calculated composite stress-strain curves appear to be within a scatter range of variation which can be expected from one specimen to another. It may, therefore, be said that the two methods of obtaining full-section data confirm each other in obtaining the shape of the stress-strain curve and the tensile yield point of the section. This agreement between the full-section tensile and the calculated stress-strain curves indicates that residual stresses which may be present do not have significant effects on full-section stress-strain curves. This conclusion is of importance in determining theoretical buckling loads of cold-formed compression members in the inelastic range and will be used below.

The full-section tension stress-strain curves for the T3 and T4 press-braked hat sections [see Fig. 2(*c*) for specimen T4] were sharp yielding. For the roll-formed track section, Fig. 3(*c*), the roll-formed channel section, Fig. 4(*c*), and the roll-formed joist chord section, Fig. 5(*c*), the full-section stress-strain curves are more gradual yielding than those of the press-braked hat sections. Thus, the variation in the yield strength of the cold worked material affects the shape of the stress-strain curve more in roll-formed than in press-braked sections.

The elongation in 2 in. was approximately 48%, 33%, and 32%, for the press braked, cold reduced killed hat, the roll-formed channel, and the roll-formed joist chord sections, respectively (Table 3 and 4). This shows that the cold work of forming leaves ample amounts of ductility in full sections although member ductility decreases as the amount of cold-worked material in the section increases.

Table 3. Full-Section Test Results

Section Type	Section Number	Length, in inches	Laterally Supported Compressive Yield Strength, in kips per square inch	Tensile Yield Strength, in kips per square inch	Tensile Ultimate Strength, in kips per square inch	Percentage Elongation in 2 inches
(1)	(2)	(3)	(4)	(5)	(6)	(7)
CRK16-38.3 press-braked hat	Strips			39.6	51.8	
	T1[a]	30		39.6	49.0	
	T2[a]	30		39.3	48.7	48
	Strips		38.0			
	C1	8	36.8			
	C2	8	38.7			
HRSK16-37.5 press-braked hat	Strips			42.5	51.0	
	T3[b]	30		42.5		
	T4[a]	30		41.3	51.1	
	Strips		45.1			
	C3A	4 3/4	44.0			
	C3B	4	45.4			
	C3	8	44.9			
	C4	8	45.2			
HRSK16-37.5 roll-formed track	Strips			46.0	54.9	
	T5[b]	30		45.3		
	T6[b]	30		48.5		
	T10	30		46.0		
	Strips		50.8			
	C5	8	50.9			
	C6	8	51.2			

Note: "Strips" indicates values obtained from stress-strain curves calculated from data from narrow strip specimens.

[a] Achieved failure in central portion of specimen.

[b] Specimen tore at end weld.

Laterally-Supported Full-Section Compression Test Results.—Full-section compression stress-strain curves are not included, because the same general

Table 4. Full-Section Test Results for Laterally Unsupported

Section Type	Section Number	Compressive Yield Strength of Flats, in kips per square inch	Laterally Supported Compressive Yield Strength, in kips per square inch	Laterally Unsupported Compressive Yield Strength, in kips per square inch
(1)	(2)	(3)	(4)	(5)
HRSK 10-37.0 Roll-formed channel	C9	49.8		49.1
	C16			49.1
	Strips			
	C7		53.0	
	C8		56.3	
	C9A		54.6	
	Strips		52.3	
	T7[f]			
	T8[f]			
	T9[f]			
HRSK 9-30.7 Roll-formed joist chord	C21	48.1		52.0
	C22			51.2
	Strips		54.0	
	C23		53.5	
	Strips			
	T14[f]			
	T15[f]			
16-gage HR press-braked lipped angle	C10	42.2		44.7
	C11	42.2		44.7
	C19	42.2	48.1	
	C20	42.2	47.1	
	T13[f]			
16-gage HR press-braked channel	C12	42.2	44.3[c]	41.7
	C13	42.2	44.3[c]	42.7
	T11[f]			
16-gage CRK 16-38.3 press-braked hat	C14	36.0		41.3
	C15	36.0		39.3
	C17	36.0	41.7	
	C18	36.0	41.6	
	T12[f]			

[a] Test not carried to ultimate compressive load.
[b] Torsional buckling. Buckling became visible after maximum load.
[c] Estimated—no laterally unsupported full-section test made for this section.
[d] Slight waving noticeable in simple lips.

shape characteristics and agreement between experimental and calculated curves were obtained in compression as in tension. Yield strengths obtained in laterally supported compressive full-section tests are compared to those calculated from strip specimens in Tables 3 and 4. Yield strengths of laterally unsupported full-section compressive tests are included in Table 4. From this data, it is seen that the compressive full-section yield-strength values were somewhat larger than the tensile values for all the sections tested except for

Compared to Laterally Supported and Full-Section Tension Specimens

Laterally Unsupported Ultimate Compressive Strength, in kips per square inch (6)	Average Strain at Lateral Unsupported Ultimate Compressive Strength, in (inches per inch) $\times 10^{-3}$ (7)	Local Buckling First Noted at Stress, in kips per square inch (8)	Tensile Yield Strength, in kips per square inch (9)	Tensile Ultimate Strength, in kips per square inch (10)	Percentage Elongation in 2 inches (11)
a	a	50.2			
55.8	27.1	52.2			
			48.9	61.8	
			47.9	59.4	
			47.7	59.0	33
			47.8	60.0	26
55.4	16.3	52.8			
a	a	53.8			
			52.3	62.3	
			50.0	61.7	34
			51.3	63.3	31
44.7	3.4	b			
44.7	3.6	b			
			42.8	49.8	
42.5	4.9	42.0			
42.7	>2.6	42.0			
			40.9	49.6	
41.7	4.0	34.4[d]	38.9[e]		
41.6	4.1	32.8[d]	37.2[e]		
			42.4	50.2	

[e] Simple lips and corners buckled outward.
[f] Achieved failure in central portion of specimen.

"Strips" indicates values obtained from stress-strain curves calculated from data from narrow strip specimens.

the CRK16-38.3 hat sections.[5,6] For that section, the full-section yield strengths averaged only 4% lower in compression than in tension.

Stub Column Test Results.—Two stub column tests (i.e., laterally-unsupported full-section compression tests) were conducted for each of the cold-formed shapes shown in Figs. 7(*c*), 7(*d*), 7(*e*), 7(*f*), and 7(*g*). Test results are given in Table 4, and section properties including moments of inertia, w/t ratios, and the form factor, Q are shown in Table 5. The yield strengths were

Table 5. Properties of Stub Column Specimens

Section Type	Area, in square inches	I_x, in inches^4	I_y, in inches^4	$\frac{L}{r_y}$	Maximum Width to thickness ratios for		Q
					Stiffened elements	Unstiffened elements	
	(1)	(2)	(3)	(4)	(5)	(6)	(7)
HRSK 10-37.0 roll-formed channel	0.58	0.395	0.082	5.6	11.3	6.8	1.00
HRSK 9-30.7 roll-formed joist chord	0.702	0.646	0.117	8.8	4.2	5.8	1.00
16-gage HR press-braked lipped angle	0.234	0.100	0.034	6.9	19.4	5.7	1.00
16-gage HR press-braked channel	0.227	0.057	0.039	5.5	15.5	18.7	0.72
CRK16-38.3 press-braked hat	0.337	0.159	0.126	6.7	28.7	8.0	1.00

Notes: 1. The effective length L is taken as 0.6 times the total length of specimens, assuming that the milled ends were nearly fixed.
2. Dimensions averaged from tensile and compressive full-section specimens are shown in Figs. 7 (*c*), 7 (*d*), 7 (*e*), 7 (*f*), and 7 (*g*).
3. I_x and I_y are the principal moments of inertia of the sections.

taken either as the 0.2% offset (specimens C9, C16, C12, C21, and C22) or as the maximum load sustained (specimens C10, C11, C13, C14, and C15). The form factor, Q has been defined elsewhere.[7] This factor is used in the design of sections containing one or more flat elements with large w/t ratios. Its purpose is to provide safety against (1) local buckling and consequent member collapse and (2) excessive local deformations.

The yield strengths of stub columns were below those of companion laterally-supported compressive specimens for all except the cold-reduced killed steel hat section. The compressive yield strengths of laterally-unsupported compression specimens are all moderately above the full-section tensile yield strengths for the specimens made from aging sheet steels, and only slightly below for specimens made from the nonaging (cold-reduced killed) material.

Values of the form factor Q were computed to be 1.0 for all of the stub column specimens except that of 16-gage press-braked channels, for which Q = 0.72 (Table 5). If, for the 16-gage channel section having Q less than 1, the

[7] "Specification for the Design of Light Gage Cold-Formed Steel Structural Members," Amer. Iron and Steel Inst., New York, N. Y., 1962, Sect. 3.6.1.

laterally-supported full-section compressive yield strength (44.3 ksi) is multiplied by Q, namely, 0.72, a value of 31.9 ksi is obtained. This is considerably lower than the average laterally-unsupported full-section compressive yield strength (42.2 ksi). This tends to indicate that the form factor requirements[7] may be quite conservative for some sections with Q less than 1. However, the following examination gives possible reasons for the apparent large difference for the 16-gage channel sections. The compressive strength of this section is probably governed by local buckling in the simple lips. In turn, local buckling in the simple lips is controlled largely by two factors: (1) The aspect ratio (i.e., length to width ratio) of the lips; and (2) the amount of fixity along their inside edge. Criteria chosen for calculation of the Q factor were necessarily conservative; i.e., for simple lips, it was assumed that the aspect ratio was infinite and that there was zero fixity along the inside edge. In regard to the first factor, it is well known that as the aspect ratio of plates increases, the critical buckling load approaches a minimum. If the 16-gage channels were longer, local buckling would have commenced at lower stresses, permitting less maximum load to be carried by the section. Also, with regard to the second factor, there is probably some fixity along the inside edge of simple lips, which would tend to make the calculated Q factor somewhat conservative for any aspect ratio.

Buckling or failure always began in the flat elements, spreading to the corners after additional loading. Fig. 8 shows the manner in which inelastic local buckling developed. Evidently, the flats, having a lower yield point, began to buckle locally at an average cross-sectional stress at or slightly above their own lower yield point, preventing the higher yield point of the corners from becoming fully effective. The average stresses at which local buckling of the flat plate elements was first noted are given in Table 4.

In the CRK16-38.3 press-braked hats, (for example, see specimen C14, Fig. 8), a slight waving in the simple lips was noted at about 80% of the maximum load. At about 90% of the maximum load both the simple lips and the corners began to buckle outward. (Note that the depth of the simple lips of the 16-gage hats more than satisfies the minimum requirements for edge stiffeners.[8]) Local buckling did not become visible in the other four sections until about 95% or more of the yield strength had been reached. Therefore, it seems reasonable to conclude that at working load levels, the deflection of flats would probably not be serious for any of these five sections used as compression members.

There is a striking contrast between the stress-strain curves of the less compact and the more compact sections. Curves typical for these two types of sections are shown in Fig. 9. The less compact 16-gage channel, 16-gage press braked lipped angle, and 16-gage hat sections reached the ultimate compressive load at strains in the range of from 3 to 5 $\times$ 10^{-3} in. per in.,

[8] Ibid., Sect. 2.3.2.1.

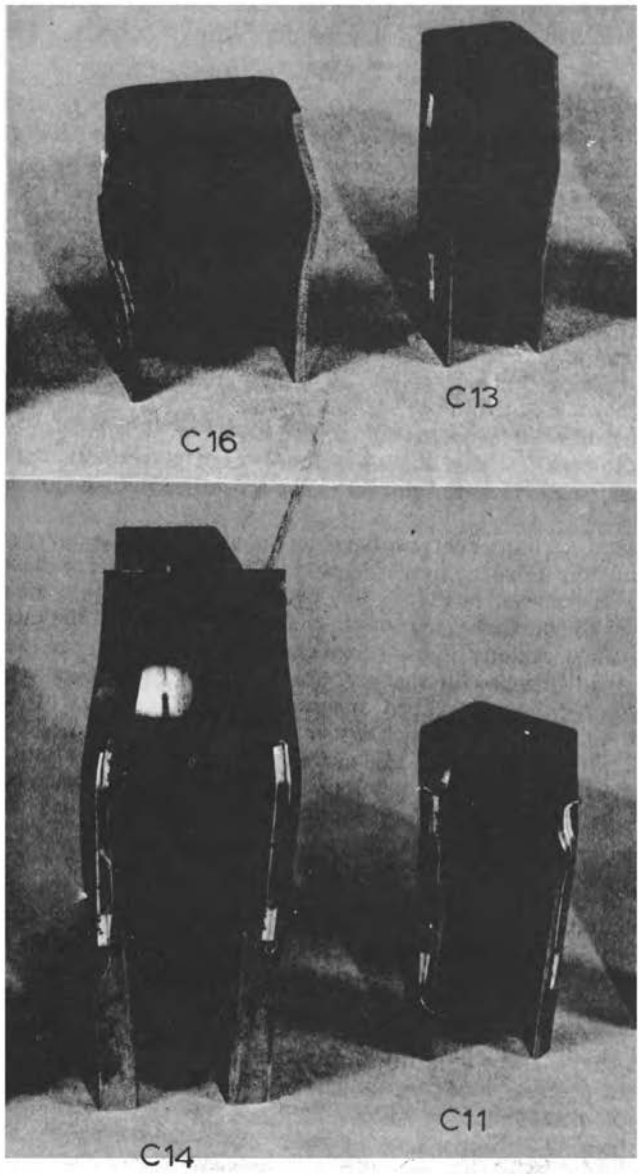

Fig. 8. Local buckling in stub column specimens.

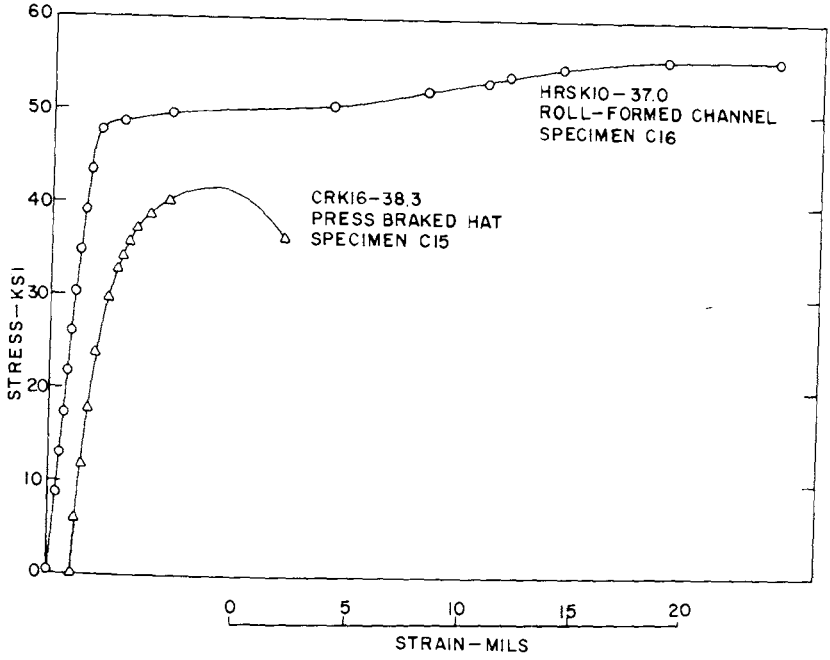

Fig. 9. Stress-strain curves showing contrasting behavior of compact and non-compact stub column specimens.

after which, the load dropped off sharply. The more compact 10-gage roll-formed channel and 9-gage joist chord specimens showed long yield plateaus and reached the ultimate load at much higher values of strain (i.e., 16 to 27 X 10^{-3} in. per in.). The behavior of the more compact shapes is similar to that of compact hot-rolled sections in such tests.[9] This may have some bearing with regard to the choice of safety factors for low slenderness compression members.

The main conclusions of the stub column investigation are as follows. The high value of corner yield strength is not completely effective in laterally-unsupported stub column tests of cold-formed sections because of local buckling in the flat plate elements which commences at or about the lower yield strength of the flats themselves. Therefore, the yield strength of laterally-unsupported full-section specimens is lower than that of similar specimens which are laterally supported. However, for the specimens tested,

[9] Haaijer, B., and Thurlimann, B., "On Inelastic Buckling in Steel," Journal of the Engineering Mechanics Division, ASCE, Vol. 84, No. EM2, Proc. Paper 1581, April, 1958.

this reduction was not large. The laterally-unsupported full-section compressive yield strengths were slightly larger than the full-section tensile yield strength for all sections tested except the one in which the two values were approximately equal. At working load levels, local distortions were not visible in any of the sections tested. The most compact stub columns exhibited stability to reasonably large values of plastic strain, i.e., had long stable yield plateaus. Because of local plastic buckling in the flat plate elements, the less compact sections, having reached the yield strength, exhibited instability at relatively low values of plastic strain, after which the load dropped off rapidly. These stub column findings will be used below in connection with column buckling in the inelastic range.

PREDICTION OF FULL-SECTION YIELD STRENGTH

Full-section tests, whether tensile or compressive, are tedious and time consuming. For this reason, it may be more convenient to correlate or predict the yield strength of the full section from simpler tests or from the virgin properties of the material.

It has been shown that the tensile may be used in lieu of the compressive full-section yield strength because the tensile yield strength is almost always slightly conservative when compared to the compressive full section or the stub column yield strengths. If, rather than the entire stress-strain curve, only the full-section tensile yield strength is desired, it may be calculated by simply taking a weighted average of the yield strengths of the corners, σ_{yc}, and flat elements, σ_{yf}, of the cross section. For the flats, the weighted average yield strength, σ_{yf}, may be obtained from coupon yield strengths by summing the product for each flat of the average yield strength for that flat and the ratio of the area in that flat to the total area of flats in the cross section. With σ_{yf} computed and the corner yield strength σ_{yc} computed from Eq. 1, the full-section tensile yield strength of the section is given by

$$\sigma_{ys} = C\,\sigma_{yc} + (1 - C)\,\sigma_{yf} \tag{6}$$

in which C is the ratio of corner area to total cross-sectional area. This is not an exact procedure, but even for gradual yielding materials, the error is quite small. For example, for a member made from a sharp yielding material such as the HRSK16-37.5 press braked hat of Fig. 7(*a*), the computation gives 65.8 $\times$ 0.08 + 39.7 $\times$ 0.92 = 41.8 ksi. Here 0.08 and 0.92 are the ratios of corner and flat areas to total cross sectional area, respectively. This compares favorably with the average tensile yield strength, 42.5 ksi, from the two full-section tension tests performed on this member. A similar computation for ultimate strength of this member gives: 69.5 $\times$ 0.08 + 49.5 $\times$ 0.92 = 51.0 ksi. This compares favorably with 51.1 ski obtained from full-section tension test T4.

Table 6. Calculated Versus Measured

Specimen Description	Virgin Yield Strength		Virgin Ultimate Strength σ_u, in kips per square inch	Inside Radius Divided by Thickness, a/t	Ratio of Corner Area, C	Calculated Tensile Corner Yield Strength, σ_{yc}, in kips per square inch
	Tensile σ_y, in kips per square inch	Compressive, in kips per square inch				
(1)	(2)	(3)	(4)	(5)	(6)	(7)
CRK16-38.3 press-braked hat	38.3	34.6	51.1	1.05	0.082	63.5
HRSK16-37.5 press-braked hat	37.5	40.5	49.0	1.00	0.082	61.2
HRSK16-37.5 roll-formed track	37.5	40.5	49.0	1.49	0.17	56.9
HRSK10-37.0 roll-formed channel	37.0	38.5	57.5	0.89	0.148	74.7
HRSK9-30.7 roll-formed joist chord	30.7	32.0	52.9	1.48	0.307	59.1

Full-section tensile yield strengths computed from Eq. 6, using the calculated corner yield strength, Eq. 1, for σ_{yc} are given in Col. 9 of Table 6 for a selection of five cold-formed cross-sections for which C (Col. 6) varies from 8% to 31%. The sections which have been chosen for illustrative purposes are shown in Figs. 7(*a*), 7(*b*), 7(*c*), and 7(*g*). Test values of the tensile full-section yield strength for each of these sections are given in Col. 10. Col. 7, σ_{yc}, was computed using Eqs. 1 through 5. Col. 8, σ_{yf}, gives the weighted average from tensile test specimens taken from the flats of the cold-formed members. The last two columns of Table 6 show the measured tensile and compressive full-section yield strengths divided by the calculated tensile full-section yield strength. The next to last column, computed by dividing Col. 10 by Col. 9 values, shows that the predicted values of tensile yield strength compare well with test values, being a maximum of 4% on the unconservative side. The last column, computed by dividing Col. 11 by Col. 9 values, shows the predicted

Full-Section Yield Strength

Average Flat Tensile Yield Strength, σ_{yf}, in kips per square inch	Calculated Tensile Full-Section Yield Strength, σ_{ys}, in kips per square inch	Full-Section Tests			Ratio of Tensile Yield Strength to Calculated tensile Full-Section Yield Strength	Ratio of Compressive Yield Strength to Calculated tensile Full-Section Yield Strength
		Tensile Yield Strength, in kips per square inch	Compressive Yield Strength, in kips per square inch	Ultimate Strength, in kips per square inch		
(8)	(9)	(10)	(11)	(12)	(13)	(14)
37.9	40.0	39.4	37.8	48.8	0.98	0.94
39.7	41.5	42.5	44.9	51.1	1.02	1.08
43.8	46.0	45.6	51.0		0.99	1.11
45.6	49.9	47.8	55.4	59.5	0.96	1.11
46.8	50.6	50.0	53.5	61.7	0.99	1.06

tensile yield strength to be conservative by 6% to 11% for all but one material, the press-braked hat section made from the cold-reduced killed material, where the difference is only 6% on the unconservative side.

No attempt is made to calculate full-section compressive properties because (1) the method of predicting the yield strength of corners used above, i.e., by Eq. 1, is based on basic material properties obtained from tensile tests,[4] and (2) the compressive strength was found to be somewhat larger than the tensile full-section yield strength for all sections except those formed from the cold-reduced killed material. However, for press-braked hats made from this material, the full-section yield strengths averaged not more than 4.5% lower in compression than in tension. Consequently, it appears that the design use of the tensile in lieu of the compressive full-section yield strength would be somewhat conservative in most cases and extremely close in those cases where the compressive is smaller than the tensile yield strength.

Inelastic Buckling Theory.—Axially-loaded columns with uniformly distributed materials properties buckle inelastically at a critical stress close to that given by the tangent modulus equation.[10]

$$\sigma_{cr} = \frac{\pi^2 E_t}{\left(\frac{L}{r}\right)^2} \tag{7}$$

in which E_t, the tangent modulus, replaces the modulus of elasticity in the Euler equation; L is the effective length of the column; and r is the radius of gyration in the plane of bending.

Osgood[11] extended the tangent modulus theory to cases where (because of the influence of residual stresses), the stress-strain characteristics are not uniform throughout the cross section of a column. His method of locating the neutral axis of monosymmetric cross sections appears to be questionable. A more rigorous approach is proposed as follows.

Consider a mono- or nonsymmetric column section such as that shown in Fig. 10. Assume that the section is constrained to buckle about the y-y axis.

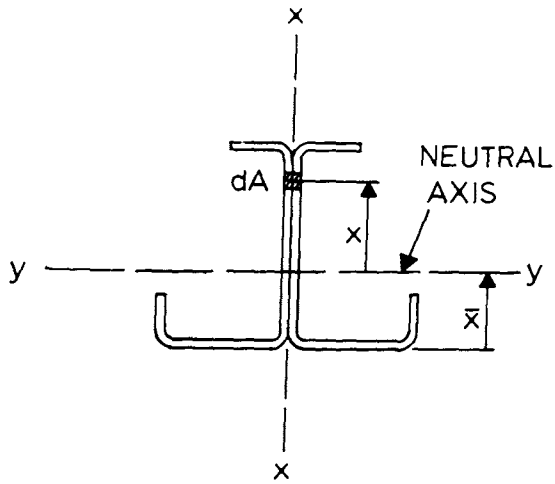

Fig. 10. Column cross section.

Also, assume that the stress-strain characteristics of the material are distributed symmetrically with respect to the x-x axis but not the y-y axis. The column is considered to be axially loaded, pin-ended, and perfectly straight.

[10] Shanley, F. R., "Inelastic Column Theory," The Journal of the Aeronautical Sciences, New York, N. Y. Vol. 14, No. 5, May, 1947, p. 261.

[11] Osgood, W. R., "The Effect of Residual Stresses on Column Strength," Proceedings, 1st U. S. Natl. Congress of Applied Mechanics, New York, N. Y., June, 1951.

It is further assumed that the column has been compressed beyond the proportional limit. The minimum load at which such an ideal column can, and generally will, begin bending is the tangent modulus load.[10] Therefore, at a load infinitesimally smaller than the tangent modulus load, the column will have uniform compressive strains. However, because the column is stressed beyond the proportional limit, the compressive stress is not uniform in the cross section. Let $\bar{x}$ be the distance from an arbitrary reference line to the neutral axis y-y. The distance $\bar{x}$ must be such that

$$M = \int_A \sigma x \, dA = 0 \tag{8}$$

in which x = the distance from the neutral axis y-y to an element of area dA as shown in Fig. 10.

A procedure for establishing a column curve for such a section is outlined as follows: (1) Assume a value of strain ϵ above the proportional limit; (2) establish the stress distribution in the cross section from known stress-strain relationships of the individual elements of the cross section, (for example, see the stress-strain curves in Fig. 11); (3) establish the location of the neutral axis for this strain by trial from Eq. 8; (4) compute the average stress corresponding to ϵ from

$$\sigma_{cr} = \frac{1}{A} \int_A \sigma \, dA \tag{9}$$

(5) in Eq. 7, because the tangent modulus is not constant, it must be retained inside the integral for flexural rigidity, $\int_A E_t x^2 \, dA$. Find the column length, L, corresponding to σ_{cr} of Eq. 9 from

$$\sigma_{cr} = \frac{\pi^2}{A L^2} \int_A E_t x^2 \, dA \tag{10}$$

Divide L by the radius of gyration r (computed without regard to the distribution of materials properties) to obtain the slenderness ratio; (6) repeat steps (1) through (5) for various assumed values of ϵ and plot the column curve.

Yang, Beedle, and Johnston[12] further modified the tangent modulus theory and applied it to steel wide-flange columns subject to residual cooling stresses. This investigation was continued and completed in 1954 by Huber and Beedle.[13] Even though, as yielding progresses, the residual stresses are eliminated and all of the material finally ends up at the same yield stress, the

---

12 Yang, C. H., Beedle, L. S., and Johnson, B. G., "Residual Stress and the Yield Strength of Steel Beams," Welding Journal, New York, N. Y., (Research Supplement), Vol. 31, No. 4, 1952, pp. 205s–229s.

13 Huber, A. W., and Beedle, L. S. 'Residual Stress and the Compressive Strength of Steel," Welding Journal, New York, N. Y.. (Research Supplement), Vol. 33, 1954, pp. 589s–614s.

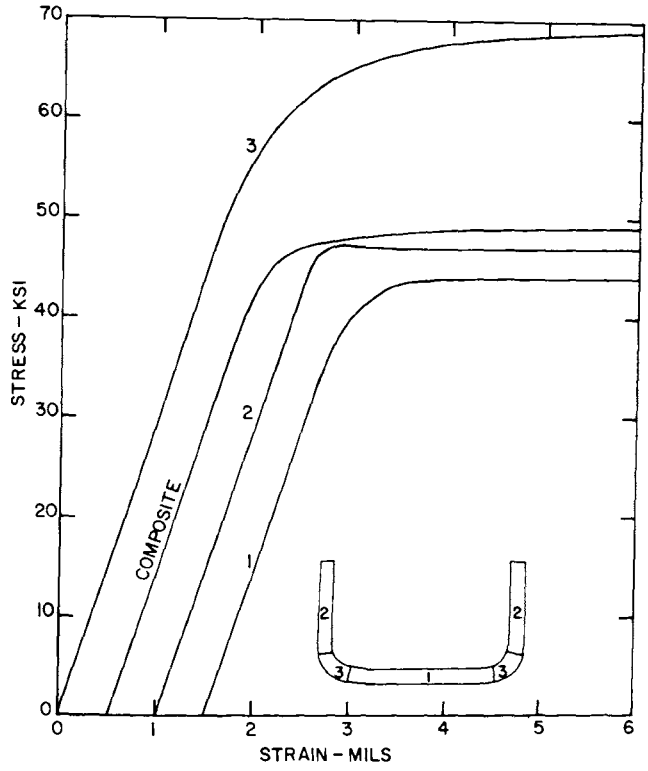

Fig. 11. Tensile stress-strain curves for elements of HRSK10-37.0 channel sections.

presence of residual stresses lowers the buckling load of compression members in the inelastic range. That part of the cross section with the highest compressive residual stress yields first. Theoretical column curves are obtained by considering that only the moment of inertia of the unyielded part of the cross section is effective. The critical stress σ_{cr} (i.e., the buckling load divided by the total cross-sectional area) may be found from

$$\sigma_{cr} = \frac{\dfrac{\pi^2 E I_e}{I}}{\left(\dfrac{L}{r}\right)^2} \tag{11}$$

in which I_e = the moment of inertia of the unyielded part of the cross section, I = the moment of inertia of the total cross section, and E = the modulus of elasticity of the idealized material. Note that Eq. 11 is a special case of Eq. 10.

In 1952, F. Bleich[14] proposed a parabolic equation

$$\sigma_{cr} = \sigma_y - \frac{\sigma_p (\sigma_y - \sigma_p)}{\pi^2 E} \left(\frac{L}{r}\right)^2 \tag{12}$$

as an approximation for the tangent modulus equation (Eq. 7). Eq. 12 may not be used for $\sigma_p < 1/2\ \sigma_y$. If the proportional limit, σ_p is taken as one-half the yield strength, σ_y, Eq. 12 becomes

$$\sigma_{cr} = \sigma_y - \frac{\sigma_y^2}{4 \pi^2 E} \left(\frac{L}{r}\right)^2 \tag{13}$$

Eq. 13 applies for short and intermediate length columns for which the slenderness ratio, L/r, is less than $\sqrt{2\ \pi^2 E/\sigma_y}$. Of course, for larger L/r ratios, the Euler equation for elastic buckling applies. In 1960, the Column Research Council (CRC) proposed[15] the use of Eq. 13 as a compromise between the strong and weak axis buckling curves obtained in the Lehigh University residual stress study.[13] Eq. 13 is sometimes referred to as the "CRC formula." It was adopted as the basic column design formula for the specification of the American Iron and Steel Institute (AISI)[16] in 1946 and for that of the American Institute of Steel Construction (AISC)[17] in 1961.

Peterson and Bergholm[18] applied Osgood's development to bisymmetric members in which the tangent modulus of the material is not constant throughout the cross section. Here, all of the material does not end up at the same yield stress after complete plastification of the section. For bisymmetric sections, the neutral axis is located at the geometric center of the cross section. If the cross section were composed of j subareas, having constant materials properties over each subarea, Eq. 10 could be written as

$$\sigma_{cr} = \frac{\pi^2}{A L^2} \sum_{i=1}^{j} E_{ti} I_i \tag{14}$$

---

[14] Bleich, Friedrich, Buckling Strength of Metal Structures, McGraw-Hill Book Co., Inc., New York, N. Y., 1952.

[15] "Guide to Design Criteria for Metal Compression Members," Column Research Council, New York, N. Y., 1960.

[16] "Specification for the Design of Light Gage Cold-Formed Steel Structural Members," Amer. Iron and Steel Inst., New York, N. Y., 1962.

[17] "Specification for the Design, Fabrication, and Erection of Structural Steel for Buildings," Steel Construction Manual, Amer. Inst. of Steel Construction, New York, N.Y., 1963.

[18] Peterson, Robert E., and Bergholm, Axel O., "Effects of Forming and Welding on Stainless Steel Columns," Aerospace Engineering, Inst. of Aerospace Sciences (presently, Amer. Inst. of Aeronautics and Astronautics), New York, N. Y., Vol. 20, No. 4, April, 1961.

in which E_{ti} is the tangent modulus of the i^{th} subarea at a particular value of strain, and I_i is the moment of inertia of the i^{th} subarea about the neutral axis of the total cross section. By application of a form of Eq. 15, Peterson and Bergholm were able to obtain excellent correlation between experimental critical stresses and analytical column curves for compact bisymmetric sections fabricated from stainless steel.[18]

The method of Eq. 14 is better suited for application to the tests described herein than the method of Eq. 11 because: (1) The effects of residual stresses on the stress-strain curves of the cold-formed full-section specimens tested were found to be negligible; (2) the main factor that affects behavior of hot-rolled steel sections is that of residual stresses, whereas in cold-formed steel shapes, as in stainless steel columns, the main factor involves changes in materials properties caused by cold working; and (3) the stress-strain curves of corners from cold-formed members are gradual yielding rather than sharp yielding as is assumed in the use of Eq. 11. The analysis of two different cold-formed column shapes by means of Eq. 14 is examined below.

Column Test Specimens.—Several lengths of each of two types of bisymmetric column cross sections (Fig. 12) were built up by connecting monosymmetric sections back to back. These shapes were fabricated from roll-formed 10-gage HRSK10-37.0 channels and 9-gage HRSK9-30.7 joist chords. Six channel columns were fabricated by bolting at 2-in. centers with 3/16-in. mild steel bolts. Two channel and four joist chord columns were fabricated by cold-riveting with 3/16-in. rivets at 1-in. centers. Both of the column shapes tested had a value of $Q = 1$.

Column Test Procedures.—The milled ends of the columns were supported on knife-edge fixtures parallel to and in the plane of the weak axis of the specimens. The weak axes of the columns were placed in the plane of the screws of the testing machine. Type SR-4 strain gages were mounted at the two quarter points at the center of each specimen as shown in Fig. 12. Four dial gages (one at the upper head, at each quarter point, and at the center point) were arranged to measure deflection perpendicular to the weak axis of the columns (Fig. 13).

The columns were centered geometrically before any load was applied. The centering was checked and adjusted in trial runs in which the maximum applied load was approximately two-thirds the theoretical maximum load. Eccentricity adjustments, by means of opposing pairs of set screws were made with the dual objectives of minimizing differences in strain readings and of minimizing deflections.

Opposing gages were read in pairs to eliminate possible local bending effects from the strain readings. All of the sets of gages were read up to a load of about two-thirds the analytical buckling strength, after which only the center-line gages were read. Deflections were measured at stages throughout the loading. Straining was continued in several of the specimens until the stabilized load had decreased to about two-thirds the maximum load attained.

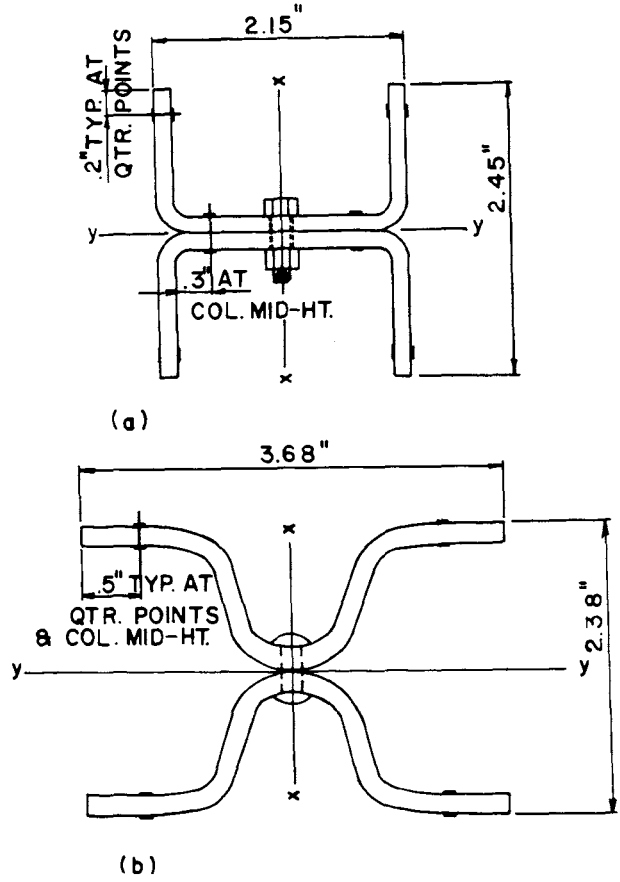

Fig. 12. SR-4 strain-gage locations for column test specimens.

Once the maximum load had been reached, strain and deflection readings were taken only after the load and strains had stabilized.

No correction was necessary for the larger moment of inertia of the end fixtures for these tests of axially loaded pin-ended columns.[19]

Results of Column Tests.—Eq. 14 was used to develop analytical curves for comparison with test data obtained for weak axis buckling of the channel and joist chord columns.

The procedure was as follows:

1. The area of the cross section was divided into three or more regions. Each area was considered to have constant stress-strain characteristics. For

---

[19] Osgood, W. R., "Column Strength of Tubes Elastically Restrained Against Rotation at the Ends," NACA (presently NASA), Washington, D. C., Report No. 615, 1938.

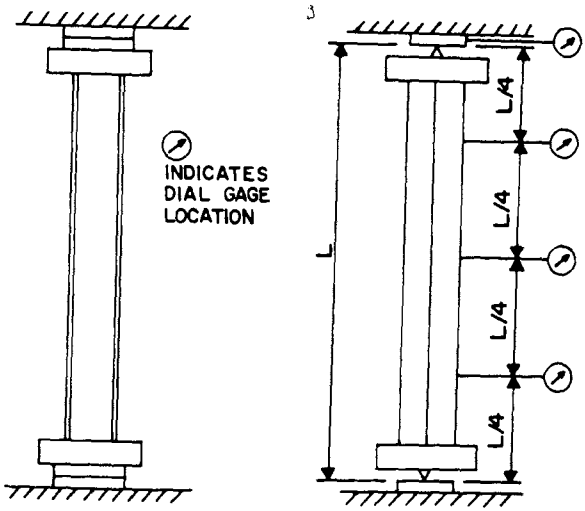

Fig. 13. Schematic of test arrangement for axially loaded pin-ended columns.

example, the channel was divided into three regions as shown in Fig. 11.

2. Average stress-strain curves were established for each region of the cross section from tensile and compressive corner and flat specimens. Tensile and compressive composite stress-strain curves were computed for the full sections.
3. The tangent moduli of the stress-strain curve of each region were determined graphically for a number of convenient values of strain.
4. The stress corresponding to each of the above-mentioned strains was read from the composite stress-strain curve. Each of these values represents the average stress, σ_{cr}, on the section at a particular value of strain.
5. The section properties of the full section and of each of the subregions were computed.
6. For each value of strain chosen, the values of E_t and σ had now been determined. Values of I and I_i were computed for the section. The slenderness ratio L/r corresponding to σ_{cr} was calculated from Eq. 14. Theoretical column curves were computed in this manner based separately on the compressive and tensile stress-strain curves of flat and corner cross-sectional elements.

Column curves for weak-axis buckling are compared to experimental column buckling stresses in Figs. 14 and 16. Column curves for strong axis buckling are included in Figs. 15 and 17. Direct application of the tangent modulus theory (Eq. 7) to cold-formed members using stress-strain curves from stub column tests, is not a completely rigorous procedure. However,

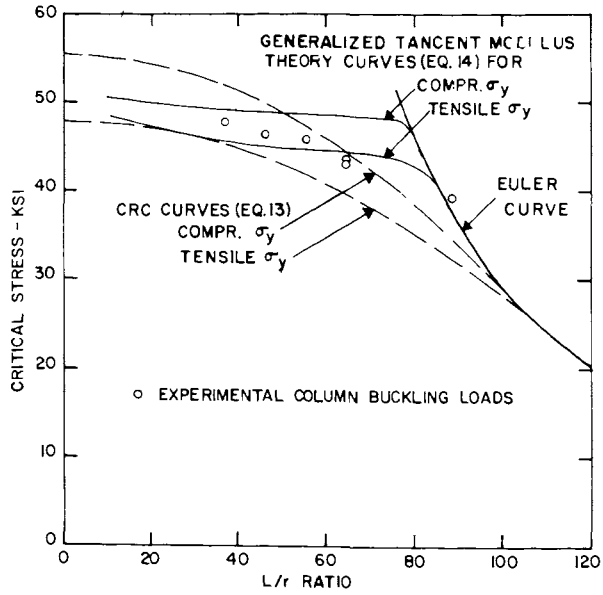

Fig. 14. Test results for inelastic buckling of 10-gage channel columns

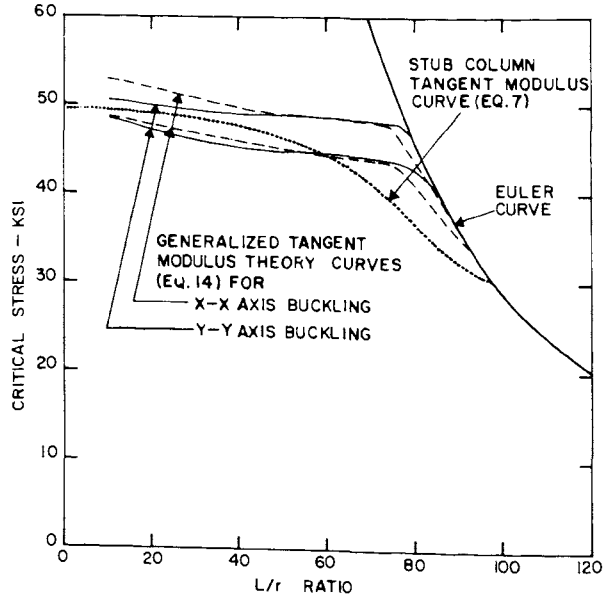

Fig. 15. Comparison of column curves for 10-gage channel columns.

column curves so obtained are shown in Figs. 15 and 17. These Eq. 7 column curves are based on tangent moduli from the stress-strain curves of stub column specimens C9 and C27, respectively. Curves plotted from the CRC formula (Eq. 13), are included in Figs. 14 and 15. Average values of the 0.2% offset yield strength from tensile and compressive full-section tests (values are given in Table 4) were used for this purpose.

The column curve calculated from Eq. 14 and based on tensile properties is lower than that based on compressive properties for both the channel and the joist chord columns. The difference between the two curves is larger for the channel columns (Fig. 14) than for the joist chord columns (Fig. 16). For the former, the experimental points correlate better with the Eq. 14 curve computed from the tensile than from the compressive stress-strain curves, for L/r ratios smaller than 60. This is reasonable because local plastic buckling reduced the compressive yield strength 11% from an average of 55.4 ksi for laterally supported specimens to an average of 49.1 ksi for laterally unsupported full-section compression specimens. The latter value is close to the average full-section tensile yield strength of 47.8 ksi. For L/r ratios less than 60, the experimental points fall between the two Eq. 14 curves and are close to the Eq. 7 curve. For the joist chord columns of Fig. 16, the experimental maximum column stresses appear to correlate better with the Eq. 14 curve based on the tensile than with the compressive properties for L/r ratios greater than 70. However, the difference between these two curves is quite small for the joist chord columns. For L/r ratios less than 70, the experimental points fall closer to the compressive than the tensile Eq. 14 curve and are closest to the Eq. 7 curve. For both channel and joist chord columns, there is little difference between the column curves for strong and weak axis buckling.

For both kinds of columns, the upper CRC curve (Eq. 13), based on the average, laterally supported compressive full-section yield strength, gives unconservative predictions for critical stress for L/r values less than 65 (Figs. 14 and 16). The lower CRC curve, based on the average full-section tensile yield strength, gives conservative and reasonable results over the entire inelastic range. Furthermore, if the lower CRC curves were plotted on Figs. 15 and 17, they would form bound curves to all of the other column curves for both the channel and joist chord columns.

In summary, the following conclusions may be drawn from the results of tests of axially loaded pin-ended columns. Analysis of two compact cold-formed column shapes by means of a generalized tangent modulus equation (Eq. 14) gives column curves in good agreement with test results. Exact agreement cannot be expected because: (1) The influence of local plastic buckling cannot be completely eliminated, even in compact shapes; (2) there is a variation in the yield strength of the steel within even a modest-size sheet; (3) there is, undoubtedly, some error involved in obtaining stress-

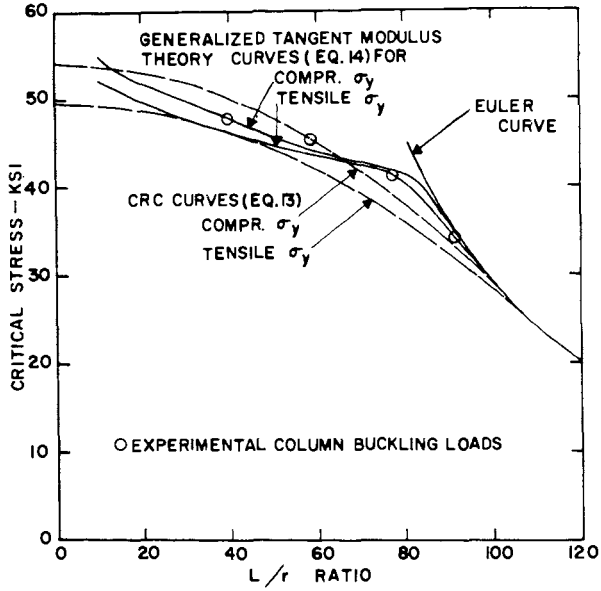

Fig. 16. Test results for inelastic buckling of 9-gage joist chord columns.

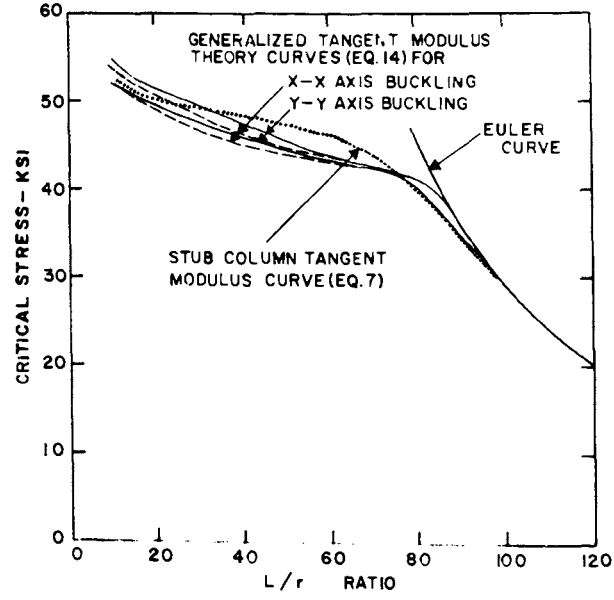

Fig. 17. Comparison of column curves for 9-gage joist chord columns.

strain curves and in determining tangent moduli from them; and (4) there are unavoidable imperfections in cold-formed column specimens.

Despite these minor sources of error, the analytical method used (Eq. 14) gives good correlations with test data. Alternatively, column curves obtained by direct application of the tangent modulus equation (Eq. 7), using stress-strain curves from stub column tests, were either on the conservative side of or close to experimental values. It was also found that for design simplification, the CRC column curve gives conservative and reasonable results when based on the full-section tensile yield strength. Alternatively, it would be reasonable to use the laterally unsupported full-section compressive yield strength for this purpose, but it would not be conservative to use the laterally supported full-section compressive yield strength in this manner.

Both materials in these two cold-formed shapes were hot-rolled semikilled, i.e., aging, steels with the proportional limit equal to or greater than one-half the yield strength. If a cold-reduced nonaging steel (such as the cold-reduced killed sheet steel) with a gradual yielding stress-strain curve having a proportional limit less than one-half the yield strength were used, Eq. 13 would not be applicable.

SUMMARY AND CONCLUSIONS

1. The yield strength of corners, cold-formed either by roll-form or press brake, was measured to be up to 102% larger than the virgin yield strength of the material.[4] The increase in tensile ultimate strength is not as large, up to 47% of the virgin value in this investigation. The stress-strain curves of corner specimens are gradual yielding because of the varying amounts of plastic strain throughout the corner. The reduction in percentage elongation of corners as compared to that of the virgin material may be as large as 90%. Full details on cold-formed corners are available.[4]
2. In the flat portions of cold-formed sections, increases in yield strengths may be attributed mainly to (1) the strain hardening and aging from stretcher-straightening of sheets stored as coils and (2) the normal pressures present in the roll-forming operation. Item (1) is the only factor that contributes significantly to the increase in yield strength of the flats of press-braked members. Both factors contribute to the increase in yield strength of flats of roll-formed members.

   The largest tensile yield-strength increase for flats found in this investigation was 52% for the roll-formed joist chord section made from hot-rolled semikilled steel. For press-braked sections, the change in the tensile yield strength of flats was +6% for the hat section made of hot-rolled semikilled steel and −1% for the hat section made of cold-reduced killed steel. (Percentage increases in compressive yield strengths were approximately the same as for the tensile yield strength.) It follows

that roll-forming produces larger increases in yield strength in the flats than brake-forming, and that larger increases are found in flats made from aging materials than from nonaging materials. For practical purposes, the yield strength in flats of press-braked material may be taken as the virgin value. If it is desired to use the increases in yield strength in the flats of roll-formed members, they may be determined from tension coupons cut from the cold-formed members.

Percentage increases in ultimate tensile strength of flats resulting from the cold work of forming were much smaller than the increases in yield strength. The maximum percentage increase in ultimate strength was 10% for the flats of the roll-formed joist chord mentioned in 3 above. The change in ductility of cold-formed flats is generally quite small. The largest reduction in percentage elongation (as compared to that of the virgin material) was 26% for the same roll-formed joist chord.

3. Regarding behavior of full cold-formed sections, the following conclusions and trends may be seen from studying the test results.
   a. Composite stress-strain curves calculated from the stress-strain curves of strip specimens from the flats plus those of corner specimens match the stress-strain curves for both tensile and laterally supported full-section test specimens quite well. This implies that any longitudinal residual stresses which may be released by the cutting of strip specimens are sufficiently small so that they have no significant effect on the mechanical properties of the full section.
   b. Increases above virgin values in both the full-section tensile and full-section compressive yield strengths were larger for the roll-formed sections than for the press braked sections tested.
   c. Compressive yield strengths of laterally supported full-section specimens were higher than the full-section tensile yield strengths for all the sections except for the press-braked hat section made of cold-reduced killed steel.
   d. Compressive yield strengths of laterally supported full sections were larger than yield strengths of unsupported stub columns for all of the sections except for the same hat section. Local plastic buckling of the flat plate elements at or slightly above the compressive yield strength of the flats prevented the higher yield strength of corners from becoming fully effective. However, the maximum stress reached in the stub columns was slightly larger than the full-section tensile yield strength for all sections except the same press-braked hat section.
   e. Local buckling of flats did not become noticeable in the most compact stub column sections until the maximum stub column load was reached. For the less compact sections, local buckling of flats became visible at loads about 10% to 20% less than the maximum

stub column loads. Therefore, it can be assumed that distortions at working loads would not be serious in any of these sections.

f. The least compact specimens, the 16-gage press-braked channel, lipped angle, and hat sections of Fig. 7(*d*), 7(*e*), and 7(*f*) reached the ultimate compressive load at strains in the range of from 3 to 5 $\times$ 10^{-3} in. per in., after which the load dropped off suddenly. The more compact sections, the roll-formed 10-gage channel and 9-gage joist chord specimens of Figs. 7(*c*) and 7(*g*) showed long, stable yield plateaus and reached the ultimate load at much higher values of strain, i.e., from 16 to 27 $\times$ 10^{-3} in. per in. This difference in behavior may have significance with regard to the choice of safety factors for column design, i.e., a higher safety factor may be indicated for the less compact sections.

g. Percentage increases in the full-section ultimate strength values were much smaller than in either the tensile or the compressive yield strengths.

h. The final percentage elongation in 2 in. appears to be in excess of 30% for both roll-formed and press-braked full-section tensile specimens (Table 3 and 4) showing that all sections, including those with large increases in yield strength, still have ample ductility.

4. Determination of the full-section tensile yield strength by calculation rather than by full-section testing requires a sufficient number of standard tensile coupon tests of the virgin steel to establish representative yield and ultimate strengths, σ_y and σ_u, for the material. With these material properties established, the corner tensile yield strength, σ_{yc}, may be calculated from Eqs. 1 through 5. Next, the average tensile yield strength of the flats, σ_{yf}, is established from standard tensile coupons, taken from the flats of cold-formed sections. The value of σ_{yf} may be substantially larger than σ_y, particularly in roll-formed sections. However, if it is not considered worthwhile to test to determine σ_{yf}, σ_y may be used conservatively in its place. The full-section tensile yield strength, σ_{ys}, may then be computed from Eq. 6.
5. The full-section compressive yield strength may be satisfactorily approximated by the calculated tensile yield strength. This is true because the tensile full-section yield strength was found to be slightly smaller than either the stub column or the laterally supported full-section compressive yield strengths for all sections tested except a hat section press braked from the nonaging cold-reduced killed material. See Conclusions 3(c) and 3(d).
6. The aging and nonaging steels tested in this investigation show marked differences in materials properties, both before and after cold-forming. Only one of these, the cold-reduced killed steel, could be classified as nonaging. This steel has a gradual yielding stress-strain curve both before and after cold-forming. The other, i.e., the aging, steels have sharp yielding

stress-strain curves before cold-forming and either sharp or gradual yielding stress-strain curves after cold-forming, depending on the type and amount of cold work involved.

7. Tests of axially loaded pin-ended columns were made on eight specimens fabricated by bolting or cold-riveting two roll-formed 10-gage channels back to back, and on four specimens fabricated by cold-riveting 9-gage roll-formed joist chord sections together. Both of these compact shapes had a value of $Q = 1$, where Q is defined by the AISI. Direct application of the tangent modulus theory by using the stress-strain curve from a stub column or other full-section test is not a completely rigorous procedure. Therefore, analytical column curves for these two column shapes were computed from stress-strain curves of flats and corner coupons taken from the cold-formed sections. A generalized form (Eq. 14) of the tangent modulus equation for column buckling (Eq. 7) was used for this purpose. Column test results were found to be in best agreement with the analytical (Eq. 14) column curves based on tangent moduli obtained from tensile corner and flat specimens from column cross sections. The use of stub column stress-strain properties in the tangent modulus equation (Eq. 7) gave column curves which were close to experimental results for slenderness ratios smaller than about 65 and which were conservative for larger slenderness ratios.
8. For design simplification, it was found that the CRC column curve (Eq. 13) gives conservative and reasonable results when based on either the full-section tensile or the stub column compressive yield strength.

ACKNOWLEDGMENTS

This investigation is part of a continuing research program regarding light-gage cold-formed steel structures, sponsored at Cornell University, Ithaca, N. Y., by the American Iron and Steel Institute.

The unfailing cooperation of W. G. Kirkland, Vice-President, AISI, Tappan Collins, Chairman of the Light-Gage Steel Subcommittee, and C. R. Clauer, Chairman of the Task Group on the Effects of Cold Work, is gratefully acknowledged.

APPENDIX.–NOTATION

The following symbols are used in this paper:

A = cross-sectional area;
a = inside corner radius;
b, n = empirical constants;

C = ratio of corner area to total cross-sectional area;
E = initial modulus of elasticity of a material;
E_t = tangent modulus of a stress-strain curve at a point above the proportional limit;
E_{ti} = tangent modulus of the i^{th} element of a cross section;
I = moment of inertia of a complete cross section;
I_e = moment of inertia of the unyielded part of a partially yielded cross-section;
I_i = moment of inertia of the i^{th} element of a cross section about the neutral axis of the total cross section;
k = strength coefficient, having same units as stress;
L = effective length of a column;
n = strain hardening exponent, nondimensional;
Q = "form factor," used in the design of sections containing one or more flat plate elements with large w/t ratios; its purpose is to provide safety against local buckling[7];
r = radius of gyration in the plane of bending;
t = thickness of sheet, element, or corner;
x = a variable of integration or of distance;
y = vertical distance of a point from midsurface of undeformed sheet (except where defined otherwise);
σ = allowable column design stress;
σ_{cr} = stress at the critical buckling load of a member;
σ_p = proportional limit determined by 0.02% offset method;
σ_u = ultimate strength;
σ_y = yield strength determined by 0.2% offset method;
σ_{yc} = yield strength of corner;
σ_{yf} = yield strength of flats of cold-formed member; and
σ_{ys} = yield strength of full section.

EFFECTS OF COLD-FORMING ON LIGHT-GAGE STEEL MEMBERS[a]

Discussions by Max Reiss and John N. Macadam

MAX REISS.[20]—In comparing the test results of a 16 gage H. R. press braked channel section with the results predicted by the use of the form factor[21] Q, the authors have found a significant difference of about 24% and conclude that the form factor requirements may be conservative for some sections.

The first point made by the authors in explanation of the discrepancy relates to the aspect ratio. It is known that the critical buckling stress of a plate

$$\sigma_{cr} = \frac{k\pi^2 E}{12(1-\nu_x^2)} \left(\frac{t}{b}\right)^2 \tag{15}$$

is a function of the aspect ratio $1/b$. For the tested channel and the aspect ratios of the web $1/b_w = 4$ and the flange $1/b_f = 3.70$, there is only a slight deviation from the minimal stress factor k (Fig. 18). The critical buckling stress of a whole section can similarly be described by

$$\sigma_{cr} = \frac{k_w \pi^2 E}{12(1-\nu^2)} \left(\frac{t}{b_w}\right)^2 \tag{16}$$

in which the stress factor k_w is dependent on the aspect ratio and can be seen (Fig. 18) to be practically equal to the minimum for the given aspect ratio. This confirms that the aspect ratio has only a minor effect in this case.

The second point considered by the authors relates to the neglect of the transverse continuity in the Q factor. The Q factor of a member composed of stiffened and unstiffened members is based on the assumption that the useful limit will be reached when its weakest unstiffened element buckles.[22]

In the case under discussion an estimate of the ultimate strength of the section is required. The ultimate strength of a single stiffened element can be predicted by Winter's empirical equation[23]

---

[a] February, 1967, by Kenneth W. Karren and George Winter (Proc. Paper 5113).

[20] Visiting Prof., University Coll., London, England,

[21] Light-Gage Cold-Formed Steel Design Manual, American Iron and Steel Institute, 1962.

[22] Winter, G., commentary on Light-Gage Cold-Formed Steel Design Manual, American Iron and Steel Institute, 1962.

[23] Winter, G. "Cold-Formed, Light-Gage Steel Construction," Journal of the Structural Division, ASCE, Vol. 85, No. ST9, Proc. Paper 2270, Nov., 1959.

$$\sigma_{max}/\sigma_y = (\sigma_{cr}/\sigma_y)^{1/2} [1-0.25 (\sigma_{cr}/\sigma_y)^{1/2}] \quad (17)$$

which is based on many experiments and has been adopted in the AISI Specifications for light gage steel cold-formed steel elements. From a comparison of this equation with Winter's experimental results for unstiffened

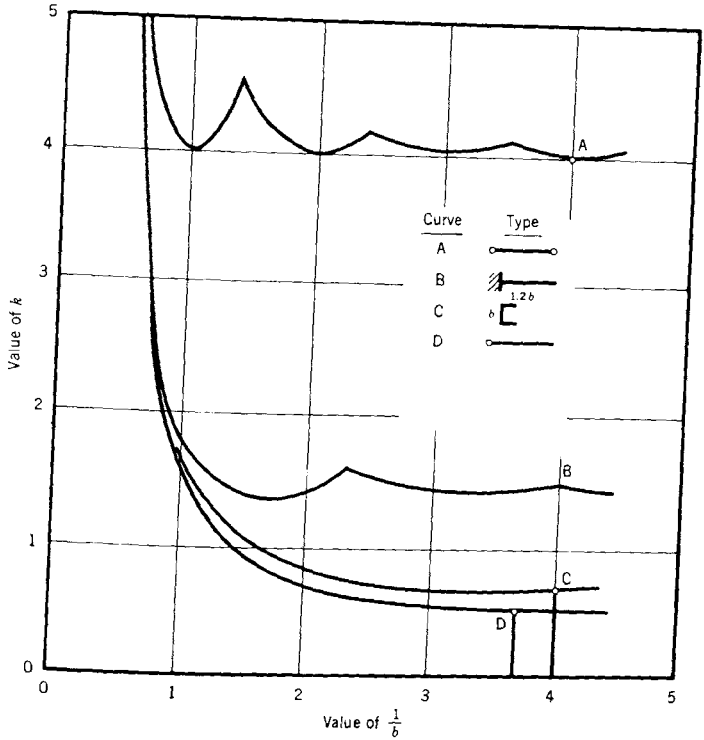

Fig. 18. Buckling coefficients.

plates,[24] it appears that the same equation can be used to predict the ultimate buckling stress of unstiffened plates as well. Furthermore, the same relationship holds for whole sections if the critical stress for the whole transversely continuous section from Eq. 16 is used. This can be seen in Fig. 20, where Eq. 17 is compared with the results of some 200 collapse tests on short length steel struts (Fig. 19).[25]

[24] Winter, G., commentary on Light-Gage Cold-Formed Steel Design Manual, American Iron and Steel Institute, p. 20.

[25] Kenedi, Chilver, A. H., Griffin, and Smith, "Cold Formed Sections in Britain," International Association for Bridge and Structural Engineers, Vol. 20, 1960, pp. 137–150.

Hertel[26] has come to the same conclusion, that a single function can describe the average collapse stress of plates and sections.

Computing the critical stress for the discussed channel section

$$\sigma_{cr} = \frac{k_w \pi^2 E}{12(1-\nu^2)} \left(\frac{t}{b_w}\right)^2 = \frac{0.69 \pi^2 E}{12(1-\nu^2)(15.5)^2} = 76.5 \text{ ksi}$$

in which k_w is a factor defining the minimum buckling stress of the whole

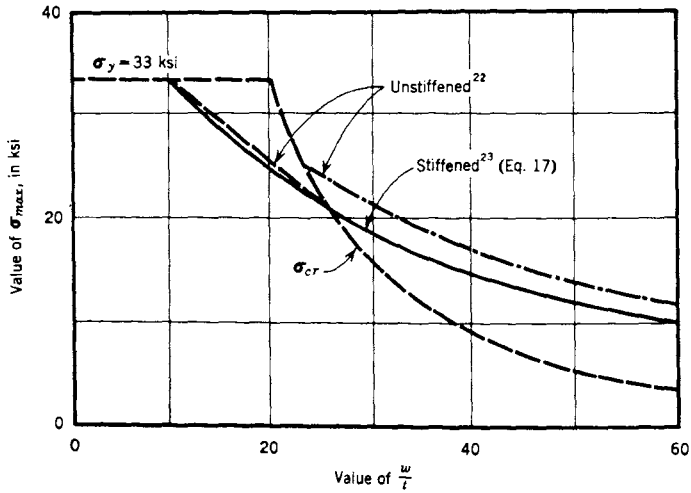

Fig. 19. Ultimate buckling stress of unstiffened elements.

section,[27] and inserting this in Eq. 17, the ultimate stress for the whole section is computed as

$$\sigma_{max} = 44.3\,(76.5/44.3)^{1/2}\,[1-0.25\,(76.5/44.3)^{1/2}] = 39.0 \text{ ksi}$$

which differs by only 9% from the test results.

It might be appropriate to mention here that the form factor may overestimate the strength of a section. This is discussed elsewhere[28] and will be demonstrated by the example of a lipped channel (Fig. 21) with a yield stress of σ_y = 44.3 ksi. The form factor for this section is Q = 0.89. From the critical stress of the whole section,

---

26 Hertel, H., Leichtbau, Springer Verlag, Berlin, Germany, 1960.

27 Sutter, K., "The Local Buckling of Aluminum Plate Elements," RP-83, Aluminum Development Association, 1959.

28 Chilver, A. H., and Reiss, M. "A Note on the Computation of Post-buckling Strength," (to be published).

$$\sigma_{cr} = \frac{k_w \pi^2 E}{12(1-\nu^2)} \left(\frac{t}{b_w}\right)^2 = \frac{5.5 \pi^2 E}{12(1-\nu^2)(60)^2} = 40.4 \text{ ksi}$$

in which k_w has been taken from Chilver.[29] The ratio of the ultimate

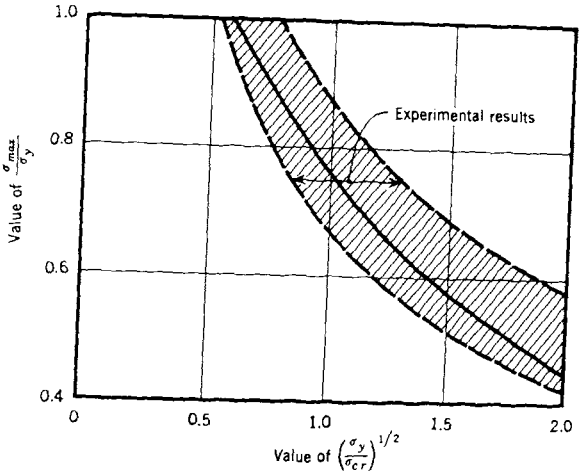

Fig. 20. Comparison of eq. 17 with results of collapse tests.

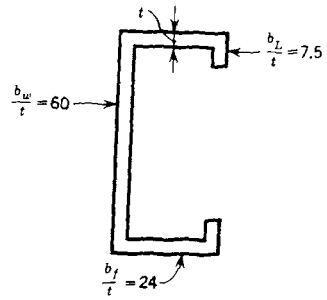

Fig. 21

buckling stress to yield stress is computed by

$$\sigma_{max}/\sigma_y = (40.4/44.3)^{1/2} [1-0.25(40.4/44.3)^{1/2}] = 0.73$$

It can be seen that this is smaller than the form factor, the difference being 18% on the unsafe side. These comparisons seem to suggest that the validity of the Q method should be reviewed completely.

[29] Chilver, A. H., "Structural Problems in the Use of Cold-Formed Steel Sections," Proceedings, Institution of Civil Engineers, 1961, pp. 233-250.

JOHN N. MACADAM,[29] M. ASCE.—Karren and Winter have presented a significant contribution to the understanding of structural members cold-formed from light gage steel. Now designers should be able to achieve some economy by taking advantage of this as-formed strength in many applications.

The writer has investigated the effects of cold forming on three light gage lipped-channel sections (Fig. 22); (1) 6 in. by 2-1/2 in. by 0.06 in. thick (designated 0.06-37), 37,000 psi minimum yield strength, mechanically capped heat—hot rolled roll-formed; (2) 6 in. by 2-1/2 in. by 0.09 in. thick (designated 0.09-50), 50,000 psi minimum yield strength, mechanically

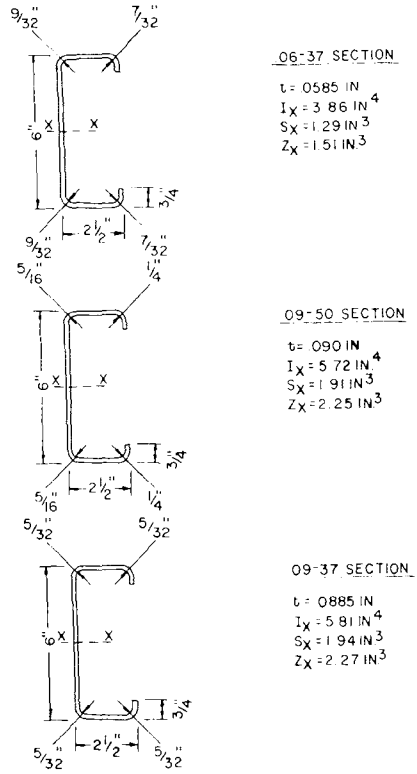

Fig. 22. Cold-formed lipped-channel sections.

capped phosphorus bearing heat—hot rolled roll-formed; and (3) 6 in. by 2-1/2 in. by 0.09 in. thick (designated 0.09-37), 37,000 psi minimum yield strength, mechanically capped heat—hot rolled press-brake-formed.

In a manner similar to that used by Karren and Winter, tension and compression coupon tests were made to show the variation of cold work effects

[29] Research Engr., Armco Steel Corp., Middletown, Ohio.

around the cross section. Full section tension tests were compared to the weighted average of the coupon tests. In addition, beam tests were made to verify the utilization of cold-work-increased properties in response to flexural loading.

Although Karren and Winter do not mention flexural members, the Light Gage Design Specification,[16] since 1962, has permitted use of increased properties from cold forming in the design of sufficiently compact flexural members. In this case, the specification stipulates tests on flange section specimens to determine the yield point. Such specimens are to consist of one complete flange plus a portion of the web of such flat width ratio that the value of Q for the specimen is unity. The yield point to be used is the lower of the values determined in tension and compression tests. Flange section tension and compression tests were made on each of the three sections in accordance with these requirements.

Each section was subdivided into small coupon elements as shown in Fig. 23. Tension yield strength variations around the cross section are shown graphically in Figs. 24, 25, and 26. Compression yield strength results vary in a similar manner. Although flat strip properties were not obtained, it is reasonable to assume that the average of the interior flat element properties represents the virgin material properties for these sections.

Increases in corner yield strength from 30% to 60% occur in the corner elements due to cold work. A slight increase in yield strength of the flat

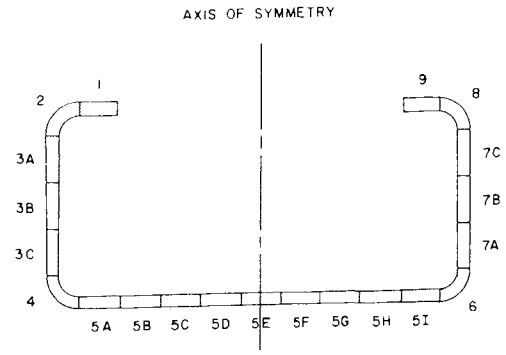

CROSS SECTION SUB-DIVIDED INTO COUPON ELEMENTS

I) 2, 4, 6, 8 CORNER ELEMENTS

II) 1, 3, 5, 7, 9 FLAT ELEMENTS

A. 1, 3A, 3C, 5A, 5I, 7A, 7C, 9
FLAT ELEMENTS ADJACENT TO CORNER ELEMENTS

B 3B, 5B, 5C, 5D, 5E, 5F, 5G, 5H, 7B
ASSUMED TO BE UNSTRAINED ELEMENTS

Fig. 23. Identification of coupon elements.

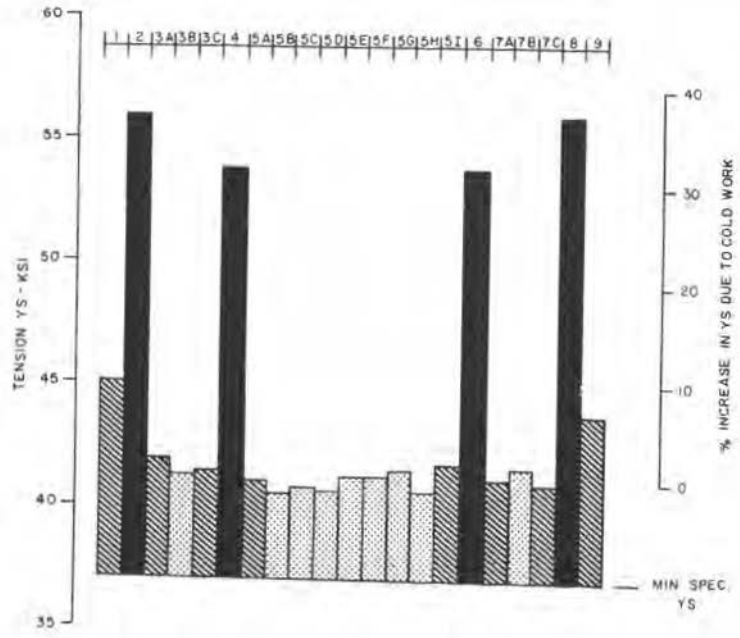

Fig. 24. Variation in tension yield strength in 0.06-37 roll-formed section.

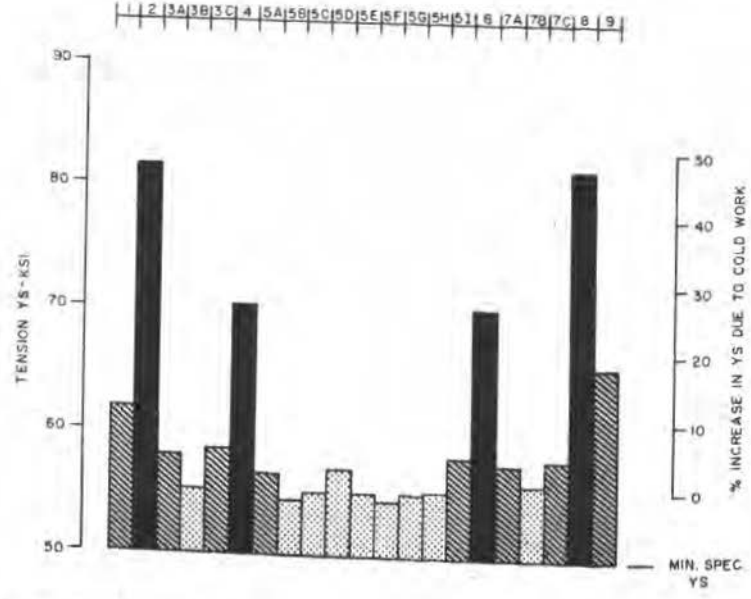

Fig. 25. Variation in tension yield strength in 0.09-50 roll-formed section.

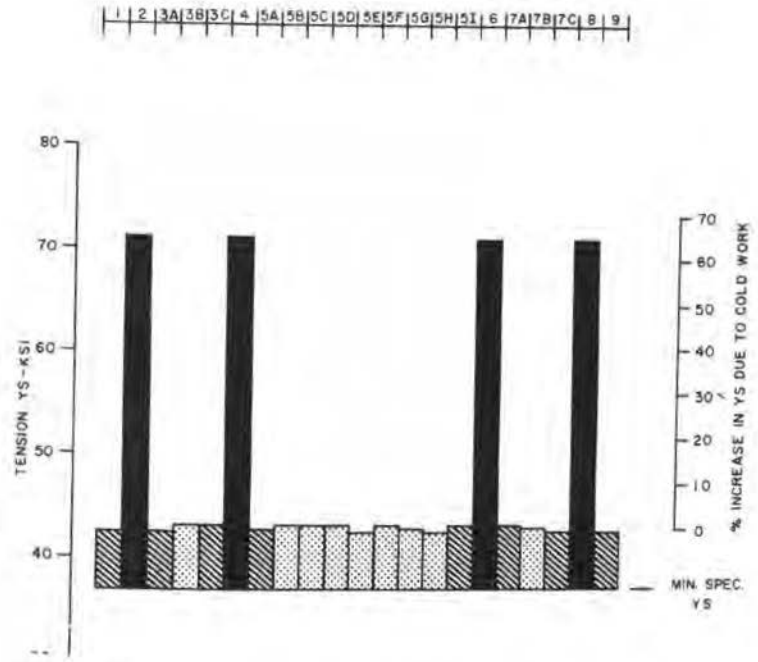

Fig. 26. Variation in tension yield strength in 0.09-37 brake-formed section.

elements, particularly the lips, adjacent to the corners is evident in the roll-formed sections. However, in the press-brake-formed section, the effect of cold work is present in the corners only. These results are in agreement with Karren and Winter's conclusions.

Karren's formulas (Eqs. 1, 2, 3, 4, and 5) for corner yield strength give excellent agreement with tension and compression yield strengths of the corner elements [Table 7(*a*)].

Results from (1) full section tension, (2) flange section tension, and (3) laterally unsupported compression tests, are given in Table 7(*b*). The flange section consisted of the flange plus a portion of the web equal to 10*r*. The length of the flange section compression test specimen was three times the least dimension of the section. Test results compare well with computed yield strengths based on weighted averages of the coupon test values.

Beam tests were made on the three lipped-channel sections using back-to-back members on a 9 ft total span. Use of symmetrical loads resulted in a 30-in. constant moment span in the center of the specimens. Bearing stiffeners and sufficient lateral bracing were provided to achieve full bending capacity of the sections. Strain gages were mounted at midspan on both sections.

In the continuing research program at Cornell University on the effects of cold-forming, referred to by Karren and Winter, a computer program has been

presented[30] for the analytical solution of flexural members including effects of cold work. This program was adapted to compute the theoretical moment versus maximum strain relationship for the lipped-channel sections tested by the writer. The comparison to test results is shown in Fig. 27. In the initial portion of each curve, which reflects elastic conditions only, the experimental data agree well with the theoretical curve, as expected. At increasing values of applied moment, the effects of cold work increases in section yield strength begin to occur. None of the sections tested were capable of attaining full plastic moment capacity (based on increased yield strength from cold work).

Table 7. Yield Strength

(*a*) Corner Elements

Section	Corner	Tensile Yield, in pounds per square inch	Compressive Yield, in pounds per square inch	Karren's Formula, in pounds per square inch
0.06-37	2-8	55,700	54,800	54,100
	4-6	53,600	54,300	51,500
0.09-50	2-8	81,300	63,100	80,200
	4-6	70,000	78,200	76,600
0.09-37	2-8	71,000	68,600	71,300
	4-6	70,600	63,100	71,300

(*b*) Flange and Full Sections

Section	Tension Yield in kips per square inch			Compression Yield in kips per square inch		
	Unstrained Elements	Computed by weighted average	Test Value	Unstrained Elements	Computed by weighted average	Test Value
0.06-37	41.0			43.0		
flange		44.4	43.1		46.6[a]	48.2[a]
full		43.4	42.6			
0.09-50	55.2			56.8		
flange		62.1	61.1		65.4	63.2
full		60.0	57.8			
0.09-37	42.8			43.4		
flange		46.9	45.9		47.1	48.7
full		45.7	44.8			

[a] Based on gross section

Little plastic rotation could be developed before local buckling failure of the compression flanges.

Results of the beam tests are summarized in Fig. 28. Three values of bending moment strength are of interest:

[30] Uribe, J., "Effects of Cold-Forming on the Flexural Behavior of Light-Gage Steel Members," essay presented to Cornell University, at Ithaca, N. Y., in 1966, in partial fulfilment of the requirements for the degree of Master of Science.

1. Elastic Moment Based on Unstrained (Virgin) Yield Strength computed using the section modulus and average tension yield strength from coupon tests on unstrained elements. This value is used as the base for the bar graphs in Fig. 28.
2. "Elastic" Moment Based on Cold Work Yield Strength computed using the section modulus and the lower yield strength from tension and compression tests on flange sections. This moment value follows that given in the Light Gage Design Specification[16] for permissible increase in flexural strength due to cold work effects. An increase of 5% to 11%, which would be applicable in design, is indicated for these lipped-channel sections. (The Specification would not permit any benefit from as-formed strength for the 0.06-37 section because the flange w/t ratio results in a Q value slightly less than unity.)

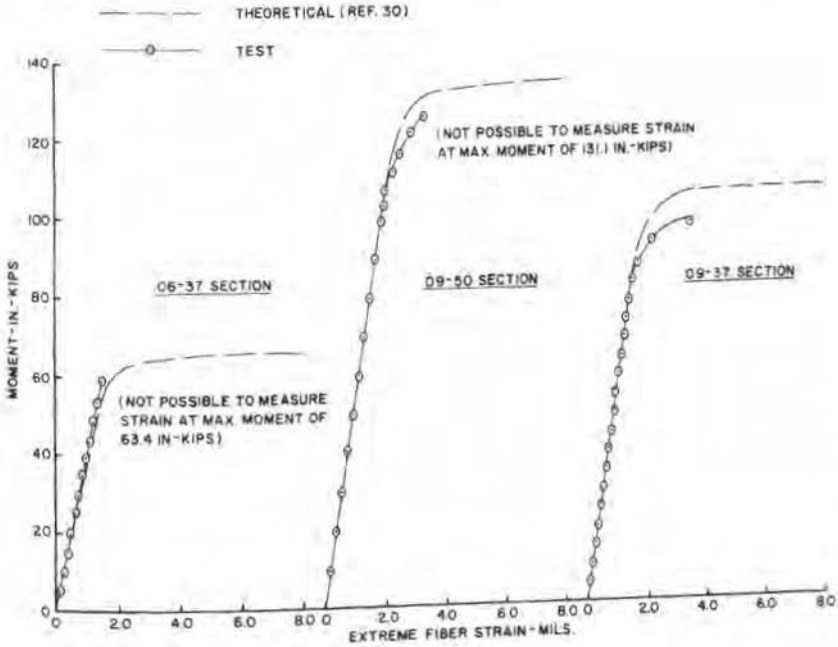

Fig. 27. Moment versus extreme fiber strain.

3. Plastic Moment Based on Cold Work Yield Strength computed using the plastic modulus and the lower yield strength from tension and compression tests on flange sections. This moment represents the maximum potential of the section in bending.

The maximum test moments were greater than the elastic moments based on cold work yield strength, thus verifying the utilization of as-formed yield strength in flexural members of these sections.

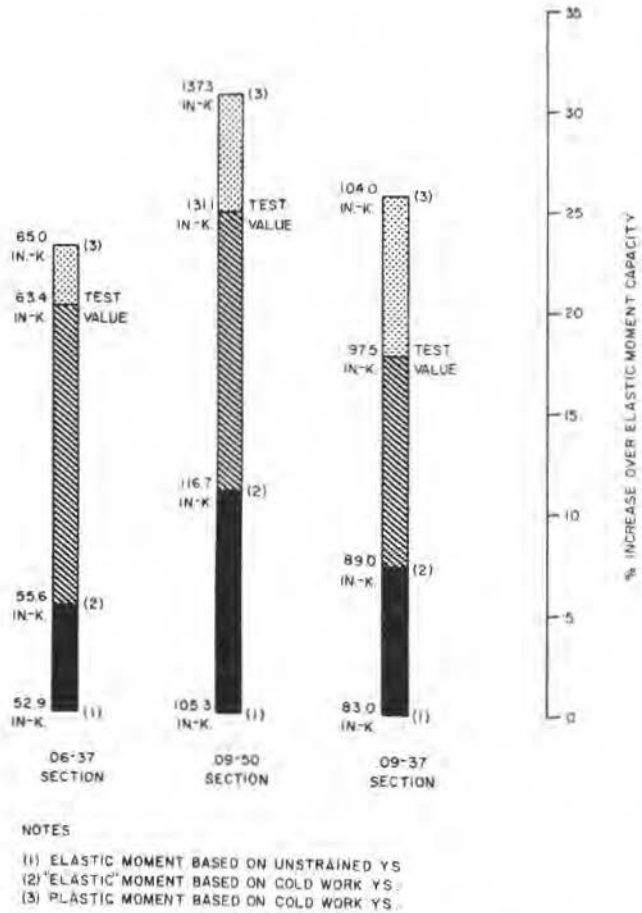

Fig. 28. Graphical interpretation of beam test results.

Plastic design methods used for compact hot-rolled sections depend on the development of plastic moments and sufficient rotation capacity at plastic hinges to form a collapse mechanism. Although test results of this study were into the plastic range, the full plastic moments were not reached, and little rotation could be sustained before failure by local buckling. Hence, these light gage cold-formed sections do not fully satisfy the conditions for plastic design in its present form.

EFFECTS OF COLD-FORMING ON LIGHT-GAGE STEEL MEMBERS[a]

Closure

KENNETH W. KARREN,[31] M. ASCE AND GEORGE WINTER,[32] F. ASCE.—The writers wish to thank J. N. Macadam for his cogent contribution. Their paper included a treatment of axially loaded cold-formed light gage steel compression members, but made no mention of the behavior of flexural members. Hence, Macadam's experimental data coupled with his use of Uribe's[30] computer program for flexural strength, complements the paper nicely.

Macadam's tests show that the maximum moment capacity for sections with $Q = 1$ can be significantly larger than that computed from the section modulus times the yield strength of the virgin material. In fact, his maximum test moments are closer to the calculated plastic moments than to the elastic moments computed from the section modulus times the yield strength determined from flange tests which include the effect of cold-work. Macadam used the lower of the yield points determined from tensile and compressive flange tests in accordance with the American Iron and Steel Institute (AISI) 1962 edition of the Specification.[7] As was reported by the writers, full section yield strengths were determined experimentally from: (1) Tensile and compressive strip specimens taken from the corners and flats of the cross sections; (2) full section tension tests; and (3) laterally unsupported full section compression (stub column) tests. It was found that yield strengths determined in these various ways did not vary more than a few percent. This is true largely because the influence of the Basuchinger effect is negligible in cold-formed corners. Furthermore, Macadam's tests show a large margin (more than 10%) between the maximum test moments and elastic moments calculated on the basis of the lower of the yield strengths determined in compliance with the 1962 AISI Specifications. Thus, it seems well established that the yield stress used as a basis for the design stress need not be restricted to the lowest of the tensile or compressive flange section yield strengths. Either the tensile or the compressive yield strength would be entirely satisfactory for this purpose. The forthcoming edition of the AISI Specification will contain significantly more liberal provisions for the use of cold-work, based on research since 1962.

Macadam states that these light gage sections do not reach the plastic moment capacity and do not sustain adequate rotation capacity for plastic

[a] February, 1967, by Kenneth W. Karren and George Winter (Proc. Paper 5113).

[31] Assoc. Prof., Dept. of Civ. Engrg., Brigham Young Univ., Provo, Utah; formerly Research Asst., Cornell Univ., Ithaca, N. Y.

[32] 1912 Prof. of Engrg. and Chairman, Dept. of Structural Engrg., Cornell Univ., Ithaca, N. Y.

design. This is to be expected, since the sections are non-compact in the sense of plastic design[9] and illustrates the fact that simple plastic design cannot be applied to cold-formed structures except with special safeguards.[22] However, it may be expected that compact (in the sense of plastic design) cold-formed sections would perform satisfactorily for plastic design. More study may be needed of the limits between truly compact and non-compact sections both for flexural and for axially loaded members. (See Fig. 9 and accompanying discussion regarding axially loaded members.) Results of such a study would apply to both cold-formed and hot-rolled sections.

Finally, it should be mentioned that a slight improvement (2) could be made to Eqs. 1 through 5 for predicting the corner yield strength σ_{yc}. For a slightly better fit they should be replaced by

$$\sigma_{yc} = \frac{kb}{(a/t)^n} \tag{18}$$

in which

$$b = 0.94 - n \tag{19}$$

$$k = 2.80\,\sigma_u - 1.55\,\sigma_y \tag{20}$$

$$n = 0.225\left(\frac{\sigma_u}{\sigma_y}\right) - 0.120 \tag{21}$$

and a/t = the ratio of the inside corner radius to the thickness of the material.

Reiss does not touch on the main theme of the paper: the effects of cold-forming on member behavior. He takes the writers' brief comments on the conservative result of one of the many cited tests as a point of departure to discuss the approach to post-buckling strength developed by the senior writer many years ago and utilized ever since in the AISI Specification[7] and elsewhere. In doing so he ascribes to the senior writer Eq. 17 which describes post-buckling strength in terms of an average stress; this stress Mr. Reiss designates as σ_{max} but herein it will be termed σ_{ave} to distinguish it from the actual maximum stress σ_{max} which occurs at the stiffened edge or edges. Eq. 17 is contrary to the form in which it was originally published and is presently used in design, namely in terms of an effective width b_{eff} rather than an average stress σ_{ave}. The two concepts of treating post-buckling strength—i.e., average stress on the one hand and effective width at actual maximum edge stress on the other—are schematically shown on Fig. 29. They are identical when dealing with the ultimate strength of an isolated compressed plate, but are not when dealing with this plate as part of a structural shape, the actual situation. This is so because the effective width method permits not only the calculation of the maximum stress (which induces

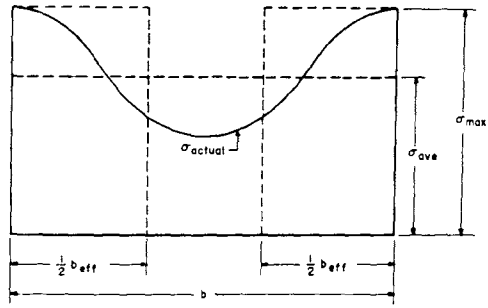

Fig. 29

failure when it becomes equal to the yield strength) but also of edge strains and consequent effective rigidities, curvatures, deflections, migrations of neutral axis under increasing load etc., at subultimate as well as ultimate loads. None of these can be calculated from an average stress, but all of them are necessary in the structural design process.

The effective width equation for plate components stiffened along both longitudinal edges was originally presented by the first form of Eqs. 22 and subsequently, as a shorthand notation, by the second.

$$\frac{b_{\text{eff}}}{b} = \frac{1.9}{\frac{b}{t}}\sqrt{\frac{E}{\sigma_{\max}}}\left(1 - \frac{0.475}{\frac{b}{t}}\sqrt{\frac{E}{\sigma_{\max}}}\right)$$

$$= \left(\frac{\sigma_{cr}}{\sigma_{\max}}\right)^{1/2}\left[1 - 0.25\left(\frac{\sigma_{cr}}{\sigma_{\max}}\right)^{1/2}\right] \qquad (22)$$

In calculating design values, such as Q, hinged edge conditions are always used for the component plates, contrary to Reiss' proposal of accounting for continuity. Not only is this procedure much simpler but it is also borne out by the senior writer's numerous tests, all of which were carried out on structural shapes rather than on isolated plates as Reiss seems to assume. It appears that, particularly when approaching yield failure (i.e., when the material at the edges is in the increasingly plastic state), the beneficial effect of rotational edge restraint is lost.

Reiss refers to Fig. 20 to support the contrary view. Unfortunately no conclusions can be drawn from such a broad undifferentiated band of test results which has a width of some 40% of the mean. The senior writer's view that the beneficial effect of edge restraint is practically negligible is supported

not only by his own but also by a recent British test series by J. B. Dwight and A. T. Ractliffe (1). These tests were made on isolated plates with fully hinged as well as fully fixed longitudinal edges, the most extreme conditions which can be produced. Their results, reproduced in Fig. 30 show that the difference between these extreme conditions is small and erratic and support their conclusion that "The typical increase in strength obtained by clamping appears to be less than 10%, and not enough to warrant higher design stresses. The difference predicted by Chilver between the simply supported and clamped strengths is considerably more than that which the present tests would suggest".

Based on this evidence there seems to be little justification for Reiss' contention that "the validity of the Q-method should be reviewed completely." The Q-method is a practical design tool rather than a rigorous research method, and relates not only to ultimate strength but also to excessive distortion as clearly stated in Ref. 24, to which Reiss refers.

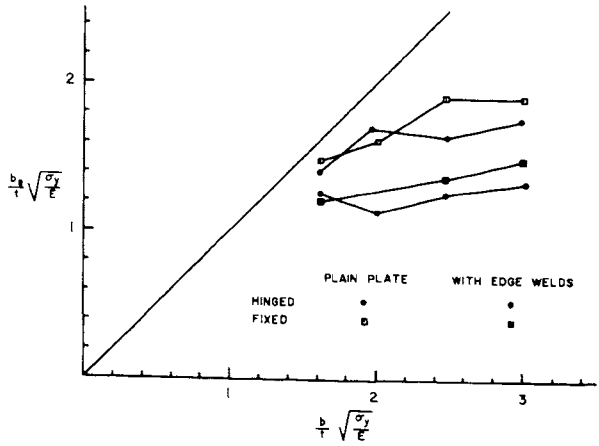

Fig. 30

APPENDIX.–REFERENCES

1. Dwight, J. B., and Ractliffe, A. T., "The Strength of Thin Plates in Compression," Thin Walled Steel Structures Symposium at University College of Swansea, Crosby Lockwood & Sons Ltd., London, 1968.
2. Karren, K. W., closure to "Corner Properties of Cold-Formed Steel Shapes," *Journal of the Structural Division*, ASCE, Vol. 94, No. ST6, Proc. Paper 5966, June, 1968.

COLD FORMING EFFECTS IN THIN-WALLED STEEL MEMBERS

by Jairo Uribe and George Winter

INTRODUCTION

Cold-forming causes a significant increase in yield strength of corners of thin-walled steel members. When the members are formed by cold-rolling, increases in yield strength also may be large in the flat portions of the sections. Thus, cold-formed members have non-uniform material properties throughout the cross-section, with an average yield strength larger than that of the sheet or strip before forming.

Extensive research has been carried out on the behavior of such cold-formed thin-walled members and most of the findings have been used in the Specification for the Design of Cold-Formed Steel Structural Members[1]. Special attention has been given to the effects of cold-forming on the properties of the material [2, 3, 4, 5, 6, 7] and the way in which they affect the behavior of structural members[8, 9, 10, 11], since quantitative information on these topics will permit a more rational and economical design.

The first step in evaluating the effects of cold-forming was an investigation by Chajes, Britvec and Winter[2], which provided some fundamental understanding of the response of ductile carbon sheet and strip steels to simple, uniform cold stretching. Karren and Winter [4, 5, 9] investigated three aspects of this subject: (1) the strengthening effects of cold-work on the properties of corners of formed sections, (2) the effective mechanical properties of full sections, and (3) the inelastic buckling strength of axially loaded pin-ended columns not subjected to local buckling.

Presented herein is the third phase of this investigation on the effects of cold work covering the following topics: (1) as-formed strength of the flat portions (which will be called the flats) of joist chord sections, (2) strength of flexural members, and (3) column buckling of bisymmetrical sections subject to local buckling.

No theoretical method is available to predict the as-formed strength of cold-rolled flats, and because of the many factors involved such a prediction has to be made on a statistical basis. Coupons taken from the flats of 32 joist chord sections were tested both in tension and compression. Based on the test results, information is given on the average increase in yield strength of flats which is likely to be exceeded in 90% of sections of this type.

The experimental behavior of 4 compact and 2 slightly non-compact beams is compared with calculated Moment-Curvature relationships and with predictions of the failure moments based on Elastic Section Modulus and Plastic Hinge methods, both considering and neglecting the strengthening effects of cold-forming. A design procedure is recommended. Tests of another

investigator[10] are also analyzed here to further verify the proposed design method. The terms "compact" and "non-compact" are used in this paper in the sense defined by reference 1 (which will be explained later in the paper) and refer to the ability of a thin-plate element to withstand a given compression stress without occurrence of local buckling.

Three types of non-compact thin-walled columns of channel, hat and lipped-hat configurations were tested. They were designed to accentuate the influence of location of strain-hardened material on the overall effect of cold-forming for this type of loading. The experimental failure loads are compared with those predicted by existing theories and the corresponding AISI Specification.

COLD FORMING METHODS

Two methods of cold-forming are used in the production of thin-walled structural members. One, known as brake forming, is a semi-manual process in which straight bending is applied to a sheet or strip of metal to produce the desired shape. The second method is cold-roll forming, a process for rapid shaping of sheet, strip or coiled flat metal in which the stock is fed longitudinally through successive pairs of rolls, each pair forming progressively the material until the desired cross section is produced[20].

EFFECT OF COLD-WORK ON FLAT PORTIONS OF COLD-ROLLED JOIST CHORD SECTIONS

Introduction.—Karren[4,5] studied the effects of cold-forming on the properties of corners of formed sections and arrived at a semi-empirical equation relating the ratio of corner yield strength to pre-forming or virgin yield strength. He also studied briefly the extension of corner plastic strain effects into the adjacent flats and the variation of tensile and compressive yield strengths and tensile ultimate strength in flats. He found that in press-braked sections the change in properties of the flats became negligible at a distance of one sheet thickness from the edge of the corner. In roll-formed sections on the other hand, increases in yield strength of flats, although smaller than for the corners, were significant, being of the order of 17, 23, and 52 percent of the virgin yield strength for a track, channel and joist chord section tested.

The change in mechanical properties of cold-rolled flats was attributed mainly to the strain hardening and aging resulting from: (1) stretcher-straightening of the coil previous to roll-forming, (2) normal pressure of the rolls, (3) warping of flats with accompanying shearing strains during the forming process. These in turn depend on many conditions such as type of

steel, temperature of coiling, wear of the rolls, skill of the roll operator and design of the rolls. Because of the number of factors to be considered and the impossibility of evaluating them even approximately, it became apparent that any prediction of the change of properties in flats of cold-rolled sections had to be made on a statistical basis. Presented here are the findings of such an investigation concerning joist chord sections.

Materials.—Joist chord sections are widely used commercial shapes that experience extensive cold work during forming and 31 of them were included in the present study. Diagrams of all sections are shown in Fig. 1 and their dimensions are given in Table 1. Sections 1 to 6 were furnished by Manufacturer I; sections 8 to 17 by Manufacturer II, and sections 18 to 32 by Manufacturer III. Manufacturer II also provided partially formed pieces cut after each stage of forming of section 8. One of these intermediate sections was tested as section 7. For all sections corresponding strips of virgin material were available, i.e., strips cut from the coils from which the sections were formed. Sections 7 to 11 and 18 to 20 were accompanied by one strip each, presumably cut from a location in the coil close to that from which the section was formed. For sections 1 to 6 and 21 to 32 two strips were available, one cut from the beginning and the other from the end of the coil. Sections 12 to 17 were accompanied by three strip pieces, cut from the beginning, the middle and the end of the coil No information is available on the locations in the coil of the material from which sections 1 to 6, 12 to 17 and 21 to 32 were formed.

The material for all of the above sections was hot-rolled carbon steel strip of structural quality.

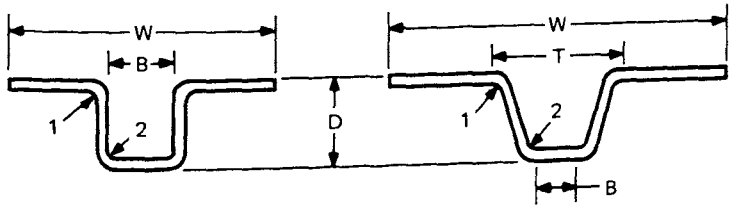

MANUFACTURERS I AND III SECTIONS

MANUFACTURER II – B SECTIONS

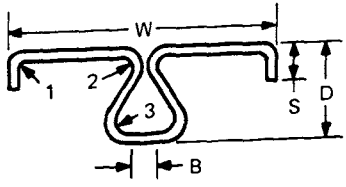

MANUFACTURER II – A SECTIONS

Fig. 1. Cross-sectional shapes.

Table 1. Dimensions of Joist Chord Sections (All dimensions in inches)

Section No.	Thickness	Developed Width	Width	Depth	Bottom Flange	Upper Opening	Lip	Corner Radius*	
								Actual Corner 1	Actual Corner 2
	t		W	D	B	T	S		
1	.100	4.69	2.81	1.23	1.24			–	–
2	.124	5.68	3.86	1.25	1.19			–	–
3	.160	5.18	3.36	1.38	1.12			–	–
4	.160	6.44	4.61	1.38	1.12			–	–
5	.196	7.20	5.34	1.50	1.05			–	–
6	.090	4.20	2.32	1.22	1.26			–	–
7	.114	7.38	5.70	1.40	0.50			–	–
8	.114	7.38	3.62	1.36	0.50		.56	–	–
9	.085	7.20	3.38	1.35	0.50		.50	0.19/0.12/0.12	
10	.128	8.01	4.25	1.38	0.50		.62	0.18/0.20/0.10	
11	.149	9.75	5.88	1.40	0.50		.88	0.27/0.20/0.10	
12	.057	6.57	2.81	1.31	0.50		.56	0.29/0.23/0.23	
13	.099	4.41	3.19	1.04	0.56	1.71		0.23	0.23
14	.124	5.27	4.06	1.06	0.56	1.71		0.23	0.22
15	.173	4.50	3.38	1.11	0.56	1.71		0.23	0.22
16	.173	6.10	4.94	1.11	0.56	1.71		0.23	0.23
17	.223	7.28	6.12	1.16	0.56	1.83		0.19	0.19
18	.096	4.25	2.76	1.10	1.00			0.23	0.22
19	.158	6.00	4.56	1.16	1.00			0.23	0.20
20	.234	6.00	4.63	1.23	1.00			0.23	0.19
21	.140	4.25	2.80	1.14	1.00			0.25	0.23
22	.118	5.00	3.53	1.12	1.00			0.23	0.23
23	.158	5.00	3.56	1.16	1.00			0.20	0.20
24	.198	5.00	3.60	1.20	1.00			0.31	0.31
25	.218	5.00	3.62	1.22	1.00			0.20	0.19
26	.158	6.00	4.56	1.16	1.00			0.23	0.23
27	.198	6.00	4.60	1.20	1.00			0.23	0.23
28	.218	6.00	4.62	1.22	1.00			0.23	0.25
29	.096	4.25	2.76	1.10	1.00			0.23	0.31
30	.124	4.25	2.79	1.12	1.00			0.23	0.23
31	.138	5.00	3.55	1.14	1.00			0.23	0.22
32	.178	5.00	3.58	1.18	1.00			0.23	0.23

*See Fig. 1 for corner locations.

Testing Procedures.—The mechanical tensile properties of the virgin materials were determined by testing 9 in. long standard tensile specimens. Three specimens were prepared from each strip accompaning sections 7 to 11 and 18 to 20. For the other sections, two tensile specimens were cut from each available strip. The specimen was held in the testing machine by self-aligning grips. The load-strain relationship was automatically recorded with a 2 in. gage extensometer. Final elongation in 2 inches was measured.

Companion compression specimens, equal in number, were 3 in. long and 0.5 in. wide. Because of the small thickness of many of the specimens it was necessary to prevent buckling while applying the load. This was accomplished by using a greased jig made of two serrated I-shaped steel pieces held together by connecting screws. The dimensions of the jig were such as to allow mounting of a 1 in. microformer gage on the protruding edges of the specimen.

As-formed mechanical properties across the section were determined by testing at least one tensile coupon, 10 in. long and 0.25 in. wide, cut from each flat of half the formed section. Because of symmetry, it was not considered necessary to take coupons from the other half although this was done occasionally for checking purposes. For seven of the sections, compression specimens of the same dimensions as for the virgin material, taken as companion specimens to the corresponding tension coupons, were tested in the manner described before.

Test Results and Discussion

The mechanical properties given in this paper are average figures of all the coupons from the same strip or section unless specified otherwise. Yield strengths were determined by the 0.2% offset method.

Virgin Material.—Prior to forming all of the material studied here had tensile yield strengths ranging from 36 to 49 ksi (Table 2) and ultimate strengths from 54 to 75 ksi. Ratios of ultimate to yield strengths ranged from 1.22 to 1.61 for all but section 28 which had a ratio of 1.83. Elongations in 2 inches ranged from 25 to 41 percent.

There was considerable scattering in virgin properties of coupons taken from different locations along a given coil. The maximum variation from the mean in specimens from the same coil ranged from 0.6 to 16.5 percent for the tensile yield strength, from 0.2 to 18.2 percent for the compressive yield and from 0.9 to 13.1 percent for the tensile ultimate strength. Average values for such maximum variations were in turn 8.5, 6.5 and 4.1 percent of the arithmetic means. The standard deviations of the virgin properties, although not very significant because of the small number of coupons (3, 4 or 6), are presented in Table 2 to help at least roughly in analyzing the change in strength produced by cold work. The values given there are based on the average of all the virgin specimens available for each section and reflect the differences in strength resulting from different locations in the coil. This is

Table 2. Average Mechanical Properties of Virgin Materials

Section No.	Material*	Gage	Compress. Properties Yield Strength		Tensile Properties				% Elong. in 2"	$\frac{\sigma_u}{\sigma_y}$
					Yield Strength		Ultimate Strength			
			Average ksi	Std. Dev. ksi	Average ksi	Std. Dev. ksi	Average ksi	Std. Dev. ksi		
1	HR-SK	12	41.6	1.8	42.1	2.1	67.0	0.6	33.9	1.59
2	HR-SK	11	41.3	1.4	39.8	1.1	61.3	0.6	36.0	1.54
3	HR-SK	8	42.0	1.9	42.8	2.2	67.6	1.5	30.4	1.58
4	HR-SK	8	43.0	1.7	42.0	1.9	66.1	0.5	33.2	1.58
5	HR-SK	6	46.6	4.0	43.6	4.7	66.9	1.6	31.4	1.53
6	HR-SK	13	50.6	0.6	48.5	0.2	71.5	1.7	28.9	1.47
7-8	HR-SK	12	36.6	0.2	36.5	3.1	57.5	1.7	37.5	1.58
9	HR-SK	13	40.5	0.2	42.5	3.4	59.3	1.2	36.2	1.40
10	HR-SK	11	41.6	1.0	40.3	3.6	64.4	1.4	33.5	1.61
11	HR-SK	9	38.3	0.6	37.3	2.1	57.5	0.6	37.7	1.54
12	HR-R	17	51.6	4.8	44.9	4.1	60.4	2.1	33.7	1.35
13	HR-SK	13	50.4	5.0	48.0	3.3	58.7	2.2	24.8	1.22
14	HR-C	11	40.8	2.0	45.8	2.6	63.5	0.9	32.8	1.39
15	HR-SK	8	41.0	2.2	39.5	2.6	59.9	1.5	41.2	1.52
16	HR-R	7	37.8	2.0	36.4	2.0	58.0	2.3	38.7	1.59
17	HR-C	4	39.3	3.3	38.6	3.7	58.5	2.8	38.6	1.52
18	HR-R	12	50.2	0.0	48.6	0.7	70.4	0.5	28.7	1.45
19	HR-R	8	40.9	3.3	42.2	3.5	59.2	3.5	32.2	1.40
20	HR-R	3	43.6	1.0	41.5	3.8	54.2	1.3	33.3	1.31
21	HR-R	9	35.9	1.8	35.7	0.8	49.1	0.8	37.9	1.38
22	HR-R	11	46.8	1.4	44.8	2.2	61.3	2.8	35.6	1.37
22A					43.6	2.4	60.1	2.8	37.0	1.38
23	HR-R	8	44.3	1.9	44.2	2.8	65.4	0.4	36.9	1.48
24	HR-R	6	43.6	0.5	41.8	1.2	61.1	0.4	37.1	1.46
25	HR-R	5	42.7	1.0	43.2	2.1	55.8	1.4	35.9	1.29
26	HR-R	8	44.6	0.6	42.2	1.8	68.1	3.1	32.5	1.61
27	HR-R	5	41.6	2.2	40.2	1.3	57.0	1.2	37.2	1.42
28	HR-R	4	41.8	2.2	41.0	3.9	75.1	3.6	31.8	1.83
29	HR-R	12	41.9	1.8	42.6	1.6	60.1	3.1	36.1	1.41
30	HR-R	11	54.0	1.0	49.2	1.6	69.3	1.4	28.5	1.41
31	HR-R	9	40.9	4.3	39.8	4.3	56.2	2.8	39.2	1.42
32	HR-R	7	40.0	2.6	38.8	3.3	55.7	4.3	41.2	1.44

*HR – Hot Rolled, SK – Semi-killed, R – Rimmed, C – Capped

important because, as mentioned before, the locations in the coil of the material from which the sections were formed were unknown.

Comparison of tensile and compressive yield strengths of all the virgin materials of this study seems to confirm the trend indicated earlier by Karren[4] that the tensile yield strength can be used as a conservative but reasonably close value of the compressive yield strength.

As-formed Sections.–The as-formed properties of all the sections are presented in Table 3. Changes in yield and ultimate strengths of flats, when compared with the virgin material, are expressed as percentages of the virgin properties in Table 4. To estimate what proportion of the change might be due to natural scattering of virgin properties, it is useful to remember that for a normal distribution the probability for a measurement to fall farther away from the mean than three standard deviations is only 0.3 percent. The standard deviations of virgin material properties were given in Table 2.

Yield and Ultimate Strengths.–The increase in yield strength of flats ranged from 2 to 54 percent of the virgin value if section 7, an unfinished shape, is excluded (Table 4). Changes in ultimate strength ranged from a decrease of 14 to an increase of 16 percent of the virgin ultimate strength. With the same exception, above, changes in individual coupons ranged from 13 percent below to 96 percent above the virgin tensile yield strength and from 17 percent below to 34 percent above the virgin ultimate.

Figure 2-a shows a typical variation of yield and ultimate strengths across joist chord sections. In all cases the flat portions at the bottom of the hat had the largest yield strengths, ranging from 11 to 96 percent above the virgin values. This is mainly due to bending of the bottom of the hat during early roll passes, being flattened out only in the last stages of forming, and perhaps to a larger normal pressure of the rolls. Figure 2-b is interesting because it shows the considerable increase in yield strength experienced by the same strip in going from the section 7 configuration to that of section 8. When compared with the virgin yield and ultimate strengths, the average increases of flats at stage 8 (section 7) are 34.1 and 10.1 percent respectively against 54.3 and 15.9 percent at stage 12 (section 8).

A main concern of this investigation was to seek adequate parameters to correlate material and/or geometrical properties of the sections with the effects of cold work upon their flat portions. Taking into account the findings of earlier investigators[4, 5, 9] attention was concentrated on four parameters: ratio of virgin ultimate to yield strengths, thickness, blank width, and virgin yield strength. The data presented in Table 4 suggest that greater benefit from cold work in the flats will be obtained the larger the virgin ultimate to yield strengths ratio, the thicker the sheet, the wider the blank width, and the smaller the yield strength are. Since thickness and blank width counteract each other in design, fairly detailed investigations may be worthwhile when new shapes are developed to indicate their best combination for optimum design. Unfortunately, quantitative correlation between the above parameters and the test results could not be found.

Table 3. Changes in Yield and Ultimate Strengths of Flats as Percentage of Virgin Values

Section No.	Thickness (in.)	# of Coupons Tested	Increase in Strength as Percentage of Virgin Values							
			Yield Strength				Ultimate Strength			
			Min.	Max.	Average	Std. Dev.	Min.	Max.	Average	Std. Dev.
1	.100	5	- 3.8	21.4	9.4	5.0	-12.7	- 9.1	-10.9	0.9
2	.124	4	17.6	46.2	25.2	2.7	1.1	9.5	3.5	1.0
3	.160	3	2.1	38.0	15.6	5.3	15.2	- 3.1	-12.0	2.2
4	.160	7	18.3	49.8	26.3	4.4	- 4.2	8.9	- 1.4	0.8
5	.196	5	17.9	62.1	24.6	10.8	0.3	18.2	3.7	2.3
6	.090	3	- 8.5	11.5	2.9	0.4	-17.2	-10.6	-13.7	2.4
7	.114	5	29.3	48.2	34.1	8.4	8.2	12.3	10.1	3.0
8	.114	3	38.9	89.0	54.3	8.4	8.5	33.6	15.9	3.0
9	.085	3	0	39.8	20.5	8.1	- 5.2	6.9	- 1.5	2.0
10	.128	4	17.9	79.7	36.8	8.8	- 1.6	18.5	3.6	2.2
11	.149	6	19.0	96.2	38.7	5.7	1.6	34.1	6.6	1.1
12	.057	7	-13.1	14.7	1.7	9.0	- 4.3	8.6	2.1	3.5
13	.099	3	6.9	20.0	14.7	6.9	- 0.7	5.6	3.0	3.8
14	.124	4	21.0	38.4	25.1	5.6	4.7	10.9	6.0	1.4
15	.173	3	36.4	67.3	43.7	6.5	2.8	17.0	6.6	2.5
16	.173	7	29.4	54.4	38.7	5.4	- 4.3	9.8	2.7	4.0
17	.223	5	31.6	70.2	47.3	9.6	3.6	23.2	11.9	4.8
18	.096	3	8.2	37.4	24.1	1.5	- 3.9	6.8	2.4	0.6
19	.158	4	14.0	58.5	25.5	8.3	1.7	22.5	7.0	6.0
20	.234	4	9.2	36.9	18.2	9.1	- 3.3	12.0	1.6	2.4
21	.140	5	21.3	47.6	36.5	2.1	1.6	15.5	10.0	1.7
22	.118	3	14.5	9.4	- 9.4	4.9	-10.9	- 9.5	-10.6	4.5
22A	.118	5	-14.0	12.4	- 6.4	5.6	- 9.2	- 7.0	- 8.3	4.7
23	.158	3	11.1	43.7	20.5	6.3	- 4.7	6.7	- 2.4	0.6
24	.198	3	27.5	50.2	32.2	2.8	0.2	9.2	2.1	0.7
25	.218	3	24.8	39.4	27.8	4.8	6.5	17.4	9.2	2.5
26	.158	4	14.7	48.1	22.6	4.1	-12.9	5.0	- 7.0	4.6
27	.198	7	16.9	48.0	26.0	3.3	- 3.7	12.5	1.4	2.1
28	.218	4	25.1	60.7	39.5	9.5	- 0.9	2.5	0.7	4.8
29	.096	3	17.4	33.6	23.5	3.7	- 1.0	2.8	0.6	5.1
30	.124	3	12.4	43.5	28.2	3.2	- 1.9	14.3	5.9	2.1
31	.138	4	17.3	51.5	30.5	10.9	0	15.1	4.8	4.9
32	.178	4	15.7	36.3	24.8	8.5	- 2.7	15.0	0.4	7.6

Table 4. Strength Increase Grouped by Type of Section

Section No.	Manufacturer	Material	Nominal Thickness (in)	Nominal Area (in^2)	Nominal Developed Width (in)	Virgin Yield Strength ksi	Virgin $\frac{\sigma_u}{\sigma_y}$	Average Increase		Average Increase	
								Yield Str. (% of Virgin)	Std. Dev. (% of Virgin)	Ult. Str. (% of Virgin)	Std. Dev. (% of Virgin)
6	I	HR-SK	.090	.378	4.20	48.5	1.47	2.9	0.4	−13.7	2.4
1		HR-SK	.100	.469	4.69	42.1	1.59	9.4	5.0	−10.9	0.9
3		HR-SK	.160	.830	5.18	42.8	1.58	15.6	5.3	−12.0	2.2
5		HR-SK	.196	1.410	7.20	43.6	1.53	24.6	10.8	3.7	2.3
2		HR-SK	.124	.704	5.68	39.8	1.54	25.2	2.7	3.5	1.0
4		HR-SK	.160	1.030	6.44	42.0	1.58	26.3	4.4	− 1.4	0.8
12	II-A	HR-R	.057	.374	6.57	44.9	1.35	1.7	9.0	2.1	3.5
9		HR-SK	.085	.612	7.20	42.5	1.40	20.5	8.1	− 1.5	2.0
10		HR-SK	.128	1.025	8.01	40.3	1.61	36.8	8.8	3.6	2.2
11		HR-SK	.149	1.453	9.75	37.3	1.54	38.7	5.7	6.6	1.1
8		HR-SK	.114	.841	7.38	36.5	1.58	54.3	8.4	15.9	3.0
13	II-B	HR-SK	.099	.436	4.41	48.0	1.22	14.7	6.9	3.0	3.8
14		HR-C	.124	.654	5.27	45.8	1.39	25.1	5.6	6.0	1.4
16		HR-R	.173	1.054	6.10	36.4	1.59	38.7	5.4	2.7	4.0
15		HR-SK	.173	.778	4.50	39.5	1.52	43.7	6.5	6.6	2.5
17		HR-C	.223	1.623	7.28	38.6	1.52	47.3	9.6	11.9	4.8
22	III	HR-R	.118	.590	5.00	44.8	1.37	− 9.4	4.9	−10.6	4.5
20		HR-R	.234	1.404	6.00	41.5	1.31	18.2	9.1	1.6	2.4
23		HR-R	.158	.790	5.00	44.2	1.48	20.5	6.3	− 2.4	0.6
26		HR-R	.158	.948	6.00	42.2	1.61	22.6	4.1	− 7.0	4.6
29		HR-R	.096	.408	4.25	42.6	1.41	23.5	3.7	0.6	5.1
18		HR-R	.096	.408	4.25	48.6	1.45	24.1	1.5	2.4	0.6
32		HR-R	.178	.890	5.00	38.8	1.44	24.8	8.5	0.4	7.6
19		HR-R	.158	.948	6.00	42.2	1.40	25.5	8.3	7.0	6.0
27		HR-R	.198	1.188	6.00	40.2	1.42	26.0	3.3	1.4	2.1
25		HR-R	.218	1.090	5.00	43.2	1.29	27.8	4.8	9.2	2.5
30		HR-R	.124	.527	4.25	49.2	1.41	28.2	3.2	5.9	2.1
31		HR-R	.138	.690	5.00	39.8	1.42	30.5	10.9	4.8	4.9
24		HR-R	.198	.990	5.00	41.8	1.46	32.2	2.8	2.1	0.7
21		HR-R	.140	.595	4.25	35.7	1.38	36.5	2.1	10.0	1.7
28		HR-R	.218	1.308	6.00	41.0	1.83	39.5	9.5	0.7	4.8

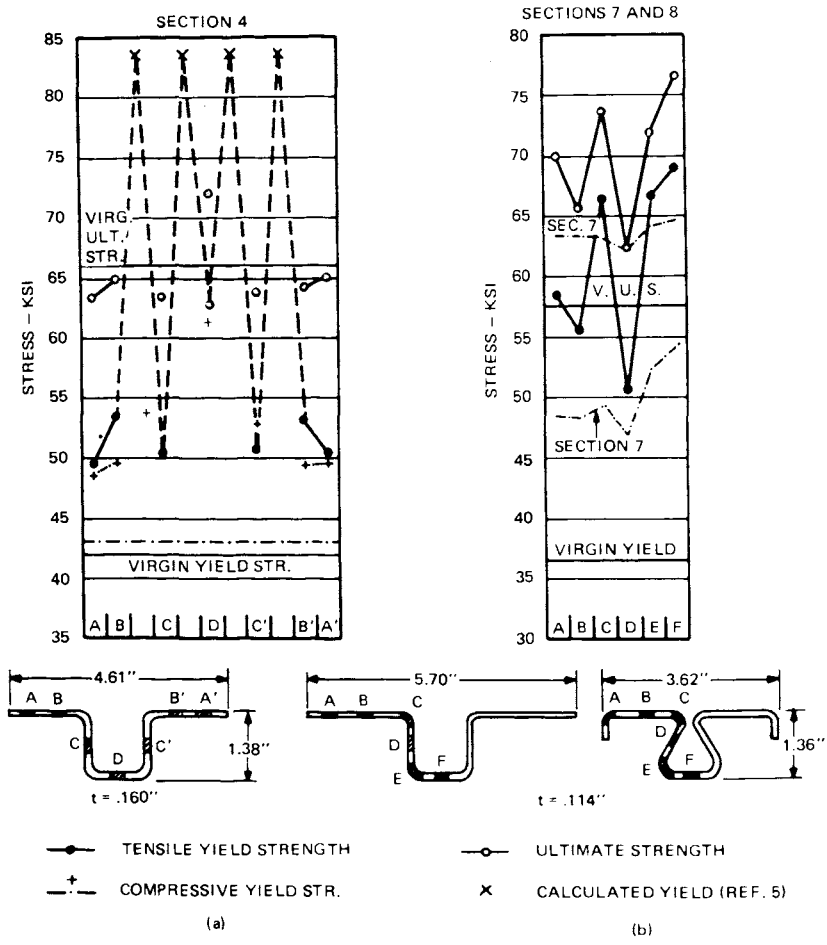

Fig. 2. a) Typical variation of yield and ultimate strengths across a joist chord section. b) Comparison of strengths at stage 8 (section 7) and stage 12 (section 8).

Changes in ultimate strength of flats do not seem to correlate with the same parameters which affect increase in yield strength.

Ductility.—The increase in yield strength caused by cold work is accompanied by a decrease in ductility. For these sections it was found that the reduction in average ductility of the flats ranged from 0 to 58 percent of the virgin elongation. However, only 4 out of 138 coupons of as-formed material showed elongations in 2 in. less than 10 percent, the lowest single value being 7.5 percent. Average elongations of all the flats in each section ranged from 14.1 to 29.8 percent. The average ductility of the whole section will be smaller when corners are included. However, research now underway suggests that these residual ductilities are amply adequate structurally.

Statistical Analysis of Results

General.—A major goal in a statistical investigation is to find an equation which correlates the experimental data with one or more parameters. As discussed before, although qualitative correlation with some parameters could be detected it was impossible to evaluate them quantitatively. On the other hand, the many factors involved, some of them random, preclude attempts at a theoretical approach. In such circumstances it is only possible to study the frequency distributions and cumulative frequency curves of the experimental data in order to find specific values of change in virgin strengths which are likely to be exceeded, for instance, in 90 percent of the cases.

Yield Strength.—Considering all the sections studied here as a single population, the frequency distribution and cumulative frequency curves of the weighted average increases in yield strengths of the flats of each section are presented in Figs. 3-a and 4-a. The highest frequency lies at an average increase of about 25 percent of the virgin yield strength, with 90 percent of the sections showing average increases larger than about 8 percent of the virgin yield strength.

Thickness and blank widths of these joist sections can be combined in such a manner that by establishing a lower limiting cross-sectional area of 0.5 in^2 all but one of the sections showing less than 15 percent increase in yield strength are eliminated. Ninety percent of the remaining sections then showed increases larger than 19 percent of the virgin yield strength (Figs. 3-b and 4-b).

Ultimate Strength.—The highest frequency for the average change in ultimate strength of flats of each section lies at an increase of about 2 percent (Fig. 5-2). Fig. 6-a shows that ten percent of the sections had average decreases larger than 9 percent of the virgin ultimate strength.

Limiting the sections again to those with an area larger than or equal to 0.5 in^2, the distributions of Figs. 5-b and 6-b are obtained. The highest frequency for average change increases to 6 percent and the ninety percent probability value increases to -7 percent.

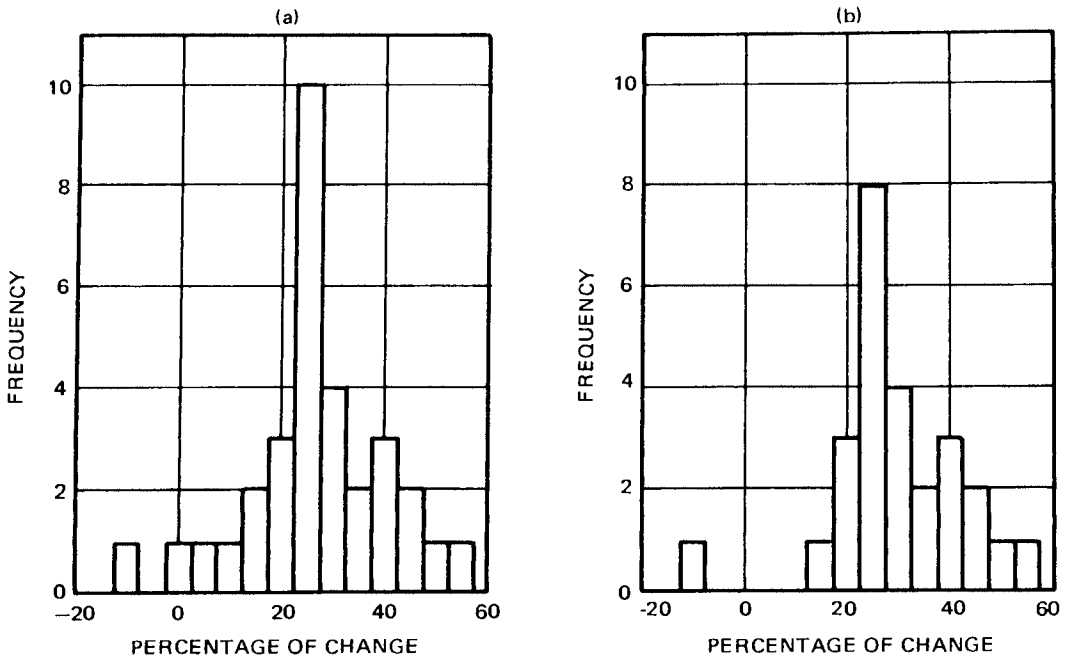

Fig. 3. Column Diagrams: distribution of average change in yield strength of flats of joist chords - a) All sections included - b) Sections with area larger than 0.5 sq. in.

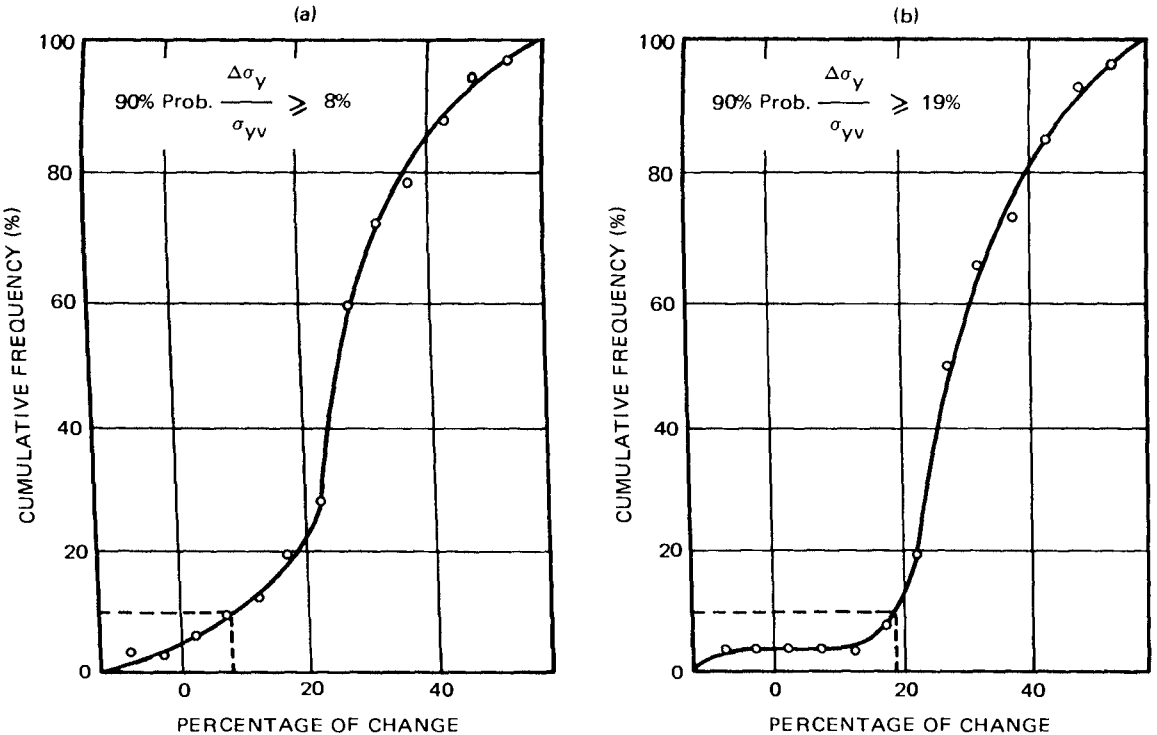

Fig. 4. Cumulative frequency curves: distribution of average change in yield strength of joist chords - a) All sections included - b) Sections with area larger than 0.5 sq. in.

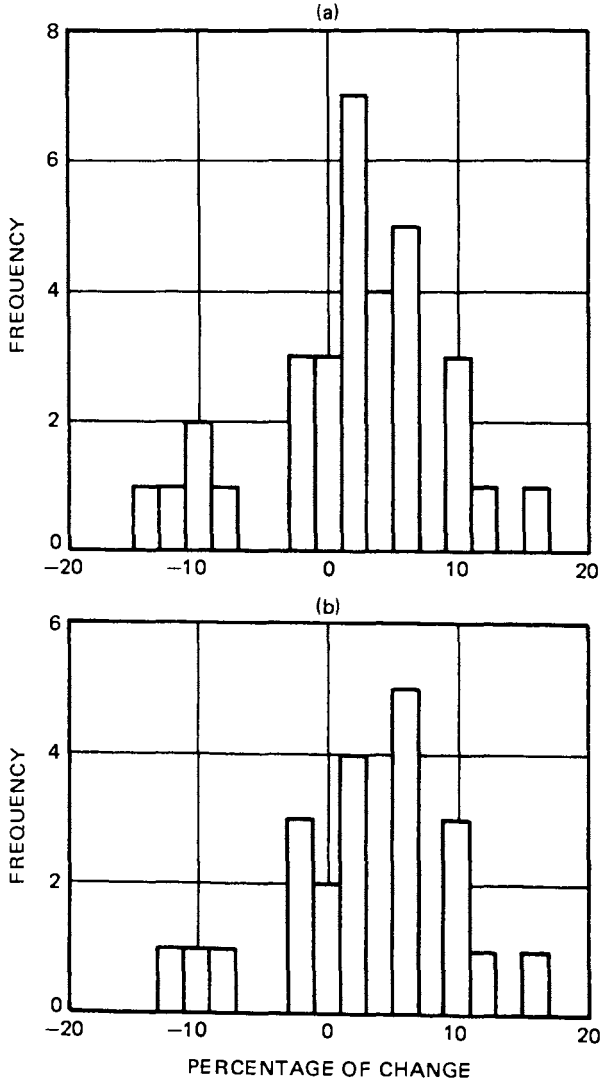

Fig. 5. Column diagrams: distribution of average change in ultimate strength of flats of joist chords - a) All sections included, b) Sections with area larger than 0.5 sq. in.

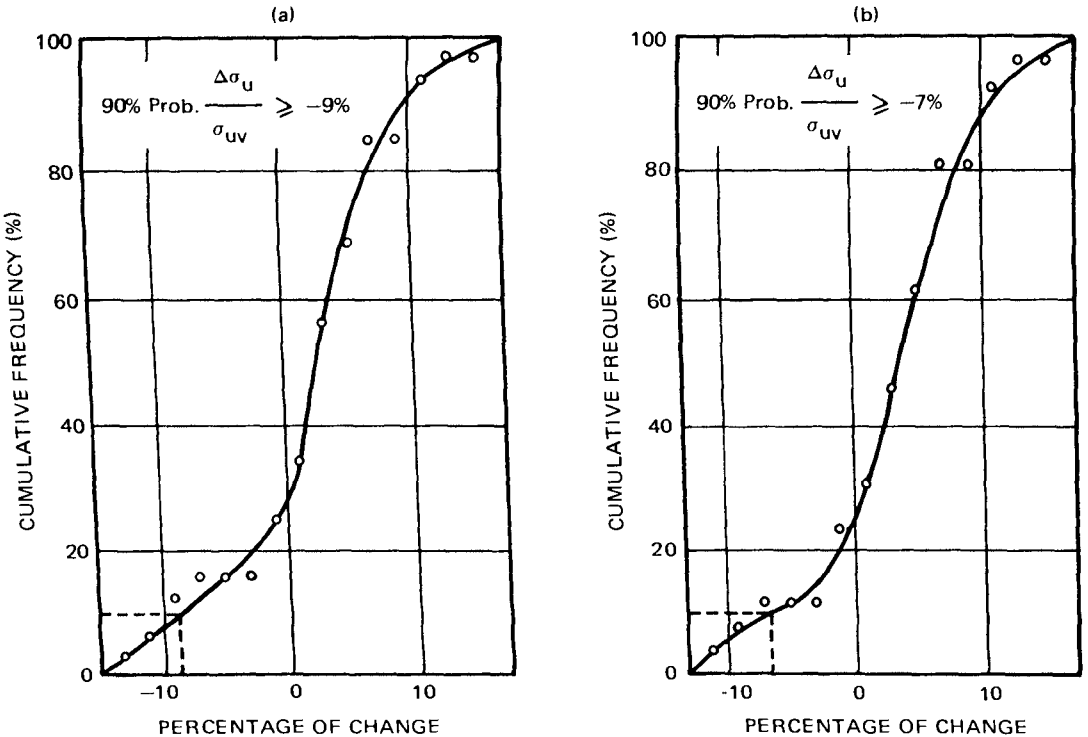

Fig. 6. Cumulative frequency curves: distribution of average change in ultimate strength of joist chord flats - a) All sections included - b) Sections with area larger than 0.5 sq. in.

It is emphasized that the above values may be valid only for the manufacturers and types of sections covered in this study. These are believed to be representative for cold-rolled shapes but the results suggest the advantage for each manufacturer of performing similar statistical investigations of his own products. This would result in greater and more reliable benefits of utilizing the strengthening effects of cold-forming obtained in the particular specific shape.

EFFECT OF COLD-FORMING ON THE BEHAVIOR OF THIN-WALLED STEEL BEAMS

Introduction.–Knowing the distribution of strength across the section, it is possible to calculate the expected behavior of cold-formed members[9, 11, 12]. In the case of thin-walled flexural members, the required computations can best be performed by using a computer program[11, 12]. Such a program was developed for the basic section shown in Fig. 7-a. Some of the common shapes which can be derived from that basic section are shown in Fig. 7-b.

The computation of properties of the section is done in the first part of the program by using the so-called linear method[21] in which the material of the section is considered to be concentrated at the axis of the sheet, and the section composed of straight and curved linear elements. The thickness of the plate is introduced only at the end of the computations to find the properties of the actual section.

The computation of the flexural strength for a given section is done in the second part of the program which gives the moments corresponding to arbitrarily selected maximum strains of the most stressed fiber. With these values, Moment vs. Curvature diagrams of the section may be drawn. The program can be adapted to any stress-strain relation. Different relations for different parts of the section, or for elements in tension and compression may then be taken into account.

Computations using this program indicated the importance of considering cold-forming effects both on corners and flats[11, 12]. However, since the flats yield at a much lower stress than the corners, it is conceivable for the latter to be prevented from reaching their increased yield strength before failure occurs. Also it was doubted whether adequate rotation capacity would be available to permit full plastification of the section, the experimental evidence to date being very limited[10]. The tests were designed to obtain information on these points.

Experimental Investigation.–In designing thin-walled structural members it is necessary to consider the reduction in strength that results from local buckling when the flat-width ratio w/t of the thin-walled elements exceeds certain values. For stiffened compression elements safe load determinations are made by using the effective width concept, i.e., by considering that only

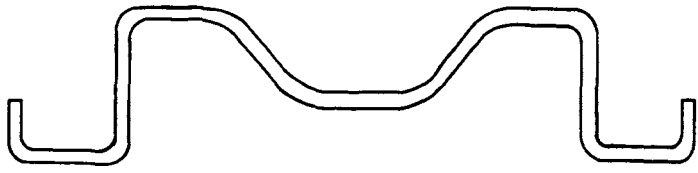

a – BASIC SECTION

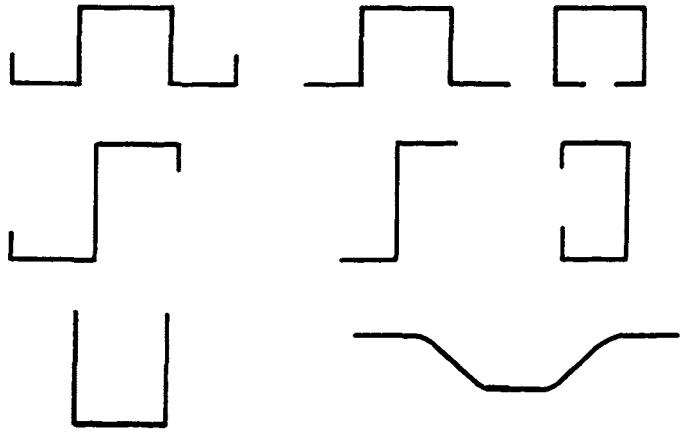

b – COMMON SHAPES DERIVED FROM THE BASIC SECTION

Fig. 7. Basic and common shape sections used in the computer program to study flexural behavior of light-gage members.

the portions of any such element adjacent to its stiffened edges are structural effective. The determination of effective width in the 1968 edition of the AISI Design Specification[1] was based on the expression:

$$\frac{b}{t} = 1.9\sqrt{\frac{E}{\sigma_{max}}}\left[1 - 0.415\frac{t}{w}\sqrt{\frac{E}{\sigma_{max}}}\right] \qquad (1)$$

where

b = effective width

t = thickness

w = flat width of compression element

E = modulus of elasticity

σ_{max} = edge stress in the compression element

Eq. 1 should be used whenever the w/t ratio is larger than:

$$\left(\frac{w}{t}\right)_{lim} = 1.28 \sqrt{\frac{E}{\sigma_{max}}} \qquad (2)$$

For unstiffened elements exceeding certain limiting w/t values local buckling is avoided by basing their design upon a reduced allowable unit stress which decreases with increasing w/t. The 1968 edition specifies that for w/t greater than $63/\sqrt{\sigma_y}$ but not greater than $144/\sqrt{\sigma_y}$ the reduced allowable unit stress σ_c to be used with the full, unreduced area of the element is given by

$$\sigma_c = \sigma_y \left[0.767 - \left(\frac{2.64}{10^3}\right)\left(\frac{w}{t}\right)\sqrt{\sigma_y}\right] \qquad (3)$$

where σ_y is the yield strength in ksi.

In the case of compression members the above procedures are simplified by using a form factor "Q", defined as follows:

"1. For members composed entirely of stiffened elements, Q is the ratio between the effective design area, as determined from the effective design widths of such elements, and the full or gross area of the cross section.
2. For members composed entirely of unstiffened elements, Q is the ratio between the allowable compression stress σ_c for the weakest element of the cross section (the element having the largest flat-width ratio) and the basic design stress $0.60\sigma_y$.
3. For members composed of both stiffened and unstiffened elements the factor Q is the product of a stress factor, Q_s, computed as outlined in paragraph (2) above and an area factor, Q_a, computed as outlined in paragraph (1) above, except that the stress upon which Q_a is to be based shall be that value of the stress σ_c which is used in computing Q_s; and the effective area to be used in computing Q_a shall include the full area of all unstiffened elements."

Sections with a Q factor of 1 are here called "compact" sections while those with Q less than 1 are called "non-compact".

Six beams were tested and the results compared with theoretical predictions. Section configurations and dimensions are shown in Fig. 8-a. All the sections were press-braked with the exception of beam B-2 which was roll-formed. All beams were "compact" according to the 1968 AISI Specification,

though beams B-4 and B-4a had w/t-ratios barely below $(w/t)_{lim}$. Compact sections were chosen because the ratio of area of the corners to total area would be very small for large flat-width ratios; for press braked sections this would result in a very small effect of cold work on the flexural behavior of the member.

Material Properties.—Virgin material was available for beams B-1, B-3 and B-4, and the virgin properties of beam B-2 were known from prior tests [4,5].

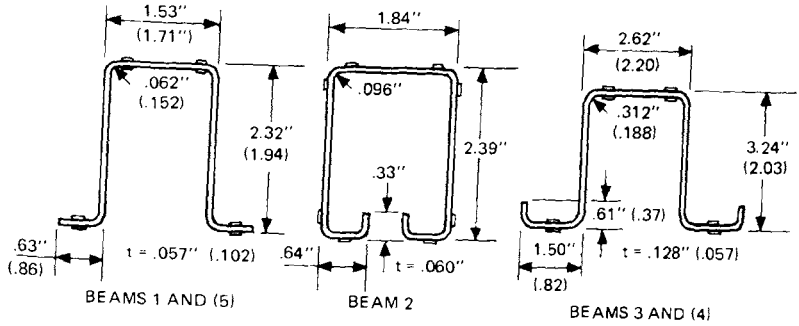

a – BEAM SECTIONS AND LOCATION OF STRAIN GAGES

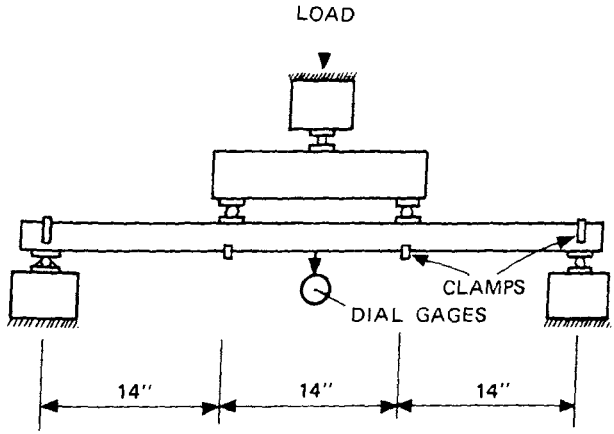

b – LOADING SCHEME

Fig. 8. Beam sections, location of strain gages and loading scheme.

Neither virgin material nor information about its properties were available for beam B-5. Three tensile and compressive tests of each available virgin material were made. The dimensions and testing procedures of these specimens were identical to those described before.

Coupons of flats and corners were taken at regular spacings across the sections and tested both in tension and compression. Dimensions and testing procedures for the flat coupons were those described before. Tensile coupons of corners were 15 in. long and were tested in a manner similar to that used for tensile coupons of flats. Compressive coupons of corners were 3 in. long for beams B-3 and B-5, and 1.5 in. long for the other beams. The testing procedure was one used by Karren[5] and involved mounting of an SR-4, A-12 strain gage at the center on the exterior side of the corner, water-proofing, greasing and wrapping of the specimen in aluminum foil to allow free longitudinal movement, and casting in hydrostone to provide lateral support and prevent buckling. Aluminum pipe sleeves provided adequate enclosure.

Flexural Tests.—The beams were simply supported on a span of 42 inches. Equal concentrated loads were applied at the third points of the span, resulting in a constant moment zone 14 in. long. Clamps were applied at the supports and under the loads to maintain the geometrical shape of the section. They proved to be effective and necessary.

Each beam was instrumented at midspan with eight SR-4, A-12, strain gages located close to the corners as shown in Fig. 8-a. Deflections at midspan were measured with two dial gages connected to the bottom flanges and reading to 0.0005 in. Fig. 8-b shows schematically the loading arrangement.

In testing, the load was applied in small increments at a rate of separation of crossheads of about 0.005 in/min., and was kept constant while deflection and strain readings were taken by means of a strain indicator and a switching box.

Test Results and Discussion

Average virgin and as-formed material properties obtained by the above procedures are shown in Table 5. The flats of the roll formed section showed weighted average increases in tensile yield and ultimate strengths of 20.3 and 10.6 percent of the virgin values respectively. Flats of press braked sections showed changes in those properties smaller than 5 percent, which is within the scattering range of virgin strengths.

Increases in tensile yield strength of corners ranged from 34 to 65 percent above the virgin values; increases in ultimate strength from 4 to 26 percent.

Strength Distribution Across the Section.—The graphs of strength distribution across the section (not shown here) indicate that the strength of flats is relatively uniform across each section[13]. The only exceptions were the bottom flanges of beam B-2, due perhaps to higher roll pressure in the forming process required by the short distance between adjacent corners, and

Table 5. Virgin and As-Formed Materials Properties of Beams and Columns

Specimen	Virgin Material			As-Formed Strength					
	Tension		Compression	Flats			Corners		
	Yield ksi	Ultimate ksi	Yield ksi	T. Yield ksi	Ultimate ksi	C. Yield ksi	T. Yield ksi	Ultimate ksi	C. Yield ksi
B-1	32.7	47.9	35.7	34.2	47.5	37.2	54.0	60.3	55.4
B-2*	37.5	49.0	40.5	45.1	54.2	46.6	61.2	66.5	64.5
B-3	45.8	67.7	46.4	45.4	65.1	47.0	61.7	70.5	65.2
B-4, 4A	44.2	63.3	43.5	44.8	65.9	42.7	59.2	68.6	60.0
B-5				28.1	43.0	31.9	51.2	57.4	51.9
UC-1 SK-18	43.4	61.8	41.1						
& SK-19	45.8	65.8	43.7						
UC-2 SK-22	41.9	60.3	41.3	41.5	62.1	39.6	69.5	66.8	63.8
SC-1 SK-1	42.0	56.9	42.2						
SK-2	39.5	55.6	39.4	39.1	54.9	40.5	57.3	65.3	62.1
SK-4	38.8	55.1	39.5						
SC-2 R-17A	41.7	54.5	43.1						
R-17B	41.0	53.9	44.2	39.6	52.2	40.7	60.9	65.4	60.7
R-19A	41.5	54.1	44.0						
R-19B	42.5	55.3	44.3						

*Virgin Properties as determined in Reference 5.

the top flange of beam B-3 which was first bent and then flattened out in order to form the section. This flange presented at the center a tensile yield strength higher than that of the adjacent corners.

The distribution of compressive yield strengths was similar to the tensile one. The compression values were in general somewhat larger than the tensile yield strengths with the exception of beam B-4 for which the compressive yield strength was slightly smaller.

Moment-Curvature Relationship.—The experimental Moment-Curvature relations were compared with those calculated by the computer program mentioned before, utilizing the material properties from coupon tests. It was assumed that the yield strength of flats was uniform across the section. Six different relations were computed for each beam: the first one uses a sharp yielding stress-strain relation for both corners and flats based on the tensile yield strength of the virgin material, i.e., it neglects completely the effects of cold work. The second uses the weighted average of tensile yield strength of flats and the experimental tensile yield strength of corners, assuming in both elements a sharp yielding curve. The third uses the same values of 0.2% offset tensile yield strength as the second but a sharp yielding stress-strain relationship for the flats and the following gradual yielding curve for the corners:

$$\sigma = \frac{\sigma_y \quad e^{\beta}}{1 + e^{\beta}} \tag{4}$$

where

$$\beta = \frac{4E\epsilon - 2\sigma_y}{\sigma_y} \tag{5}$$

and σ is the stress at a given strain ϵ. Eqs. 4 and 5 are obtained by integrating an expression for tangent modulus given in Ref. 14 and are used for strains larger than half the yield strain. For smaller strains Hooke's Law is used. Any other reasonable equation such as Ramberg-Osgood's with appropriate parameters could have been used. All three methods were repeated using the pertinent compression properties.

Moment-Curvature relations of a typical compact section are presented in Fig. 9, and of the least compact section (B-4A) in Fig. 10. The theoretical curves in those figures correspond to the first and third method described above.

After analyzing similar curves for each beam tested it was concluded that utilizing the as-formed tensile yield strength of flats and corners (third

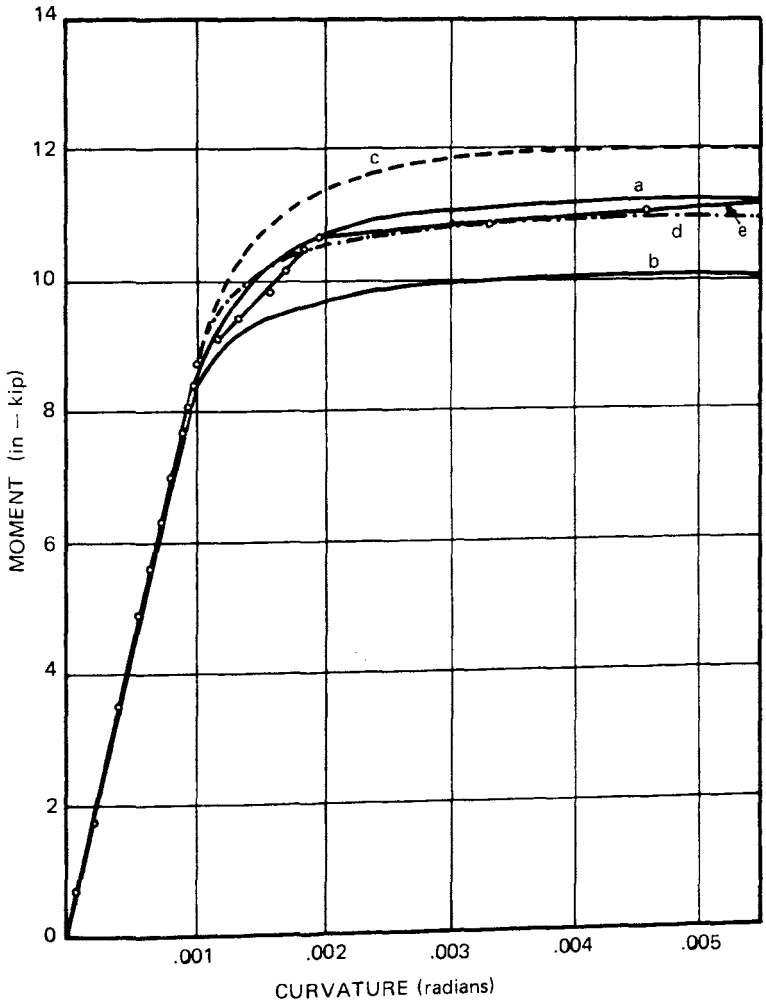

Tensile Properties: a) Cold Forming Considered; b) Cold Forming Neglected. Compressive Properties: c) Cold Forming Considered; d) Cold Forming Neglected. e) Experimental

Fig. 9. Moment-curvature characteristics of beam 1.

method above) gave close and conservative estimates of curvatures for all compact sections with small flat-width ratios. The second best approximation for press-braked compact sections would be to use the virgin compression properties. However, for roll-formed sections such as B-2, this last method would be very conservative. Beams B-1, B-3 and B-5 reached curvatures larger than 0.005 radians before failure occurred. The beams with the largest flat-width ratios, B-2 with w/t = 25.6, and B-4 and B-4A with w/t = 33.1, failed when the curvatures were about 0.0023, 0.0030 and 0.0033 respectively.

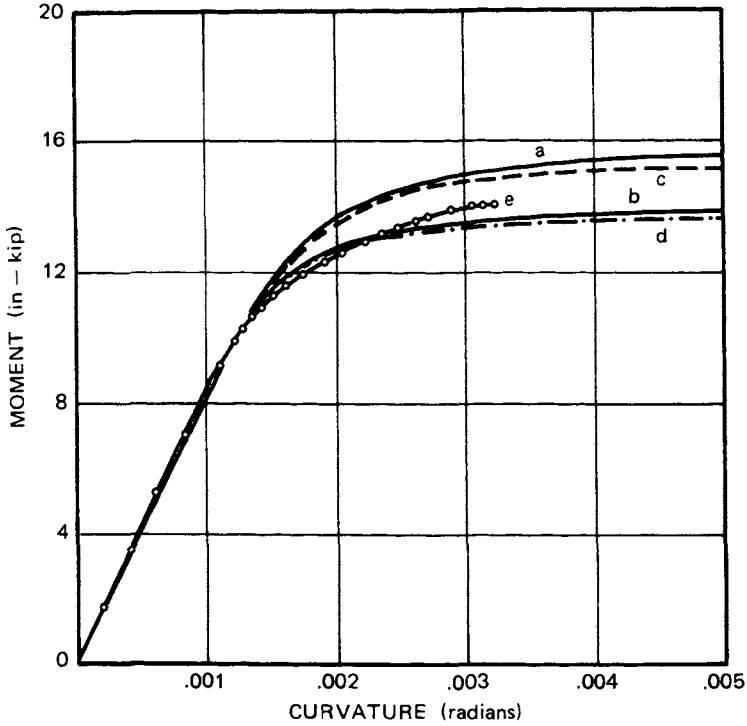

Tensile Properties: a) Cold Forming Considered; b) Cold Forming Neglected. Compressive Properties: c) Cold Forming Considered; d) Cold Forming Neglected. e) Experimental

Fig. 10. Moment-curvature characteristics of beam 4A.

Therefore, for press braked sections with w/t values of the order of $(w/t)_{lim}$ it is considered better to utilize the virgin properties in calculating Moment-Curvature relations.

Ultimate Beam Capacity.—There are two main approaches to computing the ultimate capacity of a beam. The first uses the Elastic Section Modulus concept and considers that failure occurs when the extreme fiber reaches a defined yield strength. The second uses the Plastic Hinge concept and defines failure as the moment at which the section is fully plastified, i.e., all fibers have reached a defined yield strength. The two methods will be referred to as E and P respectively, and diagrams explaining the assumed stress distributions for the different variations described below are shown in Fig. 11.

The Elastic Section Modulus method admits three alternatives: a) neglecting completely the effects of cold work by using the virgin materials properties all across the section (E-a), or b) considering such effects only on the flats and limiting the stress in the corners to the as-formed yield strength of the flats (E-b), or c) using a weighted average tensile yield strength which

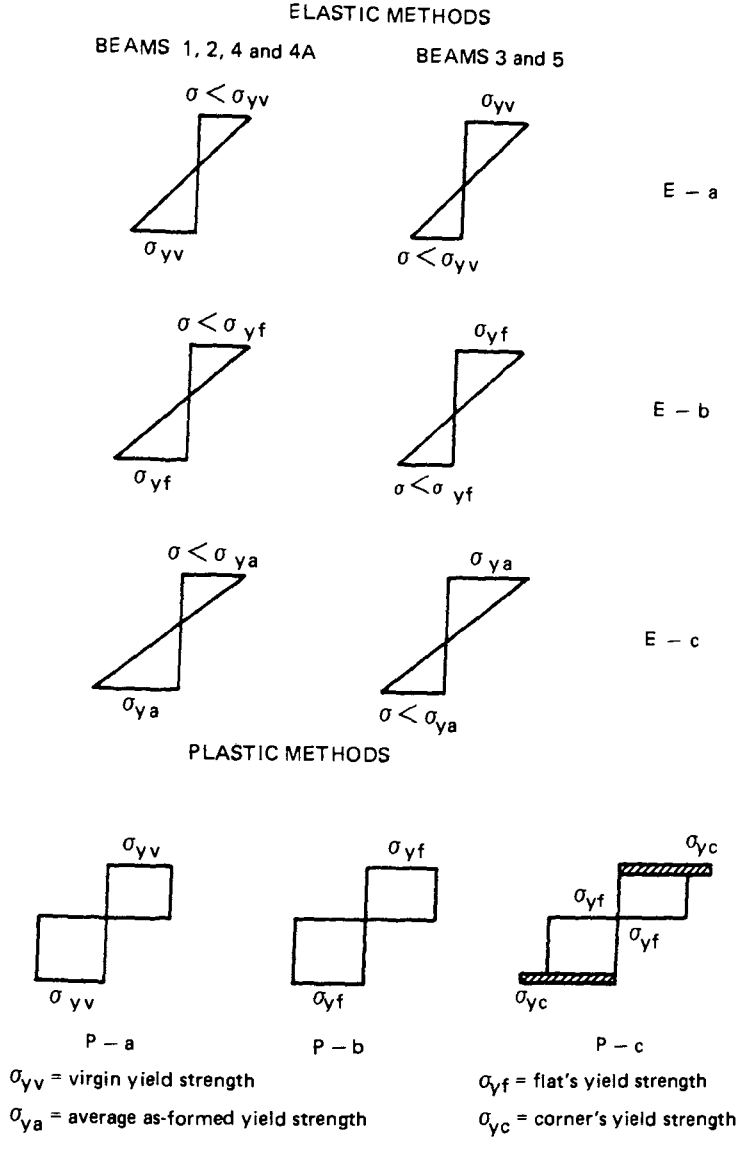

Fig. 11. Stress distributions assumed in computing the ultimate capacity of beams.

includes both corners and flats[1] (E-c). The average yield strength σ_{ya} assumed in design to be uniform across the section would be given by:

$$\sigma_{ya} = C\sigma_{yc} + (1 - C)\,\sigma_{yf} \tag{6}$$

where

C = ratio of the total corner area to the total cross-sectional area of the full section

σ_{yc} = tensile yield strength of corners

σ_{yf} = weighted average tensile yield strength of flats.

Eq. 6 was first proposed by Karren and Winter[9].

The Plastic Hinge method in turn also admits three alternatives: to the two limiting stresses assumed in (a) and (b) above, which lead to the stress distributions P-a and P-b, it is necessary to add a third one, P-c, in which full consideration is given to the effects of cold work by assigning to the corners their proper as-formed 0.2% offset yield strength.

A rigorous analysis would require to differentiate between elements in tension and compression for each alternative. However, since the yield strengths in tension and compression are very close to each other for ordinary low carbon steel, the simpler approach of using either the tensile or the compressive yield strengths for the whole section was followed. Other assumptions in the analysis are the uniformity of yield strength of the flats, which is approximately true for all sections except the tension flanges of beam B-2 and the compression flanges of beam B-3, and the definition of limiting stress as the 0.2% offset yield strength obtained from coupons. This last assumption is good for flat elements of fairly sharp yielding steel, but conservative for the corners and those flat elements with gradual yielding stress-strain relationships.

The values predicted by the above methods are compared with the experimental results in Tables 6, 7, and 8. The experimental failure moments were defined as the maximum moments obtained in the tests for all beams except B-5 for which failure was arbitrarily defined as the moment at which the deflection at midspan was equal to one fiftieth of the span length.

Computations of ultimate beam capacities by the Elastic Section Modulus method based on the tensile virgin yield strength (E-a, Table 6), underestimated the experimental ultimate moments by amounts ranging from -40.8 to -17.6 percent, with an average of -28.8 percent. By using the Plastic Hinge method and the compressive virgin yield strength (P-a, Table 7), improved estimates were obtained which averaged -8.5 percent below the experimental strengths. The same method using actual measured flats properties (P-b) further improved the estimates but only slightly.

The best strength estimates for the most compact sections, i.e., beams B-1, B-2, B-3, and B-5, were obtained by the Plastic Hinge method with the as-formed tensile properties of corners and flats (P-c). The predicted ultimate capacities were from -13.4 percent below to +0.5 percent above those found experimentally. The average deviation was -3.5 percent.

Table 6. Comparison of Experimental and Calculated Beam Capacities Using Tensile Properties

Specimen	Experimental Failure Moment (in-kip)	Elastic Method Based on: Virgin Properties E-a		Elastic Method Based on: Flat's Properties E-b		Plastic Method Based on: Virgin Properties P-a		Plastic Method Based on: Flat's Properties P-b		Plastic Method Based on: Flats + Corners P-c	
		M	%	M	%	M	%	M	%	M	%
B-1	11242	7946	−29.3	8311	−26.1	10063	−10.5	10525	−6.4	11234	−0.1
B-2	18305	11441	−37.5	13737	−25.0	14241	−22.2	17116	−6.5	18400	+ 0.5
B-3	96775	57342	−40.8	56841	−41.3	74687	−22.8	74035	−23.5	83816	−13.4
B-4	13650	11253	−17.6	11420	−16.3	13802	+ 1.1	13981	+ 2.4	15485	+13.4
B-4A	14000	11337	−19.0	11518	−17.7	13915	−0.6	14095	+ 0.7	15614	+11.5
B-5	15035*			10158	−32.4			12366	−17.8	14897	−0.9

*Arbitrarily defined at defl. = L/50.

Table 7. Comparison of Experimental and Calculated Beam Capacities Using Compressive Properties

Specimen	Experimental Failure Moment (in-kip)	Elastic Method Based on: Virgin Properties E-a		Elastic Method Based on: Flat's Properties E-b		Plastic Method Based on: Virgin Properties P-a		Plastic Method Based on: Flat's Properties P-b		Plastic Method Based on: Flats + Corners P-c	
		M	%	M	%	M	%	M	%	M	%
B-1	11242	8675	−22.8	9040	−19.6	10987	− 2.3	11448	+ 1.8	12100	+ 7.6
B-2	18305	12357	−32.5	14218	−22.3	15381	−16.0	17677	− 3.4	19103	+ 4.4
B-3	96775	58093	−40.0	58884	−39.2	75665	−21.8	76644	−20.8	87553	− 9.5
B-4	13650	11092	−18.7	10914	−20.0	13593	− 0.4	13354	− 2.2	15159	+11.0
B-4A	14000	11188	−20.1	10978	−21.6	13705	− 2.1	13464	− 3.8	15288	+ 9.2
B-5	15035*			11532	−23.3			14039	− 6.6	16230	+ 8.0

*Arbitrarily defined at defl. = L/50.

Table 8. Comparison of Experimental and Calculated Beam Capacities Using Virgin and Overall Average Tensile Properties

Specimen	Virgin Yield Strength	Average Yield Strength	Experimental Failure Moment	Virgin Properties (E-a) M_1	$\frac{M_1}{M_{exp.}}$	Average Properties (E-c) M_2	$\frac{M_2}{M_{exp.}}$	$\frac{M_2}{M_1}$
B-1	32.7	36.2	11242	7946	.707	8797	.782	1.107
B-2	37.5	46.8	18305	11441	.625	14279	.780	1.248
B-3	45.8	53.2	96775	57342	.592	66607	.688	1.162
B-4	44.2	49.5	13650	11253	.824	12677	.929	1.127
B-4A	44.2	49.5	14000	11337	.810	12781	.913	1.127
B-5	28.1*	32.3	15035	10158	.676	11676	.777	1.149

*Assumed equal to the yield strength of as-formed flats.

For the beams with largest w/t ratios, B-4 and B-4A, estimates by the Plastic Hinge method with the as-formed tensile properties of corners and flats exceeded the experimental capacities by 13.4 and 11.5 percent respectively. From Fig. 10 and the information given before on amount of rotation at failure, it seems that hat sections with w/t ratios of the order of $(w/t)_{lim}$ (Eq. 2) may be prevented from developing enough rotation to utilize fully the increased strength of the corners. Therefore for such sections it is suggested to compute the ultimate strength by the Plastic Hinge method with the more conservative (tension or compression) average yield strength of flats (if roll-formed) or of virgin material (if press braked). To do so would result for this particular case in predictions only -0.4 and -2.1 percent below the experimental capacities of beams B-4 and B-4A respecitively. However, additional experimental evidence, especially on roll formed sections, would be necessary before attempting definite conclusions on non-compact members.

Macadam[10] reported tests on three beams made by welding two lipped-channel sections back to back. He concluded that although the Elastic Section Modulus method always underestimated the failure moments, little plastic rotation could be developed before local buckling of the compression flanges occurred and therefore none of the sections tested were capable of attaining the full plastic moment based on yield strength increased by cold work. Since this was also the case for beams B-4 and B-4A, above, it was thought that perhaps the method suggested above for this type of section might also be used for Macadam's beams. The results are presented in Table 9 together with Macadam's values. It is seen that this method in which the effects of cold work on roll formed flats are included but the stress of corners is limited to that of the flats because of low rotation capacity, closely estimates Macadam's experimental ultimate moments, being conservative by amounts ranging from -3.5 to -0.5 percent with an average of -2 percent.

Notice that all of Macadam's beams are compact according to the 1968 edition of the Specification[1]. However because of their configuration, once the lips yield the compression flanges lose most of their support along the outer edges. This would explain the difference in behavior from that of the more compact hat sections (with both edges stiffened by webs) which reached their full plastic moment.

The method based on the Elastic Section Modulus and an overall weighted average tensile yield strength of both corners and flats (E-c) underestimated the capacities of the beams tested here by amounts ranging from -31.2 to -7.1 percent of the experimental strengths with an average deviation of -18.8 percent (Table 8). The capacities calculated by this method were from 10.7 to 24.8 percent above those computed by using the virgin yield strengths. The average gain was 15.3 percent and is certain to be even larger for roll formed sections. When applied to Macadam's beams, method E-c underestimated the beam capacities by amounts ranging from -12.3 to -8.7 percent with an average of -10.7 percent. It offered gains between 5.1 and 10.8 percent with

Table 9. Macadam's Tests (Reference 10)

Specimen	.06-37	.09-50	.09-37	Average
w/t	32.2	19.5	22.4	
$M_{exp.}$ (k-in)	63.4	131.1	97.5	
M_1*	52.9	105.3	83.0	
$(M_1/M_{exp.}-1)$ (%)	−16.6	−19.7	−14.9	−17.1
M_2*	55.6	116.7	89.0	
Dev. (%)	−12.3	−11.0	−8.7	−10.7
M_2/M_1	1.051	1.108	1.072	1.077
M_3*	65.0	137.3	104.4	
Dev. (%)	+2.5	+4.7	+6.7	+4.6
M_4*	61.2	128.5	97.0	
Dev. (%)	−3.5	−2.0	−0.5	−2.0
A_c/A	.148	.177	.106	
Forming Method	roll formed	roll formed	press braked	

*M_1 = Elastic Section Modulus method with assumed virgin properties (Ref. 10).

M_2 = Elastic Section Modulus method with weighted average of corners and flats (Ref. 10).

M_3 = Plastic Hinge method with weighted average of corners and flats (Ref. 10).

M_4 = Proposed Plastic Hinge method with the strength of corners limited to the as-formed yield strength of flats.

respect to the E-a method based on virgin properties. Because of its simplicity safety, and economical advantage this method is recommended for the design of compact sections with $w/t \leq (w/t)_{lim}$.

Deflections. – Fig. 12 shows the contrasting behavior of compact beams with small (B-1) and large (B-4A) w/t-ratios, caused by the small rotation capacity of the latter. Estimates of deflections at working loads, (i.e. for 0.6 times the moments obtained by the Elastic Section Modulus method using the weighted average tensile properties) underestimated the experimental values only

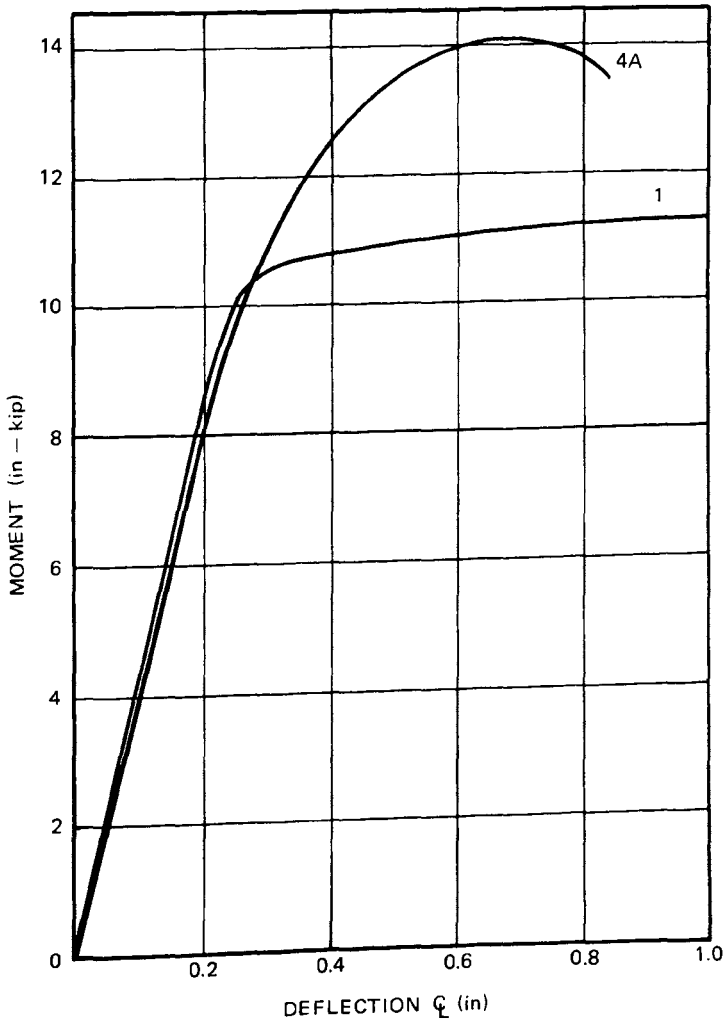

Fig. 12. Load vs. midspan deflection, beams 1 and 4-A.

slightly for four beams, the average deviation being -3.9 percent. The other two beams had deviations of -21.2 and -11.4 percent. The deflection/span ratios obtained for the above working loads ranged from 1/200 to 1/344. When working loads were based on the Plastic Moments based on discriminated as-formed tensile properties and a factor of safety of 1.65, deflections ranged from 1/157 to 1/268 of the span. These deflections may be too large to meet architectural requirements and allowable deflections rather than strength may become the limiting factor in designing this type of sections.

EFFECT OF COLD-FORMING ON STRENGTH OF NON-COMPACT COLUMNS

Introduction.—It was found in the investigation of flexural behavior that even mildly non-compact beams may not develop enough rotation to permit full use of the raised yield strength of corners. It was desirable then to investigate the extent to which the strengthening effects of cold work affect the behavior of non-compact thin-walled columns concentrically loaded, and the results of such investigation are presented next. A similar study was carried out by Karren and Winter[9], but was limited to compact sections. The one reported here follows basically their testing procedures.

The Engesser-Shanley[15] theory of column action predicts that a centrally loaded column will start bending in the inelastic range at the stress:

$$\sigma_t = \frac{\pi^2 E_t}{(L/r)^2} \tag{7}$$

where the tangent modulus E_t is the slope of the stress-strain curve at the level of the stress σ_t, L is the effective length of the column, and r is its radius of gyration with respect to the neutral axis.

Eq. 7 assumes uniform material properties across every column section. Osgood[16] indicated in 1951 how the Engesser-Shanley theory may be used to evaluate the effects of residual stresses on column strength. Petersen and Bergholm[17] in 1961 developed a method to compute the strength of columns with non-uniform materials properties across the section. They arrived at an equation identical to that found by Osgood.

Karren and Winter[9] used this method to study the effects of cold work on the behavior of compact columns. By dividing the cross section into j subareas each of which having its own stress-strain relationship, Osgood's equation becomes:

$$L^2 = \frac{\pi^2 \sum_{i=1}^{j} E_{ti} I_i}{\sigma_{cr} A} \tag{8}$$

where E_{ti} is the tangent modulus of the i_{th} element at the average stress σ_{cr}, I_i is the moment of inertia of the same element about the pertinent principal axis of the total cross-sectional area.

The solution of Eq. 8 involves the following steps: (1) assume a uniform longitudinal compressive strain ϵ; (2) from the stress-strain relationships of the material, such as those shown in Fig. 13, find for each subarea of the cross section the tangent moduli E_{ti} corresponding to the assumed strain ϵ; (3) from the composite stress-strain curve find the stress σ_{cr} corresponding to the assumed ϵ; (4) compute the moments of inertia of each sub-area about the buckling axis of the total cross section; and (5) from Eq. 8 find the length

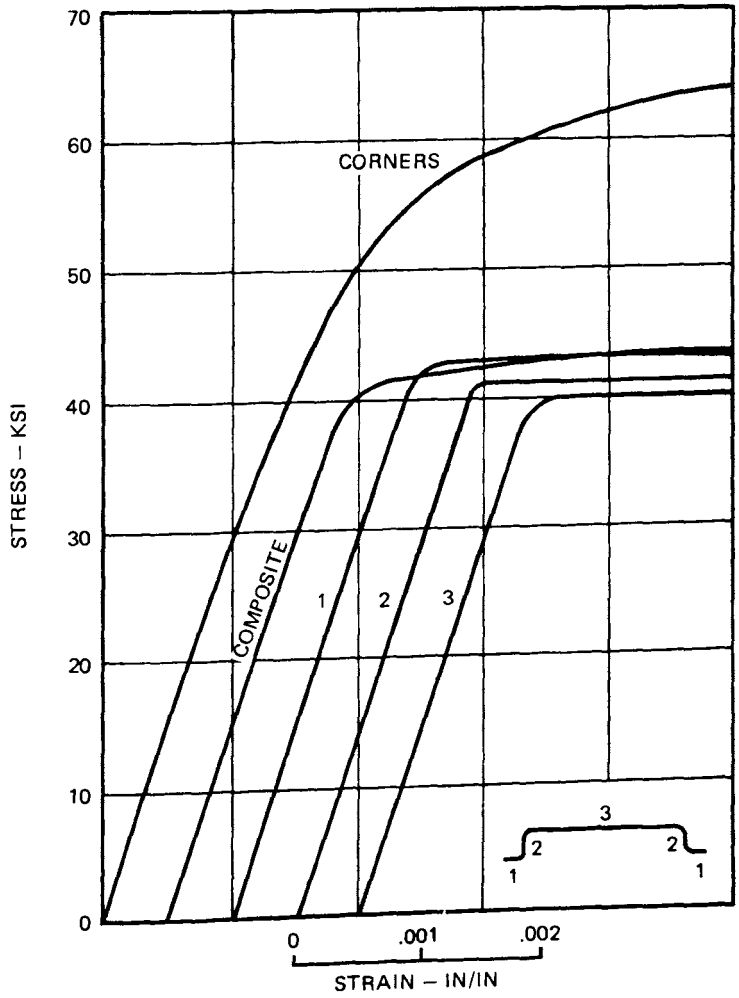

Fig. 13. Compressive stress-strain curves for elements of hat sections, series SC-1.

of the column which is on the verge of buckling under the stress σ_{cr}. By repeating the process for different ϵ the relation between the average critical stress σ_{cr} and the slenderness ratio $L/\sqrt{I/A}$ can be found for any desired range.

The AISI Specification[9] bases its design stresses on dividing by a safety factor the stresses given by the equation:

$$\sigma_{cr} = Q\sigma_y - \frac{Q^2 \sigma_y^2}{4\pi^2 E} \left(\frac{L}{r}\right)^2 \tag{9}$$

where the effect which local buckling of thin-walled elements can have in reducing column strength is taken into account by introducing the form factor "Q"[18]. Eq. 9 is not valid for materials with a proportional limit smaller than half the yield strength and is applicable only up to:

$$\left(\frac{L}{r}\right)_{lim} = \pi \sqrt{\frac{2E}{Q\sigma_y}} \tag{10}$$

The Specification's method provides adequate safety not only against actual collapse but also against excessive local distortions.

The test results of the investigation reported here will be compared with values predicted by Eq. 8 using the stress-strain curves from tensile and compressive coupons of corners and flats, such as those of Fig. 13. A comparison will be made also with the column capacities computed from Eq. 9 by using (a) the 0.2% offset yield strength obtained in laterally supported stub column tests, (b) the overall weighted average yield strength of the section (Eq. 6) and (c) the average yield strength of the flats. Finally, they will be compared whenever possible with the values obtained by direct application of Eq. 7 in connection with the stress-strain curve from a stub column test without lateral support, although this is not a completely rigorous procedure.

Experimental Investigation

Fabrication of Test Specimens.—Three types of sections were investigated. One was a double channel, i.e., a section composed mainly of unstiffened elements; the other two were double hat and lipped-hat sections and therefore composed mainly of stiffened elements. The channel columns will be designated as Series UC-1 or 2, while the hat and lipped-hat sections will be known as Series SC-1 and SC-2 respectively. Section configurations and dimensions are shown in Fig. 14. The material and geometrical properties were such that the channel section columns had a Q factor ranging from 0.818 to

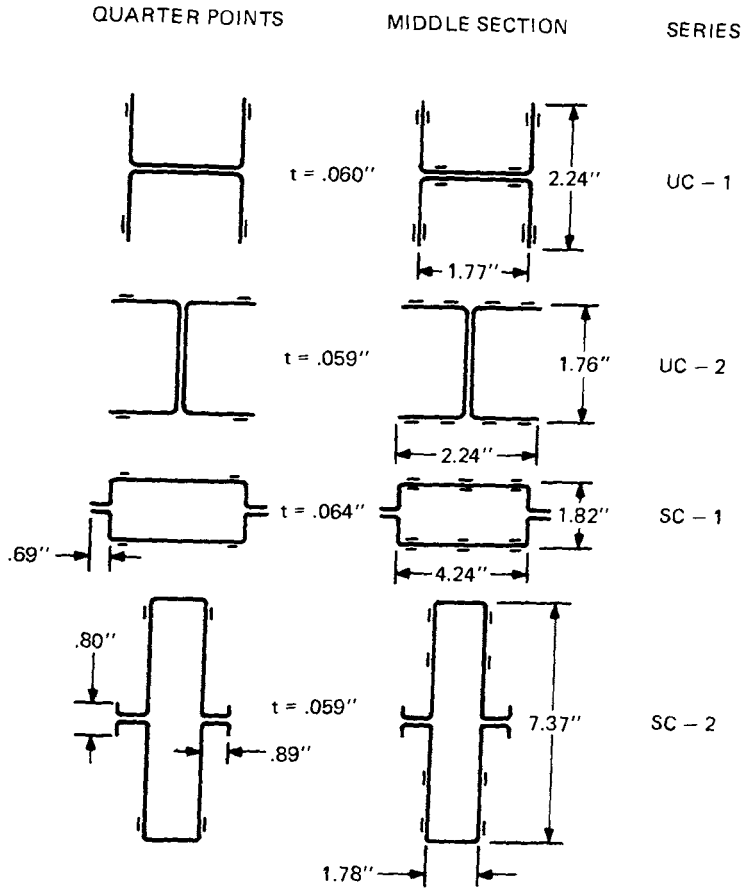

Fig. 14. Section configurations, dimensions, and strain gage location for pin-ended column tests.

0.843 according to the 1968 edition of the Specification and depending on the yield strength used in the computations, while the hat and lipped-hat sections had Q factors ranging from 0.814 to 0.834.

All the sections were formed by press braking. The lipped-hat sections had to be bent at the middle and straightened after the upper bends were made. The specimens were fabricated by bonding together two identical sections to form bisymmetrical members, using a structural adhesive. After fabrication, the specimens were saw-cut to the desired length and the ends were either milled or ground flat and parallel, and perpendicular to the longitudinal axis.

The specimens were designed and tested in such a manner as to have in some cases many and in others few of their corners situated far from the buckling axis, so that the influence of location of cold-worked portions could be more easily detected.

Testing Procedures.—Yield and ultimate strengths of the virgin material and the formed sections were found in a manner similar to that used for the joist chords or the flexural members. A length of 1.5 in. was used for all compression coupons of corners.

A stub column test, a laterally supported stub column test (to eliminate local buckling) and three pin-ended column tests of different lengths were carried out for each type of section. Testing procedures were identical to those described in Reference 9. In addition, three pin-ended channel columns (Series UC-2) were forced to buckle about their strong-axes. To achieve this lateral support was provided at the middle by means of a heavily greased guide made of 2 1/2 x 2 1/2 in. angles.

Test Results and Discussion

Material Properties.—Average virgin and as-formed material properties for each series of columns are presented in Table 5. Corners experienced average increases of 45.2, 49.8, and 16.5 percent in their tensile and compressive yield and ultimate strengths respectively. Recorded strength changes of flats were negligible and within the natural scatter range of virgin properties.

The yield and ultimate strengths of flats were relatively uniform across the sections except for the top flange of the lipped-hat, which was bent and later straightened during the forming process. The compressive yield strength distributions were very close to the tensile distributions in all cases.

Columns Composed Mainly of Unstiffened Elements (Channel Tests)

Stub Column Tests.—The stub column curve of the channel (Fig. 15) followed very closely the laterally supported stub column curve up to about the 0.2% offset yield strength. The stub column was very stable, sustaining 97% of the maximum load at strains larger than 0.006 in/in. Local buckling was slightly visible at a stress 4.1% below the yield stress obtained from the laterally supported test, or 5.9% below the calculated average compressive yield strength, or 0.8% above the average yield strength of flats (Table 10). The ratio of local buckling stress of the stub column to yield stress of the laterally supported stub column was 0.959 although the Q values for these columns ranged from 0.818 to 0.843.

Table 10. Stub Columns: 0.2% Offset Yield Strengths and Failure Loads

Series	UC-1, 2	SC-1	SC-2
Corners Area/Total Area	.1164	.1280	.1186
Tensile Yield Strength:			
Flats	41.5	39.1	39.6
Corners	59.5	57.3	60.9
Overall Average	43.6	41.4	42.1
Composite Curve	43.4	41.3	41.9
Compressive Yield Strength:			
Flats	39.6	40.5	40.7
Corners	63.8	62.1	60.7
Overall Average	42.4	43.3	43.1
Composite Curve	42.3	43.0	43.0
Laterally Supp. Stub Col.	41.6	42.3*	44.9
Stub Column:			
Failure	41.0+	36.0	37.4
Init. Strain Reversal	39.9++	34.5	36.1
Stub/Lat. Supp.	.986	.852	.833
In. Str. Rev./Lat. Supp.	.959	.812	.804
Stub/Overall Comp. Avg.	.968	.832	.869
In. Str. Rev./Ov. Comp. A.	.941	.798	.838
Stub/Comp. Avg. Flats	1.035	.889	.918
In. Str. Rev./Comp. Avg. Fl.	1.008	.852	.887

*Corrected from 42.4 ksi to take into account differences in virgin yield strength.

+0.2% offset yield strength.

++Local buckling slightly visible.

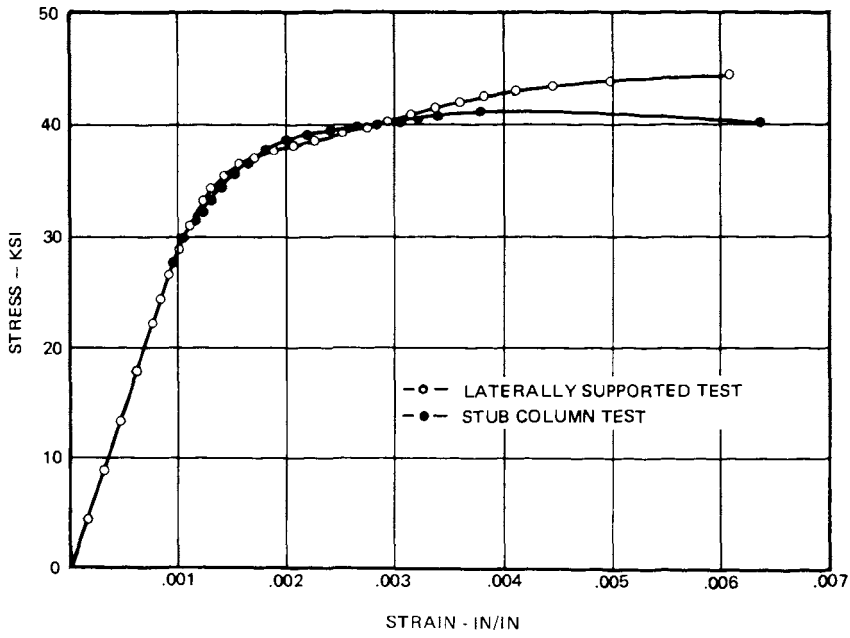

Fig. 15. Comparison of full section compressive stress-strain curves for laterally supported and stub column tests; channels series UC-1 and UC-2.

Pin-Ended Tests.–The strong and weak-axes column curves obtained from Eq. 8 disregarding local buckling, are very close to each other. The test results were remarkably close to these curves which are based on the calculated average compressive stress-strain relationships using tests of corners and flats (a and b of Fig. 16). Ratios between experimental failure loads and the compressive theoretical values by the above equation (Table 11) ranged from 0.945 to 1.074 for columns buckling about the weak axis (series UC-1) and from 0.925 to 1.054 for those buckling about the strong axis.

Experimental failure stresses also were very close to a column curve based on direct application of the tangent modulus equation (Eq. 7) and on the stub column stress-strain relationship (Fig. 16-f). Such a curve approximately follows the theoretical curves based on average calculated compressive properties of corners and flats in the slenderness ratio range between 40 and 80.

The experimental failure stresses of series UC-1 were from 3.0 to 14.8 percent above the values computed from the AISI Specification formula (Eq. 9) using the appropriate Q and the average compressive yield strength of flats (Table 13 and Fig. 16-c). Corresponding figures for the UC-2 columns were from 4.8 to 18.3 percent above calculated values (Table 13 and Fig. 16-d). Although the Specification's method is intended to prevent not only failure but also excessive distortion, and failure loads larger than predicted should be expected, it was noted that local buckling was visible before failure occurred

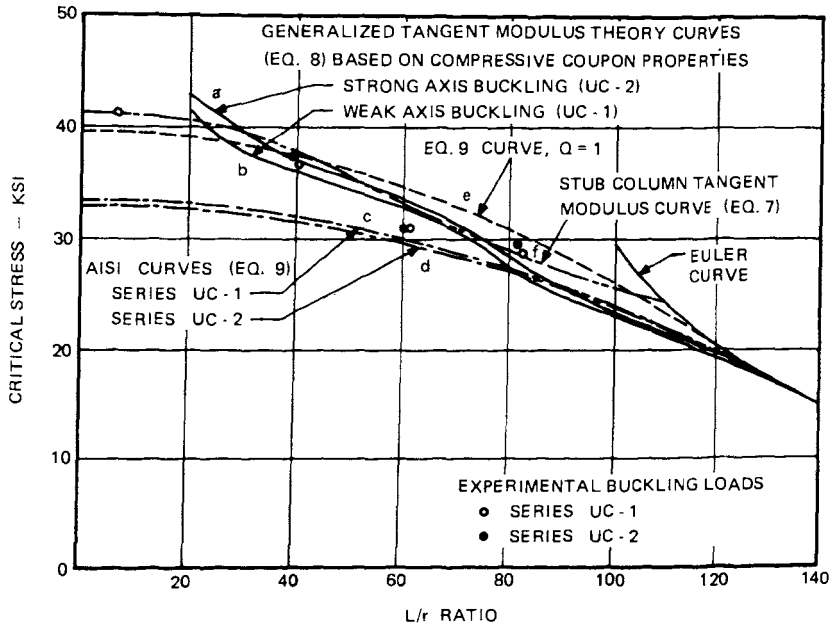

Fig. 16. Comparisons of test results and column curves for series UC-1 and UC-2.

in one test only. This shows when strain-hardening in the corners is neglected that the Specification leads to conservative predictions, especially for buckling about the strong axis since the effects of cold work are more beneficial in this case. An alternate method of computing the Q factor of sections composed of unstiffened elements is proposed next.

The determination of effective widths of stiffened elements in the 1968 edition of the Specification[1] is based on the equation:

$$\frac{b}{w} = \sqrt{\frac{\sigma_{cr}}{\sigma_{max}}} \left(1 - 0.22 \sqrt{\frac{\sigma_{cr}}{\sigma_{max}}}\right) \tag{11}$$

where

$$\sigma_{cr} = K \frac{\pi^2 E}{12 (1 - \mu^2) (w/t)^2} \tag{12}$$

In the case where one edge is supported by a thin web while the other, outer edge is unsupported, K is equal to about 0.5. Using this value in Eq. 12, and substituting this equation into Eq. 11 results in:

$$\frac{b}{t} = 0.672 \sqrt{\frac{E}{\sigma_{max}}} \left(1 - 0.148 \frac{t}{w} \sqrt{\frac{E}{\sigma_{max}}}\right) \tag{13}$$

Table 11. Summary of Column Tests – Series UC-1 and UC-2

	Sheet	$\frac{L}{r}$	σ_y Virgin Compress.	σ_f Failure Stress	σ_{SR} Strain Reversal Stress	σ_{fc} + Corrected Failure Stress	σ_{SRC} + Corrected Strain Reversal Stress	σ_{cr} from Eq. 19	$\frac{\sigma_{fc}}{\sigma_{cr}}$	$\frac{\sigma_{SRC}}{\sigma_{cr}}$
Tension Coupons	SK-22		41.3	43.6*						
Compr. Coupons	SK-22		41.3	42.4*						
Lat. Supp. Test	SK-22		41.3	41.6						
Stub Column T.	SK-22	7.1	41.3	41.0*	40.3	41.0	40.3			
UC-11	SK-22	40.3	41.3	36.5	33.7	36.5	33.7	36.0	1.013	.936
UC-12	SK-22	61.2	41.3	30.7	28.7	30.7	28.7	32.5	.945	.883
UC-13	SK-22	82.4	41.3	28.8	27.1	28.8	27.1	26.8	1.074	1.011
UC-21	SK-19	39.2	43.7	39.5	39.5	37.3	37.3	37.2	1.002	1.002
UC-22	SK-19	60.5	43.7	32.7	32.3	30.9	30.5	33.4	.925	.913
UC-23	SK-18	81.4	41.1	29.3	28.9	29.4	29.0	27.9	1.054	1.039

+ Correction based on compression virgin yield strength of stub columns.
* 0.2% offset yield strength.

which gives the effective width of unstiffened elements. For stub column tests σ_{max} may be taken as the average compressive yield strength of flats, while for pin-ended column tests σ_{max} may be replaced by the critical stress obtained from Eq. 9 using Q = 1 as a first approximation.

By computing the effective width of unstiffened elements in this manner and redefining the Q-value of channel sections as the ratio of effective area to total area, i.e., the same definition as for sections composed entirely of stiffened elements, the Q-values of series UC-1 and UC-2 would range from 0.928 to 0.971 with averages of 0.955 and 0.945 respectively, i.e., significantly larger than per AISI Specification (Table 13). These averages compare well with 0.959, i.e., the ratio of local buckling stress of the stub column to yield strength of the laterally supported stub column mentioned before. The corresponding column curve (not shown) falls only slightly below that for Q = 1 on Fig. 16 and agrees well with test results.

Columns Composed Mainly of Stiffened Elements (Hat and Lipped-Hat Sections)

Stub Column Tests.–The stub column tests of the hat (series SC-1) and lipped-hat (series SC-2) sections showed sudden failure at 85.2 and 83.3 percent of the stresses reached in the respective laterally supported stub tests. Fig. 17 presents the stub column curves for series SC-2. Those for series SC-1, not shown, were similar. Calculated Q values, based on the yield strengths obtained in laterally supported stub column tests were 0.817 for both series. It is seen that for these sections Q-values calculated by the AISI Specification method are in good agreement with test results.

Pin-Ended Tests.–For the column buckling tests, the ratios between experimental failure loads and theoretical predictions disregarding local buckling (Eq. 8) ranged from 0.880 to 0.890 for series SC-1 (Table 12 and Fig. 18-b) and from 0.911 to 0.986 for series SC-2 (Table 12 and Fig. 19-a). This indicates that consideration of local buckling by the Q-method is mandatory. Here again, it seems that having the corners far from the buckling axis (series SC-2) helped to increase the inelastic buckling load.

An approximate method to include the effects of local buckling in connection with Eq. 8 would be to modify step 3 in the procedure described before. Instead of finding σ_{cr} from a composite curve calculated for the full area of all the elements, compute the effective width of the stiffened elements at the stress σ_{fi} corresponding to the assumed strain ϵ from Eq. 1. Then, compute the stress σ_{cr} from the equation:

$$\sigma_{cr} = \Sigma(A_{eff})_{fi} \ \sigma_{fi} + \Sigma A_{ci} \sigma_{ci} \qquad (14)$$

Table 12. Summary of Column Tests – Series SC-1 and SC-2

	Sheet	$\frac{L}{r}$	σ_y Virgin Compress.	σ_f Failure Stress	σ_{SR} Strain Reversal Stress	σ_{fc} + Corrected Failure Stress	σ_{SRC} + Corrected Strain Reversal Stress	σ_{cr} from Eq. 8	$\frac{\sigma_{fc}}{\sigma_{cr}}$	$\frac{\sigma_{SRC}}{\sigma_{cr}}$
Tens. Coupons SC-1	SK-2		39.4	41.4*						
Comp. Coupons SC-1	SK-2		39.4	43.3*						
Lat. Sup. (LSSC-1)	SK-4		39.5	42.4		42.3				
Stub Column (SSC-1)	SK-2	5.7	39.4	36.0	34.5	36.0	34.5			
SC-11	SK-4	31.2	39.5	37.0	35.6	36.9	35.5	41.1	.899	.865
SC-12	SK-2	59.8	39.4	35.0	33.4	35.0	33.4	39.8	.880	.839
SC-13	SK-1	82.2	42.2	34.8	33.5	32.5	31.2	36.7	.886	.850
Tens. Coupons SC-2	R-17B		44.2	42.1*						
Comp. Coupons SC-2	R-17B		44.2	43.1*						
Lat. Supp. (SSC-2)	R-17B		44.2	44.9						
Stub Column (LSSC-2)	R-17B	5.9	44.2	37.4	36.1	37.4	36.1			
SC-21	R-17A	38.2	43.1	35.9	35.9	36.8	36.8	40.4	.911	.911
SC-22	R-19A	59.6	44.0	37.0	37.0	37.2	37.2	39.6	.939	.939
SC-23	R-19B	82.9	44.3	35.2	35.2	35.1	35.1	35.6	.986	.986

* 0.2% offset yield strength.
\+ Correction based on stub column test.

Table 13. Comparison of Experimental, Predicted and Specified Critical Stresses, ksi

Column	Experimental Failure	Predicted by Eqs. 8 and 14	Exp. Fail. / Predicted	AISI Failure	Exp. Fail. / AISI	Modified Q*
UC-11	36.5			31.8	1.148	.943
UC-12	30.7			29.8	1.030	.953
UC-13	28.8			26.9	1.070	.971
UC-21	37.3			31.5	1.183	.928
UC-22	30.9			29.5	1.048	.941
UC-23	29.4			26.8	1.097	.965
SC-11	36.9	34.0	1.086	32.4	1.139	
SC-12	35.0	32.5	1.077	29.9	1.171	
SC-13	32.5	30.5	1.065	26.9	1.208	
SC-21	36.8	34.0	1.081	32.4	1.136	
SC-22	37.2	33.6	1.107	30.5	1.219	
SC-23	35.1	31.8	1.102	27.0	1.300	

*Based on effective width determinations for both stiffened and unstiffened elements.

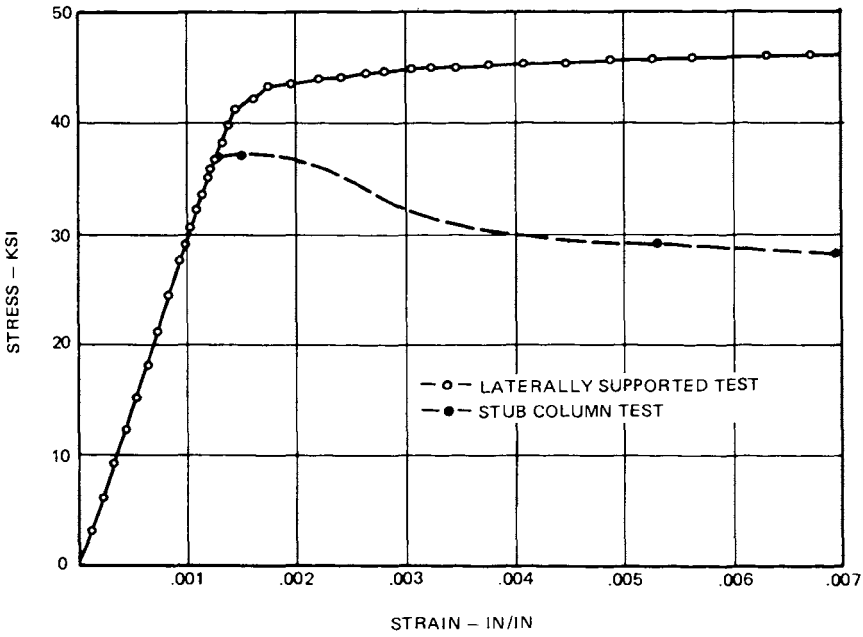

Fig. 17. Comparison of full section compressive stress-strain curves for laterally supported and stub column tests; series SC-2.

where

A_{ci} = area of the i_{th} corner

$(A_{eff})_{fi}$ = effective area of the i_{th} flat at the stress σ_{fi}

σ_{ci} = stress of the i_{th} corner at the assumed strain ϵ

σ_{fi} = stress of the i_{th} flat at the assumed strain ϵ

The other steps in the procedure remain unchanged. By using this approximation, curves e of Fig. 18 and d of Fig. 19 were obtained. The ratios between experimental and calculated failure loads ranged then from 1.065 to 1.086 for series SC-1 and from 1.081 to 1.107 for series SC-2 (Table 13).

The experimental failure stresses of series SC-1 columns were from 13.9 to 20.8 percent higher than those predicted from the Specification using specified Q factors (Table 13 and Fig. 18-c). Corresponding figures for the SC-2 columns ranged from 13.6 to 30.0 percent above the Specification values (Table 13 and Fig. 19-b). This points out, again, the conservative nature of the Specification's method.

It was found in all the columns composed mainly of stiffened elements that the length of the specimen affects only slightly its ultimate strength within the intermediate and low slenderness ratio range under study. This

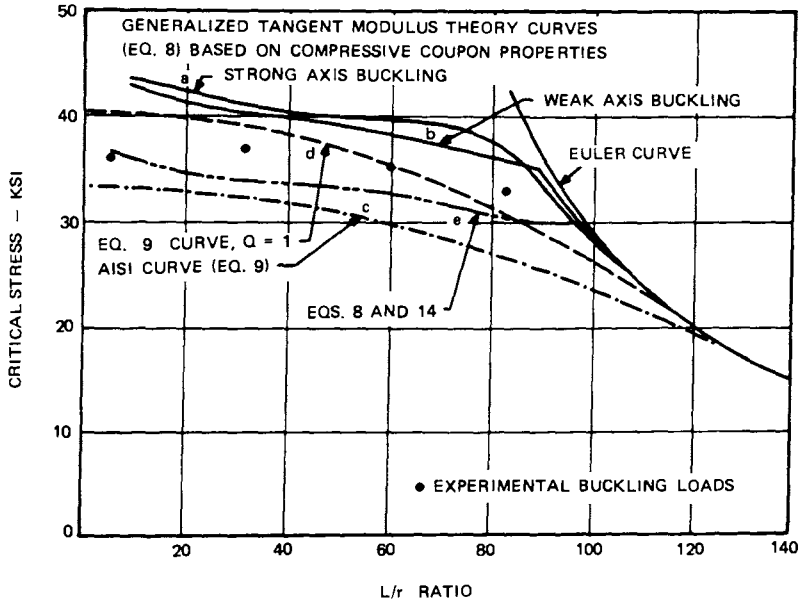

Fig. 18. Comparison of test results and column curves for series SC-1.

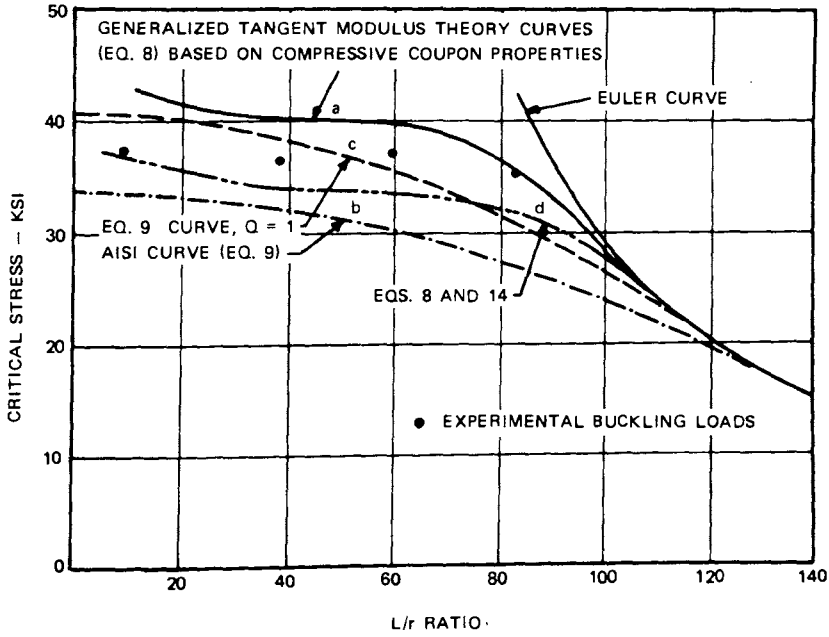

Fig. 19. Comparison of test results and column curves for series SC-2.

agrees with the results of other investigators[19], and indicates that the shape of the basic CRC-AISI column-curve is over conservative for cold-formed members produced in press-brakes. For this type of forming only the corners present a gradual yielding stress-strain curve and since they constitute generally a small percentage of the total area, the inelastic range of the column curve begins at a much higher fraction of the yield stress than reflected in the basic CRC curve on which the Specification is based. However, the difference between the actual buckling curve and the CRC-AISI curve should be smaller for the more frequent cold-rolled than for the tested press-braked sections since not only the corners but also the flats of the former are of the gradual yielding type.

SUMMARY AND CONCLUSIONS

Cold-forming causes a significant increase in yield strength of corners and to a lesser degree of flats of thin-walled steel members. This paper presents the third phase in a long range investigation on the effects of such cold-work. The topics studied here, though all related to effects of cold-work on thin-walled steel structural members are somewhat independent from each other. For this reason detailed evaluations are given under the heading "Test Results and Discussion" at the end of each individual topic. The reader is referred to these for more detailed information; the following is only a brief overall review.

A–Flats of Cold-Rolled Joist Chord Sections

No theoretical method is available to predict the as-formed strength of flat portions of cold-rolled sections; because of the many factors involved such predictions have to be made on a statistical basis. Coupons of flats from 32 joist chord sections showed increases in average yield strength up to 54 percent over the virgin yield strength. Ninety percent of the sections offered average increases in yield strength of flats greater than 8 percent of the virgin value. The ultimate tensile strength decreased by more than 9 percent of the virgin ultimate in ten percent of the sections. It was found that the benefit from cold-work will be greater the higher the ratio of virgin ultimate to yield strength, the thicker the material, the wider the blank width and the smaller the yield strength.

If one attempts to obtain a safe estimate for effects of cold work in flats without actual testing, then for compact sections such as those of Fig. 1, it seems reasonable to assume a 10 percent increase in yield strength and an 8 percent decrease in ultimate strength. The much greater strength increase in corners can be calculated from Ref. 5.

B—Behavior of Beams

Six thin-walled beams were tested and the results compared with theoretical predictions. Computed Moment-Curvature relationships based on the as-formed tensile yield strength of flats and corners were close to the experimental curves and on the conservative side. The following recommendations are made:

For design, compute the beam capacities of compact sections by the Elastic Section Modulus method based on the overall weighted average tensile yield strength of both corners and flats.

For greater accuracy where permissible, or for research purposes, compute the ultimate beam capacity of sections with low w/t ratios by the Plastic Hinge method based on as-formed tensile properties of corners and flats. In case of compact hat sections with w/t ratios close to $(w/t)_{lim}$ or compact beams made by connecting two lipped-channels back to back, use the Plastic Hinge method with the more conservative (tension or compression) average yield strength of flats (if roll-formed) or virgin material (if press-braked), disregarding corner strengthening.

C—Behavior of Non-Compact Columns

The inelastic buckling behavior of channel, hat and lipped-hat sections connected to form non-compact bi-symmetrical columns was investigated. The experimental results of the non-compact channel section columns followed closely theoretical column curves based on a modified form of the tangent modulus equation disregarding the effects of local buckling. This suggests that the method given in the AISI Specification[9] for computing the form factor Q of sections composed mainly of unstiffened members is quite conservative. A modification of the method is proposed. For the non-compact hat and lipped-hat section columns the experimental results were below the column-curves based on the modified form of the tangent modulus equation disregarding local buckling, indicating that consideration of local buckling is mandatory for sections composed mainly of stiffened elements. Q-values of hat and lipped-hat sections calculated by the AISI Specification method were in good agreement with test results.

It is finally concluded that the Specification's method leads to conservative results, especially for press-braked sections with corners located far from the buckling axis. The degree of conservatism seems to be larger for sections composed mainly of stiffened elements than for those composed mainly of unstiffened elements and is probably larger for the tested press-braked sections than for roll-formed shapes. The paper presents a more rational approach to predict the failure loads by using Eq. 8 and the average calculated compressive stress-strain curves from tests of corners and flats, with adequate

provisions for local buckling. For sections composed mainly of stiffened elements this can be accomplished by using the effective width of each sub-element in computing the stress σ_{cr} to be used in that equation. However, the amount of work involved is such as to make the method inappropriate for use in routine design.

ACKNOWLEDGMENTS

This investigation is part of a continuing research program relating to thin-walled cold-formed steel construction, sponsored at Cornell University by the American Iron and Steel Institute. The unfailing cooperation of W. G. Kirkland, Vice-President, AISI; D. S. Wolford, Chairman of the Research and Specifications Subcommittee on Building Research and Technology; and C. R. Clauer, Chairman of the Task Group on the Effects of Cold Work, is gratefully acknowledged.

APPENDIX.—NOTATION

A = cross-sectional area
A_{ci} = area of the i_{th} corner element of a cross-section
$(A_{eff})_{fi}$ = effective area of the i_{th} flat element of a cross-section
b = effective width of a thin-walled element
C = ratio of corner area to total cross-sectional area
E = modulus of elasticity
E_t = tangent modulus of a stress-strain curve at a point above the proportional limit
E_{ti} = tangent modulus of the i-th element of a cross section
I = moment of inertia of the total cross-section about its neutral axis
I_i = moment of inertia of the i-th element of a cross-section about the neutral axis of the total cross-section
K = coefficient used in determining the critical stress of a plate
L = effective length of a column
Q = "form factor" used in the design of sections containing one or more flat plate elements with large w/t ratios
r = radius of gyration in the plane of bending
t = thickness
w = flat width of a compression element
β = auxiliary variable defined by Eq. 5
ϵ = strain assumed uniform across the section
μ = Poisson's ratio of the material

σ = stress corresponding to the strain ϵ

σ_c = reduced allowable unit stress for an unstiffened compression element

σ_{ci} = stress of the i-th corner element of a cross-section

σ_{cr} = stress at the critical buckling load of a member

σ_{fi} = stress of the i-th flat element of a cross-section

σ_{max} = edge stress in a compression element

σ_t = stress at which bending starts according to the Engesser-Shanley theory of column action

σ_u = ultimate tensile strength

σ_y = yield strength determined by the 0.2% offset method

σ_{ya} = average yield strength of the total section

σ_{yc} = tensile yield strength of corners

σ_{yf} = weighted average tensile yield strength of flats of a cold-formed member

σ_{yv} = yield strength of virgin material

REFERENCES

1. Specification for the Design of Cold Formed Steel Structural Members – American Iron and Steel Institute, New York, N.Y., 1968 edition.
2. Chajes, A., Britvec, S. J., and Winter, G., "Effects of Cold-Straining on Structural Sheet Steels", J. of the Structural Div., ASCE, Vol. 89, No. ST2, Proc. Paper 3477, April 1963, pp. 1–32.
3. Hlavacek, V., "Calculation of the Increase in Yield Strength Due to the Effects of Cold Work of Forming", Final Report, 8th Congress, International Association for Bridge and Structural Engineering, New York, September 1968, p. 273.
4. Karren, K. W., "Effects of Cold-Forming on Light-Gage Steel Members", Ph.D. Thesis, Cornell University, Ithaca, New York, 1965.
5. Karren, K. W., "Corner Properties of Cold-Formed Steel Shapes", J. of the Structural Div., ASCE, Vol. 92, No. ST1, Proc. Paper 5112, February 1967, pp. 401–432.
6. Kenzo Kato, "A Basic Study on Cold-Roll Forming Technique", Nippon Kokan, Technical Report Overseas, No.1, June 1963, pp. 44–54.
7. Marx, S., et al., "Probleme der Kaltverfestigung im Stahlleichtbau", Final Report, 8th Congress, International Association for Bridge and Structural Engineering, New York, September 1968, p. 259.
8. Griffin, E., Discussion on the paper "Structural Problems in the Use of Cold-Formed Steel Sections", by Chilver, A. H., Proceedings, The Institution of Civil Engineers, October 1961, Paper No. 6495, Vol. 23, pp. 270–297, October 1962.

9. Karren, K. W., and Winter, G., "Effects of Cold-Forming on Light-Gage Steel Members", J. of the Structural Div., ASCE, Vol. 93, No. ST1, Proc. Paper 5113, February 1967, pp. 433–469.
10. Macadam, J. M., Discussion on the paper "Effects of Cold Forming on Light-Gage Steel Members"' by Kenneth W. Karren and George Winter., J. of the Structural Div., ASCE, Vol. 93, No. ST5, October 1967, pp. 654–660.
11. Uribe, J., "Effects of Cold Forming on the Flexural Behavior of Light Gage Steel Members", M. S. Thesis, Cornell University, Ithaca, New York, 1966.
12. Winter, G., and Uribe, J., "Effects of Cold Work on Cold Formed Steel Members", Symposium on Thin Walled Steel Structures at University College of Swansea, September 1967. Crosby Lockwood & Son Ltd., London, 1969.
13. Uribe, J., "Aspects of the Effects of Cold-Forming on the Properties and Performance of Light-Gage Steel Structural Members", Ph.D. Thesis, Cornell University, Ithaca, New York, 1969.
14. McGuire, W., Steel Structures, Prentice-Hall, Englewood Cliffs, N. J., 1968, pp. 485.
15. Shanley, F. R., "Inelastic Column Theory", Journal of the Aeronautical Sciences, Vol. 14, No. 5, May 1947, p. 261.
16. Osgood, W. R., "The Effect of Residual Stresses on Column Strength", Proc. 1st. U. S. Natl. Congress of Applied Mechanics, New York, June 1951, p. 415.
17. Peterson, R. E., and Bergholm, A. O., "Effect of Forming and Welding on Stainless Steel Columns", Aerospace Engineering, Inst. of Aerospace Sciences (presently, Amer. Inst. of Aeronautics and Astronautics), New York, N. Y., Vol. 20, No. 4, April 1961.
18. Winter, G., Commentary on the 1962 Edition of the Light-Gage Cold-Formed Steel Design Manual, American Iron and Steel Institute, New York, N.Y., 1962.
19. Graves Smith, T. R., "The Ultimate Strength of Locally Buckled Columns of Arbitrary Length", Symposium on Thin Walled Steel Structures at University College of Swansea, September 1967, Crosby Lockwood & Son Ltd., London, 1969.
20. Kirkland, W. G., "Cold Roll Forming Practice in the United States", American Iron and Steel Institute, New York, N.Y., April 1966.
21. Light Gage Cold-Formed Steel Design Manual. American Iron and Steel Institute, New York, N.Y., 1962.